

DISSERTATION

Ecotoxicology of nanoparticles – effects on organisms from activated sludge in wastewater treatment plants

zur Erlangung des akademischen Grades
DOCTOR RERUM NATURALIUM (Dr. rer. nat.)

vorgelegt am 29.02.2016 von Corinna Burkart,
geboren am 11. Mai 1985 in Hannover, Deutschland

Technische Universität Dresden, Fakultät Umweltwissenschaften,
Institut für Hydrobiologie

Gutachter: Prof. Dr. rer. nat. habil. Thomas U. Berendonk, TU Dresden
Prof. Dr. rer. nat. habil. Jörg Oehlmann, Goethe Universität Frankfurt
Dr. Marianne Matzke, Center for Ecology and Hydrology Wallingford, UK

Ort und Datum der Verteidigung: Dresden, 21.11.2016

Ich bestätige hiermit die Übereinstimmung dieses Exemplares mit dem Original
meiner Dissertationsschrift mit dem Titel „Ecotoxicology of nanoparticles – effects on

organisms from activated sludge in wastewater treatment plants”, vorgelegt am 29.02.2016 von Corinna Burkart, mit Verteidigung am 21.11.2016 in Dresden.

Ort, Datum

Unterschrift Corinna Burkart

Contents

Contents.....	I
Abbreviations and Symbols.....	IV
1 General introduction	1
2 Nanomaterials.....	9
2.1 Silver nanoparticles	9
2.1.1 Properties of silver nanoparticles	9
2.1.2 Characterization methods for nAg.....	9
2.2 Titaniumdioxide Nanoparticles.....	15
2.2.1 Properties of titanium dioxide nanoparticles.....	15
2.2.2 Characterization of nTiO ₂ in test media.....	15
3 Single Species tests with Ciliates.....	16
3.1 Introduction - Ciliates.....	16
3.2 Growth kinetics under experimental conditions for <i>P. tetraurelia</i>	18
3.2.1 Materials and Methods for <i>P. tetraurelia</i> growth kinetics	18
3.2.2 Results and Discussion for <i>P. tetraurelia</i> growth kinetics	20
3.3 Toxicity tests with <i>P. tetraurelia</i> and nAg	23
3.3.1 Materials and Methods for <i>P. tetraurelia</i> toxicity tests with nAg.....	23
3.3.2 Results and discussion of nAg toxicity tests with <i>P. tetraurelia</i>	28
3.4 Toxicity tests with <i>P. tetraurelia</i> and nTiO ₂	42
3.4.1 Materials and methods for nTiO ₂ toxicity tests	42
3.4.2 Results and discussion of nTiO ₂ toxicity tests	44
4 Single species tests with bacteria	52
4.1 Introduction – Bacteria in WWTPs and tested species	52
4.2 Experiments with <i>Raoultella planticola</i>	53
4.2.1 Introduction – <i>R. planticola</i>	53
4.2.2 Growth kinetics of <i>R. planticola</i> at experimental conditions	53
4.2.3 Toxicity tests with <i>Raoultella planticola</i> and nAg	60
4.3 Experiments with <i>Hyphomicrobium sp.</i>	74

4.3.1	Introduction – <i>Hyphomicrobium</i> and denitrification	74
4.3.2	Growth kinetics of <i>Hyphomicrobium</i> under experimental conditions	75
4.3.3	Toxicity tests with <i>Hyphomicrobium</i> and nAg	78
4.4	Experiments with <i>Nitrobacter vulgaris</i>	88
4.4.1	Introduction – <i>Nitrobacter</i> and nitrification	88
4.4.2	Growth kinetics of <i>Nitrobacter vulgaris</i>	89
4.4.3	Toxicity tests with <i>Nitrobacter vulgaris</i> and nAg	95
5	Accumulation tests with nAg in a simple food chain	102
5.1	Introduction - accumulation of nanoparticles	102
5.2	Materials and Methods for accumulation experiments	103
5.2.1	Characterization of nAg in conditioned CM at exposure concentrations	105
5.2.2	Acute biomagnification experiments with <i>R. planticola</i> and <i>P. tetraurelia</i>	105
5.2.3	Chronic biomagnification experiments with <i>R. planticola</i> and <i>P. tetraurelia</i>	108
5.3	Results and discussion for acute accumulation experiments	110
5.3.1	Comparison of single species tests with nAg in conditioned CM and ABC	110
5.3.2	UV-vis characterization of nAg in conditioned CM at exposure concentrations of final accumulation assay	111
5.3.3	Results and discussion of acute accumulation experiments with <i>R. planticola</i> and <i>P. tetraurelia</i>	112
5.3.4	Results and discussion of chronic accumulation experiments with <i>R. planticola</i> and <i>P. tetraurelia</i>	117
6	Activated Sludge Community Tests	121
6.1	Introduction – Activated sludge	121
6.2	Acute toxicity test with activated sludge community	125
6.2.1	Materials and Methods for acute toxicity test with activated sludge	125
6.3	Results and Discussion of acute toxicity test with activated sludge community	136
6.4	Chronic toxicity test with activated sludge community	151
6.4.1	Materials and Methods for chronic toxicity test	151
6.4.2	Results and Discussion of chronic toxicity test	153
7	Conclusions & Prospects	155
8	Summary	161
9	References	163

10	Danksagung	173
	List of figures.....	176
	List of tables.....	178
	Erklärung zur Eröffnung des Promotionsverfahrens	179
	Übereinstimmungserklärung	180
	References to own original publications used in this thesis	181
	Curriculum Vitae	182
	Annex I: Protocol for Axenic Broth for Ciliates (ABC)	i
	ANNEX II: Protocol for 0.25% Cerophyl-Medium (CM)	iii
	ANNEX III: Protocol for R2A Medium	iv
	ANNEX IV: Protocol for Nitrobacter medium 756.c	v
	ANNEX V: Protocol for aniline violet staining	vi

Abbreviations and Symbols

ABC	axenic broth for ciliates
%v/v	volume percent
μL	microliter
μg	microgram
μm	micrometer
Ag ⁺	silver ion
AMO	ammonium monooxygenase
ANOVA	analysis of variance
AOB	ammonia oxidizing bacteria
BOD	biological oxygen demand
CCA	canonical correspondence analysis
CFU	colony forming units
CI	confidence interval
CM	cerophyl medium
COD	chemical oxygen demand
d	day(s)
d _[nm]	diameter in nanometer
DIS	dispersant
DLS	dynamic light scattering
DLVO	Derjaguin Landau Verwey Overbeck
DO	dissolved oxygen
DSMZ	Deutsche Sammlung von Mikroorganismen und Zellkulturen
EC	European commission
EC _x	effect concentration at which x percent of the tested organisms are affected
ERA	Environmental risk assessment
EU	European Union
F/M	food to microorganism ratio
FCVK	fluorometric cell viability kit I
Fig.	figure
g	gram
<i>gt</i>	generation time
h	hour(s)
HAO	hydroxylamine oxidoreductase
ICP-MS	inductively coupled plasma mass spectroscopy
ICP-OES	inductively coupled plasma optical emission spectroscopy
λ _{max}	lambda max (wavelength at peak maximum)
LC _x	lethal concentration at which x percent of the tested organisms are killed
LME	linear mixed effects

LOEC	lowest observed effect concentration
mg	milligram
ML	mixed liquor
mL	milliliter
MLSS	mixed liquor suspended solids
MLVSS	mixed liquor volatile suspended solids
mV	millivolt
nAg	silver nanoparticles
NaHMP	sodium hexa meta phosphate
ND	no data/ not determined
NM	nanomaterial
nm	nanometer
NOB	nitrite oxidizing bacteria
NOEC	no observed effect concentration
NP	nanoparticle
nTiO ₂	Titanium dioxide nanoparticles
OD	optical density
OECD	Organisation for Economic Co-operation and Development
PCA	principal components analysis
PD	pre-dispersion
PdI	polydispersity index
PEC	predicted environmental concentration
PFA	Para formaldehyde
pnc	particle number concentration
PNEC	predicted no effect concentration
PWHM	peak width at half maximum
RCF	relative centrifugal force
ROS	reactive oxygen species
RQ	risk quotient
sac	surface area concentration
SBI	sludge biotic index
SBR	sequencing batch reactor
SEM	Scanning electron microscope
t	time
TGD	technical guidance document
TSS	total suspended solids
TWEEN	Trading name for poly oxyethylene() sorbitan monolaurate
UV-vis	ultraviolet to visible (range of light)
v	division rate
VSS	volatile suspended solids
WWTP	wastewater treatment plant

$\times g$ times gravitational force
 ζ zeta

1 General introduction

Nanomaterials (NM) are generally understood as materials sized less than 100 nanometer (nm) at least in one dimension (Abhilash and Pandey, 2012; Handy et al., 2008). Nanoparticles (NPs) are NMs which are characterized by sizes less than 100 nm in all three dimensions. By means of their diminutive size, they exhibit unique properties compared to their bulk material. The smaller a particle's dimension, the larger is the ratio of surface area to volume, which determines high reactivity. Different shapes (spherical, triangular, cubic, polyhedral or tube shaped) influence the properties of NPs as well. Some types of NPs occur naturally, yet the majority of NPs originate from anthropogenic manufacturing.

On the basis of their special properties, NPs became popular in multifaceted applications. In recent years nanoparticle production and application increased worldwide and will continuously rise in the future (Consumer-Products-Inventory, 2009). So far, no obligation of report exists for production volume and applications of NPs. For this reason, product numbers and NM release into the environment can only be estimated based on voluntary information from manufacturers. In figure 1 estimated numbers for products containing NPs (status: year 2010) are depicted.

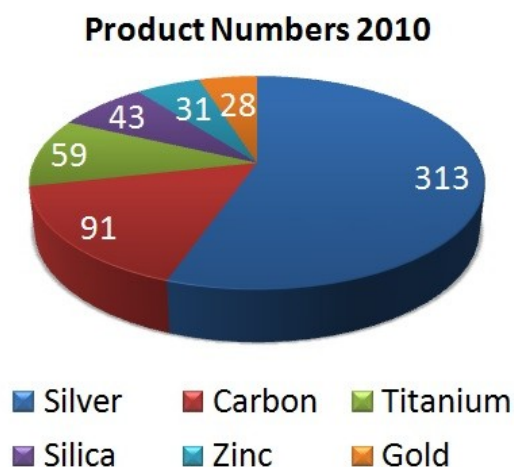


Figure 1: Estimated product numbers containing nanoparticles according to voluntary information from manufacturers (modified after Consumer-Products-Inventory, 2009).

The majority, i.e. 55% of the products in the inventory as shown in figure 1, contain silver nanoparticles (nAg). Since ancient times silver has been valued and used for its antimicrobial properties. The same accounts for the application boom of nAg in younger times. It is used in textiles, kitchen equipment, domestic appliances, medicine, personal care products and many more fields of application. Accordingly, the annual production

worldwide was estimated to be 500 tons in 2008 (Müller and Nowack, 2008) and Hendren et al. (2013) estimated the annual production in the United States only, between 2.8 and 20 tons per year.

From this huge variety of consumer products, nAg is currently and will prospectively be released into sewage and consequently wastewater treatment plants (WWTPs). As nAg is usually applied in consumer products by virtue of its antimicrobial activity, reasonable concern subsists about adverse effects towards activated sludge organisms when exposed to nAg (Blaser et al., 2008; Brar et al., 2010; Jeong et al., 2012). Currently, analytical techniques are not capable of determining the concentration of nAg in complex environmental samples. For this reason modeling approaches were undertaken to estimate environmental concentration in varying compartments, such as sewage, activated sludge and surface water. Blaser et al. (2008) modeled three scenarios of nAg release into wastewater and estimated the predicted environmental concentration (PEC) as 2 µg/L in a minimum scenario, 9 µg/L in intermediate scenario and 18 µg/L in worst case scenario. PECs modeled by Hendren et al. (2013) were estimated for nAg with different types of coatings or stabilizers. For gum arabic or polyvinylpyrrolidone (PVP) coated particles the PECs in activated sludge were estimated at 1.6 and 4.5 µg/kg, respectively. Since suspended solids content in activated sludge rarely exceeds five g/L (Viessmann and Hammer, 2005), the aforementioned concentrations can roughly be converted to 1.6 to 4.5 µg/L, on the basis of water density.

In the 2010 ranking of products containing nanomaterials, titanium dioxide nanoparticles (nTiO₂) take the third position of occurrence with a share of 10%. Although the variety of products containing nTiO₂ seems to be lower than those containing nAg, production volumes are most probably higher. Hendren et al. (2011) estimated the US production volume between 7800 and 38000 tons per year. The major fields of use for nTiO₂ are photocatalytic applications like facade and wood paintings, self cleaning surfaces or cosmetics, especially sunscreen emulsions (Kiser et al., 2009; Müller and Nowack, 2008). TiO₂ is also used as food additive E171, but it remains unclear whether it is nanoscaled. From the known fields of application, release of nTiO₂ to the aquatic environment is certain. Applied in facade painting, nTiO₂ was detected in runoff after rainstorms (Kaegi et al., 2010) and nTiO₂ washed off from sunscreens is obviously inevitable in swimming lakes, and swimming spots of rivers and sea shores. Particles ingested as food additive will be excreted with feces and enter the wastewater systems. Kiser et al. (2009) detected nTiO₂ in the tertiary effluent of a WWTP at concentrations of 10 to 100 µg/L. Müller et al. (2008) estimated the environmental concentration of nTiO₂ in surface waters between 0.7 and 16 µg/L. According to Gottschalk et al. (2009), nTiO₂ is present at the highest concentrations in all environmental compartments, relative to nAg, carbon

nanotubes and zinc oxide nanoparticles. Results of their study indicated concentrations in the sludge of sewage treatment plants accounting for 136 to 211 mg/kg on average, in effluents of WWTPs 1.8 to 4.3 $\mu\text{g/L}$ and 0.002 to 0.015 $\mu\text{g/L}$ in surface waters (Gottschalk et al., 2009).

These data, concerning both nAg and nTiO₂, clearly point out the introduction of NP into the environment via WWTPs and reveal the urgent need for hazard identification.

Characterization of NPs

When dispersed in aqueous matrices, NPs behave differently according to their size and shape dependent properties and the surrounding media. Particles can be singly dispersed, agglomerated or aggregated by different reasons (figure 2).

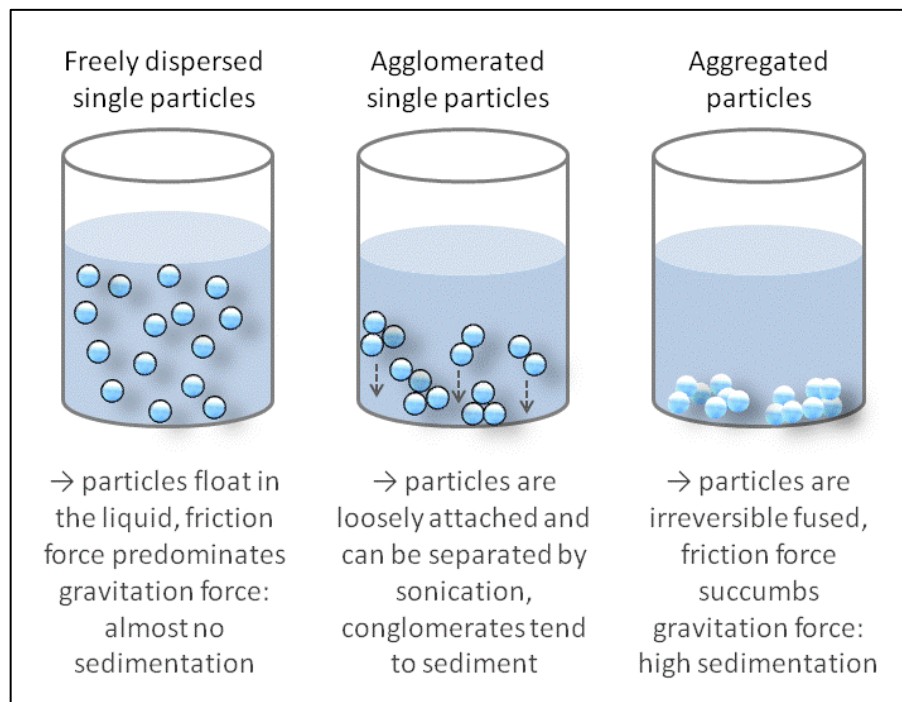


Figure 2: Dispersion, agglomeration and aggregation of particles and their tendency to sediment.

Basically, the diminutive size results in high surface areas, where friction forces become effective and outcompete the gravitational forces. In consequence particles are kept in suspence (fig. 2 left). However, these forces are not the only ones affecting dispersion stability. While electrostatic repulsion is active in dispersions of charged particles, Van-der-Waals forces cause attraction of particles (Badawy et al., 2010; Handy et al., 2008). Loosely attached groups of particles are called agglomerates (fig. 2 mid). If fusion of particle's surfaces occurs, these groups of tightly attached particles are termed aggregates (fig. 2 right; Jiang et al., 2009; Handy et al., 2011). In total, the surface area to

volume ratio is decreased in agglomerates and aggregates and the effect of gravitational forces becomes more intense than on singly dispersed NPs, leading to sedimentation. A constant exposure has to be ensured in toxicity testing, which corresponds to stable dispersions in the case of NPs. As NP behavior depends on the composition of media, the agglomeration and aggregation behavior of the NP under investigation need to be characterized in each test media for the sake of validation of toxicity tests.

Different methods for characterization of NPs are available, which focus on various parameters and each has its respective benefits and drawbacks. Generally, methods can be subdivided into “wet” and “dry”, i.e. NPs can be analyzed in dispersion or as dry powder. Dynamic light scattering (DLS), zeta potential measurement, nanotracking analysis and UV-vis spectroscopy are wet techniques, while electron microscopy is one of the dry techniques. Those methods which were used in the present work, are described in more detail in the following chapter.

Factors influencing toxicity

Toxicity of NPs has been shown to depend on different factors, including the attributes of the surrounding media or environmental conditions and the material's own properties (Beer et al., 2012; Kahru and Dubourguier, 2010). Conditions in sewage as pH, redox potential and ionic strength determine the aggregation and dissolution behavior of nAg (Boverhof and David, 2010; Lee et al., 2012). Ionic silver (Ag^+) is released from nAg by oxidation and can complex with anions, i.e. common ligands (Lee et al., 2012; Maurer-Jones et al., 2013; Xiu et al., 2011). Toxicity is affected by this mechanism through reduction of bioavailability, when complexed Ag precipitates from the surrounding medium, but can potentially be enhanced, if complexation occurs on membranes or cellular compartments of organisms. nAg itself forms complexes with sulphide, cysteine and glutathione (Choi and Hu, 2009). Another parameter potentially lowering the toxicity of nAg is the presence of dissolved organic carbon (Gao et al., 2009). Next to size and shape of the respective NPs, modifications to surfaces and addition of coatings exert influence on the mobility, consistency, reactivity, bioavailability, biocompatibility of NPs and (in the case of nAg) the amount of Ag^+ that is released (Choi et al., 2008; Kim et al., 2011; Kittler et al., 2010b; Pal et al., 2007; Wiesner et al., 2009) and thus influence their toxic potential. As diverse the parameters influencing toxicity, the versatile are the probable modes of action which are thought to provoke toxicity: nAg may attach to the cell membrane, thereby altering cell permeability and collapsing the plasma membrane potential. It affects enzymes, dissipates the proton motive force and finally leads to cell death (Dror-Ehre et al., 2009; Lok et al., 2006; Sondi and Salopek-Sondi, 2004). nAg might further induce the formation of free radicals, which damage the cell membrane (Kim et

al., 2007). Very small nAg were proven to enter cells and likely interact with sulphur- and phosphorus-containing compounds such as DNA (Morones et al., 2005). A key question regarding the toxicity of nAg is, whether it is promoted by the nanoparticle itself or by the Ag^+ released from the surface of nanoparticles (Beer et al., 2012; Kittler et al., 2010a; Kittler et al., 2010b; Xiu et al., 2012). Study results were contradictory here, depending on nanoparticle size, presence of oxygen and genera under investigation (Sotiriou and Pratsinis, 2010; Xiu et al., 2012). The majority of studies regard Ag^+ as toxic component, which interacts with thiol groups and has an impact on DNA replication (Feng et al., 2000; Liao et al., 1997). Accordingly nAg are categorized to bear low risk, although nAg still have to be considered as a source of ions, especially at very small sizes (Sotiriou and Pratsinis, 2010). Different coatings propose a major influence on the dissolution of Ag^+ from nAg (Li and Lenhart, 2012; Tejamaya et al., 2012). Size and coating specific ion release kinetics are of high interest for metallic NM risk assessment and consequently better metrics than mass concentrations are required for reporting toxicity test results for these types of NMs (Abbott and Maynard, 2010; Aitken et al., 2006; Handy et al., 2008; Teeguarden et al., 2007).

In contrast to nAg, ion release from nTiO_2 is minimal for reason of its low solubility in water (Kiser et al., 2009) and therefore negligible in toxicity testing. For this reason, generally experiments are carried out without ionic controls. Commonly toxicity of NMs is thought to be based on oxidative stress (generation of reactive oxygen species, ROS), disruption of cell membranes, disturbance of electron transport and/or entrance into the cell, probably with consequent DNA damaging (Li et al., 2008). Details on the mechanisms driving toxicity of specific NPs are still not fully elucidated, particularly for non ion-releasing NMs like nTiO_2 (Battin et al., 2009). Zheng et al. (2011) studied the effects of nTiO_2 modification on performance and microbial community of activated sludge and revealed impacts on nitrogen removal, especially ammonia oxidation. Abundances of ammonia oxidizing and nitrifying bacteria were shown to be affected by TiO_2 exposure through inhibition of specific enzymes.

NM toxicity testing with relevance to wastewater treatment plants

In Europe, treatment systems utilizing secondary (biological) treatment are predominant in wastewater purification. Aerobic biological treatment with activated sludge is one of the major and most common techniques. Activated sludge is characterized by a diverse community consisting mainly of bacteria and unicellular eukaryotes (ciliates and flagellates). Bacteria play a major role in degradation of organic matter including organic pollutants in wastewater and are commonly arranged in flocs in order to be protected from precipitation and predation. Ciliates are part of the predator community and

responsible for purification of water from freely dispersed bacteria, including potentially pathogenic microbes (Curds, 1982).

Risk is commonly defined as the probability of the incidence of harm (Fent, 2013). Thus, environmental risk of a certain material or substance is the probability of incidence of harm towards the environment. It is derived from the hazard posed by the material towards biota and their exposure in the environment (risk assessment). Environmental agencies realized the need for hazard identification and environmental risk assessment (ERA) for nanomaterials (NMs) and came to the conclusion, that to date no generally applicable guideline for nanomaterial hazard identification (European-comission, 2012) exists. Consequently, a case-by-case approach for NM ERA throughout the period of pending development of NM-suitable methods was recommended. According to technical guidance documents (Technical-Guidance-Document, 2003; hereafter referred to as TGD 2003) the base set of standard test organisms for ERA in aquatic environments are algae, cladocera (daphnids), fish and bacteria. Except for bacteria, these organisms are not meaningful as proxy species for activated sludge because they are not abundant. This fact represents an obvious contrast to the demand of case-by-case approaches.

Regarding relevant organisms, especially bacteria are considered to be affected by their degradation activities, for which reason nitrification or respiration inhibition tests have been established and documented in respective OECD guidelines for hazard identification and applied for NM toxicity testing (Hu et al., 2002; Hu et al., 2004; Jeong et al., 2012; Liang et al., 2010; Zheng et al., 2011). Results, especially for nAg, were contradictory depending on the genera and conditions used for the respective experiments and lead to different conclusions concerning the risk posed by nAg towards the functionality of WWTPs (Jeong et al., 2012; Liang et al., 2010). New test approaches are required due to an evident lack of standardized methods evaluating risk by means of WWTP specific organisms. Special emphasis should be placed on protozoa, especially ciliates, for the reason of their role in removal of bacteria from effluent waters. In this regard it is interesting, if NPs affect ciliates indirectly by inhibition of bacterial growth leading to starvation of the protozoa, or directly by contamination of bacterial food or other straight effects e.g. on cell membrane integrity. Finally, effects of NPs on functionality and performance of WWTP ecology are a matter of high interest.

Thesis outline

The aim of this work was to develop toxicity test methods, considering WWTP specific organisms and compartment specific environmental concentrations. A graphical outline of aspects in this study is shown in figure 3 (page 7): as a first step, single species tests, which focus on the susceptibility of bacteria (*Raoultella planticola*, *Hyphomicrobium sp.*

and *Nitrobacter vulgaris*) and ciliates (*Paramecium tetraurelia*) towards nAg, are developed. In a second step, indirect effects by accumulation of nAg in simple food chains are investigated. At the highest tier, effects of nAg on the WWTP (activated sludge) community are determined. Results from each toxicity test are implemented into environmental risk assessment.

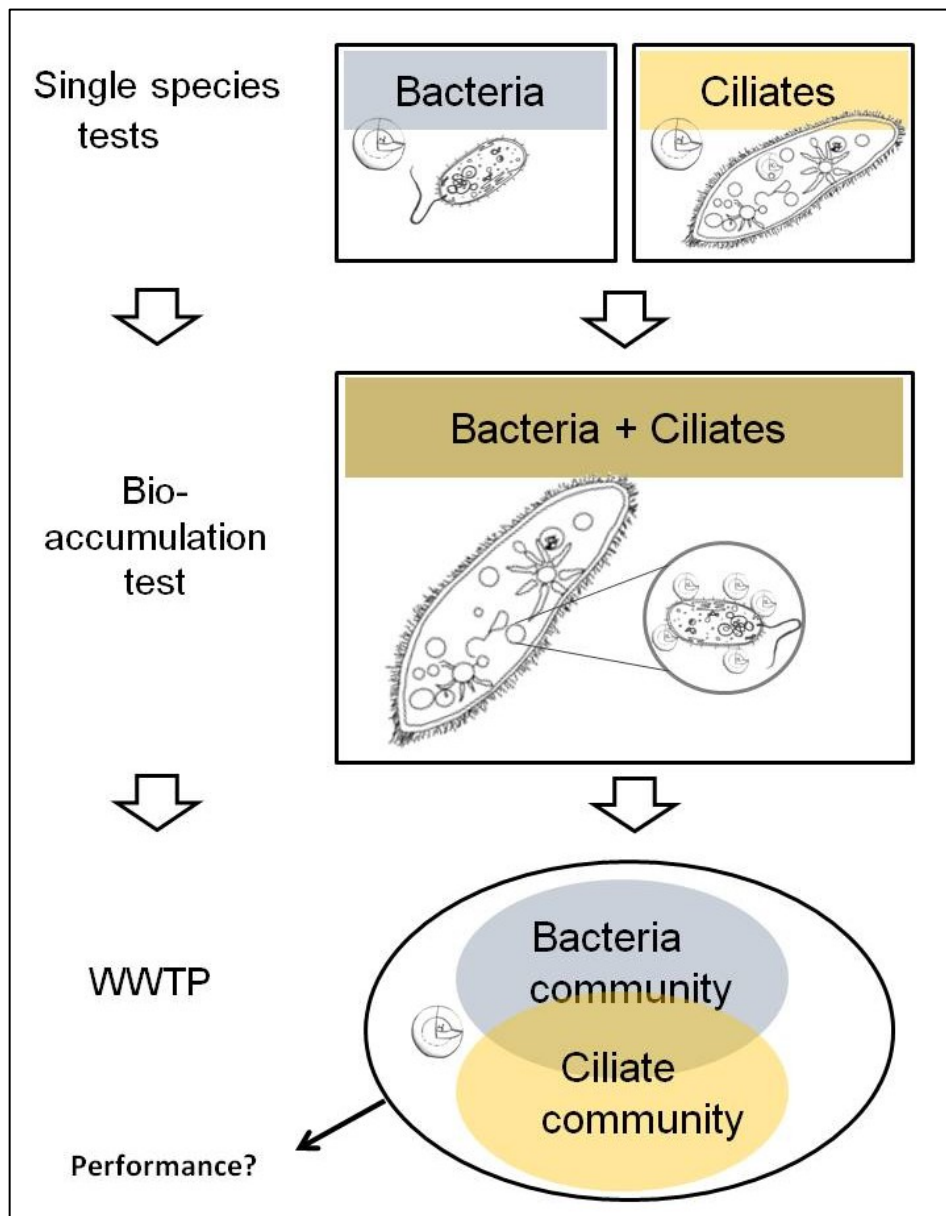


Figure 3: Flowchart of stepwise approach for studying effects of silver nanoparticles on activated sludge organisms.

The established single species test with ciliates is adapted to toxicity testing of nTiO₂. Besides the acute test, a chronic test is performed and influence of UV – light is considered to account for the photocatalytic activity of anatase modification of nTiO₂.

The following chapter (chapter 2) describes properties of nanoparticles and characterization methods which apply for several of the toxicity tests conducted in this work. Experiment specific details are given in respective sections. Further chapters refer to single species tests on ciliates (chapter 3) and bacteria (chapter 4), accumulation experiments (chapter 5) and activated sludge community tests (chapter 6). Finally, conclusions (chapter 7) and summary (chapter 8) are formulated according to the results described in the above mentioned chapters.

Within this thesis, the following hypotheses are explored:

1. The sensitivity towards nAg exposure differs between the separately tested species and organism groups (chapter 3 and 4).
2. The determined toxic effects of nAg are triggered by ions released from particles (chapter 3 and 4).
3. nTiO₂ exhibits toxic effects on *P. tetraurelia*, which are enhanced by photocatalysis through UV radiation (chapter 3).
4. Different uptake pathways in *Paramecium tetraurelia* lead to different effect concentrations of nAg in acute toxicity tests (chapter 3 and 5).
5. nAg affect the community composition and abundance of organisms from activated sludge, probably leading to deterioration of wastewater purification processes (chapter 6).

2 Nanomaterials

2.1 Silver nanoparticles

2.1.1 Properties of silver nanoparticles

Nanosilver (nAg) dispersion NM-300K (LGC standards material) was purchased from Mercator GmbH (Salzwedel, Germany) as aqueous dispersion with 4% polyoxyethylene (20) sorbitan mono-laurat (TWEEN® 20) and 4 % of polyoxyethylene glycerol trioleate. The total Ag content was 5 to 25 (+/- 0.5) wt % and Ag⁺ content was less than 0.2 (+/- 0.05) wt % according to the manufacturer. According to own analyses by inductively coupled plasma optical emission spectroscopy (ICP-OES)¹ of NM-300K stock dispersion (for details see below), total silver content of the dispersion was 121.9 g/L which corresponds to 12.2 wt %. The Ag⁺ fraction was 5.14 g/L equaling 0.5 wt % of NM-300K dispersion. The resulting nAg content was calculated with 116.7 g/L (11.7 wt %) which corresponds to 95.8% of total silver content. These data were used to establish predispersions in water to achieve respective nominal concentrations for toxicity tests.

The material data sheet describes the nanoparticles as spherical and less than 20 nm in size. Dispersant (NM-300K DIS) was purchased separately to realize a dispersant control in toxicity tests described below.

2.1.2 Characterization methods for nAg

UV-vis spectroscopy is a method for determining mean particle size and shape of primary particles in media. The basic principle of UV-vis characterization is the determination of the specific plasmon absorption band of nanosilver (Hassellöv et al., 2008; Petit et al., 1993) whichs properties depend on primary particle shape and size. Spherical nAg display a distinct peak at approximately 400 nm (Hassellöv et al., 2008; Lin and Sun, 2011; Petit et al., 1993), while nanorods or triangles show two absorption peaks at different wavelengths (Hassellöv et al., 2008; Van Dong et al., 2012). Conclusions about the dispersion stability are drawn from peak broadening and red shifting, as particles agglomerate (Hassellöv et al., 2008; Lin and Sun, 2011). Coatings however, can affect the location of absorption peak, for example TWEEN stabilized nAg have red shifted absorption maxima compared to uncoated nAg (Li and Lenhart, 2012). Using two regression functions on data reviewed by Solomon et al. (2007),

¹ conducted at TU Dresden, Chair of soil resources and land use, Dr. Thomas Klinger, Tharandt

nanoparticle size distribution as diameter ($d_{[nm]}$) is calculated according to measured peak maxima (λ_{max} ; equation 1) and peak width at half maximum (PWHM; equation 2)

$$\text{particle size 1 } d_{[nm]} = 1.526 * \lambda_{max[nm]} - 598.525$$

equation 1

$$\text{particle size 2 } d_{[nm]} = 0.682 * PWHM_{[nm]} - 29$$

equation 2

Dynamic light scattering (DLS) is a method to determine the size distribution of NPs in media, i.e. in dispersion. The dispersion is irradiated with laser light. Particles in dispersion scatter the incident light in dependence of their size (figure 4).

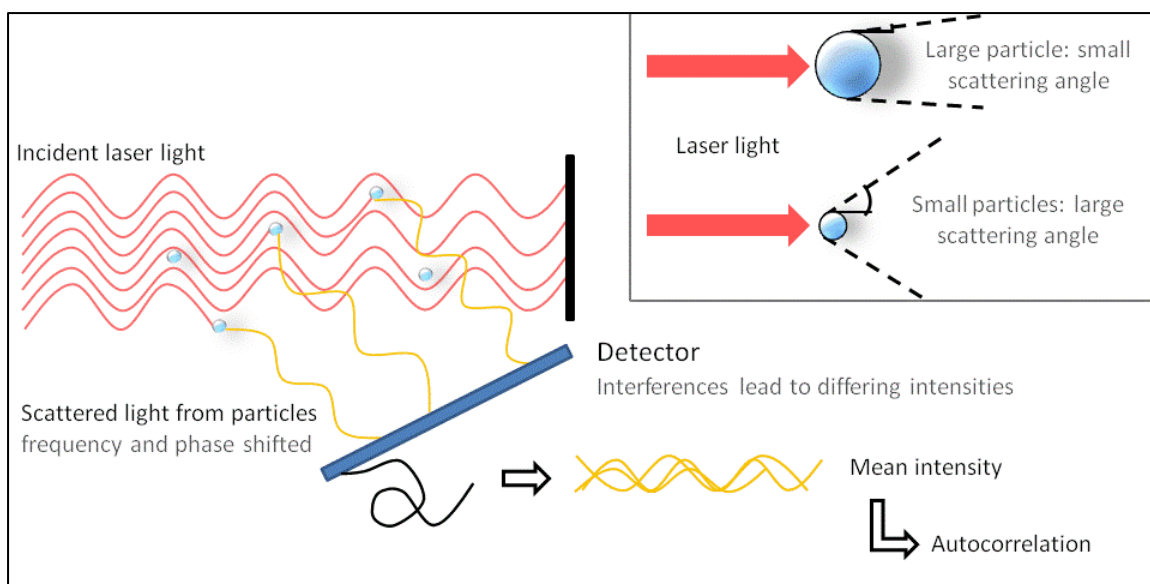


Figure 4: Principle of DLS. Modified, from R. Nitzsche². Based on scattering angles of differently sized particles (upper right corner) incident laser light is scattered, resulting frequency and phase shifts are detected and mean intensity is derived. Mean particle sizes are inferred from an autocorrelation function.

Larger particles hold smaller scattering angles than small particles. A detector records the intensity of backscattered light at an angle of 90 or 173 degrees. The measured

² R. Nitzsche (Malvern Instruments GmbH) April 2010: NETZSCH Praxistag, TU Berlin Fachgebiet Verfahrenstechnik: Partikelmesstechnik, Partikelcharakterisierung

light intensity undulations are averaged by interferences (frequency and phase shifts), and hydrodynamic diameters of the particles are derived from an autocorrelation function (Jiang et al., 2009).

Hydrodynamic diameters of nAg were determined by DLS on a Zetasizer NanoZS (Malvern, Westborough, USA)³. Universal parameters for nAg characterization were refractive index of Ag (0.54), number of runs (10) and duration per run (10 s). Experiment specific details are given in the respective toxicity test chapters.

Zeta potential measurements characterize the dispersion status of charged NPs in dispersion, e.g. silver, gold or titanium dioxide nanoparticles. On charged particle surfaces, counter ions of the surface charge accumulate (figure 5, Zeta potential), generating an electrostatic double layer according to Derjaguin, Landau, Verwey and Overbeek (DLVO) theory (Badawy et al., 2010; Handy et al., 2008).

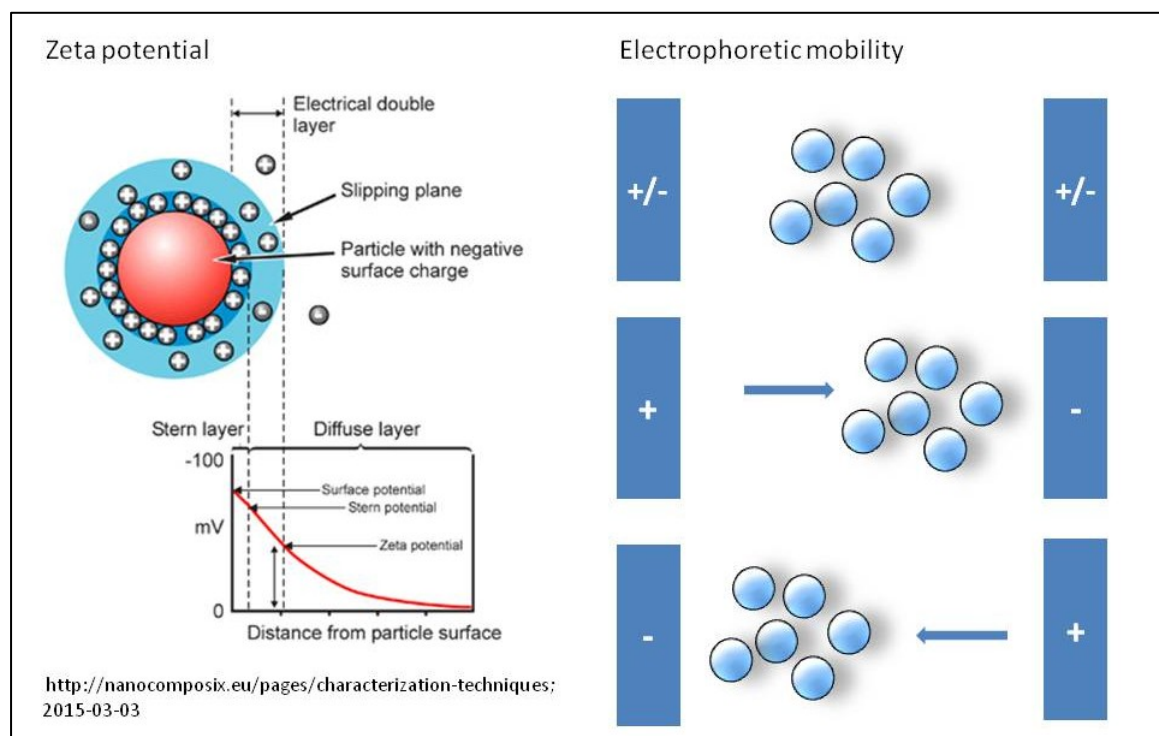


Figure 5: Illustration of zeta potential and electrophoretic mobility. Left side depicts composition of electrical double layers on charged particle surfaces with respective potentials. Right side depicts movement of positively charged particles in the alternating electric field, as used for determination of electrophoretic mobility.

³ used at TU Dresden, Chair of water supply engineering.

It consists of one layer densely packed ions directly connected to the charged surface (stern layer) and an outward layer with decreasing counter ion density, termed slipping plane. At the edge of the slipping plane, at the border to equilibrated charge in the surrounding liquid, the zeta potential is determined.

It is derived from the electrophoretic mobility (figure 5, page 11; electrophoretic mobility) of a charged particle in an alternating electric field (Jiang et al., 2009). At zeta potentials larger or equal ± 30 millivolt (mV), attraction forces between particles even the occurring repulsion forces and thus dispersions are considered steady. The closer the zeta potential is to the point of zero charge (0 mV), the more attraction forces dominate between particles, aggregates or agglomerates form and sediment. Consequently the dispersion becomes unstable. The point of zero charge is depending on pH and organic matter in surrounding media (Handy et al., 2008). Agglomeration tendency of the dispersed nAg was derived from zeta potential measures on a Zetasizer NanoZS (Malvern, Westborough, USA) in all test concentrations.

Conventional **scanning electron microscopy** (SEM) is a dry technique, which can be applied for NP characterization and allocation. In the microscopic picture two-dimensional size measures are enabled. Samples need to be dried prior to analysis and therefore are vulnerable to produce artifacts like agglomeration. Further, charge effects can influence the results. Still the technique is appropriate for primary particle size determination. SEM was carried out on a Zeiss DSM 982 Gemini⁴. Details on sample preparation are given in the respective toxicity test chapters.

Next to the method for characterization of nanoparticle shape, size and dispersion status, exposure concentrations need to be validated. **Inductively coupled plasma optical emission spectroscopy** (ICP-OES) is a common method for sample analysis. Total Ag and Ag⁺ were analyzed separately, after partitioning by centrifugation. Liquid samples at volumes of 10 to 12 mL were digested by adding few drops of 69% nitric acid (HNO₃) and burned in argon plasma of the ICP-OES device⁵. Atomic emission was detected by a CCD camera and correlated to the silver content according to calibration standards. In table 1 all characterization methods applied for nAg are summarized.

⁴ at TU Dresden, research group mechanical process engineering, Prof. Dr. Michael Stintz

⁵ Samples processed at Helmholtz centre for environmental research, Magdeburg, Dr. Norbert Scheibe and Dr. Wolf von Tümpling.

Table 1: Overview on characterization methods applied for identification of nAg (and Ag⁺) properties in respective media.

Method	Parameter determined	Sample property
UV-vis spectroscopy	mean diameter, dispersion status	wet
DLS	hydrodynamic diameter	wet
Zeta potential	electrophoretic mobility, dispersion stability	wet
SEM	primary particle size, dispersion status (prone to artifacts)	dry (dispersion in medium dried)
ICP-OES	mass concentration	wet, diluted

Currently, **environmental risk assessment** (ERA) of nanomaterials is carried out under REACH (Registration, Evaluation, Authorisation and Restriction of Chemicals) directive of the European Community Regulation on chemicals and their safe use. Accordingly, a risk quotient (RQ) is calculated as predicted environmental concentration (PEC) divided by predicted no effect concentration (PNEC). Using mass concentrations to compare toxicity data for ERA is not feasible for engineered nanomaterials (ENMs). For differing particles, especially those releasing toxic ions, metrics like particle number concentration per litre (pnc) and surface area concentration (sac) need to be applied (Teeguarden et al., 2007). These consider agglomeration behavior, probability to encounter test organisms and ion release into media. At the same mass concentration, pnc differ dramatically due to particle size, resulting in different sac values. More ions are released into media with increasing sac until a specific equilibrium is reached (Kittler et al., 2010a). The threshold concentration of this equilibrium and dissolution rate are driven by several factors (dissolved oxygen concentration, particle concentration, pH, temperature) and can be further influenced by nanoparticle coatings, ingredients of media or test organisms (Bilberg et al., 2012; Kittler et al., 2010a; Liu and Hurt, 2010; Marambio-Jones and Hoek, 2010; Sotiriou and Pratsinis, 2010; Xiu et al., 2012).

If mean particle size and concentration in exposure dispersion was available from analyses, effect concentrations were converted to pnc and sac taking into account the density of silver, according to equation 3 and equation 4 according to Teeguarden et al. (2007):

$$pnc = \frac{c}{\rho \times V}$$

equation 3

$$sac = A \times pnc$$

equation 4

where c is the determined concentration of nAg in the respective sample [g/L]. ρ is the density of bulk silver (10.5 g/cm³), V is the volume of the particles [cm³/particle] calculated from the cubic of the mean particle diameter [cm] in the sample according to UV-vis spectroscopy, multiplied with $1/6 \pi$. A is the surface area per particle [cm²/particle], calculated from the square of the mean particle diameters [cm] in the samples multiplied with π .

2.2 Titaniumdioxide Nanoparticles

2.2.1 Properties of titanium dioxide nanoparticles

Titanium dioxide nanoparticles ($n\text{TiO}_2$) are known to exist in three crystalline forms: anatase (tetragonal), rutile (tetragonal) and brookite (orthorhombic). Studies suggest that anatase and rutile have different photocatalytic properties, with anatase possessing the better combination of photoactivity and photostability, the rutile form is less photoactive (Clemente et al., 2012; Porkodi and Arokiamary, 2007). $n\text{TiO}_2$ is insoluble in water, chloric acid, nitric acid and ethanol, but is soluble in concentrated and heated sulfuric, hydrogen fluoride and alkaline media (Clemente et al., 2012).

$n\text{TiO}_2$ for toxicity experiments were delivered as dry powder "Hombikat UV100" (LGC standards Material NM101), bottled by Fraunhofer IME, Germany and provided by the federal environmental agency (UBA), Germany. The chemical composition as analyzed by Fraunhofer IME was given with 91.7% TiO_2 as uncoated anatase modification. Primary particle size was 6 to 8 nm and specific surface area according to BET was approximately 320 m^2/g . Stray ion level was low.

2.2.2 Characterization of $n\text{TiO}_2$ in test media

In order to ensure constant exposure in toxicity testing, dispersion status must be analyzed as described before (see section 1 General introduction, Characterization of NM). $n\text{TiO}_2$ were used in single species tests with ciliates exclusively in this work (see chapter 3.4). Hence characterization was undertaken in filtrated axenic broth for ciliates (ABC) exclusively, utilizing DLS and zeta potential measures. Details on the background of these techniques are given in the silver nanoparticle section above (2.1.2, page 9 ff.). Parameters for DLS using a Zetasizer Nano ZS along with clear disposable zeta cells (Malvern, Westborough, USA) were set as follows. Viscosity of the media was 1.00 cP, refractive index of media was 1.272, refractive index of $n\text{TiO}_2$ was 2.7, Absorption was 0.2, number of runs per sample were 10 and duration per run 10 seconds.

UV-vis spectroscopy is useable for determining optical properties of $n\text{TiO}_2$, however it is not possible to deduce particle size of this material by means of the method. Instead, the absorption band is determined, which is used to calculate the band gap value. This information is useful for deducing the modification of $n\text{TiO}_2$ (Dhandapani et al., 2012) and inferring photocatalytic activity for respective applications. For dispersion characterization in ecotoxicology it is not valuable. For this reason UV-vis spectroscopy was not applied for $n\text{TiO}_2$ analysis.

3 Single Species tests with Ciliates

3.1 Introduction - Ciliates

Ciliates are part of the predator community and responsible for purification of water from freely dispersed bacteria, including potentially pathogenic microbes (Curds, 1982). So far, predators as major contributors to water purification within the community were almost disregarded, although methods are available to determine sludge quality from community structure of unicellular eukaryotes (Madoni, 1994).

In this chapter a novel single species test system for acute toxicity of NM on ciliates relevant in European WWTP is reported. As a representative species for filter feeders in WWTP, *Paramecium tetraurelia* was used in axenic culture.

Paramecia (Alveolata, Oligohymenophorea, Peniculia) are a genera of the ciliates, belonging to the protozoa, unicellular eukaryotes. Ciliates are characterized by dimorphism of nuclei and the possession of cilia.

Nuclear dimorphism denotes the possession of both somatic and generative nuclei. The macronucleus (somatic nucleus) operates the cellular metabolism while the micronucleus (generative nucleus) is distinguished by retaining the cells genetic information. The number of micronuclei varies interspecifically, but loss of micronuclei in an organism is not lethal (Wichtermann, 1986).

Paramecium aurelia (MÜLLER 1773) is a syngen complex with 14 types (*P. primaurelia*, *P. biaurelia*, *P. triaurelia*, *P. tetraurelia*, and so on). They are distinguished by mating type reaction and isoenzym patterns (Sonneborn, 1975). Abundance of *P. aurelia* is cosmopolitan and all-seasonal. Mainly it occurs in the detritus and rarely in the pelagial of standing waters and in running waters (Berger et al., 1997). The ecological demands of the syngens differ sometimes even intraspecifically (Nyberg and Bishop, 1983). In the *Paramecium aurelia* – complex, three modes of reproduction occur, i.e. binary fission, autogamy and conjugation. The asexual binary fission is the most frequently appearing mode of reproduction especially in batch cultures, however, clonal age is limited species specifically. Thus, to prevent cell ageing and death, sexual reproduction by conjugation or autogamy is necessary (Görtz, 1988; Wichtermann, 1986).

Generation time depends on temperature and food quantity and quality, amongst others. For *Paramecium* grown on *Enterobacter aerogenes* as food source and a cultivation temperature of 20 °C, generation time is 17.3 h (Finlay, 1977). Cell size is

another influencing parameter: small ciliates have generation times of 2 to 4 hours, larger ciliates reduplicate in 10 to 30 h (Fenchel, 1980a). Because of these differences in growth kinetics, it is important to determine the behavior of organisms under investigation at experimental conditions, realized in this thesis as described in the following section (3.2).

The eponymous attribute of ciliates are the cilia which cover the whole cell surface of paramecia. Undulating beats of these cilia enable the cell's locomotion and phagocytosis. The latter is a manner of food intake of unicellular filter feeders. The beat of cilia generates a current of surrounding water and contained food particles in direction of the cytostome (cell mouth). Food particles are generally composed of bacteria and small cells. Uptake of particles into the ciliate cell depends on their size and shape, but not on food quality (Fenchel, 1980b; Finlay and Fenchel, 1996). Next to the uptake of particles by phagocytosis, liquids may be taken up by pinocytosis. This pathway plays a major role in the single species test described below, due to the use of axenic medium.

Undigestible components, waste products and excess water are excreted through the cytoproct and by means of contractile vacuoles.

In the experiments described below, *Paramecium tetraurelia* was used, because it is the only ciliate species which is relevant in European activated sludge and also available in axenic culture, as required for single species tests.

3.2 Growth kinetics under experimental conditions for *P. tetraurelia*

3.2.1 Materials and Methods for *P. tetraurelia* growth kinetics

Methods for growth kinetics were performed according to Leps (2011) and are described in detail subsequently.

Cultivation of axenic Paramecium tetraurelia

Axenic cultures of *P. tetraurelia* strain 7S (SONNEBORN 1975), were kindly provided by Dr. Eva-Maria Ladenburger, University of Konstanz, Germany. Axenic broth for ciliates (ABC) was prepared according to the protocol for axenic medium of (Soldo and Van Wagtendonk, 1969), modified after Kaneshiro et al. (1979) (see Annex I: Protocol for Axenic Broth for Ciliates (ABC), page i). Stock cell cultures were maintained in heat sterilized (180 °C) 10 mL test glasses covered with Kapsenberg caps in the dark at 22 ± 1°C. Once a week, 4.5 mL of fresh medium were inoculated with 0.5 mL of seven day old cell culture under sterile conditions.

Analysis of growth kinetics

Growth kinetics were studied testing two endpoints as applied in later toxicity tests, i.e. cell number by counting and viability by application of a fluorometric viability kit as described below.

In a first experiment, unfiltered ABC was used to determine stock culture growth kinetics covering the whole life of a batch culture. In a second experiment filtered ABC was tested against unfiltered ABC for growth kinetics of *P. tetraurelia* over a period of four days. ABC was filtered using syringe connected cellulose acetate PES filters (TPP, Switzerland, pore sizes 0.45 µm and 0.22 µm subsequently) for preparation of this experiment.

For determination of cell number in all experiments, an aliquot of 500 µL from stock culture was fixed by addition of Bouin's solution (Bouin, 1897) to a total concentration of 1%, for cell counting. Cell counting was carried out utilizing a modified 24-well plate as counting chamber (figure 6).

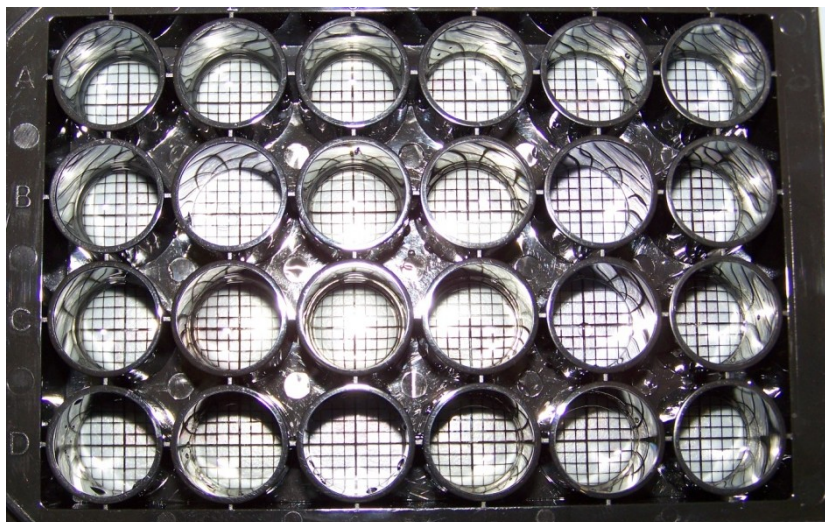


Figure 6: Modified 24-well plate as counting chamber. Transparent bottom of the plate was supplied with a counting grid.

Defined volumes (15 to 50 μL) of fixed cells were mixed thoroughly and dispersed in deionized H_2O (Milli-Q Direct8, Millipore, Merck KGaA, Darmstadt, Germany), supplied with liquid detergent, into the wells at 3 to 5 replicates. Whole sample volume per each well was analyzed with a stereomicroscope (SZX2-ILLD, Olympus, Tokyo, Japan) and mean cell number per volume was determined from all replicates. A volume of 10 mL experimental culture with cell density adjusted to 500 or 1 000 cells was prepared from stock culture with determined cell density using filtrated or unfiltrated ABC, respectively. For each day of experiment duration including day zero, 5 wells of a 96-well plate (pure grade S, transparent F-bottom, Brand GmbH & CO KG, Wertheim, Germany) were filled with 100 μL of experimental culture and 3 wells with respective medium as blank. From wells for day zero, all replicates were drawn as sample for determination of real cell number in the wells at the beginning of the experiment. In 0.5 mL reaction tubes (Eppendorf, Hamburg, Germany) samples were left for settling of dead cells. From the supernatant containing living cells, 65 μL were transferred to a fresh 0.5 mL reaction tube filled with 2 μL of Bouin solution for fixation. Cell counting was carried out as described before. 8 hours after preparation of the experimental culture, 10 μL of fluorometric cell viability kit I; (FCVK, Promo Cell GmbH, Heidelberg, Germany) were added to each well prepared for day 1 of the growth curve on the 96-well plate for cell viability determination. The plate was incubated for 16 h at 22°C in the dark. After this time, fluorescence was measured in the respective wells using a microplate reader (Polarion plate reader, Tecan Group Ltd., Switzerland) with three flashes for excitation at 545 nm and emission at 595 nm and a gain of 55. Blank values were subtracted from measured fluorescence in samples for determining relative

fluorescence. Cell number was subsequently counted as described above. Throughout the whole experiment FCVK was added daily at the same time as on day zero to respective wells and fluorescence and cell numbers were analyzed 16 h later.

Division rate v and generation time gt were calculated from viability and cell count data according to equation 5 and 6:

$$gt = \frac{1}{v}$$

equation 5

$$v = \frac{n}{t}$$

equation 6

where t is the age of the culture in hours ($t = t_{\text{end}} - t_{\text{beginning}}$) and n the change of cell number determined as

$$n = \frac{\frac{N}{N_{t_0}}}{\lg 2}$$

equation 7

with N being the cell number or relative fluorescence after time t and N_{t_0} the cell number at the beginning of the test, or relative fluorescence at first measure time.

3.2.2 Results and Discussion for *P. tetraurelia* growth kinetics

Growth kinetics were determined under culture maintenance and experimental conditions using cell density and viability as endpoints. In figure 7 growth curves for a batch culture of *P. tetraurelia* in ABC over a period of 10 days are shown.

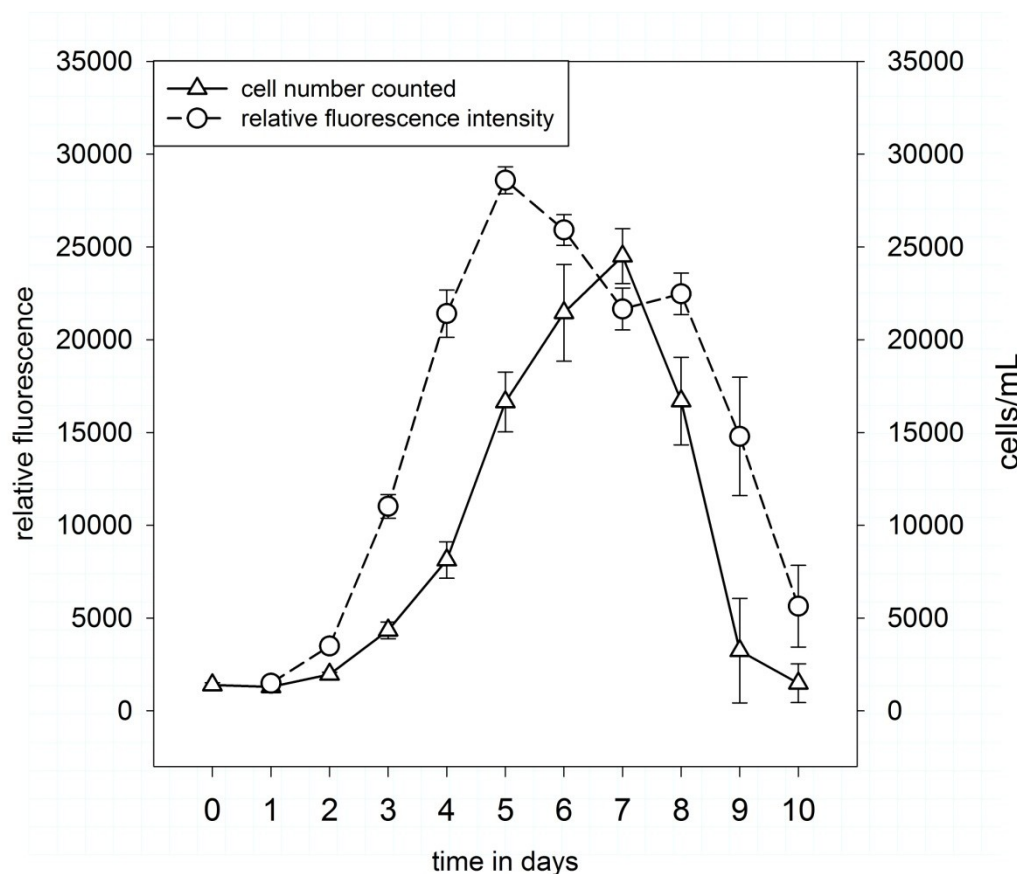


Figure 7: Ten days growth curves of *P. tetraurelia* batch culture in unfiltered ABC. Endpoints viability and cell number were investigated. Error bars indicate standard error of means.

Exponential growth begins after one day and lasts until the fourth (according to viability data) or fifth day (cell number), respectively. Stationary phase cannot be determined clearly, while mortality sets in after at least seven to eight days. Viability seems to be the more sensitive endpoint, as growth phases commenced earlier for fluorescence than for cell number. The trends exhibited by these growth curves are typical for batch cultures, where nutrient excess at the beginning stimulates division of cells. Nutrient uptake is enhanced as cells grow exponentially. Maximum capacity is reached as nutrients or oxygen become limited, or inhibiting metabolites accumulate; leading to starvation and finally extinction of the cell culture (Fuchs, 2007).

For determination of growth kinetic phases under toxicity test conditions, filtrated ABC was tested against unfiltered ABC throughout exponential growth (four days) of *P. tetraurelia* for both endpoints. In figure 8 results are plotted as growth curves. Triangles represent data from cell counting while circles refer to viability data. Filled symbols embody data from cells in filtrated medium, while open symbols display cells in unfiltered ABC.

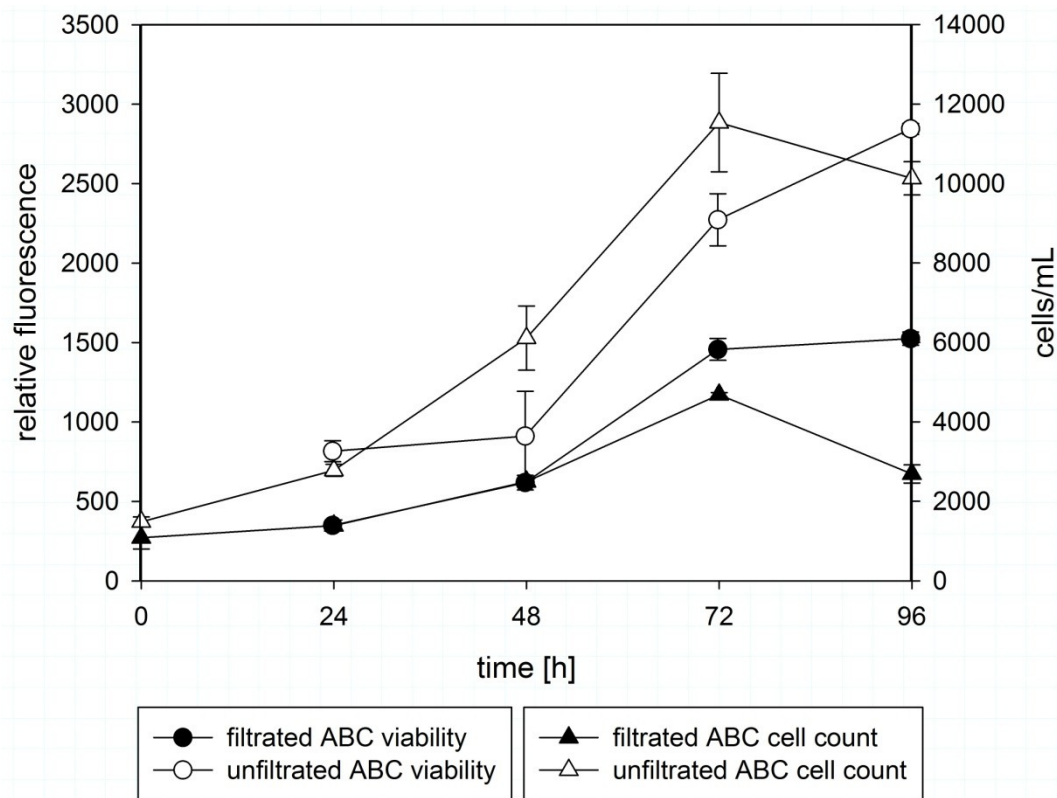


Figure 8: Growth of *P. tetraurelia* in unfiltered (open symbols) and filtrated (filled symbols) ABC for endpoints viability (circles, left y-axis) and cell number (triangles, right y-axis) over 96 hours. Note differing scales of y-axes. Error bars indicate standard deviations.

Total cell number and fluorescence were lower in filtrated ABC compared to unfiltered ABC. Growth was decreased most probably to lesser nutrient content in the filtrated media due to removal of larger particles that could be ingested by the cells via phagocytosis. However, both methods display the same pattern over time for the respective medium.

Based on mean cell numbers per sampling time, for filtrated medium division rate ν was 0.037/h between day one and three. Generation time gt was calculated with 27 h. For unfiltered ABC, ν was 0.043/h and $gt = 23.3$ h. Mean initial cell density was slightly higher in the unfiltered ABC, but no statistical significant difference was detected between both assays (t-test, $P = 0.234$). It can hence be assumed that cell growth is faster in unfiltered medium than in the filtrated which is not an effect of initial cell density, although the power of the conducted t-test was low (0.106).

The incubation time for *P. tetraurelia* cultures prior to toxicity tests was set to 3 days in filtrated ABC, to ensure exponential growth of the culture, based on the growth kinetic results presented in this section.

3.3 Toxicity tests with *P. tetraurelia* and nAg

3.3.1 Materials and Methods for *P. tetraurelia* toxicity tests with nAg

Axenic cultures maintained as described in the previous section (3.2), were used for toxicity tests. Some methods for toxicity testing were performed according to Leps (2011).

Chemicals

Preparation of stock dispersions/solutions and exposure dispersions/solutions

For all dispersion and solution preparations, 10 and 50 mL centrifuge tubes (TPP, Switzerland) were used.

For characterization of the nanomaterials and for toxicity test preparation, a 1 g/L and a 1.5 g/L stock dispersion was established from NM-300K dispersion using sterile HPLC-grade water (Chromanorm for HPLC, VWR Int., France). A corresponding concentration was used for stock solution of the dispersant NM-300K DIS (17% v/v) established with HPLC-grade water (Carl Roth GmbH + Co. KG, Karlsruhe, Deutschland) and used as dispersant control in toxicity tests.

Silver nitrate (AgNO_3) was utilized as exposure treatment for ionic silver (Ag^+) in toxicity tests. A 1 g/L AgNO_3 stock solution was prepared from silver nitrate ($\geq 99, 9\%$, p.a., Carl Roth GmbH + Co. KG, Karlsruhe, Deutschland) in sterile HPLC-grade water.

ABC was filtrated using syringe connected cellulose acetate PES filters (TPP, Switzerland, pore sizes 0.45 μm and 0.22 μm subsequently) and used in all experiments, i.e. characterization and toxicity tests, nanomaterial dispersions and precultures. Dissolved oxygen concentration in the filtrated medium was analyzed with an oxygen meter (WTW Oxi 340i).

For nanoparticle characterization, nAg stock dispersions were diluted to the respective concentrations with filtrated ABC.

For toxicity tests, predispersions were prepared from stock dispersions/solutions with filtrated ABC at 11-fold concentration of nominal exposure concentration, to compensate for dilution by cell culture added in toxicity tests. For samples with final

nAg concentrations of seven to 60 mg/L, the 1 g/L stock dispersion was used, for the highest concentration (120 mg/L) the 1.5 g/L stock was used.

Final nominal nAg and Ag⁺ concentrations in the toxicity tests are depicted in table 4 (section 3.3.2 Results and discussion of nAg toxicity tests with *P. tetraurelia*, page 35), where more experimental details are summarized.

Characterization of silver nanoparticles in exposure media

Size distribution of nAg in exposure media was analyzed by different methods. Filtrated ABC served as blank. Nanoparticle tracking analysis was rejected due to high background scattering.

UV-vis spectra were recorded over wavelengths from 250 to 600 nm (Hitachi U-2000, Hitachi, Nissei Sangyo GmbH, Düsseldorf, Deutschland) from three replicates of each test concentration of nAg. Nanoparticle size distribution as diameter (d) was calculated according to measured peak maxima and PWHM (see page 10).

Hydrodynamic diameters of nAg were determined by dynamic light scattering (DLS). Three replicates of each test concentration were analyzed as described in chapter 2.1.2. Agglomeration tendency of the dispersed nAg was derived from zeta potential measures in all test concentrations. Dispersant refractive index was 1.272 and dispersant absorption was 0.3, the dielectric constant was set to 80.

nAg size distribution was also determined by scanning electron microscopy (SEM) (Zeiss DSM 982 Gemini) and exposed cells were examined for potentially adhering nanoparticles on the cell surface. Sample preparation involved a vacuum filtration step, to deposit particulate material on a filter membrane (pore size 50 nm). Membranes were mounted on studs and sputtered with a 1 nm layer of platinum.

The pH of the different nanoparticle dispersions was measured before and after toxicity tests using a WTW pH 3110 equipped with WTW Sentix MicB electrode.

Analytics

Fractions of total Ag and Ag⁺ in NM-300K dispersion were analyzed using ICP-OES. Total silver content of the NM-300K dispersion was analyzed in two dilutions with de-ionized water on a SPECTRO CirosCCD ICP-Spectrometer (SPECTRO Analytical Instruments GmbH, Kleve). A sub-sample of the diluted NM-300K dispersion was centrifuged in Eppendorf cups (relative centrifugal force (RCF): 23,143 x g; 99 min; room temperature; Eppendorf 5403 centrifuge) and Ag⁺ content was analyzed in the supernatant. The difference between measured total Ag and Ag⁺ content is the nAg

fraction. The resulting data were used to establish predispersions in water to achieve respective nominal concentrations for toxicity tests, as depicted in table 4 (page 35).

Toxicity tests

All tests were conducted under sterile conditions, at 22°C and incubation in the dark.

Tested nominal nAg concentrations were between 7.5 and 120 mg/L resulting in nominal Ag⁺ concentrations between 0.35 and 5.64 mg/L with a spacing factor of 2, respectively. The tested nominal Ag⁺ concentrations (applied as AgNO₃) were between 3.98 and 63.6 mg/L also with a spacing factor of 2.

As toxicological endpoints, cell viability and mortality were determined, using a combined approach of viability detection using FCVK on 96-well plates (pure grade S, transparent F-bottom, Brand GmbH & CO KG, Wertheim, Germany) with additional cell count. In a first assay, the toxicity test was conducted as a separate FCVK/cell count assay with control for contamination. In a second experiment, the cell count assay was repeated for analytical purposes with a higher volume, however fewer replicates in 25 mL cell culture flasks (TPP, Switzerland). Figure 9 (page 26) shows details about replicate numbers, volumes used and procedures applied.

For all assays, axenic cell cultures were cultivated in filtrated ABC until exponential growth. Cell numbers of precultures were adjusted to 3 000 to 5 000 cells/mL by counting (see above) and adding filtrated medium directly before assay preparation. Predispersions ('PD' in figure 9) for nAg exposure and presolutions for Ag⁺ exposure were prepared as described above, added to adjusted preculture and dispersed in 96-well plates. The pH at the beginning of the test was determined using a WTW Sentix MicB electrode with WTW pH 3110. For respective blanks (six replicates per concentration) preculture was substituted by filtrated medium and for dispersant control blanks by dispersant stock solution (17% v/v). Control blanks consisted of filtrated medium only.

After four hours of exposure, resazurin from fluorometric cell viability kit was added to each well and exposure was continued until 20 h exposure time. Fluorescence was measured as indicator for viability using a Polarion plate reader (Tecan Group Ltd., Switzerland) with excitation at 545 nm and emission at 590 nm wavelength. Subsequently, surviving cells were separated from dead ones and fixed by addition of Bouin's solution as described above (chapter 3.2), for cell counting.

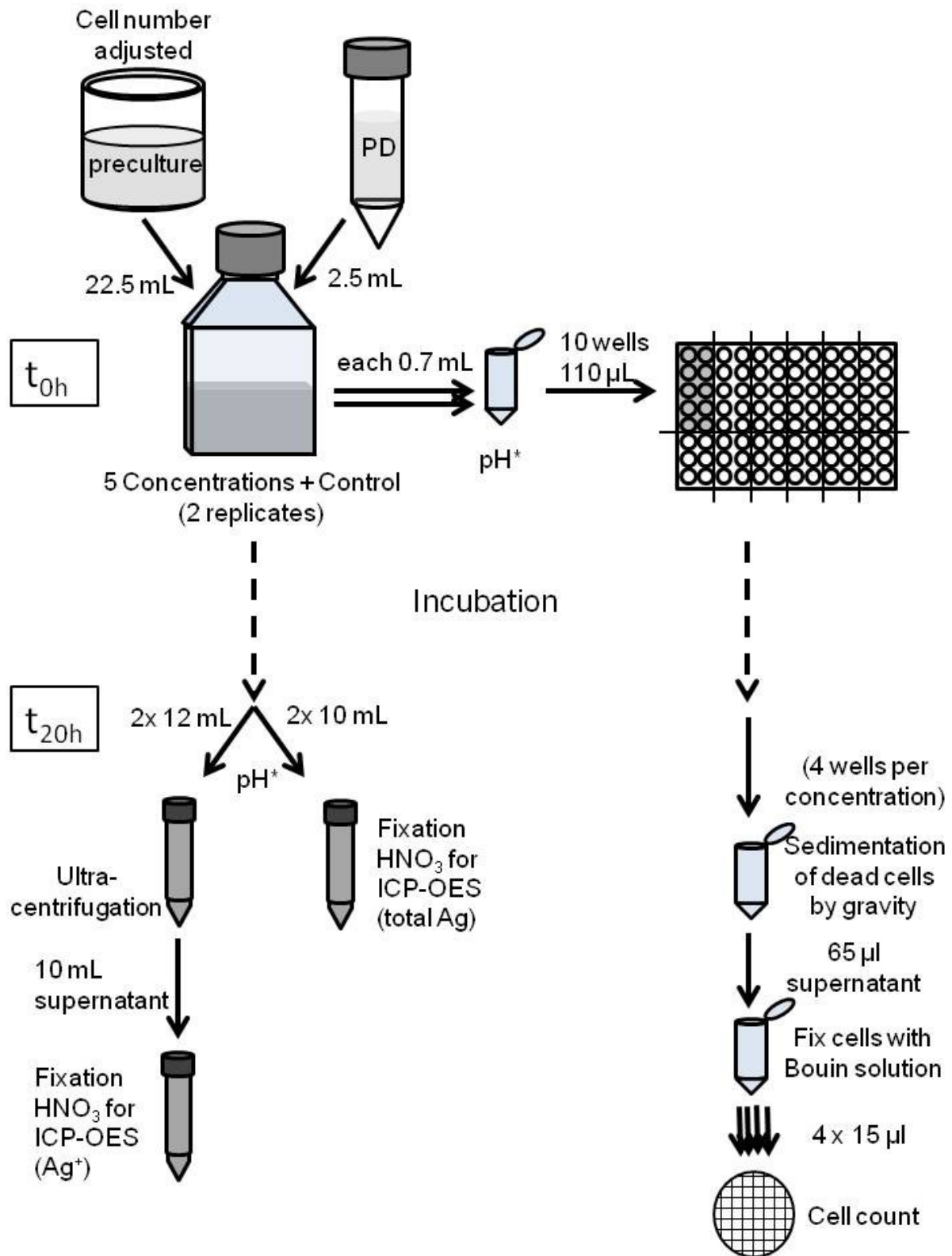


Figure 9: Experimental setup, preparation of assays and analyses. 'PD' = predispersion/presolution; pH*: determined in pooled replicates per sample

Cell counting was carried out as described before. Two replicates of each treatment, concentration and blank from 96-well plates were incubated on Mueller-Hinton agar (Carl Roth GmbH + Co. KG, Karlsruhe, Deutschland) plates for at least 48 h at 28°C to identify potential bacteria or fungi contamination. The pH at the end of the test was determined using WTW Sentix MicB electrode with WTW pH 3110 in pooled samples per treatment from 96-well plates and in samples drawn from cell culture flasks. In each treatment the Ag and Ag⁺ fractions were analyzed by ICP-OES in two replicates at the end of the second experiment. Additionally, a final nominal concentration of 30 mg/L in filtrated ABC without organisms was analyzed. For total Ag analyses exposure solution was digested with one drop of concentrated nitric acid (69% HNO₃, Sigma-Aldrich, Steinheim, Deutschland) in 15 mL polypropylene centrifuge tubes (Corning Inc., Mexico) immediately. Samples for Ag⁺ analyses were transferred to centrifuge tubes and centrifuged for 135 min with a RCF of 15,557 x g at 22°C (Eppendorf 5810 R centrifuge). The supernatants were digested with concentrated HNO₃. Samples were shaken and diluted 1:10 or 1:100 depending on nominal concentrations prior to measures and analyzed on Optima 7300 V HF Version ICP-OES Spectrometer (Perkin Elmer, Waltham, Massachusetts, USA). We calculated the nanoparticulate fraction (nAg) as difference of the results from total Ag and Ag⁺ analysis.

Data analysis

Validity criteria for the toxicity tests were:

- No mortality based on cell numbers in final controls compared to initial cell numbers
- Negative contamination checks on agar plates
- Constant pH and incubation conditions.

Toxicity test data were fitted as concentration response curves with Weibull regression and 95% confidence intervals and analyzed for effect concentrations (20-h LC₅₀ for mortality based on cell counts and 20-h EC₅₀ for inhibition of viability based on fluorometric cell viability kit) using ToxRat[®] Standard Version 2.10. Results were plotted with Sigma Plot 11.0 software. For enhanced readability, LC₅₀ values will subsequently be referred to as EC₅₀ values. For risk assessment, the determined effect values were compared to data from literature for the same material as applied.

We calculated the particle number concentration per litre (pnc) and surface area concentration (sac) for all samples from the determined nAg concentrations, mean particle size from UV-vis spectroscopy data and density of silver according to equation

3 and 4 (see section 2.1.2 Characterization methods for nAg, page 13) according to Teeguarden et al. (2007).

Surface area concentration (sac in cm²/L) was correlated to the Ag⁺ content in comparison to mass concentration. Here it was necessary to correct the determined Ag⁺ content for the known input of Ag⁺ from stock dispersion in accordance with the analyzed Ag and nAg content in NM-300K: based on the determined nAg concentration, the reference content of Ag⁺ (debit value) was calculated for each sample. The analyzed Ag⁺ in toxicity tests was then divided by the debit value.

Effect concentrations converted to sac were implemented to risk assessment. A literature survey was conducted for comparison of toxicity values of NM-300K. The obtained data were used to calculate the predicted no effect concentrations (PNECs), according to TGD (2003) for acute toxicity testing. Predicted environmental concentrations (PECs) were taken from Hendren et al. (2013), providing data for activated sludge with a lower and higher exposure scenario (for details see citation and table 5). All determined PECs and PNECs were converted to their corresponding sac as described above. Risk quotients (RQ) were calculated as PECsac divided by PNECsac.

3.3.2 Results and discussion of nAg toxicity tests with *P. tetraurelia*

Axenic cultivation and experimental design were chosen in these experiments because in acute toxicity tests water-only exposure must be ensured. Cultivation of *Paramecia* was successfully established with a generation time of 23.3 hours at 22°C. In order to cover experimental conditions, generation times were also determined for cultivation in filtrated ABC with 27 hours at 22°C. Since exposure duration in toxicity tests was below generation time of the organism, it is regarded as acute toxicity test. The advantages of this novel test system compared to other OECD standard acute toxicity tests are the low space required for cultivation of a high number (density) of test organisms and short experimental times, signifying similar time efficiency like algae or bacteria tests. Except for the need of equipment to ensure sterile working conditions there are no special demands for storing *Paramecia* cultures, which suits them well to the available facilities of most ecotoxicological laboratories. For the reason of easy culture handling and the absence of other forms such as sessile or crawling ciliates as axenic cultures, we regard *Paramecium tetraurelia* as an acceptable representative organism for filter feeders in WWTPs.

Characterization of nAg

Nanoparticle dispersions for all tests were prepared with 1 g/L stock dispersions, made from NM-300K and HPLC-grade water. Radniecki et al. (2011) showed that pre-dispersion in ion-free water leads subsequently to better stability of nanoparticles in respective exposure media and to more reproducible results in test approaches.

Characterization in exposure media was chosen because it is a prerequisite to describe exposure conditions (Navarro et al., 2008). ABC was filtrated for excluding mediumborne particles above 220 nm size from toxicity tests, to avoid interference with characterization of nAg, as previously seen in unfiltrated ABC by DLS (figure 10).

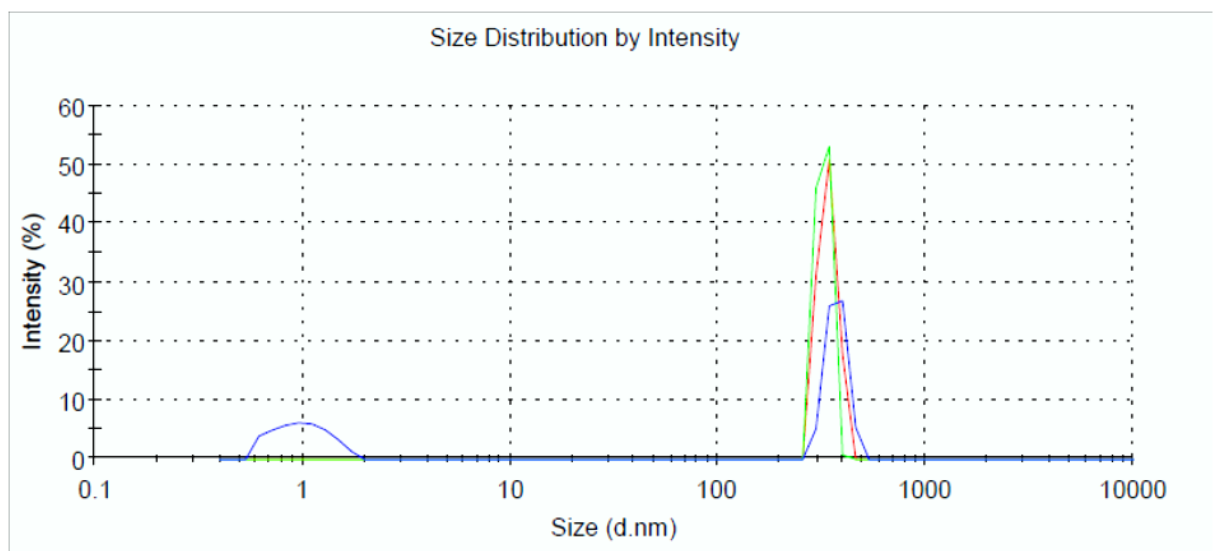


Figure 10: Intensity weighted size distribution of 0.01 mg/L nAg in unfiltrated ABC as determined by DLS measurements (three replicates, indicated by different colors). Distinct peaks are visible at particle diameters of 400 nm.

Characterization of nAg particles by DLS and UV-vis spectroscopy yielded particle diameter size distributions in filtrated ABC as displayed in figure 11 and table 2.

Table 2: nAg Particle sizes as mean diameters estimated by dynamic light scattering technique and UV-vis spectroscopy in filtrated ABC.

Sample	Dynamic light scattering Mean diameter \pm Std. dev.		UV-vis characterization Particle diameters*		
	Peak1 d[nm]	Peak 2 d[nm]	Equ. 1 d[nm]	Equ. 2 d[nm]	Mean size d[nm]
Blank	93.7 \pm 1.1	-	n.d.	n.d.	n.d.
7.5 mg/L	70.5 \pm 4.0	5.7 \pm 2.6	27	11	19
15 mg/L	66.9 \pm 8.5	3.0 \pm 0.8	27	13	20
30 mg/L	43.2 \pm 4.6	2.7 \pm 2.6	43	21	32
60 mg/L	32.3 \pm 1.4	2.6 \pm 0.8	77	19	48
120 mg/L	26.4 \pm 1.4	2.2 \pm 0.7	93	44	69

n.d.: not determined; *Standard deviations for particle sizes calculated from UV-vis absorption spectra were not applicable. Standard deviations of absorption from three replicates were always below 0.004 in UV-vis measurements and thus did not result in any differences of calculated particle sizes. Blank: plain filtrated ABC.

In filtrated medium without added nanoparticles a DLS peak was recorded at 93.7 \pm 1.1 nm, originating from media supplements. In nAg supplied medium, a second peak in low nanometer range (2.2 to 5.7 nm) occurred beneath the major DLS peak, representing the dispersant.

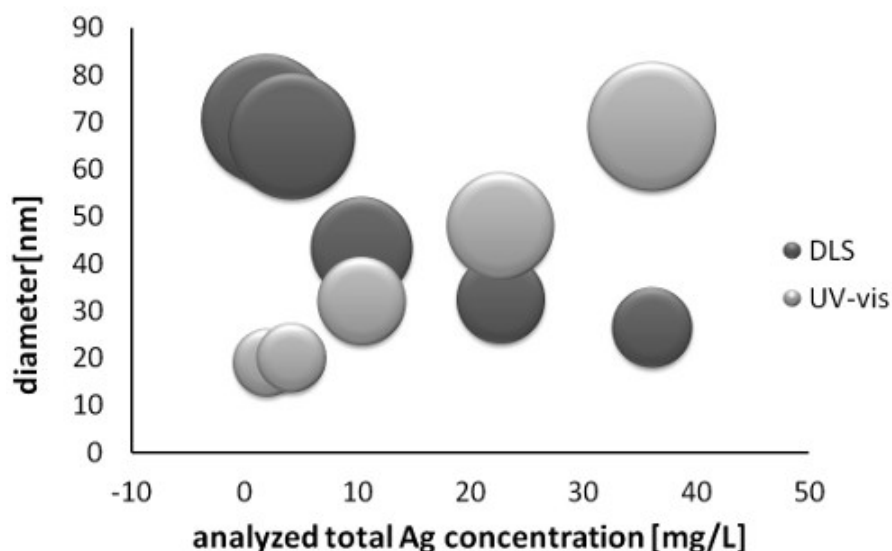


Figure 11: Concentration dependent particle diameters in filtrated ABC analyzed with different methods (DLS and UV-vis). Size of the symbols corresponds to their determined diameter by the respective technique.

Results from DLS analysis for nAg supplied medium showed a significant decrease of nAg particle diameter from 70.5 to 26.4 nm with increasing concentration (figure 11). In contrast, calculated diameters derived from UV-vis spectroscopy increased from 27 to 93 nm (figure 11). Calculation of UV-vis results with the second equation showed the same trend, however smaller particle sizes from 11 to 44 nm. The mean sizes of particles calculated from the two equations were 19 to 69 nm (figure 11). The discrepancy between DLS and UV-vis results originates from the principles of detection methods and is frequently described in the literature (Li and Lenhart, 2012; Poda et al., 2011). Since hydrodynamic diameters include the aqueous layer surrounding the particles, the core particle diameter cannot be determined exactly by DLS. A high polydispersity of samples was observed in this study. Scattering from medium born particles smaller than 200 nm interfered with DLS characterization. Against expectations, hydrodynamic diameters decreased with increasing concentration. Therefore careful interpretation of DLS results is recommended. The basic principle of UV-vis characterization is the typical plasmon absorption band of spherical nanosilver (Petit et al., 1993). Specific plasmon absorption band characteristics depend on primary particle shape and size. In this study, the maximum absorption peak was located at 410 nm at the lowest nAg concentration, which is in agreement with typical absorption peaks of singly dispersed spherical nAg at ~400 nm and findings of Li and Lenhart (2012) for TWEEN® 20 stabilized singly dispersed nAg. With increasing concentrations, maximum absorption shifted to higher wavelengths, reaching 450 nm for 120 mg nAg/L. The author assumes this red shift as an indication of agglomeration with increasing particle concentration. Broadening of the peak width with increasing particle concentration is also indicative for agglomeration processes (Tejamaya et al., 2012). Compared to DLS technique, results of mean particle sizes calculated from maximum absorption and PWHM of UV-vis spectra are biased to a lesser extent and are conform to specifications according to the manufacturer (particle size < 20 nm).

SEM confirmed a mixed dispersion state of nAg in exposure medium. Particles were present as primary particles and agglomerates of different sizes as shown exemplarily for 60 mg/L dispersion in figure 12 a) and b). Agglomeration could occur as an artifact of sample preparation. Primary particles were identifiable in the agglomerates, confirming the average diameter derived from UV-vis spectra.

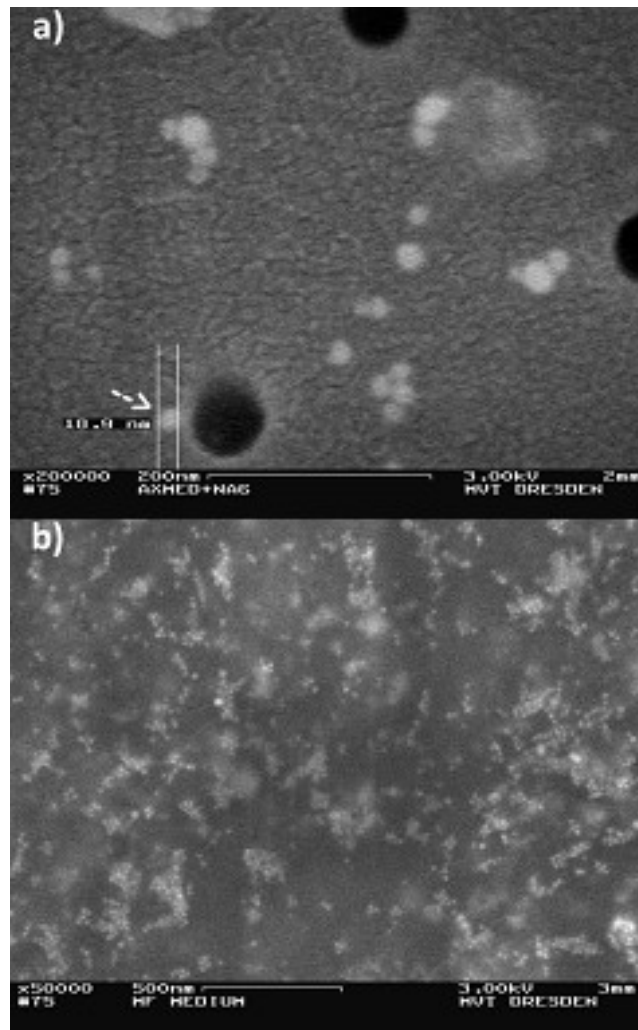


Figure 12: SEM pictures of a 60 mg/L nAg dispersion in filtrated ABC. a) nAg dispersed as primary particles (white dots) in ABC at magnification x 200000. Diameter of the measured particle (arrow) is 18.9 nm. b) Agglomerated and dispersed nAg at magnification x 50000.

Results of zeta potential analysis are depicted in table 3. Filtrated medium had a zeta potential of -22.2 mV. With increasing nAg concentration in the medium, the zeta potential changed from -23.2 towards a lower charge of -15.6 mV. The identified dispersion status for the respective exposures suggested bioavailability of nAg throughout the duration of subsequent toxicity tests.

Table 3: Results of zeta potential (ζ in mV) analyses of nAg test concentrations in filtrated ABC.

Sample	ζ [mV]
Filtrated medium	-22.2 ± 1.6
7.5 mg/L	-23.2 ± 0.1
15 mg/L	-22.3 ± 0.6
30 mg/L	-21.1 ± 0.6
60 mg/L	-17.4 ± 0.4
120 mg/L	-15.6 ± 0.2

Analytics

Under quality assurance aspects the recovery to characterize adsorption behavior of nAg and Ag^+ to exposure vessels under experimental conditions by ICP-OES analyses (figure 13, page 34) was investigated. Initial and final concentrations were the same in this test, indicating negligible adsorption to surfaces of used vessels. According to rank sum test (U-test) there were no significant differences between the analytic results according to the two methods of sample handling. It is evident, that significant differences in the amounts of Ag found in the samples are rare, indicating that adsorption of Ag to exposure vessels is negligible for explaining losses of Ag in the experiment analytics. According to U-test there is no statistical significant difference between silver contents in assays containing cells and cell free assays. Interpretation of this data requires caution, as influence of cells on the recovery of silver cannot be excluded with absolute certainty, due to the possibility of beta errors.

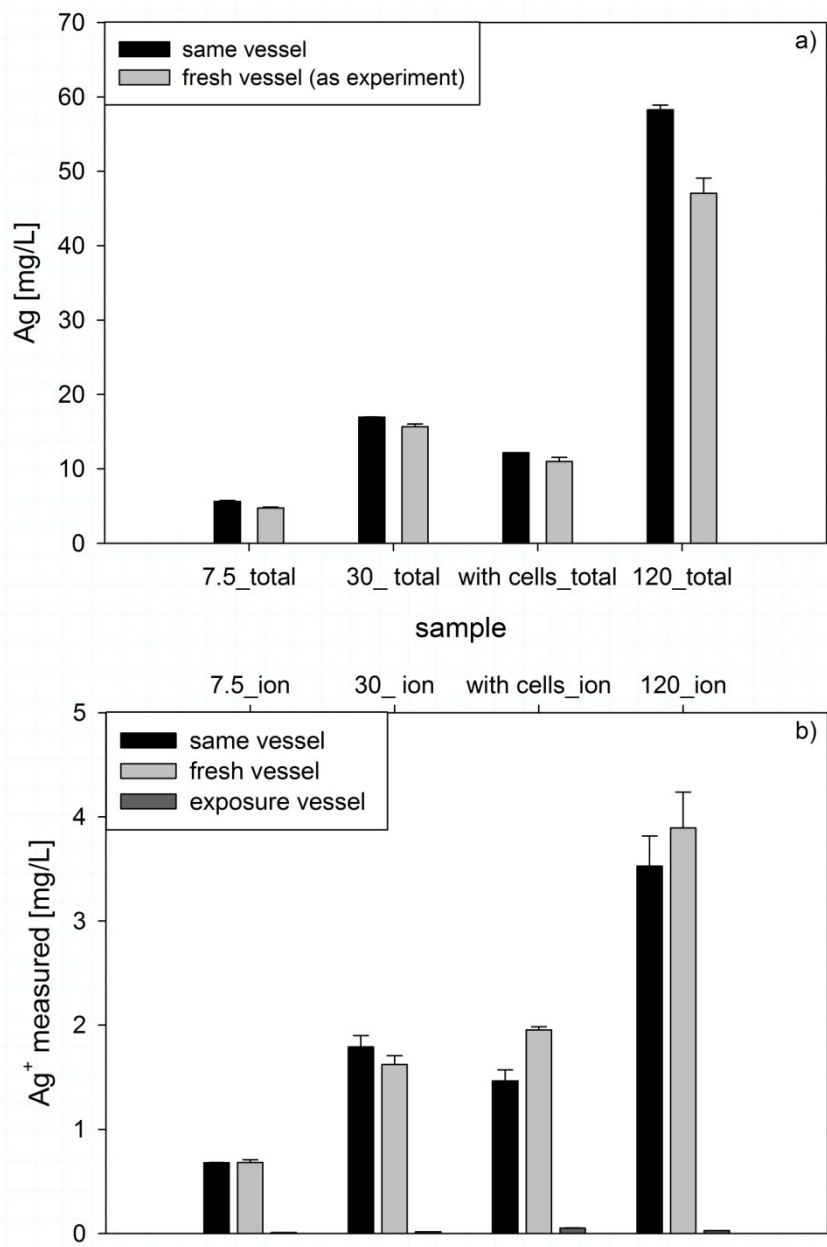


Figure 13: Analyzed values of total Ag (a) and Ag⁺ (b) in recovery experiment. Filtrated ABC was supplied with three different nominal concentrations of nAg (7.5, 30 and 120 mg/L). Additionally, cell culture (with cells_total and with cells_ion) was supplied with nAg at a nominal concentration of 30 mg/L. Black bars - samples exposed and acidified in the same vessel. Gray bars - samples transferred and acidified in fresh vessels after exposure. Dark gray bars (figure b only) - Ag⁺ content from exposure vessel after sample transfer and refilling with HPLC-grade water and acidification. Error bars indicate standard error of means.

Nominal and determined Ag and Ag⁺ concentrations of nAg and AgNO₃ exposures by ICP-OES analyses are displayed in table 4. ICP-OES analyses of exposure liquids at the end of toxicity tests showed, that total exposure Ag concentrations were significantly lower compared to targeted total nominal Ag concentrations in both nAg and Ag⁺ treatments (see recovery in table 4).

Table 4: Nominal and determined concentrations of Ag and Ag⁺ in nanoparticulate (nAg) and ionic (AgNO₃) treatments and percentile recovery of nominal concentrations

Treatment	Nominal concentration		Analyzed concentration		Recovery	
	Ag total [mg/L]	Ag+ [mg/L]	Ag total [mg/L]	Ag+ [mg/L]	Ag total %	Ag+ %
nAg	8.4	0.4	2.0	0.6	24	150
	16.7	0.7	4.2	0.8	25	118
	33.3	1.4	10.4	1.3	31	92
	66.6	2.8	22.7	2.1	34	76
	133.2	5.6	36.1	4.2	27	75
AgNO ₃	4.0		1.1	1.2	27	30
	8.0		2.3	2.2	29	28
	16.0		4.1	3.1	26	19
	32.0		9.0	8.2	28	26
	64.0		13.3	25.0	21	39

In nAg exposures, total Ag content determined by ICP-OES was on average about one third (28%) compared to nominal concentrations. Analyzed Ag⁺ concentration was similar to the calculated concentration (106%) based on stock dispersion analysis. nAg content was calculated from the difference between analyzed total Ag and Ag⁺ and was consequently lower than targeted nominal concentration, with an average recovery of 26%. In AgNO₃ exposures, the analyzed total Ag and Ag⁺ concentration were comparable and made up one third of the nominal concentration (26% and 28%, respectively). Since adsorption to test vessels was proven negligible, the lower experimental concentration certainly originated from measuring errors when weighing in minute amounts of NM-300K and AgNO₃ for stock preparation and from transferring liquids from stocks to pre-dispersions and pre-dispersions to exposure vessels due to the high viscosity of the material. For example, coating of pipette tips with the NM-300K material after transfer to liquids was observed by eye.

The 1.5 g/L stock dispersion was exclusively used to prepare the highest exposure concentration. Here, the deviation between analyzed and nominal concentration differed from samples prepared with the 1 g/L stock dispersion. These results indicate the necessity to analyze Ag content of freshly prepared stocks and (pre-)dispersions and a drawback of using stocks with different Ag mass concentrations for sample preparation. Since incomplete digestion of analytical samples still cannot be ruled out

with certainty, underestimation of experimental concentrations is possible but is not quantifiable.

Toxicity tests

In filtrated ABC the dissolved oxygen concentration was 7.6 mg/L. The pH in ABC containing different concentrations of nanoparticles was 7.05 ± 0.25 throughout repeated tests. Hence, no negative effect of oxygen content and pH was expected on viability of ciliates. Controls of microbial contamination prepared on Mueller-Hinton agar plates from FCVK replicates were negative throughout the tests. Thus, validity criteria were fulfilled.

According to TGD (2003), concentration response curves were drawn from respective analyzed mean concentrations at the end of tests for all exposures and Ag^+ and nAg concentrations at 50% effect levels were calculated. The discrepancies between nominal and analyzed silver concentrations might in the worst case have lead to an underestimation of EC_{50} values (i.e. a lower determined EC_{50} than the real EC_{50}). For risk assessment this is acceptable in terms of the precautionary principle. Effective concentration response curves are shown in figure 14.

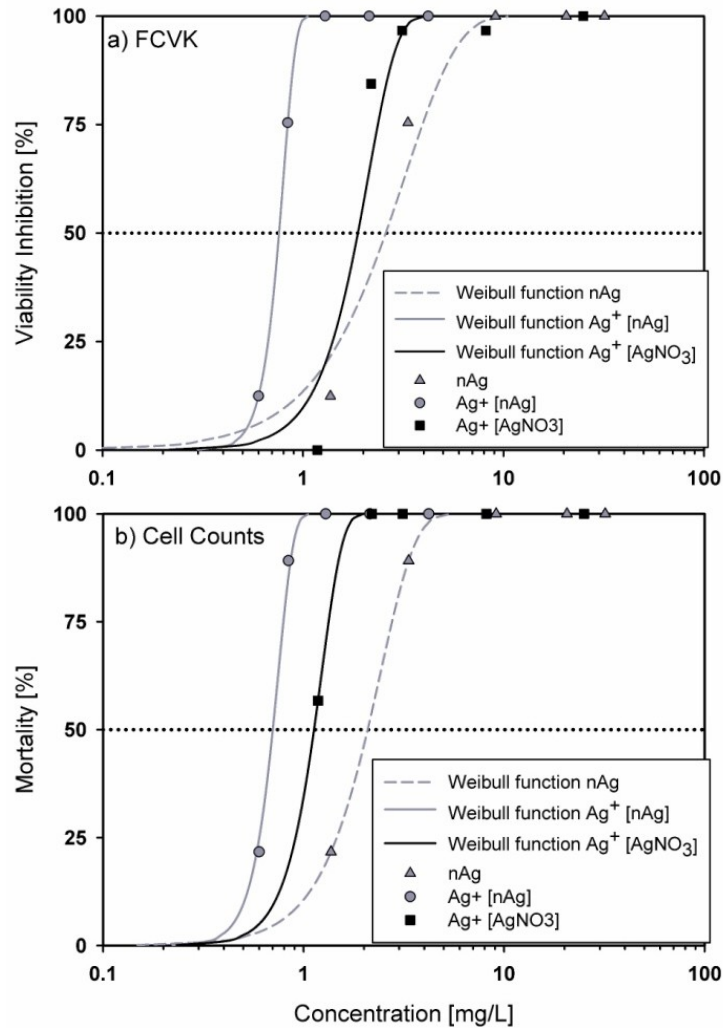


Figure 14: Concentration response curves based on effective concentrations of Ag⁺ and nAg in nanoparticulate and ionic treatment for viability assay (FCVK) and mortality assay (cell counts). 95% confidence intervals were omitted for better visibility of data, but are given for EC₅₀ values in table 5. Note logarithmic scale of x-axes.

Goodness of fit (probabilities for Chi²) for all Weibull regressions was high with $p(\text{Chi}^2) > 0.100$ and regressions were significant with $p(F) < \alpha$ ($\alpha = 0.05$) in F-tests. Differences in 20-h EC₅₀ values derived from effective concentration response curves for nAg exposure were marginal between the two toxicological endpoints viability (FCVK) and mortality (cell counts). Since concentration response curves were steep and confidence intervals (CI) overlapped, these values were considered the same. Statistical difference between two EC₅₀ values can be tested using Zajdlik's ad hoc method no.1 (Environment Canada, 2005) according to equation 8:

$$z = \frac{\log EC50_1 - \log EC50_2}{\sqrt{(\sigma^2(\log EC50_1) + \sigma^2(\log EC50_2))}}$$

equation 8

where σ is the standard error. If $|z|$ is larger than the critical value 1.96, EC_{50} values are significantly different. Based on this equation, nominal EC_{50} values of nAg tests were compared for the two toxicological endpoints and were not statistically different with $p(F) < \alpha$ ($\alpha = 0.05$). As the two endpoints yield the same results, a mean 20-h EC_{50} value was calculated for nAg exposure with 2.35 mg/L and for Ag^+ 0.73 mg/L in the same assay.

In $AgNO_3$ treatment, the mean EC_{50} for Ag^+ was 1.92 mg/L. The toxicity of Ag^+ is considered to be the same in both nAg and $AgNO_3$ treatment since concentration response curves were steep and the 95% CIs coincided. Whether the toxicity of nAg is caused by released ionic silver, or by the nanoparticles themselves (Beer et al., 2012; Bilberg et al., 2012; Kittler et al., 2010a; Kittler et al., 2010b; Lee et al., 2012; Musee et al., 2011; Sotiriou and Pratsinis, 2010; Xiu et al., 2012) is a controversial discussion in the literature. In this study results imply, that Ag^+ was responsible for toxic effects, since EC_{50} of Ag^+ were the same for both treatments, which supports the second hypothesis of this thesis. Despite these findings nAg still has to be regarded as source of Ag^+ in aqueous systems and requires reasonable ERA of the nanoparticulate material.

We calculated pnc and sac of nAg for all samples. The sac [cm^2/mL] was correlated to the Ag^+ content in comparison to mass concentration (figure 15) for demonstration of applicability. Fit of regression was better when using surface area concentration ($r^2 = 0.99$) than mass concentration ($r^2 = 0.94$) of nAg.

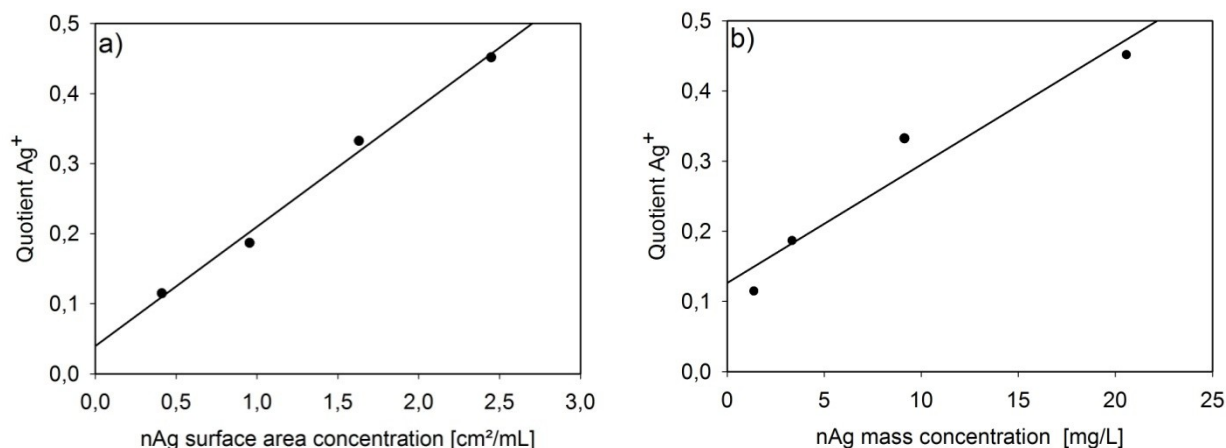


Figure 15: Regression functions of Ag^+ release quotient and a) surface area concentration: $y = 0.17 \cdot x + 0.04$; $r^2 = 0.99$ or b) mass concentration of nAg: $y = 0.02 \cdot x + 0.13$; $r^2 = 0.94$. The maximum concentration was excluded from correlations due to the use of a different stock dispersion for sample preparation.

This result indicates that sac is a powerful parameter for explaining toxicity of NPs through ion release. Although one may argue that correlation of mass concentration with ion release is still good, Liu et al. (2010a) showed that Ag^+ release of silver at different size scales (4.8 nm, 60 nm, macroscopic Ag as foil) differed significantly over several orders of magnitude in terms of mass concentration. When Ag^+ release was related to surface area, results for different materials were at the same order of magnitude. The author assumes that testing differently sized nanoparticles would illustrate the suitability of sac for toxicity evaluation.

For implementation of sac into ERA, detailed data on aging and behavior of nanomaterials in the environmental matrices is necessary. There is also a need for more detailed models for predicted environmental concentrations which consider release amounts of nanomaterials with their respective particle sizes and coating types since they significantly influence toxicity (Marambio-Jones and Hoek, 2010; Musee et al., 2011). With these information, mass concentrations applied for PECs and PNECs can be converted to sac. In this study, data from literature was considered for the same material only, as applied here (i.e. NM-300K), because ERA should be done case-by-case rather than generalized for a core material, as stated by the European commission (2012). At the moment these data are scarce. However a first attempt to predict environmental concentrations of nAg with specific coatings was made by Hendren et al. (2013), TWEEN® 20 stabilized nAg like NM-300K was not included in their study, but data for gum arabic, PVP and citrate coated nAg were provided. PVP and citrate are two of the most often used coatings/stabilizers for nAg (Badawy et al., 2010). The author assumes TWEEN® 20 stabilized nAg to be comparably abundant in the environment like gum arabic or poly ethylene glycol (PEG) coated particles. For NM-300K specific ERA we used the PECs of 1.6 to 4.5 $\mu\text{g/L}$

activated sludge and converted these into sac, equaling 0.46 to 1.29 cm²/L. The latter were applied in risk quotient calculation. The calculations were made under the assumption of particle diameters of 20 nm.

For calculating PNEC, it was necessary to compare toxicity data for aquatic organisms and identify the most sensitive species for NM-300K and then convert mass concentration values to sac. The only available aquatic toxicity data found for NM-300K explicitly was published by Wang et al. (2012). The authors reported toxicity data for algae (*Raphidocelis subcapitata*), fish (*Danio rerio*) and cladocera (*Chydorus sphaericus*), where the latter was the most sensitive species. An overview of respective EC_x values is given in table 5. Since the focus of this study was to determine a possible risk of nAg for WWTP organisms, those organisms tested by Wang et al. (2012) were considered not relevant. Hence, effects on *P. tetraurelia* (this study) were exclusively regarded for ERA.

Table 5: Toxicity values of NM-300K determined in this study compared to data from literature for different organisms. RQ: risk quotient (PECsac/PNECsac).

Organism	Type of toxicity value	Value in µg/L	PNEC in µg/L	PNECsac in cm ² /L	RQ scenario 1	RQ scenario 2	Citation
<i>Raphidocephalus subcapitata</i>	4.5-h EC ₅₀	896	0.896	0.256	0.0 [#]	0.1 ^{##}	Wang et al. (2012)
<i>Chydorus sphaericus</i>	48-h EC ₅₀	9	0.009	0.003	2.0 [#]	8.3 ^{##}	
<i>Danio rerio</i>	96-h (?) EC ₅₀	84	0.084	0.024	0.3 [#]	1.0 ^{##}	
<i>Paramecium tetraurelia</i>	20-h EC ₅₀	2340	2.34	0.67	0.7 [§]	1.9 ^{§§}	This study

[#] PECsac for freshwater, lower scenario: 0.006 cm²/L; ^{##} PECsac for freshwater, max scenario: 0.025 cm²/L; [§] PECsac for activated sludge, lower scenario: 0.46 cm²/L; ^{§§} PECsac for activated sludge 1.29 cm²/L.

Toxicity values were transformed to PNEC using an assessment factor of 1000 for acute toxicity tests and subsequently converted to corresponding sac (PNECsac). According to these data, in WWTPs no risk (RQ = 0.7) resulted at the lower estimated PEC_{sac}, but at the higher PEC_{sac} (RQ = 1.9) a possible risk for activated sludge organisms exists. Accordingly, nAg is a possible source for reduced performance of WWTP or operational deterioration. Exposure situation and extent of leaching

processes in WWTPs might still differ substantially from assumptions in acute toxicity tests to either direction. Therefore, investigation of fate, behavior and effects of nAg on organisms and whole communities in model WWTPs is necessary. First of all, stepwise approaches for understanding effects on communities need to regard bioaccumulation effects in food chains.

It has to be considered that results from calculations of pnc and sac are simplified approximations to real conditions here, because particles were assumed to be spherical and deviations from mean diameters were neglected. For agglomerates the bias of overall density, resulting from gaps between primary particles, was disregarded. Note that cross effects, like the influence on NP dissolution by dispersants or other materials in the exposure medium, were not considered in this approach. Implemented PEC values were only estimated by models and beyond that, were not restricted to NM-300K material. Nevertheless, prospectively NM release into the environment will rise along with increasing production and application. PECs will ascend and the probability of risk posed to organisms in respective compartments will strengthen, especially in respect to nAg being used for its antimicrobial properties. In this field of application we cannot expect any development of safe-by-design NPs.

As a matter of fact few data exist in literature, which describe effects of NM-300K on WWTP organisms. For this reason, this study represents a feasible explorative way of assessing risk by NM-300K for organisms relevant in activated sludge ecology. As a probable risk was identified here, more detailed investigations are required according to TGD. As the next step, more organisms are taken into account for acute toxicity testing: in chapter 4 toxicity tests with relevant bacteria and nAg are described.

3.4 Toxicity tests with *P. tetraurelia* and nTiO₂

The above described toxicity tests with *P. tetraurelia* were adapted to testing of nTiO₂. Methods were performed according to Schulze (2013) and are described in detail subsequently.

3.4.1 Materials and methods for nTiO₂ toxicity tests

Axenic *P. tetraurelia* cell cultures were maintained and applied using filtrated ABC as described in section 3.2.

Preparation of nTiO₂ stock dispersion

NM-101 nTiO₂ was delivered as powder which was dispersed in dispersant solution according to round robin test published by Nickel et al. (2014) at a final nominal concentration of 100 mg/L. For the dispersant solution (1% sodium-hexametaphosphate, (NaHMP)), 0.005 g NaHMP (Sigma-Aldrich, Steinheim, Germany) were weighed into a 500 mL Schott bottle (glass) and mixed with 600 mL HPLC-grade water by stirring. 0.01 g nTiO₂ were weighed (Sartorius RC210S) and dispersed in 100 mL of the dispersant solution. Preliminary tests with a 1 g/L nTiO₂ revealed strong agglomeration behavior.

Characterization of nTiO₂ dispersions

Particle sizes were characterized at pre-dispersion concentrations, 2.8, 5.6, 11.3, 22.5 and 45 mg/L in sterile filtrated axenic medium via DLS as described above (see chapter 2.2.2). Zeta potential was analyzed in preliminary tests for dispersions of 5 and 10 mg/L nTiO₂ in ABC.

Acute toxicity tests with nTiO₂

Pre-dispersions of nTiO₂ were prepared from 100 mg/L nTiO₂ stock dispersion and sterile filtrated axenic medium at concentrations 2.8, 5.6, 11.3, 22.5 and 45 mg/L. For the toxicity assay, 96-well plates (pure grade S, transparent F-bottom, Brand GmbH & CO KG, Wertheim, Germany) were used to realize 10 replicates of each treatment concentration and 6 replicates as blanks. Pre-dispersions were filled into the respective wells at a volume of 50 µL and 50 µL of cell number adjusted *P. tetraurelia* culture (see chapter 3.3) were added. Two control assays were prepared with 10 replicates each, one for cell number determination at the start of the experiment and one for analyses at the end of the experiment. For controls 50 µL of pure filtrated media and for dispersant control (10 replicates) 50 µL of 1% NaHMP were applied instead of pre-dispersion. Blanks were filled with filtrated media and if applying, pre-

dispersant respectively. Positive controls, for realizing 100% mortality samples, were accomplished by using 50 µL of 1 g/L AgNO₃ solution instead of pre-dispersion.

After filling the 96-well plates, controls for initial cell number determination were fixated in 5 replicates and 3 replicates per fixed sample were counted as described in chapter 3.3. pH was determined in joined samples from 3 control wells and in 2 wells from the respective blanks. The two remaining replicates from control were streaked on Mueller-Hinton agar plates and incubated at 33°C for 48 h for contamination check. 96-well plates were incubated for 4 h at 22°C and subsequently, 10 µL FCVK were added to each well. Final nominal nTiO₂ concentrations apart from controls were 1.3, 2.6, 5.1, 10.2 and 20.4 mg/L in the assay.

Incubation was continued for further 16 h. After this time, fluorescence was measured in all cavities as described in chapter 3.3 and cell numbers were determined accordingly, after an optical evaluation of the 96-well plate using a stereomicroscope (SZX2-ILLD, Olympus, Tokyo, Japan).

Acute toxicity test with nTiO₂ under UV light irradiation

Toxicity tests were prepared as described above. During the first incubation time of 4 hours, UV light irradiation at 254 nm wavelength was realized by using the sterilization facility of the clean bench (Hera Safe HS12, Heraeus Instruments, Hanau, Germany). Analysis of samples was undertaken as described before.

Data analysis

Validity criteria for the toxicity tests were:

- no mortality based on cell numbers in final controls compared to initial cell numbers
- negative contamination checks on agar plates
- constant pH (fluctuation <0.5) and constant incubation conditions.

Toxicity test results were analyzed regarding concentration response relationships using ToxRat[®] Standard Version 2.10. Student's t-tests were applied for pairwise comparison of data and results were plotted with Sigma Plot 11.0 software.

Chronic toxicity tests

For chronic toxicity testing over a period of 168 h, seven 96-well plates were prepared either containing controls or treatments at one of the five tested concentrations at the same composition as described for acute toxicity tests. Blanks were omitted, as

viability was not applicable for prolonged tests and thus fluorescence blanks were not required.

For initial cell number determination, samples were fixated immediately after preparation of the assay, as specified previously. In intervals of 24 h, samples for cell counting were drawn from controls and treatments as in the acute toxicity tests. On day four and five after assay preparation.

3.4.2 Results and discussion of nTiO₂ toxicity tests

Characterization of nTiO₂ dispersions

Intensity weighted particle size distributions from DLS analyses (figure 16) showed distinct peaks at about 200 nm diameter for concentrations from 2.8 mg/L (red line in figure 16) to 11.3 mg/L (pink line in figure 16). Peak width at these concentrations was broad, ranging from 40 to approximately 600 nm, with Pdl's of 0.27 to 0.44. For concentration of 22.5 mg/L (black line in figure 16) two comparably intense peaks were detected at about 150 nm and at 400 nm. For the concentration of 45 mg/L (blue line figure 16) a small peak at 90 to 100 nm and a second more intense peak between 400 and 500 nm occurred. Pdl's at the two concentrations were 0.52 and 0.62, respectively. The second peak at concentration 2.8 mg/L positioned at about 1100 nm is an artifact from the algorithm (pers. comm. Prof. Stintz⁶ taken from recommendations for measures with Malvern Zetasizers, 2010) and thus not regarded as particle size.

⁶ MVT TU Dresden

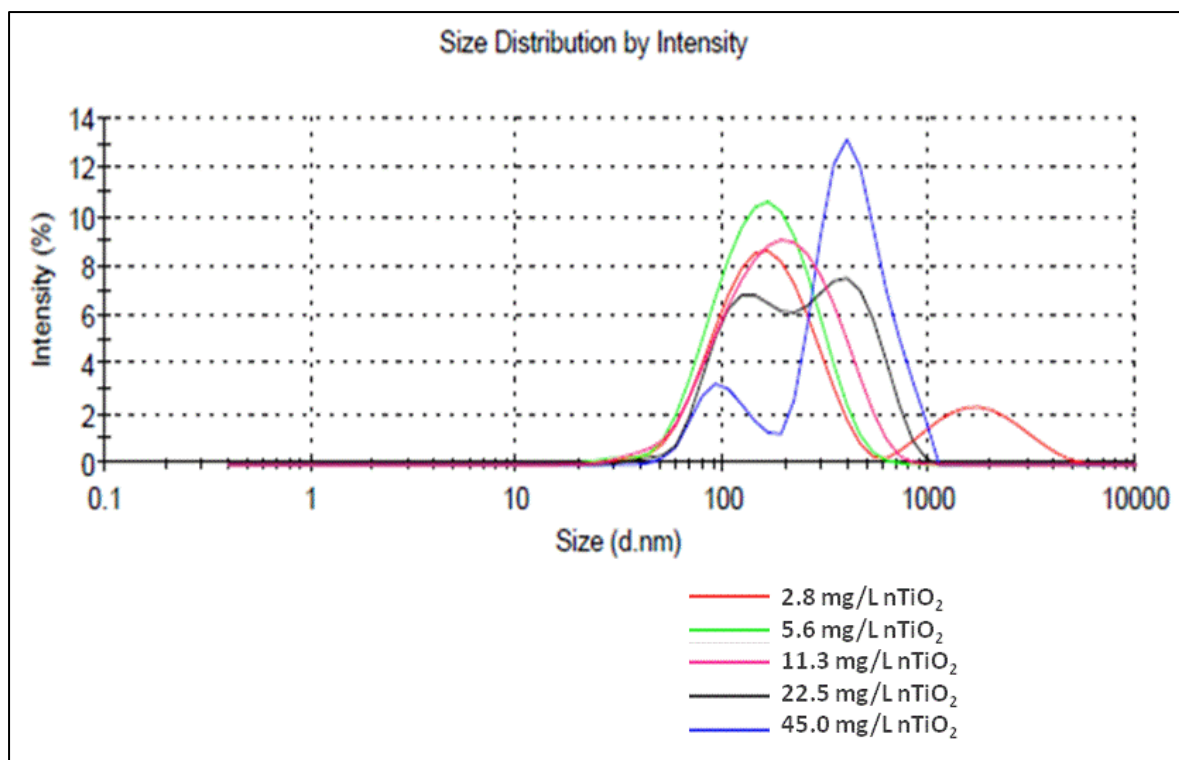


Figure 16: Intensity weighted size distribution of nTiO₂ in filtrated ABC, according to DLS.

Since manufacturer's information state primary particle size of 38 nm, these results suggest agglomeration of particles in the medium, despite the fact that DLS results are always biased towards larger particle diameters due to the hydrated sphere around the particles. At the higher concentrations agglomeration tendency seems to increase as indicated by the very intense peak at 400 to 500 nm in the 45 mg/L dispersion and the increasing polydispersity indices along with nTiO₂ concentration. With increasing agglomeration tendency, a settling of particles must be assumed, probably leading to an unstable exposure at the highest concentration of dispersions.

Zeta potential measures of 5 and 10 mg/L nTiO₂ dispersions revealed inexplicable fluctuations of positive and negative potentials probably resulting from interactions of nTiO₂ with media ingredients.

Acute toxicity test

Contamination controls were negative and the pH ranged from 6.7 ± 0.0 in the controls and blanks at beginning of the test to 6.88 ± 0.08 in the samples and 6.78 ± 0.04 in the blanks at the end of the test. No significant difference between cell numbers of controls at beginning and end of the experiment was detected, although mean cell numbers at the end of the experiment were decreased, but with a high

standard deviation. Thus mortality in controls was negated and validity criteria were regarded fulfilled. In figure 17 bar plots of the acute toxicity test results for both endpoints are depicted.

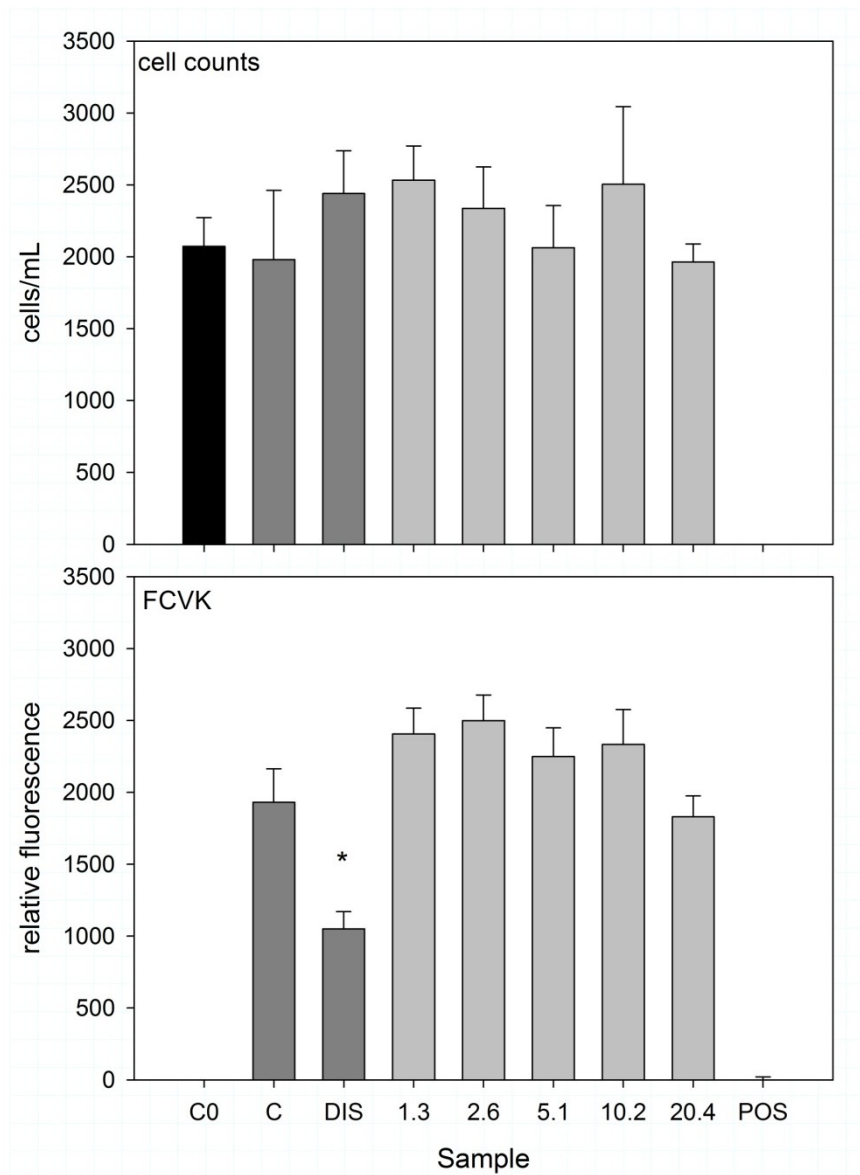


Figure 17: Bar charts for acute toxicity test results regarding cell counts and FCVK, showing mean values with standard error on y-axis. C0 = control at beginning, C = control at test end, DIS = dispersant control, numbers are nominal nTiO₂ concentrations in mg/L, POS = positive control . Asterisk indicates statistically significant difference to control according to t-test.

In the viability assay, relative fluorescence in dispersant controls was significantly lower compared to controls according to Student's t-test with $P = 0.003$. For both of

the endpoints mortality and viability, no significant differences were found between treatments and control at test end.

Concentration response relationships could not be determined. Since agglomeration and settling of nTiO₂ started at concentrations of about 45 mg/L, the maximum final nominal concentration to be tested in this assay was 20.4 mg/L. As initial cell density in the tests affected growth of *Paramecium* cultures, a higher ratio of pre-dispersion to cell culture would not be recommendable. For this reason and for the unstable exposure situation at higher nTiO₂ concentrations, determination of effect values had to be resigned in this case.

Acute toxicity tests with UV light irradiation

Results from acute toxicity tests with additional UV light irradiation of 4 h is shown in figure 18. For cell counts, mean control values at the end of the test deviated significantly from controls at the beginning of the test. As dispersant control values did not reveal mortality compared to control at beginning of the test and fluorescence values did neither, it must be assumed that the deviation of the control in the cell count assay originated from counting errors. Optical control of 96-well plates prior to fixation also supported this assumption. No significant changes in pH were observed throughout the test and contamination controls on agar plates were negative. Validity criteria were thus regarded fulfilled.

Concentration-response curves could not be determined according to results of both endpoints. For this reason, effect concentrations were not determinable. In the cell count assay no significant differences between all samples were observed. For the endpoint viability, a statistical significant difference was found between treatment at 1.3, 2.6 and 20.4 mg/L nominal nTiO₂ concentration and dispersant controls according to student's t-tests with $P < 0.05$. This unusual response might be a random result of the UV irradiation itself, rather than an effect of nTiO₂ toxicity. Assuming unstable exposure at the highest concentration however, could lead to another explanation of the observed effects on viability, such that only at low concentrations UV irradiation affects toxicity. To elucidate this issue, measures of nTiO₂ concentrations and quantification of ROS generation would be required. Regarding mortality and the weak inhibition of viability, influence of UV irradiation on NM-101 toxicity at the tested concentrations can be considered negligible. This might still not be true for higher concentrations, but since application of higher concentrations was not possible for the above mentioned reasons, no further investigations were undertaken. Thus hypothesis 3 of this thesis was rejected for acute toxicity.

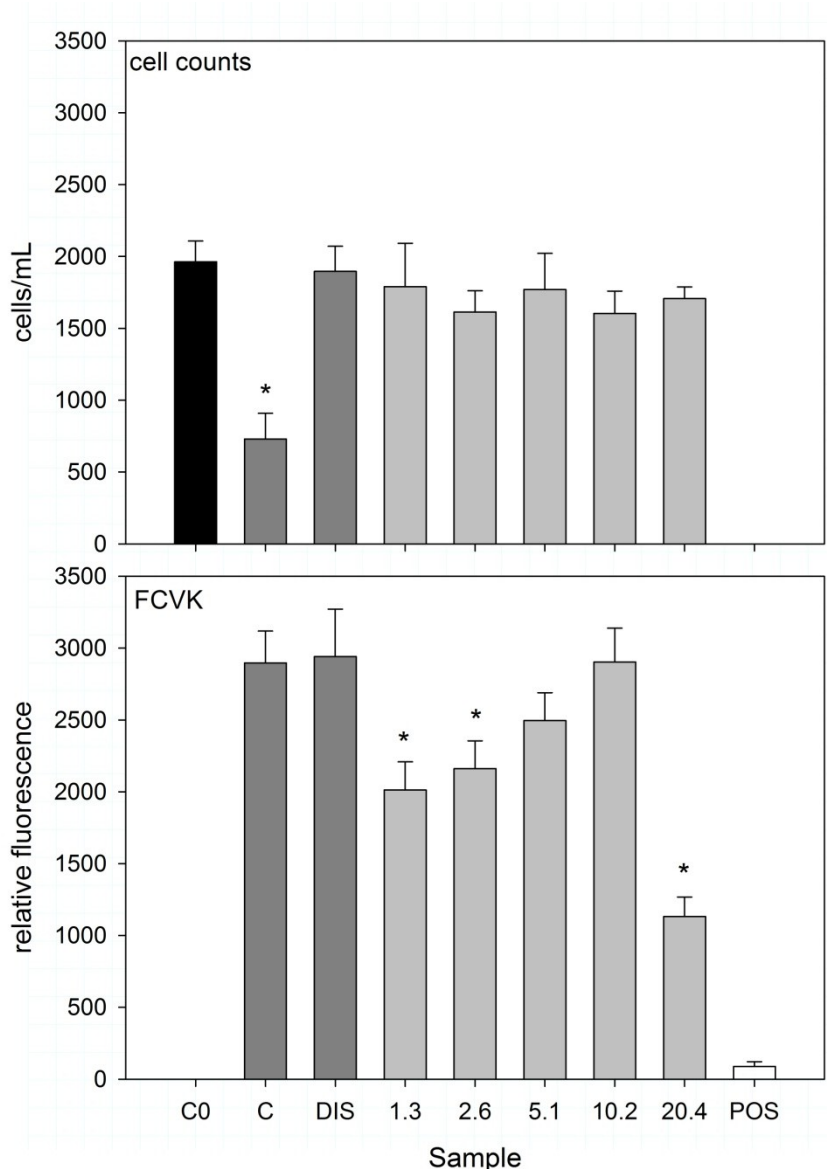


Figure 18: Bar charts of results from acute toxicity test with UV irradiation regarding cell counts and FCVK, showing mean values with standard error on y-axis. C0 = control at beginning, C = control at test end, DIS = dispersant control, numbers are nominal nTiO₂ concentrations in mg/L, POS = positive control; asterisks indicate statistically significant differences of respective treatments to dispersant control (DIS) with P < 0.05

Effect values in the mg/L range, higher than those concentrations tested here, would probably result in a risk to WWTP organisms according to risk quotient calculation on acute toxicity data. The PNEC would be in upper µg/L range, while PEC is 136 mg/L in activated sludge as estimated for Europe according to Gottschalk et al. (2009). Thus RQ would exceed 1, indicating environmental risk being present.

As described by the federal environmental agency of Germany (Wyrwoll et al., 2014), no effects were observed for standard toxicity testing with *Danio rerio*, *Eisenia foetida*

and in activated sludge respiration inhibition tests at concentrations below 100 or 1000 mg/L nTiO₂, respectively. NOEC for *Daphnia magna* was 18.5 mg/L. However, the authors stated that compared to other tests, where slight modifications of the test design were undertaken, effect values decreased to lower concentrations. For example, different endpoints or prolongation of test duration revealed differing results.

According to these findings and TGD (Technical-Guidance-Document, 2003), the next step in risk assessment would thus be to undertake more acute toxicity tests with different relevant organisms or proceeding to chronic toxicity tests. The latter was realized in this work, again applying *P. tetraurelia* as test organism.

Chronic toxicity tests

Chronic toxicity tests over 168 hours were conducted using mortality as endpoint determined by cell counts exclusively. In figure 19 results from chronic toxicity tests are displayed as growth curves. Data acquisition was not carried out at time points 120 h and 144 h.

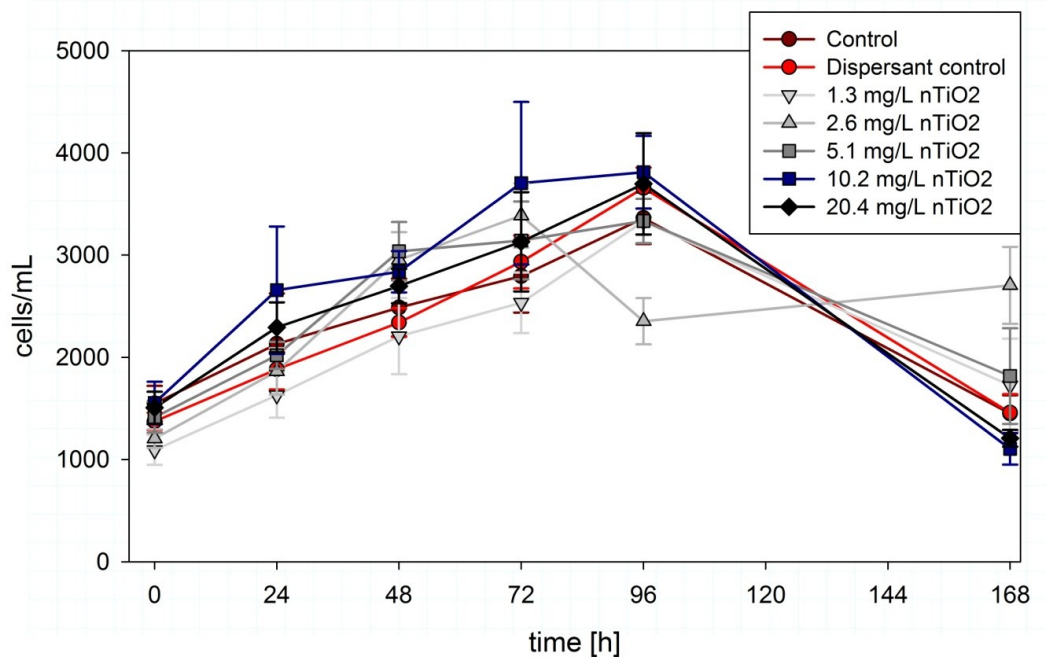


Figure 19: Chronic exposure with nTiO₂, cell density in controls and treatments over time. Error bars indicate standard error of means.

Regarding cell numbers at the beginning and end of the test (after 168 h), no statistically significant differences were found for cell density in all samples at the

beginning of the test, however, power of performed test was low. At the end of the test, significant differences between treatments with nominal nTiO₂ concentration 2.6 mg/L and the two highest concentrations were found by One-way ANOVA with $P < 0.05$. In the 2.6 mg/L treatment growth was negative in the time interval of 72 to 96 hours for unknown reasons, which increased insignificantly in the following period, resulting in the highest cell density at the end of the assay. Due to the high standard error this result should be regarded carefully and the difference of this treatment to the highest exposure treatments might be an artifact through random deviation of the sample from usual growth behavior or through counting errors. For example, it was observed that through storing of fixated samples, cells tended to stick to the walls of the reaction tubes and were not easy to transfer to counting chambers.

As shown before, stationary phase of *P. tetraurelia* growth in filtrated media ended after 96 h (see chapter 3.2). Although not all treatments had completely entered stationary phase after 96 h in chronic tests, obviously no shortening of exponential growth phase occurred due to exposure. Calculated growth rates (see figure 20) tended to zero with proceeding time and were between 0.0 and 0.3 cells per hour for the interval of 72 to 96 h throughout all samples. This indicated the immediately forthcoming end of exponential growth phase and differences between treatments could not be detected.

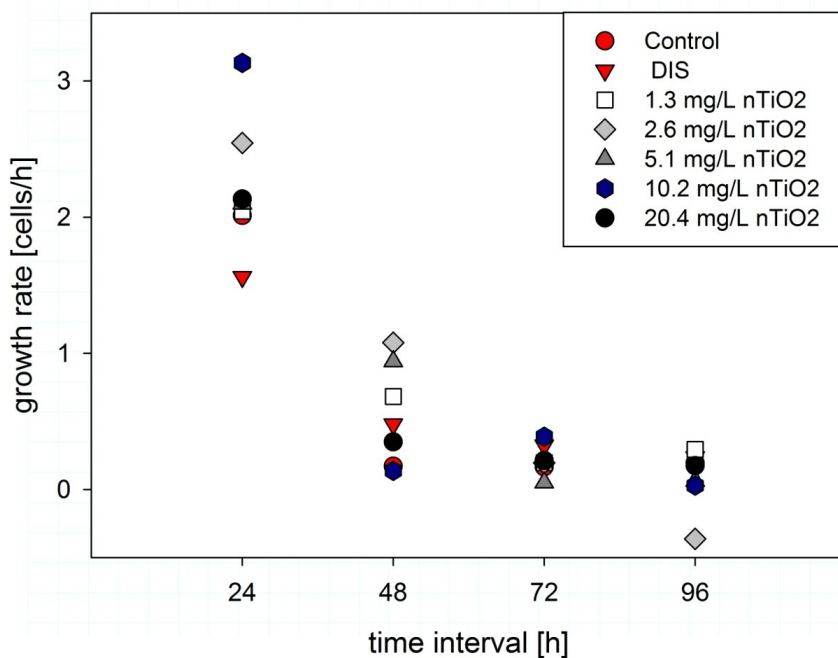


Figure 20: Growth rates as cells/h in different treatments of chronic exposure with nTiO₂ in 24 h time intervals.

No concentration response behavior was observed regarding growth parameters. According to these results, effects of NM-101 exposure to *P. tetraurelia* were not determinable and consequently risk was not assessable. Since PEC was estimated to 136 mg/L in activated sludge, still probability of occurring risk cannot be excluded for higher concentration in the mg/L range. For instance, Battin et al. (2009) investigated the toxicity of NM-101 on microbial biofilms at a concentration of 5.3 mg/L over a period of 48 h and found significant effects. However, the focus of their study was on receiving water bodies downstream from WWTP and it included UV irradiation under environmental conditions. A direct projection of these results to the conditions in activated sludge is not possible, as intrusion of light into activated sludge is not as high as in environmental waterbodies and microbial fauna and its structure differs drastically. Accordingly, also for chronic toxicity testing, the hypothesis 3 (toxicity of nTiO₂ on *P. tetraurelia*) was rejected.

Consequently, effects of NM-101 on other organisms relevant in WWTP should be regarded. Data for toxicity tests connected to activated sludge are scarce in the literature for NM-101, but for operational functioning of WWTP. Respiration inhibition test according to OECD guideline test number 209 revealed no observed effect concentrations (NOECs) higher than 1 000 mg/L (Wyrwoll et al., 2014). Although this concentration refers to a sublethal endpoint, it can be assumed that NOECs for viability and mortality might be found at similar ranges.

4 Single species tests with bacteria

4.1 Introduction – Bacteria in WWTPs and tested species

Microbes in activated sludge tend to aggregate in flocs due to the predatory pressure induced by Protozoa in the WWTP community. This process is important for WWTP operation, since biomass arranged in flocs settles better during tertiary treatment. At the outer layers of such flocs, oxygen and nutrient supply is higher than in the inner part of the flocs. Thus, in the extraneous regions of the flocs, aerobic microorganisms are more abundant, while anaerobes dominate in the center of the flocs.

Exemplarily for the aerobic and facultatively anaerobic bacterial community of activated sludge, a German WWTP (Berlin Ruhleben), was analyzed by Kämpfer et al. (1989; 1990) regarding the community composition. The most abundant genus was *Aeromonas*, with approximately 20%. Next to about 18% of unidentifiable microorganisms, the genera *Pseudomonas* and *Acinetobacter*, as well as the family of *Enterobacteriaceae* were very frequent in the community. All these groups belong to the subclass of gammaproteobacteria, which was also the most abundant subclass in a study of WWTP communities in the USA and China by Xia et al. (2010). Within the family *Enterobacteriaceae*, among other genera, *Enterobacter*, *Escherichia* and *Klebsiella* were found in the community. Nowadays, one *Klebsiella* strain is named as genus *Raoultella* (Drancourt et al., 2001). In WWTP using methanol for enhancing denitrification, facultatively methylotrophic bacteria of the genus *Hyphomicrobium*, belonging to the alphaproteobacteria, can be highly abundant (Lemmer et al., 1995). Their eponymous property of building hyphae and buds lead to the formation of large flocs or even contribute to the formation of floating sludge. Apart from this adverse aspect, *Hyphomicrobia* may play a significant role in denitrification processes (Lemmer et al., 1995). For toxicity tests of nAg on the bacterial part of the community, key species for single species tests were chosen based on abundance in activated sludge, special metabolic activities or contributions to wastewater treatment processes and for reasons of practicability in terms of transfer to food chain experiments with Protozoa. The genus *Nitrobacter* was chosen because it is involved in the nitrification process through oxidation of nitrite to nitrate. The species applied was *Nitrobacter vulgaris* as a strain isolated from a WWTP. *Raoultella planticola*, as representative of the frequently abundant *Enterobacteriaceae*, was utilized additionally for the reason of being an established food organism for *Paramecium* which was practicable for food chain experiments. *Hyphomicrobium sp.* was deployed

as WWTP isolate in toxicity tests due to its relevance for denitrification and its special physical properties.

4.2 Experiments with *Raoultella planticola*

4.2.1 Introduction – *R. planticola*

Raoultella planticola is a gammaproteobacterium and belongs to the family *Enterobacteriaceae* which is the dominating taxon in the microflora of aerated wastewater along with *Pseudomonadaceae* (Filipkowska et al., 2000).

Bacteria of the genus *Raoultella* are gram-negative, non-motile, capsulated rods of 1 to 6 μm length, which propose respiratory and fermentative metabolism and thus are able to live aerobic and facultatively anaerobic. The cells are oxidase-negative and catalase positive (Drancourt et al., 2001).

Methods and results of all *Raoultella planticola* experiments were established and obtained from the diploma thesis work of Patrick Obert-Rausser under supervision of the author of this thesis.

4.2.2 Growth kinetics of *R. planticola* at experimental conditions

The tests were performed according to Obert- Rausser (2012) and are described in detail subsequently.

4.2.2.1 Materials and Methods for *R. planticola* growth kinetics

The *Raoultella planticola* (V-236 strain) was obtained from Leibniz Institute DSMZ-German Collection of Microorganisms and Cell Cultures (Braunschweig, Germany). The bacteria were cultivated in cerophyl medium (CM) prepared according to Sonneborn (1970) modified as described by Krenek *et al.* (2011) (see ANNEX II: Protocol for 0.25% Cerophyl-Medium (CM) for details). The pH of the CM was 6.9 ± 0.09 (LF340, SenTix 61 pH electrode, WTW, Weilheim, Germany). For all liquid handling Eppendorf pipettes equipped with plastic tips were used. Centrifuge tubes (TPP, Switzerland) were used for cell cultures and experiments.

Growth kinetics of *R. planticola* were determined according to three methods: biomass by optical density (OD_{600}), viability by fluorescence and colony forming units (CFU) by agar plating. Figure 21 depicts an overview of the experimental procedure.

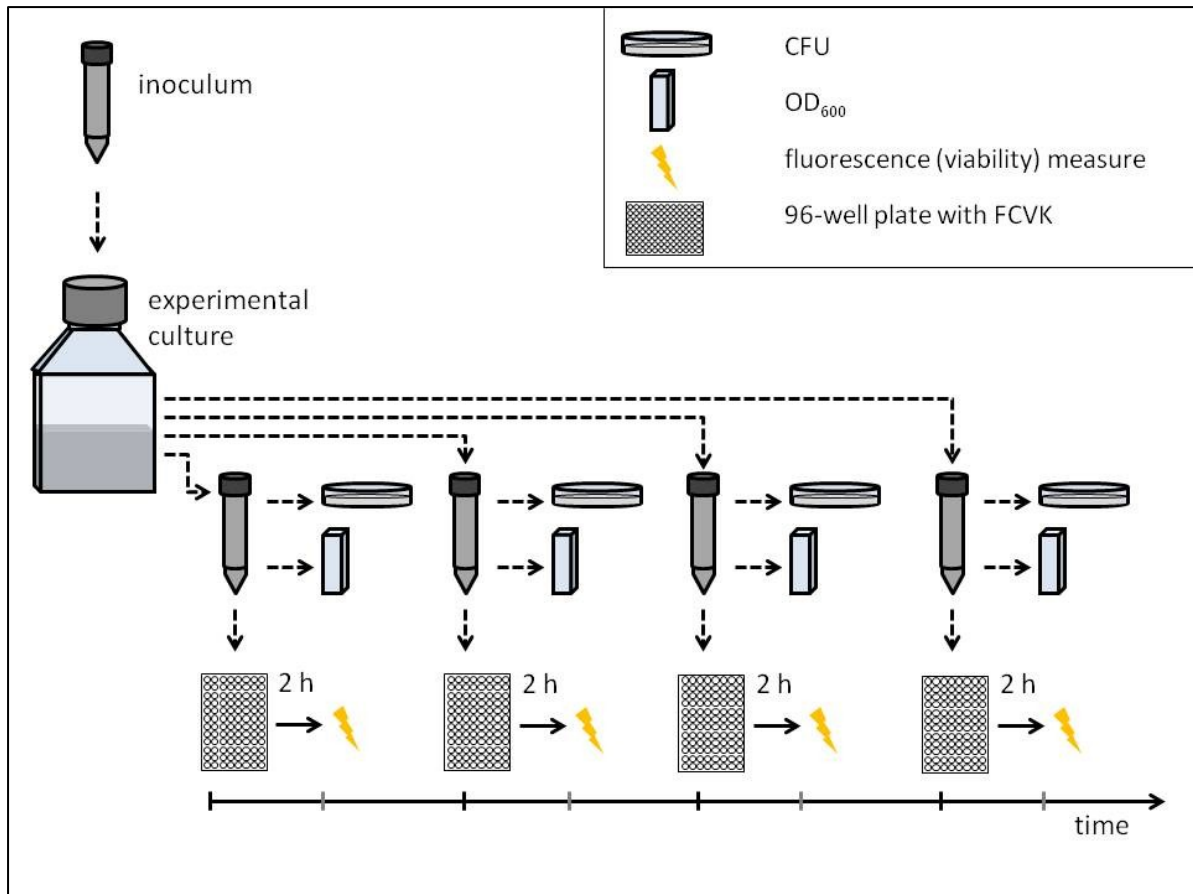


Figure 21: Flowchart of experimental setup for growth kinetic of *R. planticola*.

A liquid culture in CM, previously cultivated at 22°C on a rotation shaker (Innova 42, New Brunswick Scientific Co., Inc., Edison, NJ, USA) was used as inoculum for 50 mL fresh CM. For determination of initial number of CFU/mL a defined volume of two dilutions of the liquid culture were plated on Mueller-Hinton agar immediately after inoculation and incubated at 30°C (KB53, Binder GmbH, Tuttlingen, Germany) for 24 h. At the same time, samples were drawn for OD₆₀₀ measures in polystyrene cuvettes (Brand GmbH & Co. KG, Wertheim Germany) and absorbance at 600 nm wavelength was determined. The liquid culture was incubated at 22°C on the shaker. At regular intervals, 100 mL aliquots of the liquid culture were transferred to 96-well plates (pure grade S, transparent, F- bottom, Brand GmbH & Co KG, Wertheim, Germany) in 8 replicates. 10 µL of fluorometric cell viability kit I (FCVK, PromoCell GmbH, Heidelberg, Germany) were added to each well and incubation was continued for 2 hours. After this incubation time, fluorescence of the samples on 96-well plates was measured utilizing a Polarion plate reader (Tecan Group Ltd., Switzerland). At the same time samples from the incubated liquid culture were drawn for dilution plating

on agar and for OD₆₀₀ measures as described before. Approximately 24 h after each sampling event, CFU on the agar plates were counted.

4.2.2.2 Results and Discussion of *R. planticola* growth kinetics

In preliminary tests with OD₆₀₀ and CFU as endpoints for growth kinetics, *Raoultella planticola* cultures were prepared in the same way as for toxicity tests, i.e. cultures were adapted to 22°C temperature previous to inoculation of medium.

In these experiments, size of inocula (CFU/mL) and adaptation time to experimental conditions seemed to be parameters influencing growth kinetics, i.e. the duration of lag and exponential phase (data not shown). Longer adaptation times correlated with shorter lag phases and higher number of CFU/mL in inocula correlated with shorter exponential phases. Accordingly division rate ν and generation time gt (see equation 5 and 6, page 20) were correlated with inocula sizes and time for adaptation. In the tests conducted here, size of inocula were always connected to the longer or shorter adaptation time, thus the definitive effects of each of the two parameters cannot be inferred. As also described by Robinson et al. (2001) physiological state, previous growth environment and temperature history of the inoculation culture were shown to have profound effects on the duration of lag phase and subsequently on exponential phase. According to Robinson et al., size of inocula seemed to affect growth parameters only under suboptimal conditions for the culture. Variation of constants due to uncontrollable parameters is a known phenomenon of growth kinetics in microbial ecology (Lindqvist, 2006).

Correlation of OD₆₀₀ values with CFU/mL of a growing culture suggests a partitioned linearity of correlation for the two evaluated parameters (figure 22).

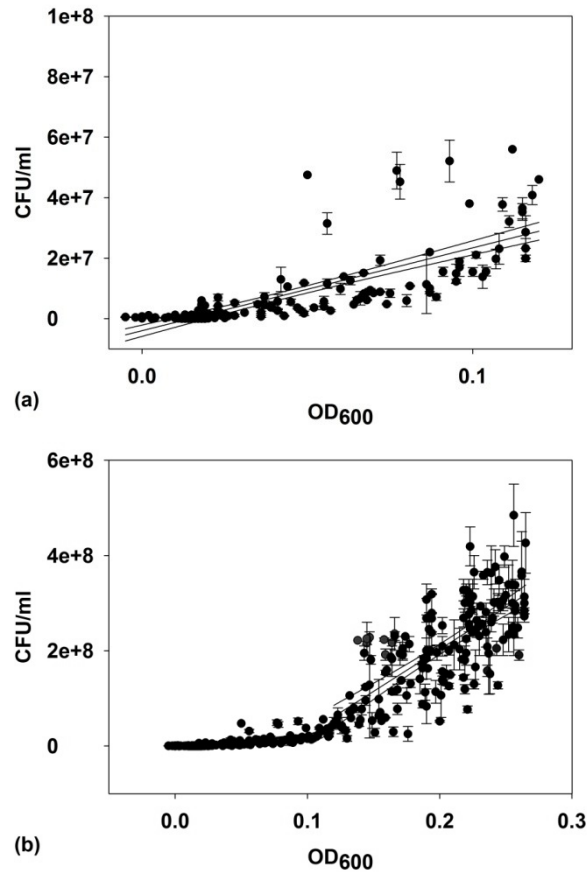


Figure 22: Correlation of CFU/mL with OD₆₀₀ values in a growing cell culture of *R. planticola*, (a) for OD₆₀₀ < 0.12 and (b) for all OD₆₀₀ measured. Regression lines (inner lines) with $r^2 = 0.6$ for a), $r^2 = 0.53$ for b) and 95% CIs (outer lines) are displayed. Error bars indicate standard error of means.

At low cell densities an increase of OD₆₀₀ up to 0.12 did not also result in significant increases of CFU/mL and slope of the regression was low, r^2 was 0.6 ($P < 0.001$). At higher cell densities, starting at an OD₆₀₀ of 0.12, the correlation was more proportional with a higher slope of regression. At high cell densities (OD₆₀₀ > 0.12 and more than $2 \cdot 10^7$ CFU/mL) fit of regression lines was lower with r^2 of 0.53 ($P < 0.001$) compared to lower cell densities (OD₆₀₀ < 0.12 and less than $2 \cdot 10^7$ CFU/mL) and scattering of CFU around the regression line increased. Reasons for these findings might be deviations in the accuracy of absorption measures, because multiple scattering of light by bacterial cells can occur at high cell densities and on the other side, not all bacteria are freely dispersed, leading to underestimation of absorbance. Both effects might lead to a bias of OD₆₀₀ values. Dilution of the cells prior to plating on agar also holds sources for errors in CFU determination. At higher cell densities dilution has to be increased leading to higher standard errors of CFU values. Nevertheless, for preparation of growth kinetics experiments at comparable conditions, a guidance value was required to quickly estimate the cell density in the

experimental culture and to select the dilution factor for agar plating at the beginning of the experiment. For this reason, based on data shown in figure 22, dilution levels were assigned to OD₆₀₀ values as depicted in table 6 and used for subsequent experiments with additional viability measurement.

Table 6: OD₆₀₀ values with assigned dilution levels for agar plating of *R. planticola* cultures.

OD ₆₀₀	Dilutions on agar plates
<0.02	10 ⁻² ; 10 ⁻³
0.02 – 0.05	10 ⁻³ ; 10 ⁻⁴
0.05 – 0.12	10 ⁻⁴ ; 10 ⁻⁵
0.12 – 0.3	10 ⁻⁵ ; 10 ⁻⁶

The CFU value of the culture used for growth experiments estimated from OD₆₀₀ was $2.2 \cdot 10^8$ per mL while agar plating yielded a CFU of $2.95 \cdot 10^8 \pm 0.255 \cdot 10^8$ per mL which is in good accordance. After inoculation of 50 mL CM with 50 μ L from this culture, CFU was estimated as $1 \cdot 10^7$ per mL and was confirmed by agar plating ($1 \cdot 10^7$ per mL). Lag phase of all determined growth curves lasted for 20 h followed by an exponential growth phase of approximately 10 h (figure 23).

While OD₆₀₀ and CFU/mL remained constant during the adjacent stationary phase throughout the observed time frame, relative fluorescence decreased after 40 h suggesting a reduction of viability of the cells. This could be due to nutrient limitation, because resources decrease rapidly in an exponentially growing batch culture. Viability seemed to be the most sensitive endpoint, reacting on suborganismic level at a point where either bacteria start to take up dormant stages or before extinction of the culture begins. As viability measures are connected to cell metabolism it is a more dynamic endpoint than OD₆₀₀ and CFU which are rather inert. Additionally, for CFU determination, scattering increases with number of CFU/mL. At higher CFU values, dilution of experimental culture prior to agar plating needs to be increased, leading to an increased dilution error accordingly.

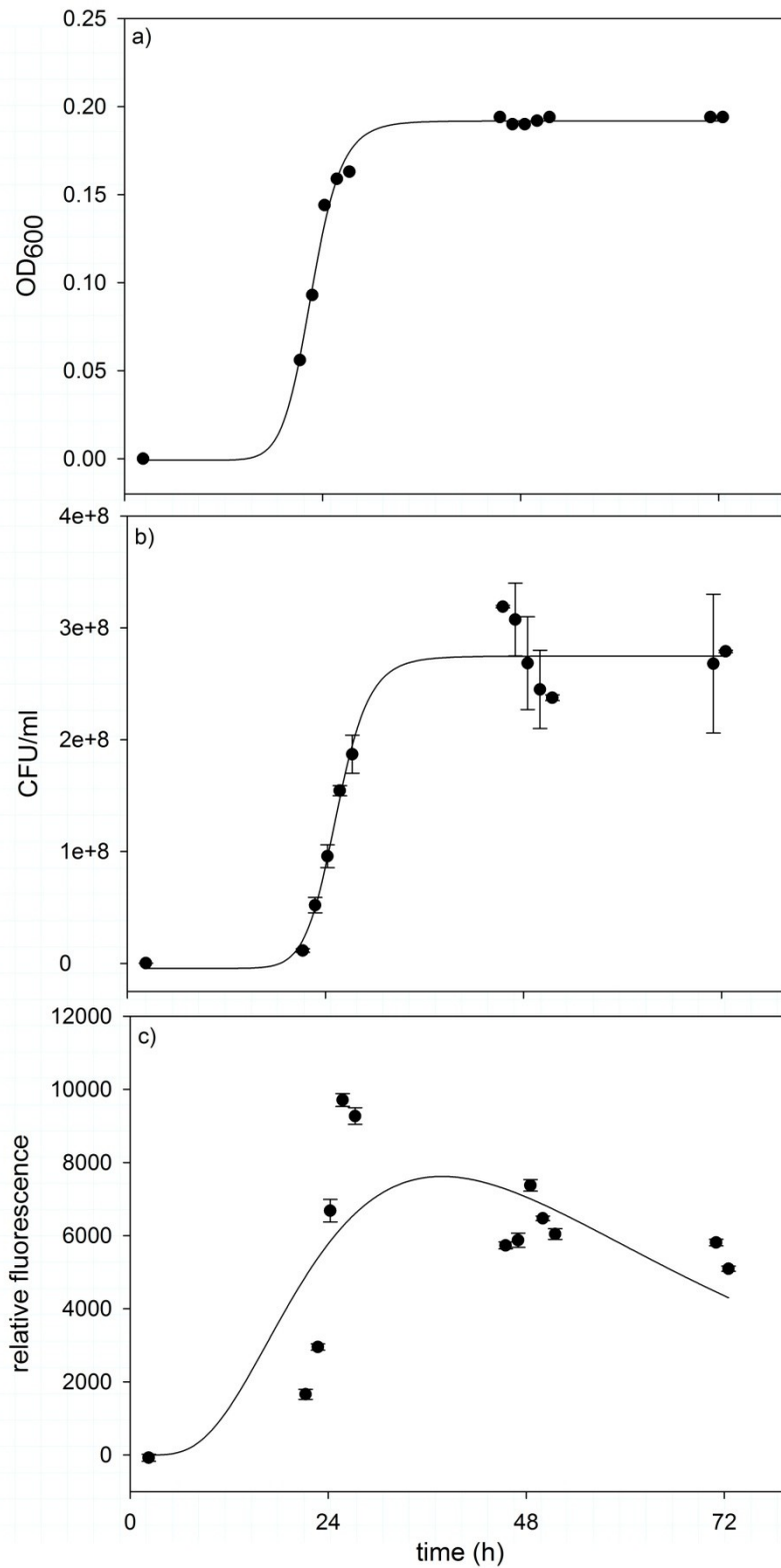


Figure 23: Growth curves obtained from a) OD₆₀₀, b) CFU/mL, and c) relative fluorescence, over 72 h. For OD₆₀₀ curve, r^2 of the sigmoid function was 0.9940 ($P < 0.0001$) and for CFU/mL $r^2 = 0.9631$ ($P < 0.0001$). For relative fluorescence r^2 of the log-normal-3-parameters function was 0.524 ($P = 0.025$). Error bars indicate standard deviation, if applicable. Error bars indicate standard error of means.

Correlations of the determined endpoints against each other are shown in figure 24.

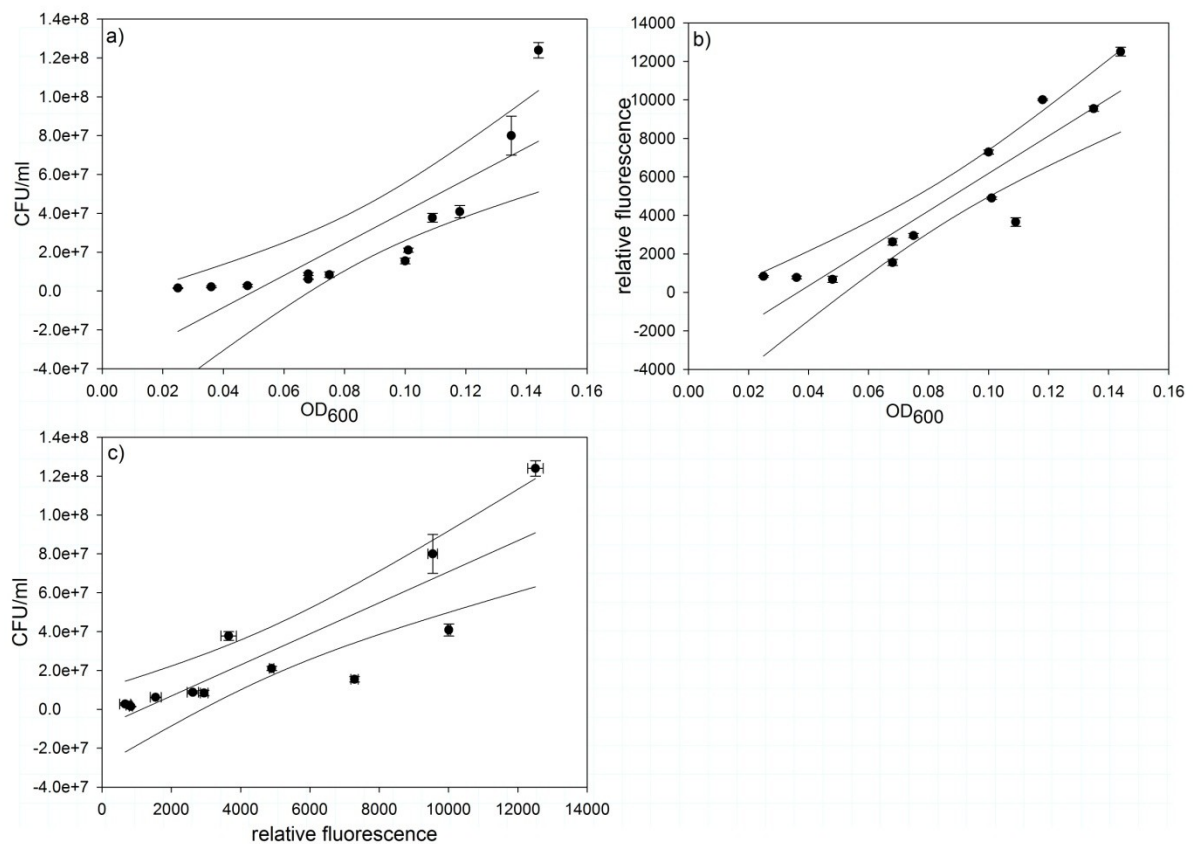


Figure 24: Correlations of all determined endpoints against each other, a) CFU vs. OD₆₀₀, $r^2 = 0.70$; b) relative fluorescence vs. OD₆₀₀, $r^2 = 0.83$; c) CFU vs. relative fluorescence, $r^2 = 0.76$. Curved lines represent 95% CI. Error bars indicate standard error of means.

The best correlation between respective endpoints was found for relative fluorescence data with measured OD₆₀₀ ($r^2 = 0.83$). These two endpoints were thus applied for subsequent toxicity tests. The correlations between CFU and the other two endpoints was probably less because of the high scattering in CFU data after 40 hours as seen in figure 23 b). Generation time was calculated for all of the three methods of growth determination according to equations 5, 6 and 7 (see section 3.2.1, page 20). Results are depicted in table 7, along with the mean value from all three methods.

Table 7: Generation time *gt* of *R. planticola* at 22°C according to different methods of growth kinetic determination.

Method	<i>gt</i>
OD ₆₀₀	0.63 h (38 min)
CFU	0.11 h (7 min)
Fluorescence	0.33 h (20 min)
Mean	0.35 h (21 min)

Generation time according to fluorescence was closest to the mean value of all methods (0.35 h). This generation time of *R. planticola* is fast, compared to growth of *E. coli* at 22°C. The values for *E. coli* in literature, however determined from steady state or continuous culture in different media, were between 1.3 (Shehata and Marr, 1975) and 3.6 h (Kovářová et al., 1996). For acute toxicity testing, the identified generation time was considered for determination of incubation period, but also other factors such as incubation time for fluorescence dye needed to be included in the experimental design.

4.2.3 Toxicity tests with *Raoultella planticola* and nAg

Cerophyl medium (CM) was employed as broth for bacteria cultivation because the bacteria suspension is also usable for feeding ciliates and thus provides the opportunity to expand research on the interactions between bacteria and ciliates. The tests were performed according to Obert- Rauser (2012) and are described in detail subsequently.

4.2.3.1 Materials and methods for *R. planticola* toxicity tests

R. planticola stock cultures were cultivated in CM at conditions described above (section 4.2.2.1).

Stock dispersions of nAg and AgNO₃ were prepared in 2 mL reaction tubes (Polypropylene, Eppendorf, Wesseling-Berzdorf, Germany) for the characterization of nAg in media and for the preparation of toxicity tests. The nAg-stock dispersion established in cerophyl medium (CM, see below) nominally contained 1.2 g/L total Ag. Stock solutions with the corresponding concentration of the dispersant were prepared using CM and NM-300K DIS. The AgNO₃-stock solutions for the toxicity tests contained 5 g AgNO₃/L in CM.

Characterization

The hydrodynamic diameter of nAg in nominal concentrations of 53.6 µg/L, 80 µg/L, 120 µg/L, 180 µg/L and 270 µg/L total Ag in CM were characterized via dynamic light scattering (DLS) using a Zetasizer Nano ZS along with clear disposable zeta cells (Malvern, Westborough, USA). Temperature was set to 22°C, the time for equilibration was 120 s, the viscosity of the CM was 1.00 and the refractive index of the CM was 1.36. For each nAg concentration 5 replicates with 10 runs each were analyzed.

UV-vis spectroscopy was applied for size analysis of nAg. The absorption spectra over a wavelength from 300 to 600 nm (U-2000, Hitachi, Düsseldorf, Germany) were recorded for nAg dispersions at the same nominal concentrations as above and additionally 6.92 mg/L nominal total Ag. For each concentration 4 replicates were analyzed. Diameter of nAg was derived from the maximum absorption and the peak width at half maximum (see page 10). Size analysis via scanning electron microscopy was carried out for CM with and without *R. planticola* and 270 µg/L nominal total Ag. Four mL of each sample were filtered through 0.05 µm-Filters (polycarbonate membrane filter, 13 mm, Sterlitech, Kent, USA) utilizing an exhaustor. The filters were sputtered with a 1 nm layer of platinum. Primary size and morphology of nAg were determined using a digital scanning electron microscope (DSM 982 Gemini, Zeiss, Oberkochen, Germany).

Toxicity Tests

Nominal test concentrations were 53.6 µg/L, 80 µg/L, 120 µg/L, 180 µg/L and 270 µg/L total Ag, which corresponds to nominal nAg concentrations of 48.2 µg/L, 72 µg/L, 108 µg/L, 162 µg/L and 243 µg/L. Potential toxic effects were also evaluated for respective concentrations of the dispersant. Exposure to AgNO₃ was performed with nominal concentrations of 4.9 µg/L, 7.4 µg/L, 11 µg/L, 16.5 µg/L and 24.9 µg/L. Negative controls (NC) without silver were employed and 1000 µg/L AgNO₃ as positive control (PC) were used in all toxicity tests performed. All tests were conducted with four replicates per concentration or control.

In 15 mL centrifuge tubes (Corning Inc., Acton, USA), 12.5 mL CM and respective nAg, dispersant or AgNO₃-liquids were mixed to attain the intended exposure concentrations after addition of the inocula. For inocula *R. planticola*-culture in CM was cultivated at 22°C on a shaking incubator (120 rpm, Innova 42, New Brunswick Scientific, Nürtingen, Germany) and OD₆₀₀ was measured (BioPhotometer plus,

Eppendorf, Hamburg, Germany) at 30 minutes intervals. At an OD₆₀₀ of 0.08, diluted samples of the culture were plated out on Mueller-Hinton Agar-plates (Carl Roth GmbH + Co Kg, Karlsruhe, Germany) to determine the colony-forming units (CFU) per mL of culture. 2.5 mL of the culture were added to each of the prepared centrifuge tubes and the OD₆₀₀ of the exposure assays were determined. Exposure assays were incubated at 22°C and 120 rpm for 5 h. Bacterial biomass was determined as cell density by measures of OD₆₀₀ and cell viability using “Fluorometric Cell Viability Kit I” (FCVK, PromoCell GmbH, Heidelberg, Germany). After three hours of exposure, 96-well plates (pure grade S, transparent F-bottom, Brand GmbH & CO KG, Wertheim, Germany) were prepared from exposure assays by adding 100 µL liquid per well and additionally 10 µL FCVK. The 96-well plates and centrifuge tubes were incubated for further two hours. After a total exposure duration of five hours, fluorescence was determined in the 96-well-plates using a fluorescence microplate reader Polarion (Tecan Group Ltd., Männedorf, Switzerland) and the OD₆₀₀ of the exposure assays in the centrifuge tubes was determined.

Analytics

ICP-OES analysis was performed to determine the amount of total Ag and Ag⁺ in the conducted toxicity tests, as described above except some minor variations. As for the ICP-OES analysis a volume of about 10 mL is required per sample, the tests were re-conducted at a higher volume of 50 mL per sample, with two replicates of nominal total Ag concentrations of 53.6 µg/L, 120 µg/L and 270 µg/L. Additionally 270 µg/L total Ag without bacteria were analyzed. Directly after the initial determination of the OD₆₀₀, 10 mL of each sample were extracted, filled into 15 mL centrifuge tubes and fixated by adding a drop of 69% HNO₃. These samples were used for the determination of the total amount of Ag at the start of the experiments. For determination of Ag⁺, particulate silver was settled by centrifugation (Eppendorf centrifuge 5810 R equipped with high-speed fixed angle rotor F-34-6-38, Eppendorf, Hamburg, Germany). 12 mL from each vessel were filled into 15 mL centrifuge tubes and centrifuged at 15 557 x g and 22°C for 135 min. Subsequently 10 mL of supernatant were transferred into fresh 15 mL centrifuge tubes and fixated as described above. After assessment of the OD₆₀₀ and the fluorescence at the end of the toxicity tests, samples were extracted and fixated as described above to evaluate the amounts of total Ag as well as Ag⁺ at the end of the experiment. ICP-OES analysis was carried out using an Optima 7300 V HF Version ICP-OES Spectrometer (Perkin Elmer, Waltham, Massachusetts, USA)⁷. Determined concentrations were compared

⁷ Carried out at Helmholtz center for environmental research Magdeburg, N. Scheibe

to nominal concentrations as derived from analysis of manufactured dispersion described above (see chapter 2 Nanomaterials).

Statistical analyses and calculation of concentration-response curves was performed with Toxrat Standard V2.10.05 (Toxrat® Solutions GmbH) software. Results were plotted using Sigma Plot 11.0 software.

4.2.3.2 Results and Discussion of *R. planticola* toxicity tests

Characterization of nAg

Results from DLS analyses of pure CM indicated a peak with an average hydrodynamic diameter of 232 ± 10 nm (table 8). The particles causing this peak originate from CM ingredients and hence were found in all other assays, too, showing an average hydrodynamic diameter of 222 ± 7 nm. The size of these particles did not differ significantly in the different exposure assays at varying concentrations of nAg ($P = 0.113$, One-way ANOVA).

Table 8: Hydrodynamic diameters of nAg in CM (Concentrations in μg of nominal total Ag per L CM, $n = 5$).

Sample	Peak 1 Mean diameter \pm SE	Peak 2 Mean diameter \pm SE
CM	232 ± 10	-
53.6 μg	237 ± 23	55 ± 8
80 μg	230 ± 9	35 ± 8
120 μg	211 ± 13	42 ± 6
180 μg	242 ± 20	54 ± 8
270 μg	181 ± 16	41 ± 3
Mean \pm SE [μg]	222 ± 7	45 ± 3

In the nAg exposure assays a second peak was found with an average hydrodynamic diameter of 45 ± 3 nm (table 1). The size of the particles affecting this peak was not significantly different in all concentrations ($P = 0.213$, One-way ANOVA). With increasing concentration of nAg, hydrodynamic diameters did not increase. Adsorption of nAg to medium borne particles was negligible, since no increase of hydrodynamic diameters along with concentration and compared to pure CM was found through analysis of peak 1.

The applied exposure concentrations for toxicity tests were too low for detection by UV-vis spectroscopy. A size of 20-27 nm was derived from the absorption spectrum at a concentration of 6920 $\mu\text{g/L}$ nominal total Ag. These diameters reflect the particle diameters of NM-300K given by the manufacturer.

In figure 25, a SEM picture of CM with 270 $\mu\text{g/L}$ nominal total Ag without bacteria is depicted. Primary nAg particles with an approximate size of 20 nm (A) and larger particles with approximately 200 nm (B) are to be seen. Black pitches (C) are the pores of the filter (50 nm).

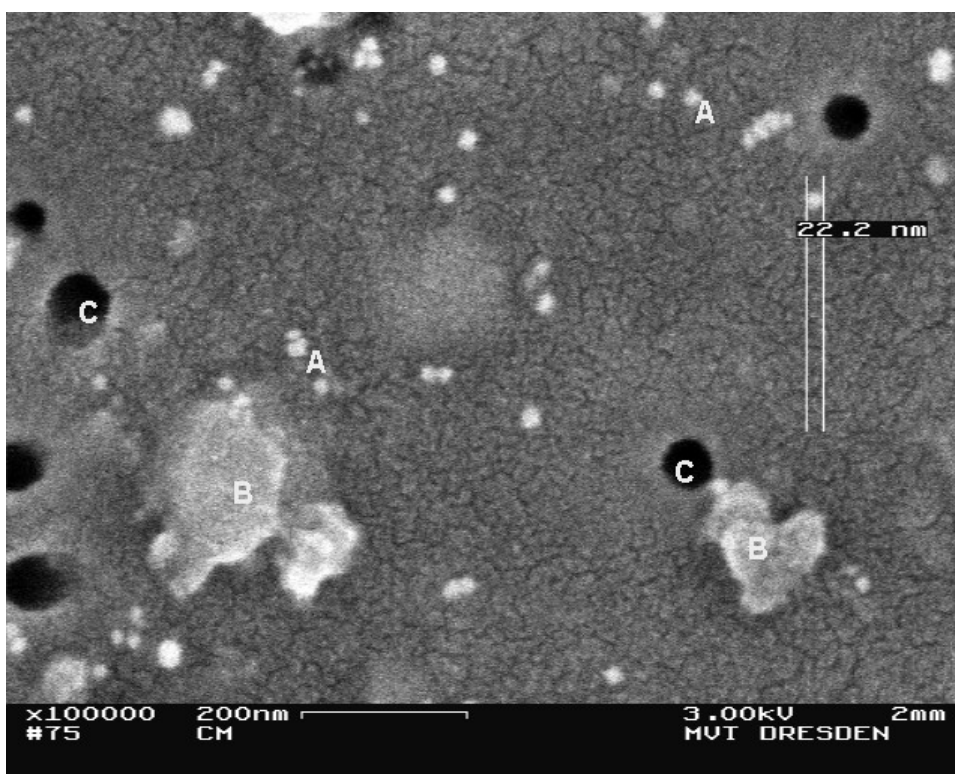


Figure 25: SEM photograph of CM with 270 $\mu\text{g/L}$ Ag at 100000-fold magnification. The vertical white lines are accessories of the SEM tool for size determination. The number displayed next to them is the size of the analyzed particle between the lines.

For reasons discussed in the previous chapter (see section 3.3.2) it is likely, that results from UV-vis spectroscopy and SEM analyses mirror the true status of particle size under exposure conditions in contrast to DLS results. Particles sized approximately 200 nm, as found by DLS and SEM, most probably originate from medium borne organic matter of CM.

Photographs of CM containing 270 $\mu\text{g/L}$ nominal total Ag with bacteria are displayed in figure 26. Rod-shaped structures with the length of approximately 1-3 μm , which represent the bacteria, cover the whole surface of the filter. Light, spherical particles are located at the intersections between the bacteria. Because of the high density of bacteria in the sample and the low size of the pores no singly dispersed cells could be detected.

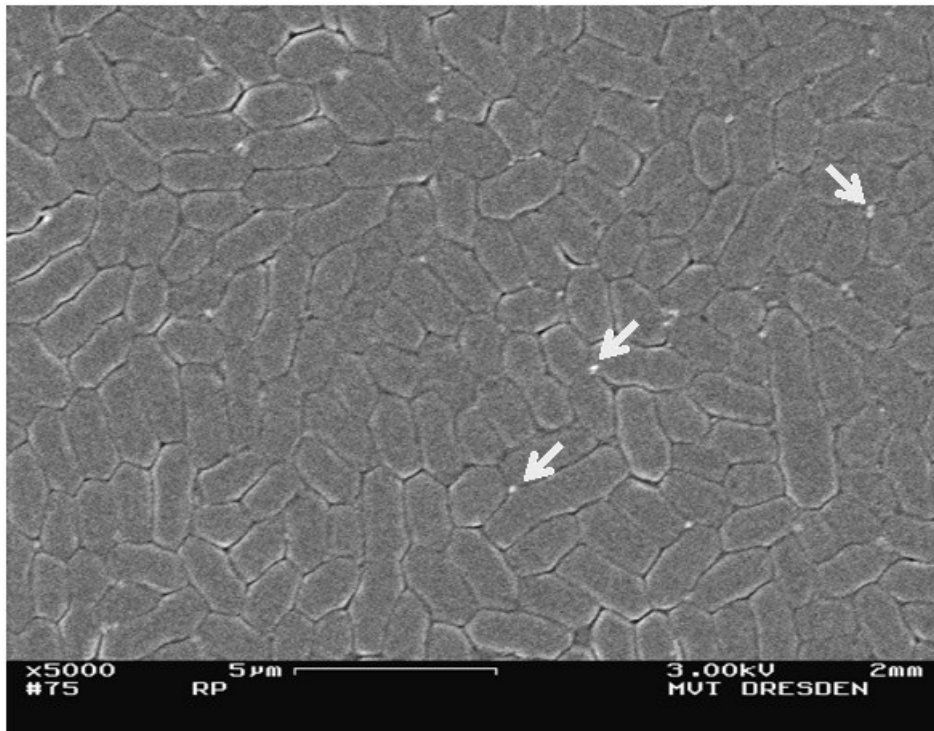


Figure 26: SEM photograph of 270 $\mu\text{g/L}$ nominal total Ag and *R. planticola* at 5000-fold magnification. Arrows exemplarily show some nanoparticles present in the sample.

Comparable pictures of bacterial cells via SEM have been recorded by Sondi & Salopek-Sondi (2004). Note that the congregation of nAg in the intersections of the cells could be artifacts of SEM-sample preparation with the exhaustor.

Analytics

The concentrations of total Ag at the beginning and the end of the experiment determined via ICP-OES analysis are shown in table 9. Measured amounts of total Ag at the beginning and the end of the experiment are statistically not significantly different. Compared to the nominal concentrations of total Ag, the determined amounts deviate by approximately 50%. Possible reasons for this discrepancy are

measuring errors from weighing in minute amounts of stock dispersion, as well as adsorption of nAg to pipette tips during liquid handling. Chemical analysis of working stocks should be undertaken in order to avoid overestimation of exposure concentrations. Presence of bacteria did not seem to interfere with analysis as results from ICP-OES did not differ significantly between exposure solution with and without bacteria.

Table 9: Ag-concentrations according to ICP-OES analysis in CM at the start and the end of the toxicity test (n = 2).

Sample	Nominal Conc. [µg/L]	Conc. Start Mean ± SD [µg/L]	Conc. End Mean ± SD [µg/L]
NC	0	Below LOD	Below LOD
PC	640	441.6 ± 8.1	433.6 ± 6.3
53.6	53.6	23.8 ± 0.6	30.3 ± 2.1
120	120	54.7 ± 2.6	57.8 ± 2.1
270	270	134 ± 1.9	134.5 ± 0.3
270 without bacteria	270	125.7 ± 9.8	124.7 ± 3.1

LOD: Limit of determination.

A linear regression with the displayed equation describes the relation between measured and nominal total Ag concentrations (figure 27). The regression function was used to derive values of contained total Ag (see table 10) in toxicity tests with nAg, in which no chemical analysis was conducted (see toxicity tests below).

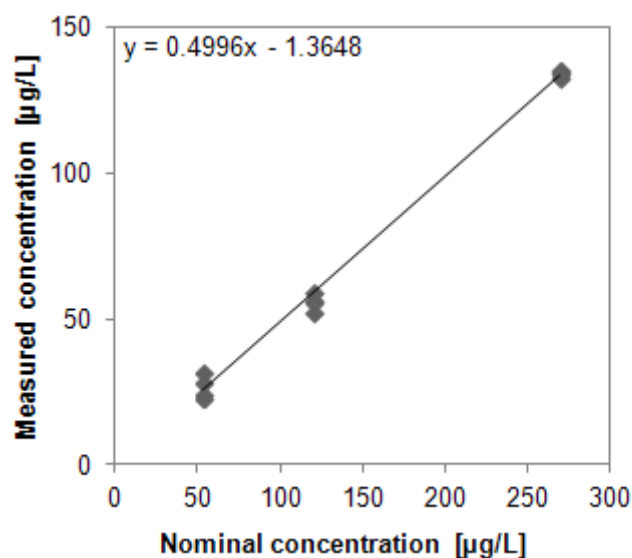


Figure 27: Measured concentrations of total Ag plotted against nominal concentrations of total Ag.

Table 10: Nominal and inferred concentrations derived from regression function in *Raoultella* toxicity tests.

Nominal Concentration [$\mu\text{g/L}$]	Derived concentration [$\mu\text{g/L}$]
0	0
53.6	25
80	39
120	59
180	89
270	134

Results of ICP-OES analyses of Ag^+ and Ag-salts were below LOD for all samples. Subsequently, inductively coupled plasma mass spectroscopy (ICP-MS) analysis was undertaken, because LOD of this method is lower compared to ICP-OES. Results were unaccountable, indicating cross contamination of the samples. For this reason, nAg fraction in the samples could not be calculated and hence consecutively all results and discussion will refer to total Ag concentrations.

Toxicity tests

The relative inhibition of bacteria at the end of the toxicity test plotted against the measured concentrations of total Ag is shown in figure 28. The calculated 5h EC_{50} for OD_{600} in the toxicity tests with nAg was 77 $\mu\text{g/L}$ total Ag and according to the fluorescence it was 111 $\mu\text{g/L}$.

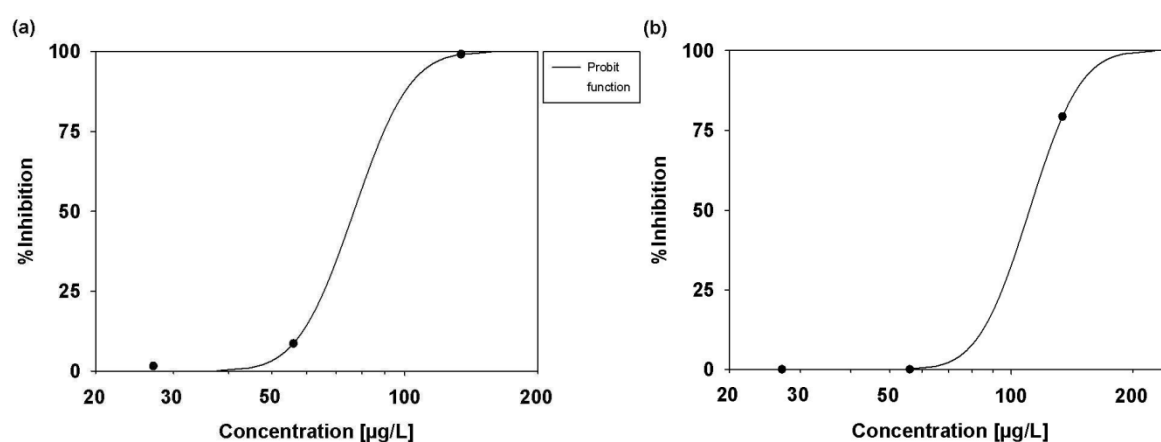


Figure 28: Relative inhibition of *R. planticola* exposed to nAg depicted as concentration-response curves. Concentrations stated as total Ag according to ICP-OES analyses. Inhibition of the OD_{600} (a) and fluorescence (b) after 5 h exposure to nAg.

A 95%-confidence interval (CI) could not be calculated by ToxRat software due to the low number of concentrations and replicates. To obtain more reliable EC₅₀ results, the test was repeated with five concentrations of nAg and higher replicate number, however without ICP-OES analysis due to practicability. Nominal concentrations were transformed to effective (i.e. derived realistic) concentrations according to regression as depicted in figure 27 and table 10 (see above).

In a parallel assay, probable effects of the dispersant were tested. No effect was observed for all tested concentrations of the dispersant (up to 220 µg/L) on *R. planticola* (P=0.155 for OD₆₀₀, P=0.949 for fluorescence, One-way ANOVA; data not shown).

Clear concentration response curves were obtained for OD₆₀₀ and fluorescence results of nAg exposure. The relative inhibition of bacteria is shown in figure 29 with cell viability and OD₆₀₀ as toxicological endpoint plotted against calculated concentrations according to table 10.

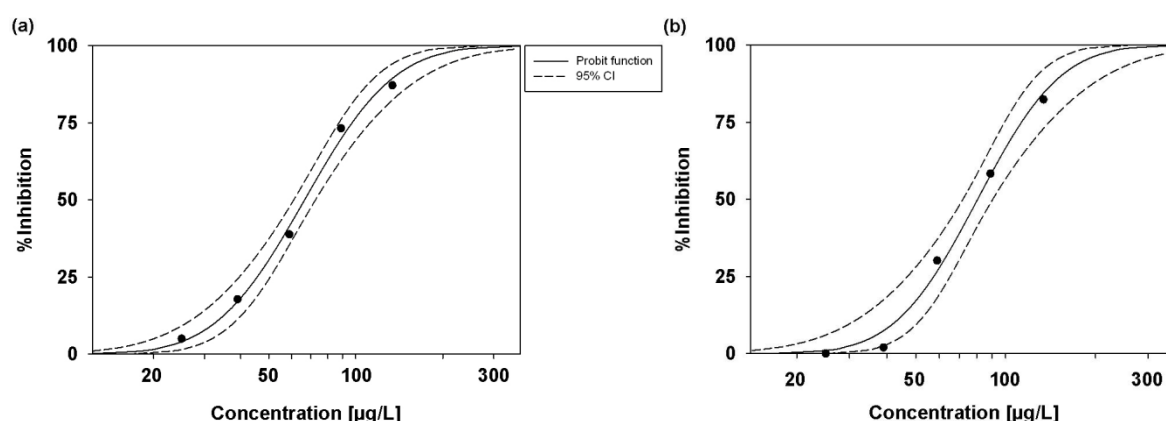


Figure 29: Derived inhibition of *R. planticola* exposed to nAg depicted as concentration-response curves. Concentrations stated as total Ag estimated according to table 10. Inhibition of the OD₆₀₀ (a) and fluorescence (b) after 5 h exposure to nAg with 95% CI.

For OD₆₀₀ the extrapolated 5h EC₅₀ of total Ag in the toxicity tests with nAg was 67 µg/L (95% CI 61-73 µg/L) and according to the fluorescence it was 81 µg/L (95% CI 72-91 µg/L). Tests were repeated to evaluate reproducibility of results. Table 11 lists the 5h EC₅₀ of measured total Ag for the first attempt accompanied by ICP-OES and 5h EC₅₀ of estimated total Ag according to the concentration values from table 10 for the second and third attempt.

Table 11: Median effective concentrations derived from the toxicity tests with nAg according to OD₆₀₀ and fluorescence.

Parameter	Method of measurement	1. attempt Accompanied by ICP-OES	2. attempt	3. attempt
EC ₅₀ [µg/L] (95% CI)	OD ₆₀₀	77	67 (61 - 73)	60 (48 - 74)
EC ₅₀ [µg/L] (95% CI)	Fluorescence	111	81 (72 - 91)	52 (40 - 66)

Statistical differences between obtained EC₅₀ values were analyzed using a formula (equation 9) taken from the guidance document on statistical methods for environmental toxicity tests (Environment Canada, 2005) which is applicable for comparison of multiple EC₅₀ values:

$$X^2 = \sum_{i=1}^k w_i \left(\log(EC50_i) - \left(\frac{\sum_{i=1}^k w_i \log(EC50_i)}{\sum_{i=1}^k w_i} \right) \right)^2$$

equation 9

Whereas

$$w = \left(\frac{1}{SE(\log EC50)} \right)^2$$

equation 10

According to this approach all of the EC₅₀ values derived from the toxicity tests with nAg are statistically not significantly different (P = 0.972).

Concentration-response relationship was determined for AgNO₃ with both methods, in the same way as for toxicity tests with nAg. The relative inhibition of *R. planticola* is depicted in figure 30. The test was carried out in duplicate and the results of the toxicity tests with AgNO₃ are shown in table 12. For the OD₆₀₀ the calculated mean 5h-EC₅₀ is 13 µg/L nominal AgNO₃ (95% CI 11-17 µg/L) and for the fluorescence 12 µg/L (95% CI 10-16 µg/L).

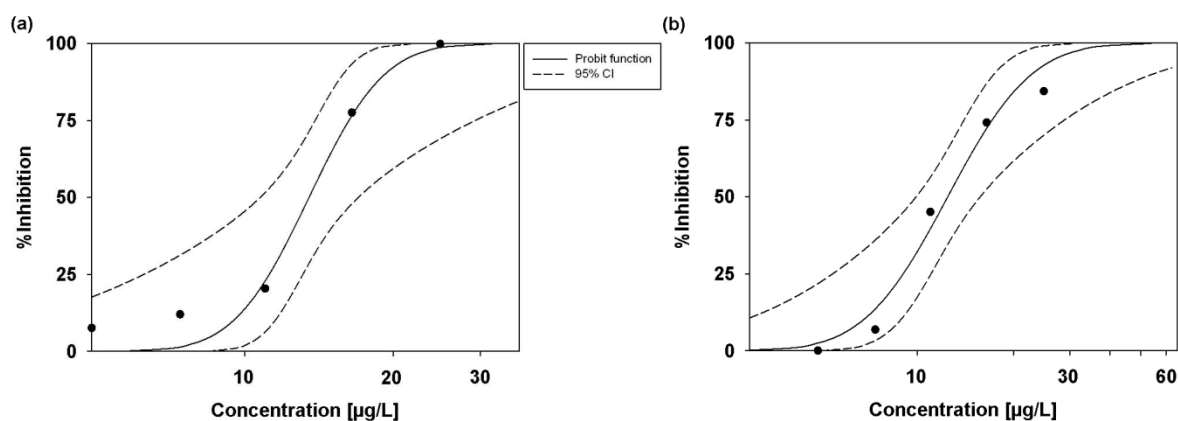


Figure 30: Relative inhibition of *R. planticola* exposed to AgNO_3 depicted as concentration-response curves. Concentration displayed as nominal AgNO_3 -content. Inhibition of the OD_{600} (a) and fluorescence (b) after 5 h exposure to AgNO_3 with 95% CI.

Table 12: EC_{50} values with CI for *R. planticola* toxicity tests with AgNO_3 derived from two toxicity tests according to OD_{600} and fluorescence.

Parameter	Method of measurement	1. attempt	2. attempt
EC_{50} [$\mu\text{g/L}$] (95% CI)	OD_{600}	14 (11 - 17)	12 (ND)
EC_{50} [$\mu\text{g/L}$] (95% CI)	Fluorescence	12 (10 - 16)	12 (10 - 14)

ND: No data.

Differences between the EC_{50} were not significant ($P = 0.993$) according to the formula described above.

In order to deduce whether the inhibition of *R. planticola* was caused by nAg itself or the released Ag^+ , the contained fractions of Ag^+ in the toxicity tests with nAg and AgNO_3 are opposed in table 13. The concentrations of total Ag in the toxicity tests with nAg are displayed as measured values for the first attempt and as calculated values for the second and third attempt. As the concentrations of Ag^+ in the toxicity tests were below LOD, the Ag^+ -fraction in the nAg tests was estimated by the ICP-OES-determined share of Ag^+/Ag -salt in the dispersion. The AgNO_3 concentrations and the contained values of Ag^+ in the AgNO_3 toxicity tests are depicted as nominal concentrations because of the lack of measured data.

Table 13: Median effective concentration according to OD₆₀₀ and fluorescence for the toxicity tests with nAg (total Ag, measured values for the first attempt, estimated according to table 10 for the rest) and AgNO₃ (nominal) and the respective corresponding fractions of Ag⁺ (calculated for the tests with nAg, nominal for AgNO₃).

Test		nAg tests		AgNO ₃ tests	
	Method	total Ag- conc. (95% CI) [µg/L]	fraction of Ag ⁺ (95% CI) [µg/L]	fraction of Ag ⁺ (95% CI) [µg/L]	AgNO ₃ -conc. (95% CI) [µg/L]
1. attempt	OD ₆₀₀	77 (ND)	3.2 (ND)	No ICP-OES accompanied test conducted	
(ICP-OES accompanied)	Fluorescence	111 (ND)	4.7 (ND)		
2. attempt	OD ₆₀₀	67 (61-73)	2.8 (2.6-3.1)	8.6 (6.8-10.8)	14 (11-17)
	Fluorescence	81 (72-91)	3.4 (3-3.8)	7.9 (6.3-10)	12 (10-16)
3. attempt	OD ₆₀₀	60 (48-74)	2.5 (2-4.3.1)	7.9 (ND)	12 (ND)
	Fluorescence	52 (40-66)	2.2 (1.7-2.8)	7.5 (6.3-9)	12 (10-14)

ND: No data.

As chemical analysis is time and cost consuming, concentrations of Ag in toxicity tests with high concentration and replicate numbers were estimated based on regression function from nominal and determined concentrations (figure 27, page 66 and table 10, page 67). For interpretation of results one needs to consider that dosage of Ag varies slightly in each assay through liquid handling and extrapolated concentrations do not always reflect exact concentrations. The extrapolated EC₅₀ for total Ag in the toxicity tests with nAg ranged from 52 to 111 µg/L according to the different methods and attempts. The extrapolated fraction of Ag⁺ ranged from 2.2 to 4.7 µg/L. For AgNO₃ the nominal EC₅₀ ranged from 12 to 14 µg/L with a fraction of Ag⁺ from 7.5 to 8.6 µg/L. These data are estimated based on the assumption, that Ag⁺ content in dispersion is the same as in the NM-300K stock and that nominal concentration of AgNO₃ was the realistic exposure concentration. Since standard errors of inferred EC₅₀ values are not available, the equation for comparing multiple EC₅₀ taken from the guidance document of Environment Canada (2005) cannot be used for comparison of data. Here, a pairwise comparison of CIs is applicable as also stated by the guidance document. If confidence intervals of two EC₅₀ do not overlap, a statistical difference of these values is assumed to be significant. According to this procedure, all EC₅₀ for Ag⁺ in nAg tests compared to those in AgNO₃ tests are statistically different. For this reason it cannot be shown that Ag⁺ causes the observed toxic effects, because EC₅₀

for Ag^+ from AgNO_3 is higher than that of Ag^+ from nAg. This finding contradicts the second hypothesis of this thesis, that toxicity is triggered by the Ag^+ released from nAg. Nevertheless it cannot be excluded, that complexation of Ag^+ occurred in the medium in one or the other assay or both, leading to deviations of realistic exposure concentration of Ag^+ from nominal concentrations. Besides this probability, a NP specific effect could lead to these results. It is generally acknowledged, that NP – cell contact causes membrane damage and in such way enables entrance of Ag^+ into the cell (Bondarenko et al., 2013).

For total nominal AgNO_3 concentrations equations 9 and 10 (page 69) were applicable for EC_{50} comparison. These results and the comparability of EC_{50} values for both methods in nAg tests suggest adequacy of both methods for effect determination. Regardless, both methods possess advantages and disadvantages. OD_{600} determines bacterial biomass by turbidity of the cell suspension. The drawback here is that dead and living cells in suspension cannot be distinguished. The fluorescence kit detects metabolic activity of bacteria and therefore does not directly reflect a change in biomass. The major drawback is that initial fluorescence cannot be measured at the beginning of the test, since transformation of resazurin to resorufin requires a minimum incubation time and thus would lead to a time shift. Both methods, OD_{600} and fluorescence determination, have been applied to cross check results for plausibility. It was shown that both methods are applicable to detect effects of toxic compounds, especially nAg. Therefore they bear the option to choose between different methods in further experiments depending on experimental purpose e.g. for biomagnification studies.

For transformation of EC_{50} values of nAg to pnc and sac (see chapter 2.1.2), the mean EC_{50} for nAg of all conducted tests was estimated as sum of all nAg EC_{50} values divided by the number of tests, where nAg EC_{50} were determined as total Ag EC_{50} minus their respective ionic fractions. Thus the mean EC_{50} of nAg was $71.5 \pm 8.1 \mu\text{g/L}$. Primary particle size as proven by UV-vis and SEM characterization was applied in equation 3 and equation 4. Accordingly, pnc was calculated with $2.27 \cdot 10^{13}$ particles/L and sac with $285.74 \text{ cm}^2/\text{L}$. For risk assessment in WWTPs with *R. planticola* as most sensitive organism, PNEC_{sac} was calculated as EC_{50} (sac) with a safety factor of 1000 for acute toxicity ($\text{PNEC}_{\text{sac}}=0.285$). PEC_{sac} values were applied as described above (chapter 3.3). For both exposure scenarios RQ was higher than 1 (1.6 for the lower and 4.5 for the higher exposure scenario), indicating a possible risk towards WWTP organisms.

Compared to the results from toxicity testing with *P. tetraurelia*, *R. planticola* was the more sensitive organism, which supports a part of the first hypothesis of this thesis (sensitivity towards nAg differs between tested organism groups).

In the literature, evidence for differential sensitivity of bacteria towards exposure with a specific nAg material exists. For example, publications reviewed by Musee et al. (2011) and Marambio-Jones and Hoek (2010) showed, that growth inhibition after 24 h differed between *E. coli* and *S. aureus* by a factor of 10. Depending on the type of nAg applied, these results varied, like in the study of Vertelov et al. (2008). Here *L. mesenteroides* was the more susceptible organism compared to *E. coli* and *S. aureus*, with the latter getting inhibited at the twofold concentration only. Differences in effects of nAg exposure were also found for gram- positive and gram-negative bacteria strains (Jin et al., 2010). Yang et al. (2014) reported in their study, that ammonia-oxidizing bacteria (AOBs) were more susceptible towards nAg exposure than nitrite- oxidizing bacteria (NOB) and, within the AOB species investigated, sensitivity was differing as well. These results suggest that nAg toxicity towards several bacteria species should be taken into account for risk assessment of nAg in WWTPs. The other part of the first hypothesis of this thesis (sensitivity towards nAg differs between tested species within a group of organisms, here bacteria) concerns this assumption. In the following sections, the focus is on inhibitory effects of nAg on bacteria strains which are representatives of those microbial groups involved in nitrification and phosphorous removal during the wastewater treatment process.

4.3 Experiments with *Hyphomicrobium sp.*

4.3.1 Introduction – *Hyphomicrobium* and denitrification

Nitrite (NO_2^-) and nitrate (NO_3^-) occurring in wastewater due to nitrification (see 4.4.1) or by direct input via inflow need to be removed during wastewater treatment because they are chemically and biologically harmful. Thus, denitrification (see 4.3.1) is usually carried out after nitrification in WWTPs.

Denitrification is a process by which NO_2^- or NO_3^- are transformed via nitric oxide (NO) and nitrous oxide (N_2O) to dinitrogen gas (N_2) (Lu et al., 2014). These reactions are conducted majorly by bacteria and require the activity of the enzymes nitrate reductase, nitrite reductase, nitric oxide reductase and nitrous oxide reductase, which in turn work best under low dissolved oxygen conditions. Some organisms are capable of only one or few types of reactions within denitrification (exclusive nitrite reducers, incomplete denitrifiers and incomplete nitrite reducers) and some bacteria are capable of conducting all types of reactions within denitrification (complete denitrifiers). The genus *Hyphomicrobium* belongs to this latter group of organisms (Lu et al., 2014).

Hyphomicrobium bacteria belong to the class of alphaproteobacteria and order of *Rhizobiales*. They are gram-negative, rod-shaped cells with lengths of 1 to 3 μm , which grow under aerobic conditions (Garrity et al., 1974), where methanol or ethanol are required as carbon source (Lu et al., 2014). As facultative anaerobic, *Hyphomicrobium* uses nitrate or nitrite as electron acceptor. Colonies grown on agar are minute in size and colorless, bright beige or brownish depending on the light source used for examination. Asexual reproduction occurs as daughter cell formation through budding. In wastewater treatment plants up to $6 \cdot 10^5$ hyphomicrobia per mL have been found in activated sludge (Garrity et al., 1974).

In this section of the thesis, the potential effects of nAg and Ag^+ on the activity of *Hyphomicrobium* as a representative of denitrifying bacteria were investigated. Experiments were carried out under aerobic conditions, as exclusion of oxygen supply from enclosed air in the test vessels was not feasible. The results of single species toxicity testing were intended to be compared to the toxicity derived for other bacteria species to test for the first hypothesis and to contribute to a comprehensive risk assessment of NM-300K nAg.

4.3.2 Growth kinetics of *Hyphomicrobium* under experimental conditions

4.3.2.1 Material and Methods for *Hyphomicrobium* growth kinetics

Hyphomicrobium sp. strain KDM2 was obtained from DSMZ (Deutsche Sammlung von Mikroorganismen und Zellkulturen GmbH, Germany) and cultured in medium 830 (R2A medium) supplied with 2 g/L methanol (see ANNEX III for details). For cell culture maintenance, 4.5 mL of fresh media were pipetted into sterile glass tubes and inoculated with 0.5 mL of a seven days old culture. Glass tubes were covered with Kapsenberg caps and kept at 28°C in the dark (New Brunswick TM Excella E24, Eppendorf AG, Germany).

Growth kinetics of *Hyphomicrobium* sp. were determined based on OD₆₀₀ measures in 96-well plates (pure grade S, transparent F-bottom, Brand GmbH & CO KG, Wertheim, Germany). 24 replicates were prepared each for blank and cell culture. 200 µL of freshly inoculated culture or fresh media as blanks were applied per replicate. The plates were incubated at 28°C and measured in Synergy H1 plate reader (BioTek Instruments, Inc., Winooski, VT, USA). Over a period of 28 h, optical density at 600 nm wavelength (OD₆₀₀) was measured in blanks and samples at intervals of 2 h.

Growth kinetic determination was repeated at higher volume (initially 10 mL) but with two replicates only, to cover a longer period of time (several days). A culture with an OD₆₀₀ of 0.161 was used to inoculate fresh R2A medium, yielding a dilution of 1:10 in each replicate. OD₆₀₀ was determined directly after inoculation and subsequently every 24 h by transferring 1 mL from each replicate to polystyrene cuvettes and measuring absorbance at 600 nm wavelength with a Hach Lange DR2800 photometer. Measures were carried out until no changes in OD₆₀₀ were observable anymore. Division rate ν and generation time gt were determined between day 1 and 5 (96 h) according to equation 5 and equation 6 (see section 3.2.1, page 20).

CFU determination was not undertaken, as colony formation of *Hyphomicrobium* is difficult to observe for reason of their minute size and pale coloring.

4.3.2.2 Results and discussion of *Hyphomicrobium* growth kinetics

OD₆₀₀ measures over the first 28 h of growth in intervals of 2 h were conducted to reveal duration of the lag phase of a freshly inoculated *Hyphomicrobium* culture. In figure 31 results are displayed. The end of lag phase is determined from the crossing point of the tangents which are fitted to the measuring points of the period at the

beginning, where OD_{600} does not change significantly and the following period, where OD_{600} values change over time significantly (see insertion in figure 31). The end of lag phase and change to exponential growth of the culture is thus determined as 12 hours after inoculation.

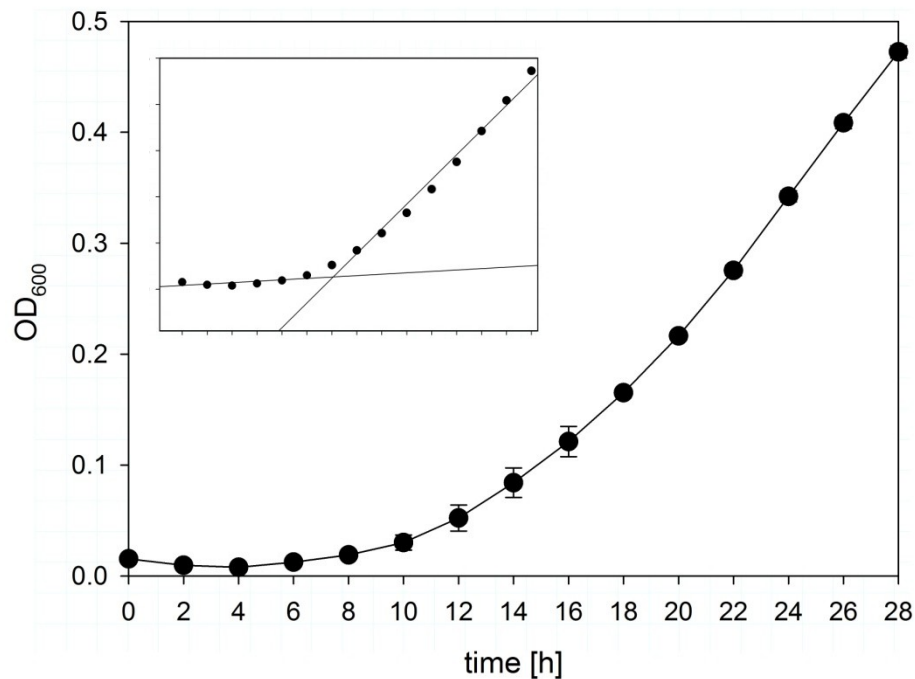


Figure 31: Growth kinetics of a freshly inoculated *Hyphomicrobium* culture over 28 h as determined by OD_{600} measures on 96-well plates. Error bars indicate standard error of means. The small insertion shows the tangents for the determination of lag phase ending.

The determination of growth kinetics over a period of several days was carried out in two replicates with a higher volume and using polystyrene cuvettes instead of 96-well plates. This approach was undertaken because on 96-well plates evaporation from wells led to strong fogging of the lid over longer periods of time and wells dried out in the end. This problem could not be overcome even by sealing of the plate and heating of the lid. The results from measures of OD with cuvettes in the photometer are displayed in figure 32. Here temporal resolution is lower so that the lag phase cannot be seen in this plot, as it covers the first 12 h after inoculation, like previously shown. Exponential growth was observed between day 1 and 5. After this period, stationary phase began and OD_{600} values evened out at about 0.16 after 8 days.

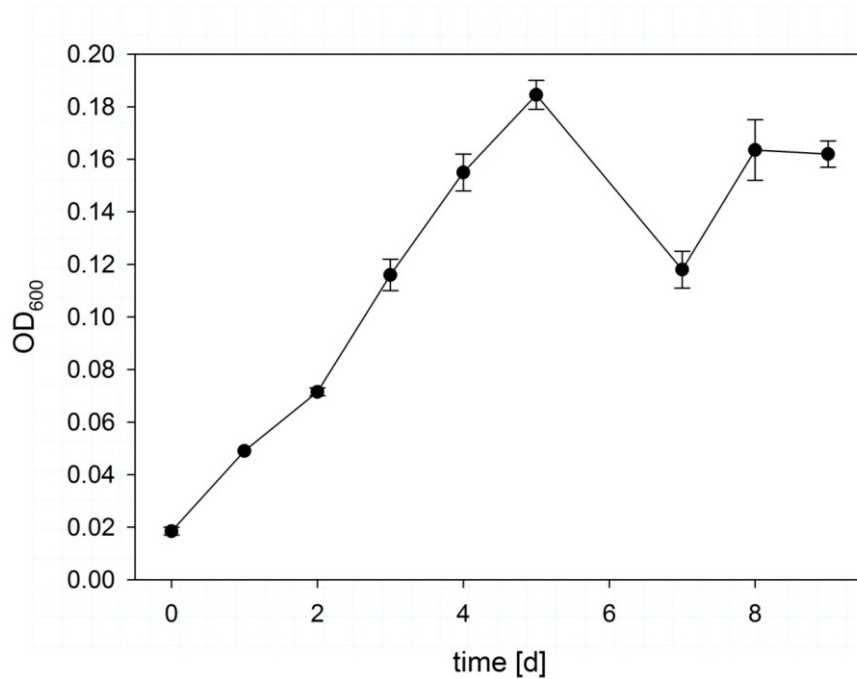


Figure 32: Growth kinetics of *Hyphomicrobium* sp. over 9 days determined as OD₆₀₀ in cuvettes. Error bars indicate standard error of means.

Division rate ν (see equation 6, page 20) was determined as 0.13/h and generation time gt (see equation 5, page 20) was 7.7 h between day 1 and day 5. This finding is in very good agreement with the division rate of 0.12 to 0.14/h reported by Hayes et al. (2010) for a *Hyphomicrobium* culture grown at pH 7 with a medium containing methanol as carbon source.

As mentioned before, methanol is the preferred carbon source during aerobic metabolism of *Hyphomicrobium*. Although the bacteria strain was chosen as representative of denitrifying bacteria, conditions for denitrification could not be realized in the growth kinetics and toxicity test experiments, because they would require anaerobic handling of the cultures. Anaerobic handling demands special vessels and gassing with oxygen free gases throughout the whole experimental procedure, which was not feasible for this work. For this reason, effects of nAg on the facultative denitrifying organism *Hyphomicrobium* were studied under aerobic conditions.

Based on the observed growth kinetics of *Hyphomicrobium* sp. in this experiment, pre-cultivation of cultures for subsequent toxicity tests was defined with 1 day (24 h) and exposure period was specified with further 24 h.

4.3.3 Toxicity tests with *Hyphomicrobium* and nAg

4.3.3.1 Materials and methods for toxicity tests with *Hyphomicrobium*

Characterization of nAg

nAg dispersions based on R2A medium were prepared from stocks of 1g nAg/L HPLC-grade water (see chapter 3.3.1) at nominal concentrations of 2.5, 3.75 and 5.63 mg/L. UV-vis spectroscopy was conducted for two replicates of each concentration over a range of 250 to 600 nm wavelength.

Particle diameters were calculated according to equation 1 and equation 2 (see chapter 2.1.2).

Preparation of toxicity test assay

Figure 33 depicts the assay preparation for toxicity tests with *Hyphomicrobium sp.* and nAg or AgNO₃.

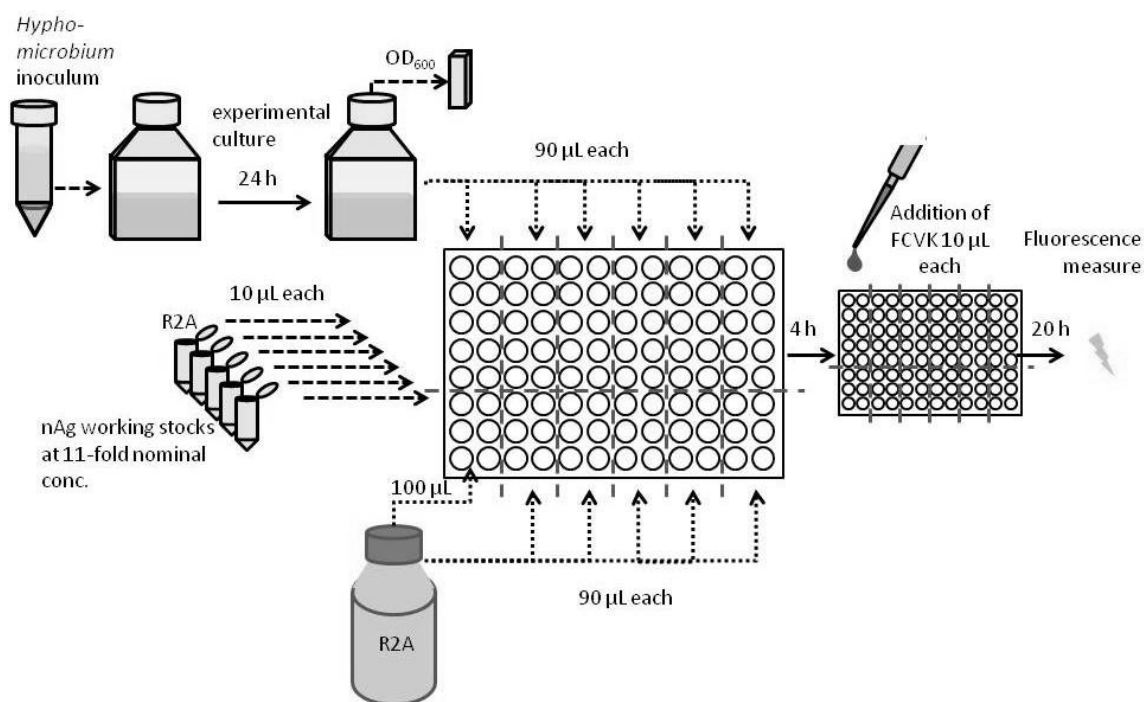


Figure 33: Scheme of toxicity test preparation with *Hyphomicrobium sp.* and nAg or AgNO₃, respectively.

A freshly inoculated cell culture of *Hyphomicrobium sp.* was incubated for 24 h and OD₆₀₀ was determined for evaluation of growth. Pre-dispersions of nAg and pre-solutions of AgNO₃ were prepared from 1 g/L stocks in HPLC-grade water and R2A

medium at 11-fold final nominal concentrations. On a 96-well plate (pure grade S, transparent F-bottom, Brand GmbH & CO KG, Wertheim, Germany) 10 replicates of each treatment were prepared applying 90 μL of cell culture. 10 μL medium were added into control wells, and 10 μL of pre-dispersion or –solution for nAg and AgNO_3 exposures, respectively. Blanks were prepared with medium instead of cell culture at 6 replicates for each treatment.

After incubation of the 96-well plate over 4 h at 28°C in the dark, 10 μL FCVK were added to each well and incubation was continued at the same conditions for further 20 h. Subsequently, fluorescence was measured at excitation wavelength of 545 nm and emission at 590 nm on a Polarion plate reader (Tecan Group Ltd., Switzerland) as described before (see chapter 3).

Nominal nAg concentrations in the range of 0.3 to 6.2 mg/L were tested within the conducted assays. The first test was carried out at concentrations of 0.3 to 5 mg/L with a spacing factor of 2. Ag^+ concentrations of 0.25 to 4.0 mg/L were tested with AgNO_3 as ion source. In the second experiment, nominal nAg concentrations of 2.75, 4.31 and 6.2 mg/L were tested and compared to Ag^+ concentrations of 2.0, 3.0 and 4.5 mg/L. In the third experiment, nAg exposure was tested exclusively at nominal concentrations of 3.5 to 5.04 mg/L with a spacing factor of 1.1. Cell density was determined as OD_{600} besides analysis of viability in this last assay.

If applicable, concentration response curves and corresponding EC_{50} values were determined using Toxrat Standard V2.10.05 (Toxrat® Solutions GmbH) software. All results were plotted using Sigma Plot 11.0 software.

4.3.3.2 Results and discussion of *Hyphomicrobium* toxicity tests

Characterization of nAg

UV-vis spectrograms of nAg dispersions prepared with R2A media were recorded for particle characterization in terms of size distribution and agglomeration behavior. Results are displayed as spectrograms in figure 34 and 35 (following pages). For the first spectrogram, concentrations were applied as tested in the second toxicity test assay. For the second spectrogram, working stocks were analyzed at 11-fold exposure concentrations as applied in the third toxicity test assay (see below).

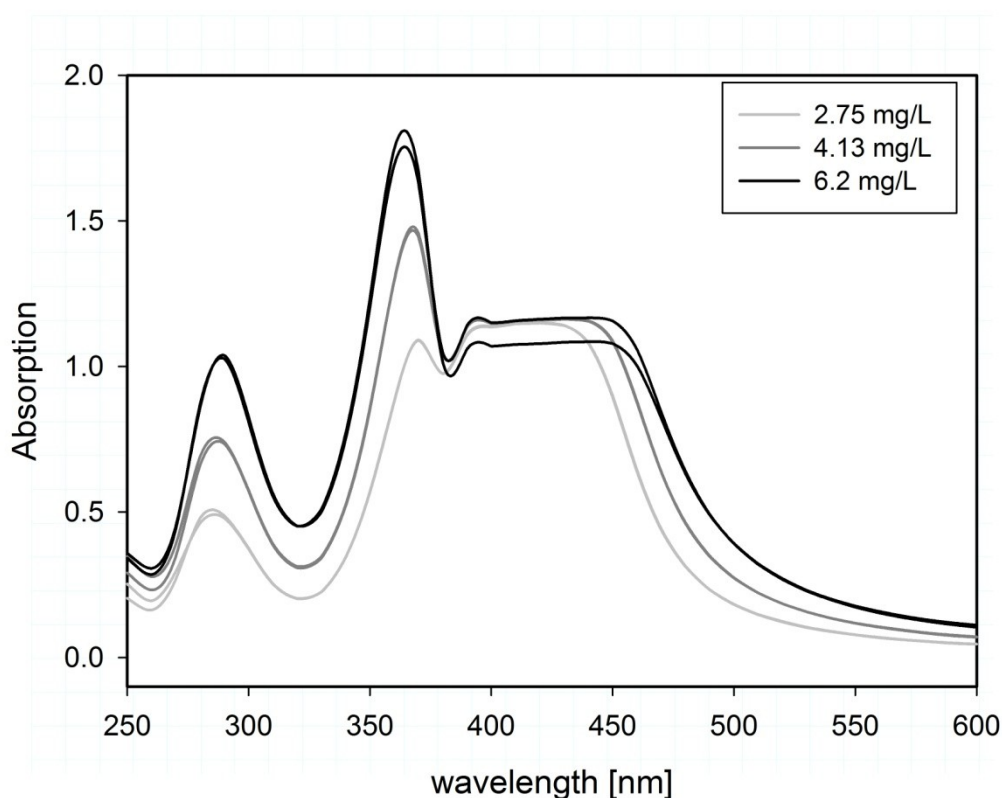


Figure 34: UV-vis spectrograms of nAg dispersions in R2A medium at concentrations used in subsequent toxicity tests.

Deviating from previous UV-vis spectra recorded with nAg in CM and ABC, the spectra at toxicity test exposure concentration displayed at least two peaks in all tested concentrations. One definite peak was observed at a maximum wavelength of approximately 290 nm and a second less distinct peak at a range of 325 to 500 nm, exhibiting a maximum at 370 nm and a plateau between wavelengths 400 and 475 nm. The valley in the second peak at 370 nm was observed before and is a technical artifact due to the change of the light source at this wavelength.

Mean particle sizes calculated as diameters from UV-vis data as displayed in figure 34, ranged from 47 nm in the lowest concentration to 54 nm in the highest concentration samples. However, for the medium and high concentration, particle sizes calculated from λ_{\max} (equation 3, page 13) had to be omitted as sizes were negative due to the strong blue shift of peak maxima. Although the determined particle sizes indicated agglomeration of primary particles, it must be considered, that either UV-vis analysis was impacted by any kind of contamination, or NP concentrations were too low for exact characterization by means of UV-vis. Results of the second analysis at higher nAg concentrations, as shown in figure 35, support this latter assumption.

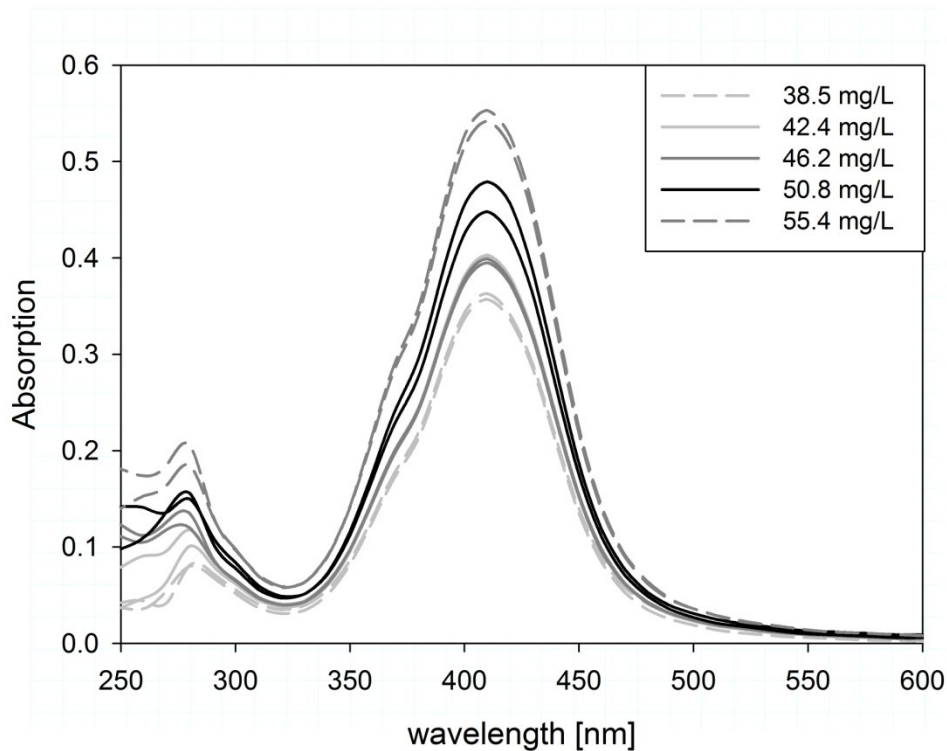


Figure 35: UV-vis spectrograms of nAg working stock dispersions in R2A medium at 11-fold concentrations as applied in the third toxicity test.

Distinct peaks were observed at 410 nm wavelength for all working stock concentrations, which is considered typical for spherical nAg as primary particles in dispersion (Hassellöv et al., 2008; Lin and Sun, 2010; Petit et al., 1993). Peak maxima, as well as the absorption at a wavelength of 250 nm increased according to increasing nAg concentrations, as expected. Particle sizes were calculated from equation 1 and equation 2, revealing particle diameters of 22.3 nm at the lowest working stock concentration to 25.8 nm at the highest working stock concentration, which is in good agreement with primary particle diameters indicated by the manufacturer (20 nm) and with results from previously described SEM analyses in ABC and CM (see 3.3.2, page 28 and 4.2.3.2, page 63). From these results, dispersion stability and a constant exposure throughout the toxicity test duration were inferred.

Toxicity test

Viability of exposed *Hyphomicrobium* cells in 24 h toxicity tests was determined as relative fluorescence. Results of the first toxicity tests did not reveal concentration response behavior in a classical sense. A steady increase of fluorescence was

observed with increasing concentrations of nAg except at the highest concentration, as shown in figure 36.

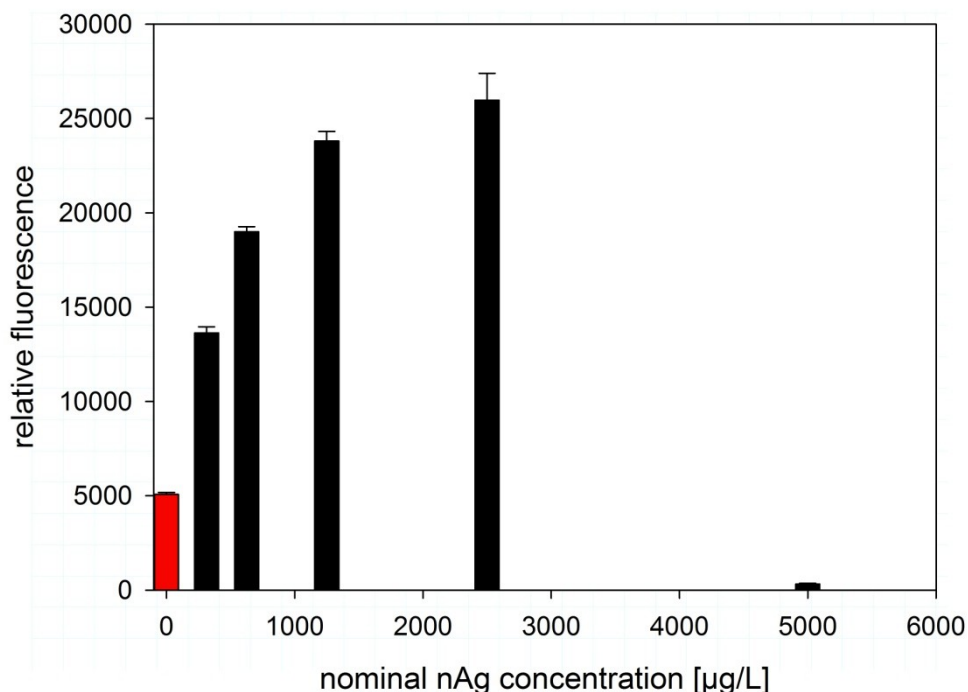


Figure 36: Viability of *Hyphomicrobium* cells exposed to nAg, as relative fluorescence. Error bars indicate standard error of means.

The increase of fluorescence signal in the range of 100 to 2500 µg/L indicates enhanced metabolic activity of the cells compared to controls. This pattern suggests the onset of some kind of stress response, for example activation of silver efflux pumps. It was assumed that concentration response behavior might occur in the range of 2500 µg/L to 5000 µg/L, if existent. At the lower concentrations of Ag⁺ treatment, fluorescence was comparable to control, but was distinctly higher at the highest nominal concentration, as depicted in figure 37. For comparison of these results to effects caused by Ag⁺ released from nAg, nominal Ag⁺ concentrations derived from Ag⁺ concentration in the nAg stock (see section 2.1.2) are depicted in the respective graph.

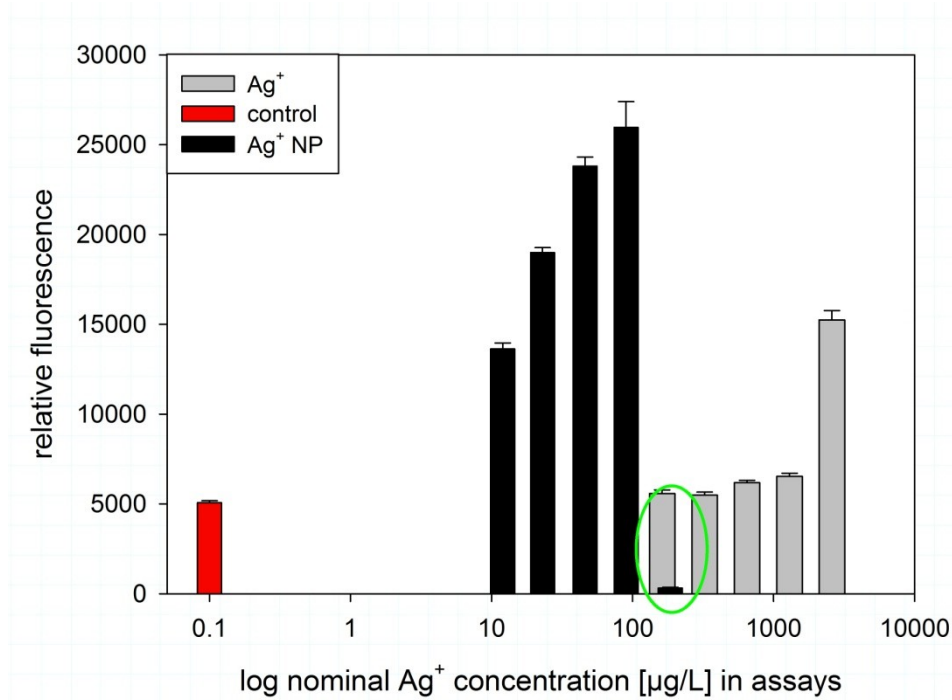


Figure 37: Toxicity test results for *Hyphomicrobium* as viability (relative fluorescence) opposed to nominal Ag⁺ concentration. Black bars indicate results from nanoparticle treatment, gray bars indicate results from AgNO₃ (Ag⁺) treatment. Error bars indicate standard error of means.

Interestingly, Ag⁺ (if not nAg itself) seems to cause an inhibitory effect in the range of 100 to 220 µg/L in the nanoparticle assay, while no effects were observable in the AgNO₃ assay at this range (see green ellipse in figure 37). It was speculated that the increase of fluorescence signal at the highest AgNO₃ concentration indicated the onset of stress response at these concentrations with probable decay at exalted concentrations, similar to the patterns observed in nAg treatment. For verification of these assumptions and of former results, a test was conducted with three nominal concentrations of nAg (2750, 4130 and 6200 µg/L), and Ag⁺ at nominal concentrations of 2000, 3000 and 4500 mg/L. Results of this assay are shown in figure 38.

The pattern observed for nAg treatment was similar to the former results. Again, concentration response was contradictory to expectations, as for the two lower nAg concentrations relative fluorescence increased compared to control and was distinctly lower at the highest concentration. For Ag⁺ treatment, all determined values for fluorescence were higher than in the control.

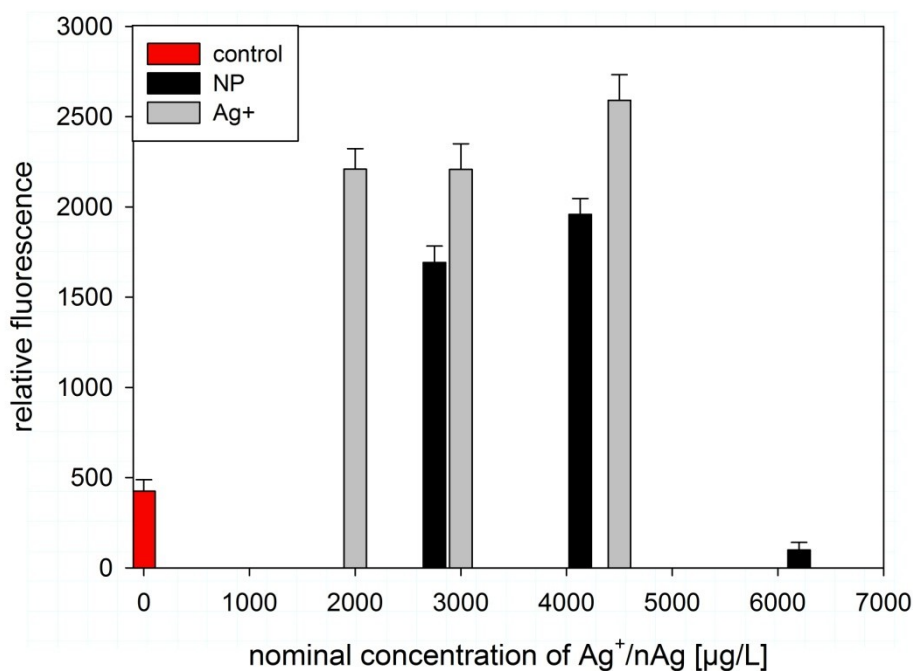


Figure 38: Viability of *Hyphomicrobium* cells after 25 h exposure to nAg and AgNO₃ at expected concentration response range. Error bars indicate standard error of means.

In order to exclude the possibility that experimental mistakes led to the respective results and to explore a narrowed concentration range for concentration-response behavior, a final assay was carried out at five nominal nAg concentrations between 3500 and 5040 mg/L with a spacing factor of 1.1, and additional recording of OD₆₀₀ values after preparation of the assay and at the end of incubation. Usually, spacing factors should not exceed 2.0, but in this case lower spacing factor was applied in order to get a higher resolution in the range where exposure response changed from 0 to 100 % inhibition.

As shown in figure 39 a), no concentration response behavior was traced for the FCVK assay, and in contrast to previous assays, inhibition of viability at the highest tested concentration was not observed. These results suggested that the tested *Hyphomicrobium* is resistant to silver up to a specific trigger concentration. In the OD₆₀₀ assay results were differing at the end of the toxicity test, showing a lower absorption along with increasing nAg exposure concentrations (figure 39 b).

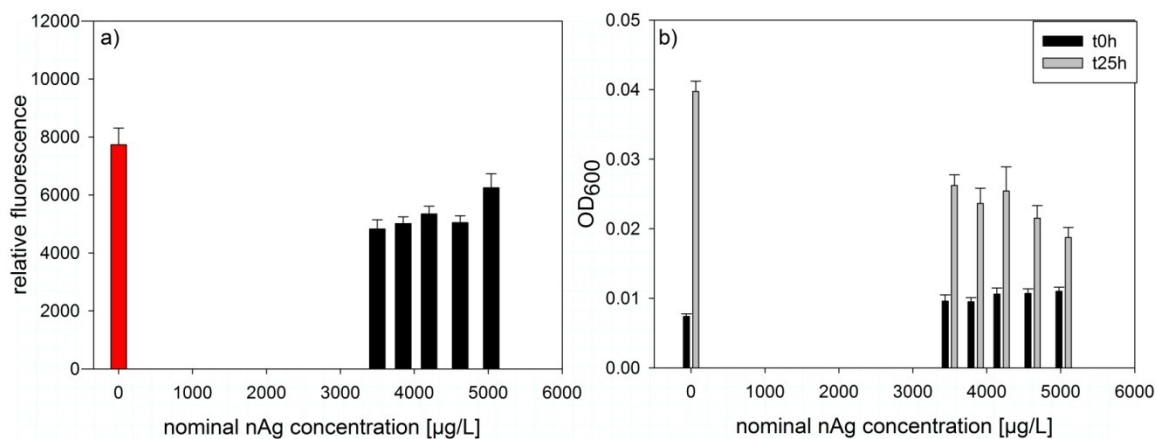


Figure 39: a) Viability of *Hyphomicrobium* after 25 h exposure to nAg in third toxicity test assay. Error bars indicate standard error of means. b) OD₆₀₀ of *Hyphomicrobium* cells after exposure to nAg as absorption in third toxicity test assay. Black bars indicate cell culture density at t_{0h}, gray bars show results after 25 h of exposure (t_{25h}). Error bars indicate standard error of means.

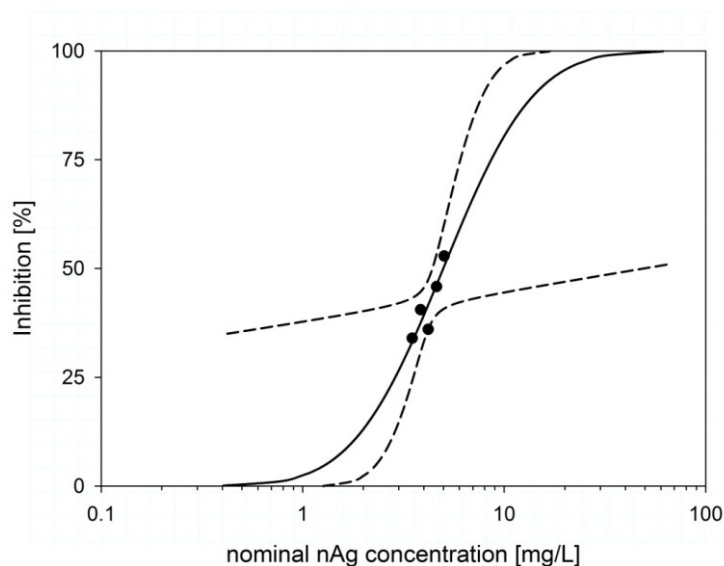


Figure 40: Concentration response curve of *Hyphomicrobium* exposed to nAg according to OD₆₀₀ analysis. Solid line: probit function. Dashed lines: upper and lower 95% CIs. Note logarithmic scale of x-axis.

However, complete inhibition of growth was not observed, as absorption after 25 h was higher compared to 0 h in all samples. Concentration-response behavior and the 25h EC₅₀ concentration was determined from probit analysis as displayed in figure 40 (see above), as 4.99 mg/L (4 990 $\mu\text{g/L}$) with 95% confidence intervals between 4.4 and 49.4 mg/L. Goodness of fit was high with $p(\text{Chi}^2) > 0.1$ and regression was significant with $p(F) = 0.04$, although the upper confidence intervals were very broad. This might be provoked by the unconventional spacing factor of 1.1 between the test concentrations. Concluding from the results presented in this section, the tested strain of *Hyphomicrobium* sp. seemed to be unsusceptible to Ag^+ from AgNO_3 , even at

comparably high concentrations, while nAg induced effects within a range of 4 to 5 mg/L. These observations can either be explained by NP-specific toxicity, or by a resistance of the strain against silver ions, premising Ag^+ removal or some kind of NP-specific toxicity as well. In the literature, generally Ag^+ is thought to be the toxic component of nAg, which is released by oxidation of the particle surface (Reidy et al., 2013). However, Ag^+ toxicity might be mitigated by complexation with inorganic ligands, such as Cl^- or S^{2-} , or organic matter (Reidy et al., 2013; Xiu et al., 2011; Yang et al., 2014). For example, Yang et al. (2014) reported significant inhibition of ammonia oxidizing bacteria by nAg in the absence of bioavailable Ag^+ . Toxicity of nAg itself is asserted to be caused by interaction of particles with the cell membrane (Bondarenko et al., 2013), especially for very small NPs (Morones et al., 2005). It is hypothesized that nAg can interact more closely with cell surfaces, damaging cell membranes and disrupting ion efflux pumps and thus opening the path for released Ag^+ to cause oxidative stress (Bondarenko et al., 2013; Hwang et al., 2008). These findings contradict the second hypothesis of this thesis, which was previously rejected according to results from chapter 4.3 (*R. planticola*), but supported concerning results from chapter 3.3 (*P. tetraurelia*).

Previous studies reported similar results as those obtained from toxicity tests in this work. Khan et al. (2011) observed nAg-tolerance in a *Bacillus pumilus* strain isolated from sewage, which in contrast was sensitive towards AgNO_3 exposure. Excretion of extracellular polymeric substances (EPS) was identified as a mechanism to bind nAg and thus mitigating their toxicity by preventing Ag^+ release. According to further studies, several mechanisms for development of tolerance against silver exist in bacteria. Zhang et al. (2014) reported a 50-fold increase of total gene copy numbers of *silE* gene, which encodes for an Ag(I)binding protein 41 days after long term exposure of nitrifying bacteria to nAg in a wastewater bioreactor. Also, an increased excretion of EPS was observed in the study, suggesting a role of these substances in silver tolerance of bacteria. Gunawan et al. (2013) adapted an environmental *Bacillus* sp. strain to Ag exposure and tested it for growth and the generation of reactive oxygen species (ROS). Up to a dosage of 10 mg/L the *Bacillus* culture was not suppressed in growth. From the comparatively low level of ROS production in the cells the authors deduced other mechanisms of tolerance induction than oxidative stress and found increased levels of cytoprotective *sil* genes, *silB* and *silP*. The first encodes for a permease, most probably of an ABC-type Ag^+ /proton antiporter, the second presumably encodes for an Ag^+ efflux P-type ATPase, or more precisely for the therein contained histidin sensor. These results indicated the presence of a silver efflux pump system, as described by Gupta et al. (1999). These antibiotic resistance genes are

assumed to be located on plasmids and thus could be transferred between bacterial strains at hotspots such as WWTPs. The *Hyphomicrobium* strain tested in this study could have received such resistance genes before its isolation from the WWTP as well, leading to the results described here. The enhanced activity of *Hyphomicrobium* cells at a wide range of concentrations of nAg and comparably high concentrations of AgNO₃ as observed in this study, is regarded as an indication for silver efflux pump activities. The occurrence of probable silver resistances in bacteria implies another kind of risk of NPs to environmental and human health, as overuse of antibacterial agents of any kind might lead to dissemination of resistances and thereby to a loss of therapeutic resources (Gupta et al., 1999; Schluesener and Schluesener, 2013).

Compared to the toxicity of nAg towards *R. planticola* (average nominal EC₅₀ of 0.082 mg/L), toxicity of nAg towards *Hyphomicrobium* sp. was very low. As the EC₅₀ for *Hyphomicrobium* is much higher than EC₅₀ of *R. planticola*, it is not useful for implementation into risk assessment, as only the most sensitive organism should be regarded for the calculation of PNEC. Based on the results obtained for *R. planticola* the conclusion is retained, that a probable risk through exposure of bacteria towards nAg (NM-300K) in activated sludge exists (see section 4.2.3.2).

4.4 Experiments with *Nitrobacter vulgaris*

4.4.1 Introduction – *Nitrobacter* and nitrification

Bacteria of the genus *Nitrobacter* belong to the subclass of alphaproteobacteria and are characterized as gram-negative, pleomorphic, but generally rod shaped cells with sizes of 1 to 2 μm in length and 0.5 to 0.9 μm in width. They tend to reproduce by budding or binary fission at very low generation times, lasting from 8 hours to several days (Spieck and Bock, 2005).

Nitrification is a two step process which is carried out by two groups of (generally autotrophic) nitrifying bacteria. In the first step ammonium-oxidizers, e.g. *Nitrosomonas*, *Nitrosococcus*, *Nitrospira*, *Nitrosolobus* and *Nitrosovibrio* (AWWA, 2002) transform ammonium (NH_4^+) to nitrite (NO_2^-) with the help of the enzymes ammonium monooxygenase (AMO) and hydroxylamine oxidoreductase (HAO) (Kim and Gadd, 2008). In the second step nitrite-oxidizers use the NO_2^- as energy source, along with hydroxylamine, to generate 4 electrons and consequently produce NO_3^- . This reaction takes place with the help of the enzyme nitrite oxidoreductase (NOR) (Kim and Gadd, 2008) and is carried out by bacterial genera such as *Nitrobacter*, *Nitrospina*, *Nitrococcus* and *Nitrospira* (AWWA, 2002; Kim and Gadd, 2008). Some heterotrophic bacteria and fungi are also capable of nitrification, however with much lower efficiency. Although nitrite is the major energy source, *Nitrobacter* are able to use organic energy sources (Koops and Pommerening-Röser, 2001).

Previously, nitrification inhibition due to nanosilver exposure has been shown (Choi 2009). No negative effects on the abundance of *Nitrobacter* were found in a long-term exposure at 100 $\mu\text{g/L}$ nAg concentration in a membrane bioreactor (Zhang et al., 2014), but Liang et al. (2010) reported that *Nitrobacter* was washed out after shock loading over 12 h with 1 mg/L nAg. In the same study, population shifts of nitrifying bacteria were observed along with an increase of NH_4^+ and NO_3^- concentration in the effluent. Yang et al. (2014) found a comparatively low sensitivity of nitrite-oxidizing bacteria towards nAg. These partially controversial results emphasize the need to determine the sensitivity of nitrifying bacteria towards specific nAg in single species tests. In this work, nAg (NM-300K) toxicity towards *Nitrobacter vulgaris* as a representative for nitrifying bacteria in WWTPs was tested. The aim of this section was to compare the sensitivity of the tested bacteria for testing of the first hypothesis and to include the results into the risk assessment for NM-300K nAg.

4.4.2 Growth kinetics of *Nitrobacter vulgaris*

Bacteria of genus *Nitrobacter* are growing very slowly, even at optimum physiological conditions (Spieck and Bock, 2005). Many species of the genus are non-cultureable on solid media. For this reason CFU determination as parameter for growth kinetics is not utilizable. In some species of the genus, absorbance measures are applicable to determine the density of bacteria culture at a wavelength of 450 nm (Grunditz and Dalhammar, 2001). For the species under investigation in this study, *Nitrobacter vulgaris* (Bock 2001), OD₄₅₀ measures did not approve to reveal growth of the cells. However, due to the ability of *Nitrobacter* to metabolize bioavailable nitrite (NO₂⁻) to nitrate (NO₃⁻), the rate of this conversion was used as an additional measure for growth (Grunditz and Dalhammar, 2001).

4.4.2.1 Materials and methods for *N. vulgaris* growth kinetics

Nitrobacter vulgaris (Bock 2001) type strain Z (DSM No. 10236) was purchased from Leibniz Institut DSMZ (Deutsche Sammlung von Mikroorganismen und Zellkulturen GmbH, Germany). Autotrophic *Nitrobacter* medium 756.c as described by DSMZ GmbH was used at pH 8.3 for cell culture, growth experiments and toxicity tests (for details see ANNEX IV).

For determination of growth kinetics, 45 mL of fresh medium was inoculated with 5 mL of a 21 day old *Nitrobacter vulgaris* culture. Different methods were tested for analysis of cell culture growth: fluorometric cell viability kit I staining (FCVK), colorimetric cell viability staining (CCVK), nitrite consumption (cuvette tests) and aniline violet staining. In a preliminary test for FCVK, different dilutions of the 21 day old cell culture were prepared (1/5, 1/10, 1/20) to determine optimal cell densities for detectable fluorescence signals. 24 replicates at a volume of 100 µL of each dilution and additionally blank medium were spread into 96-well plates (pure grade S, transparent F-bottom, Brand GmbH & CO KG, Wertheim, Germany) and 10 µL of resazurin (FCVK, Promo Cell GmbH, Heidelberg, Germany) were added. Fluorescence was measured after 2, 3 and 4 hours using a Synergy H1 plate reader (BioTek Instruments, Inc., Winooski, VT, USA) with excitation wavelength of 545 nm and emission wavelength of 595 nm with gain set to 55. Transformation of the color of the dye was checked after 24 h.

Cuvette test LCK 339 (Hach Lange GmbH, Germany) was used for determination of nitrite concentration as NO₂-N and LCK 341 (Hach Lange GmbH, Germany) for

determination of nitrate concentration as $\text{NO}_3\text{-N}$. Samples were diluted prior to cuvette preparation using ultrapure water (MilliQ) if required, to meet the measurement range of the respective cuvette test. First measure was taken 5 h after inoculation and subsequently repeated every 2 to 3 days until day 21 after inoculation.

For CCVK method, 6 columns (8 wells each) of a 96-well plate (pure grade S, transparent F-bottom, Brand GmbH & CO KG, Wertheim, Germany) were filled with medium 756.c at a volume of 110 μL and the other 6 columns were filled in the same way with a 21 day old culture of *N. vulgaris*. 10 μL CCVK (Promo Cell, Heidelberg, Germany) were added to the first column (8 replicates) of *N. vulgaris* culture and 1 blank column. Absorption at 450 nm was measured using a Synergy H1 plate reader (BioTek Instruments, Inc., Winooski, VT, USA) for these columns after 4 h of incubation at 28 °C in the dark (New Brunswick™ Excella E24, Eppendorf AG, Germany) for determination of colorimetric staining intensity at the beginning of the experiment. The averages of the determined values for blanks were subtracted from cell culture measures. The procedure was repeated 5 times, every 24 h.

For aniline violet staining, a 21 day old culture of *N. vulgaris* was dispersed at 200 μL aliquots into a 96-well plate (pure grade S, transparent F-bottom, Brand GmbH & CO KG, Wertheim, Germany). The technique is used under the assumption, that the cells under investigation form biofilms at the walls of the plate wells. At each measurement time, the liquid was withdrawn from 8 wells of the 96-well plate and the biofilm was stained with 0.1 % aniline violet solution (for a detailed protocol see ANNEX V: Protocol for aniline violet staining). Absorption was measured at 595 nm using a Synergy H1 plate reader (BioTek Instruments, Inc., Winooski, VT, USA).

4.4.2.2 Results and discussion for *N. vulgaris* growth kinetics

Growth of *N. vulgaris* was measured by different methods: FCVK, CCVK, aniline violet staining and determination of nitrite ($\text{NO}_2\text{-N}$) and nitrate ($\text{NO}_3\text{-N}$) concentrations in the medium of a growing culture over time, where the consumption rate was used as indicator of cell culture growth.

FCVK measures with diluted cell cultures revealed best results for a 1:10 dilution after 4 h (figure 41), although fluorescent units were comparably low (referred to *P. tetraurelia* or *R. planticola*) with high standard deviations and optically no transformation of the FCVK dye was determinable after 24 h.

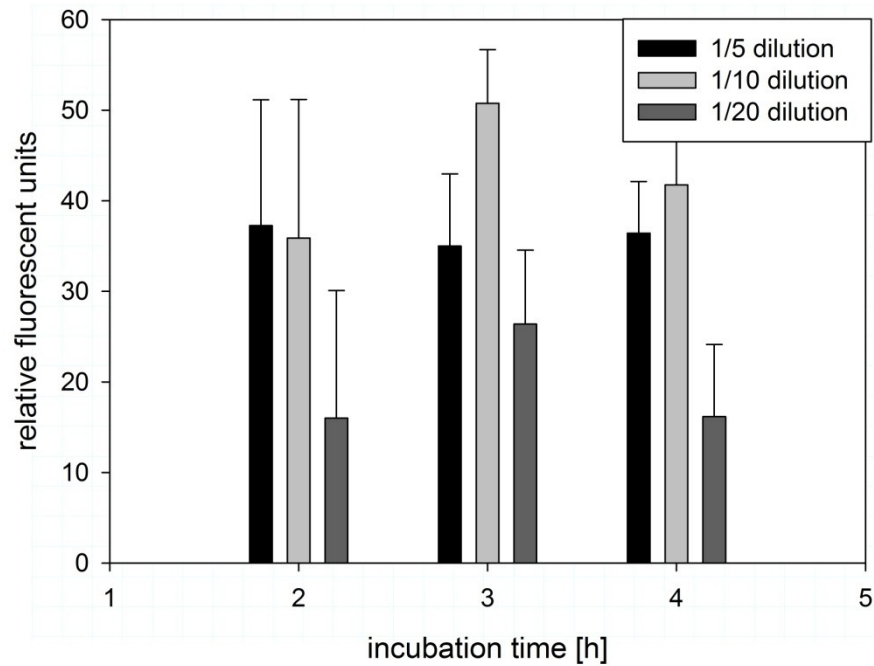


Figure 41: Results of the preliminary FCVK assays with differently diluted *N. vulgaris* culture. Error bars indicate standard error of means.

For this reason, incubation period was prolonged in subsequent tests, but at first other methods for determination of growth were tested in terms of practicability and better reliability.

Figure 42 shows the results of the $\text{NO}_3\text{-N}$ and $\text{NO}_2\text{-N}$ measurements over a period of 21 days, here displayed as time in hours. Lines indicate dynamic fit curves (exponential growth and exponential decay). Nitrite concentration was far above the detection range of the cuvette test in the first measurement (0 h) and was thus determined at 10 000-fold dilution of the medium. For determination of $\text{NO}_2\text{-N}$ after 96 and 168 hours, 1 000-fold dilutions of cell culture were prepared to meet detection range of the cuvette tests. $\text{NO}_3\text{-N}$ analyses were carried out with undiluted samples for the first ten days and subsequently with diluted samples in order to meet measurement ranges. Still, for some samples data were obtained outside of measuring range for one of the two nitrogen compounds.

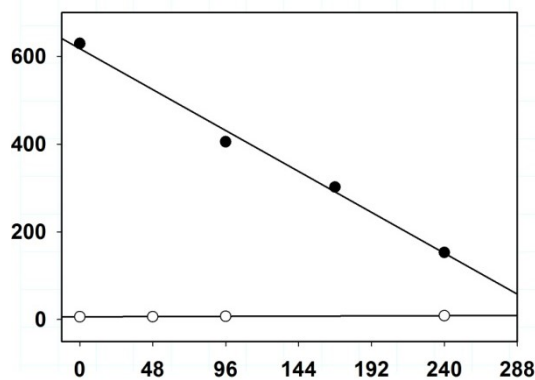
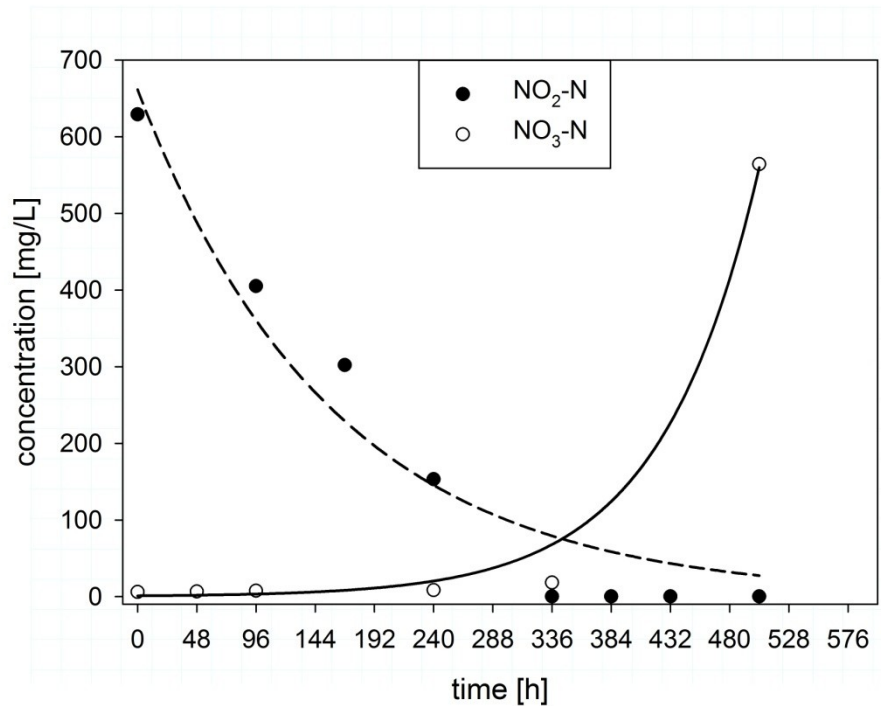


Figure 42: Nitrite consumption and nitrate release during growth of *Nitrobacter* as measure for growth kinetics. Upper graph: filled circles and dashed line (fitted curve, 2 parameters) indicate exponential decay of NO_2^- in the growing culture, while open circles and solid line (fitted curve 2 parameters) show exponential increase of NO_3^- concentration. Lower graph: detailed graph of measured concentrations during the first 240 h of the experiment. Lines represent regression functions fitted to the data. For symbol legend see upper graph.

In these cases, the respective value was excluded and only values from the complementary cuvette test were displayed. Up to 240 h after inoculation no changes in nitrate concentration were observed as revealed by $\text{NO}_3\text{-N}$ analysis, indicating low conversion rate of nitrite to nitrate. While $\text{NO}_2\text{-N}$ concentration decreased during subsequent analyses to almost 0 mg/L after 336 hours (14 days), $\text{NO}_3\text{-N}$ concentration increased only slightly after 336 hours and incremented strongly until 504 hours (21 days).

The discrepancy between the decay of $\text{NO}_2\text{-N}$ and the delayed increase of $\text{NO}_3\text{-N}$ in the medium illustrates eventual shortcomings of this method. One reason might be the concentration of 1300 mg/L nitrite present in the fresh media, which is thought to inhibit its own oxidation at much lower concentrations, i.e. 1.4 to 184 mg/L (Boon and Laudelout, 1962; Lees and Simpson, 1957). Another key parameter in nitrite oxidation is oxygen supply, which could be limiting in such assay, although the test vessel was opened and thus aerated every two days. However, these facts do not explain the delayed increase of nitrate concentration, while nitrite decayed during the first 10 days. As nitrite concentrations were too high in the initial phase of the experiment for the cuvette test, samples needed to be diluted up to 1000-fold. Due to probable dilution effects, this method is considered prone to deviations. However, if regarding the period of time between 0 h and 240 h in figure 42, the fitted hyperbola curves detract from the observation that the decline in $\text{NO}_2\text{-N}$ concentration is almost linear and $\text{NO}_3\text{-N}$ concentration remains linearly constant. This linear pattern of consumption indicates a constant cell number throughout the regarded time period. Assuming a lag phase after inoculation of the media, $\text{NO}_2\text{-N}$ concentrations would be assumed to remain constant during the first few days of the experiment. In a preliminary test over a period of 4 h, $\text{NO}_2\text{-N}$ consumption started within the first 2 hours after inoculation. Throughout this experiment, $\text{NO}_2\text{-N}$ concentration decreased at a rate of 0.01 to 0.015 mg/L*h. Hence, one cannot argue that the lag phase might have occurred during the first 96 h of the growth kinetics experiment. It remains unclear, why the $\text{NO}_2\text{-N}$ consumption rate did not increase as expected under the assumption of cell culture growth. Also $\text{NO}_3\text{-N}$ release does not elucidate this issue: up to a time period of 14 days (336 h), no increase in $\text{NO}_3\text{-N}$ concentration was observed. Between days 14 and 20, however, a steep incline was determined.

Other methods for determination of growth kinetics were explored, such as a colorimetric cell viability dye (CCVK I (WST-8) Promo Cell GmbH, Heidelberg, Germany) and aniline violet staining. In both methods, an increase of absorption (OD at a certain wavelength) refers to increase of cell number. As indicated in figure 43, scattering of measured absorption was very high for both methods at the beginning (0 h for aniline violet and 24 h for CCVK) of the experiments. For aniline violet, no increase of OD was detected over a period of 14 days (336 h) and scattering of absorption measures appeared to be varying between sampling dates. CCVK measures were conducted over a time course of only 5 days. Results suggested that the cell number of *Nitrobacter vulgaris* increased until day 4 (96 h) and subsequently the cell number entered stationary phase (no change of absorption). This result was

contradictory to the findings from nitrite consumption and also contrasted the growth kinetics information in literature (Lees and Simpson, 1957).

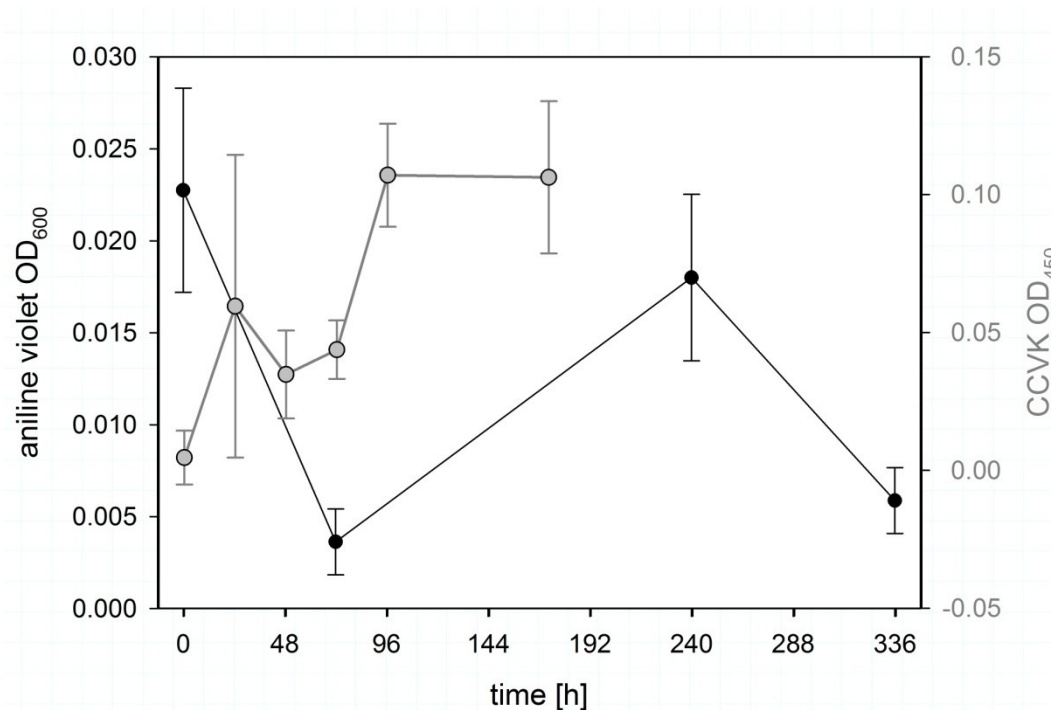


Figure 43: Growth kinetic experiments with *N. vulgaris* and aniline violet (black, scaling on the left) or CCVK (gray, scaling on the right). Error bars indicate standard error of means.

Despite the shortcomings of the nitrite consumption method, it is assumed that cell density in the culture was more or less constant at least throughout the first 10 days of the experiment, which is in consensus with data from literature. Thus, pre-culture periods for toxicity tests were determined as 10 days and exposure was carried out for 4 days in total (see below). For subsequent toxicity testing, FCVK method was chosen, because it was the most practicable and probably most reliable method, besides for the reason of comparability of test results between all conducted single species experiments.

4.4.3 Toxicity tests with *Nitrobacter vulgaris* and nAg

4.4.3.1 Materials and methods for *N. vulgaris* toxicity tests

Characterization of nAg in Nitrobacter medium

UV-vis spectroscopy was applied for characterization of nAg at toxicity test concentrations (1, 200, 1000, 2500, 5000 and 10000 µg/L) in *Nitrobacter* medium (DSMZ 765.c) at a wavelength range of 250 to 600 nm. Particle diameters were calculated according to equation 1 and equation 2, if applicable corresponding to measurement results (see section 4.4.3.2). UV-vis characterization was repeated at concentrations of 2500 to 10000 µg/L over 72 h, in order to control for dispersion stability throughout exposure duration in toxicity tests.

Particle characterization with dynamic light scattering technique was omitted, as measures in previous chapters showed strong bias towards higher diameters.

Toxicity tests

A range finder toxicity test was conducted at nominal nAg concentrations of 1, 10, 100, 1000 and 10000 µg/L. Nominal concentrations corresponded to the NP fraction as determined by ICP-OES in the NM-300K stock (see 2.1, page 9 f.) in the case of nAg dispersion and to the calculated fraction of Ag⁺ in the case of AgNO₃ stock solution. A graphical scheme of assay preparation for the toxicity test is shown in figure 44.

For assay preparation, a pre-culture was set up 10 days before the experiment. A nAg stock dispersion with 1 g nAg (NM-300K, LGC standards material, Mercator GmbH, Salzwedel, Germany) per L HPLC-grade water (Carl Roth GmbH + Co. KG, Karlsruhe, Deutschland) and a silver nitrate stock solution with 1 g AgNO₃ (≥ 99, 9%, p.a., Carl Roth GmbH + Co. KG, Karlsruhe, Deutschland) per liter HPLC-grade water were prepared. From these stocks, working stocks were prepared 11-fold concentrated compared to final nominal concentrations.

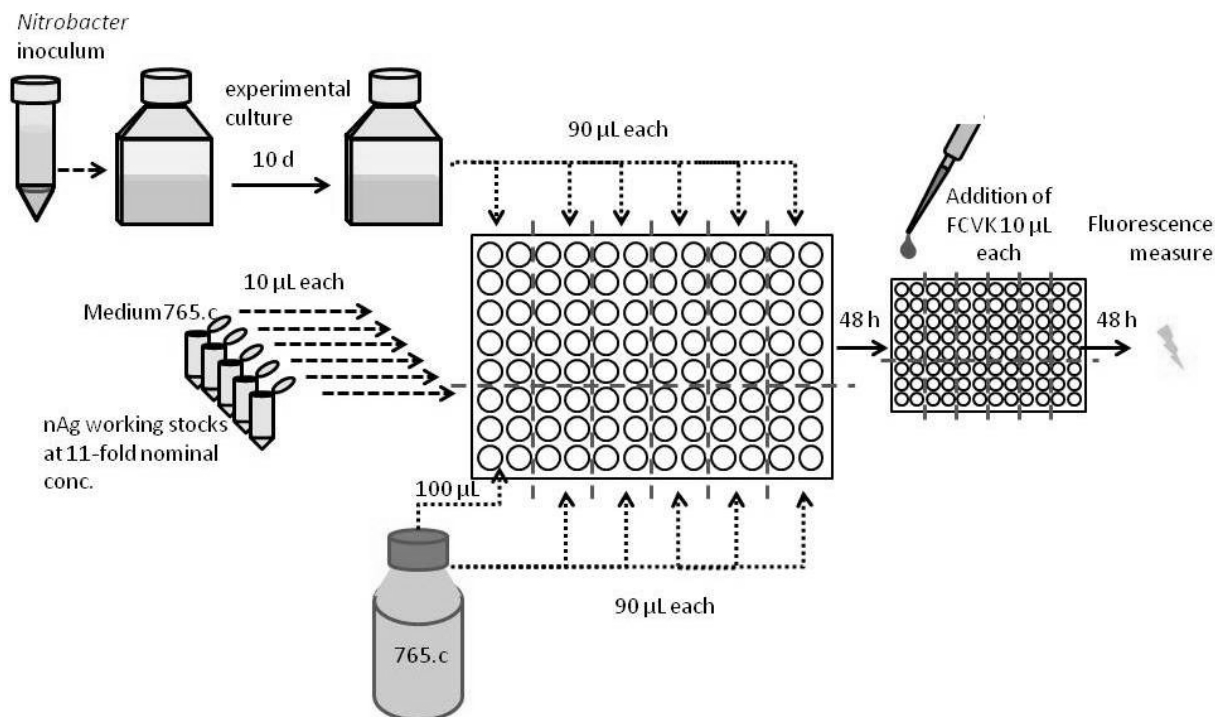


Figure 44: Scheme of toxicity test preparation with *Nitrobacter vulgaris* and nAg or AgNO₃, respectively.

Experiments were carried out using 96-well plates (pure grade S, transparent F-bottom, Brand GmbH & CO KG, Wertheim, Germany). At the beginning of the experiment (t0h), 10 wells per control and concentration of both treatments were filled each with 90 µL of the 10 days old cell culture. For blanks (6 replicates each per control and treatment concentration) plain *Nitrobacter* medium (756.c) was deployed. 10 µL of the respective working stock were added to the treatment wells and respective blanks. For controls, the same amount of plain medium was used. The plates were incubated for 48 h at 28 °C in the dark and subsequently 10 µL of fluorescent cell viability kit (FCVK, Promo Cell GmbH, Heidelberg, Germany) were added to all wells. Exposure was continued for further 48 h at 28°C in the dark, before viability measures were undertaken, using a plate reader (Polarion plate reader, Tecan Group Ltd., Switzerland) with an excitation wavelength of 545 nm and emission wavelength of 590 nm.

In subsequent experiments the tested final concentrations were 1, 50, 100, 200 and 1000 µg/L for both nAg and AgNO₃ treatment and assays were prepared in the same manner as described for the range finder experiment.

4.4.3.2 Results and discussion of *N. vulgaris* toxicity tests

Characterization of nAg in Nitrobacter medium

Preliminary results of UV-vis spectroscopy measures revealed that concentrations as applied in toxicity tests other than the range finder assay, were too low to obtain distinct peaks from nAg in *Nitrobacter* medium as shown in figure 45 (colored lines).

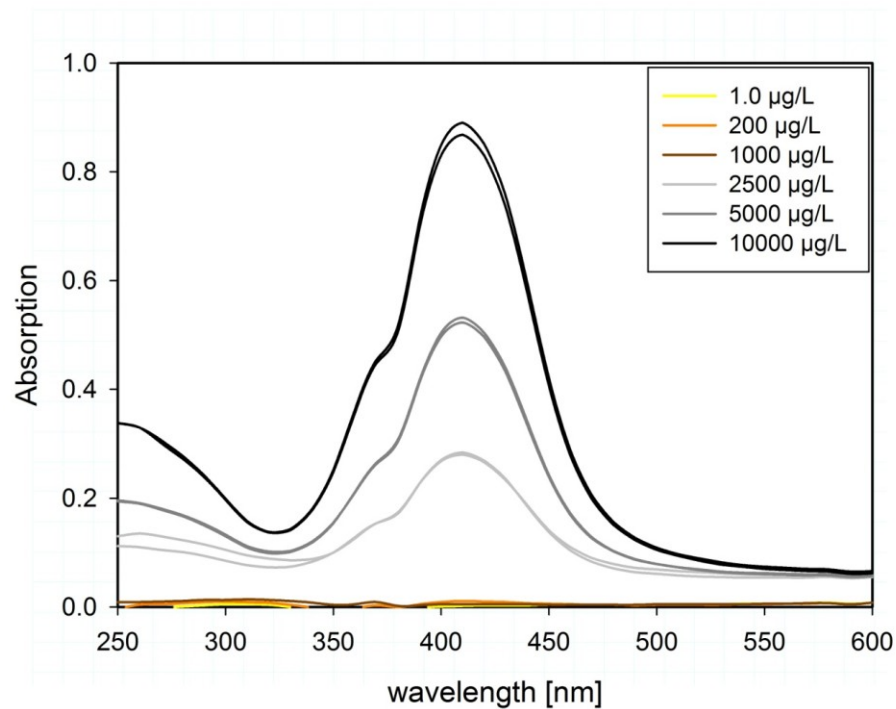


Figure 45: UV-vis spectrogram of nAg in Nitrobacter medium at exposure concentration (colored) and increased concentrations.

For higher concentrations, as used during range finder experiments, peaks were distinctly shaped and calculation of particle sizes according to equation 1 and equation 2 (see page 10) was practicable. According to these equations, mean particle diameter was 25.5 ± 1.4 nm at concentrations of 2500 to 10000 µg/L. Results from prolonged measures at these concentrations are displayed in figure 46.

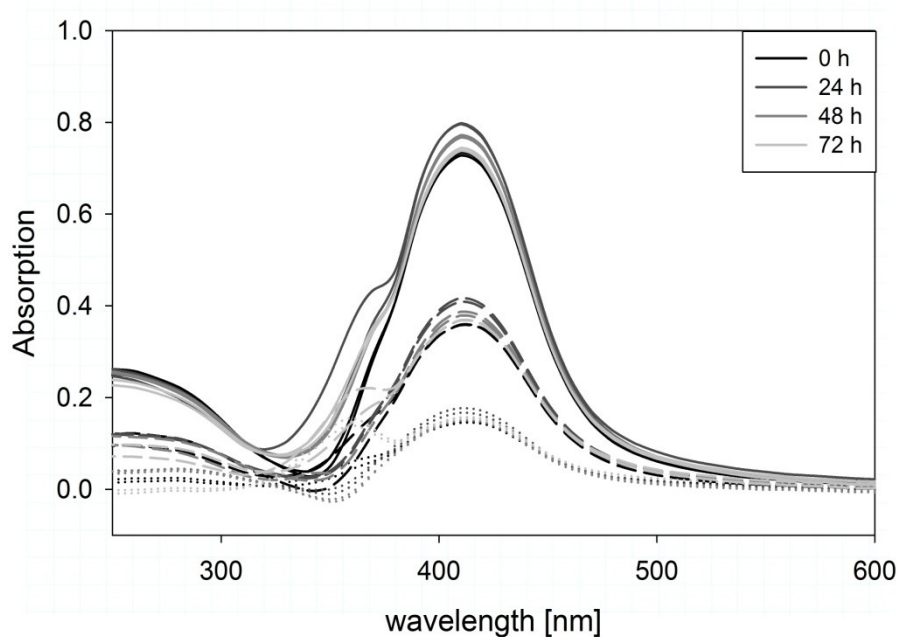


Figure 46: UV-vis spectrograms of nAg in *Nitrobacter* medium over 72 h with concentrations of 2500 µg/L (dotted lines), 5000 µg/L (dashed lines) and 10000 µg/L (solid lines). Smooth shoulders in the peaks at wavelengths of 370 to 380 nm are artifacts from the change of light source.

The peak heights and absorption at 250 nm did not differ significantly over time per nominal concentration, indicating constant concentrations of nAg in the medium throughout exposure duration.

Particle diameters calculated from these UV-vis spectra remained stable at around 20 nm for all concentrations up to 48 h. After 72 h, particle diameters increased slightly at the lowest concentration to 35 nm and at the medium concentration to 25 nm. This increase could be caused by a minor agglomeration tendency. For a more pronounced agglomeration, calculated particle sizes would reflect common multiples of the primary particle size. It must be regarded that concentrations applied in toxicity tests were lower than those analyzed here and dispersion stability might differ, especially regarding dissolution of particles. Also, probable effects of living bacteria on dispersion stability could not be considered here, as organisms would interfere with UV-vis measurements.

Toxicity tests

A preliminary toxicity test was conducted as range finder between concentrations of 1 and 10000 µg nAg/L. Results of this test are depicted in figure 47.

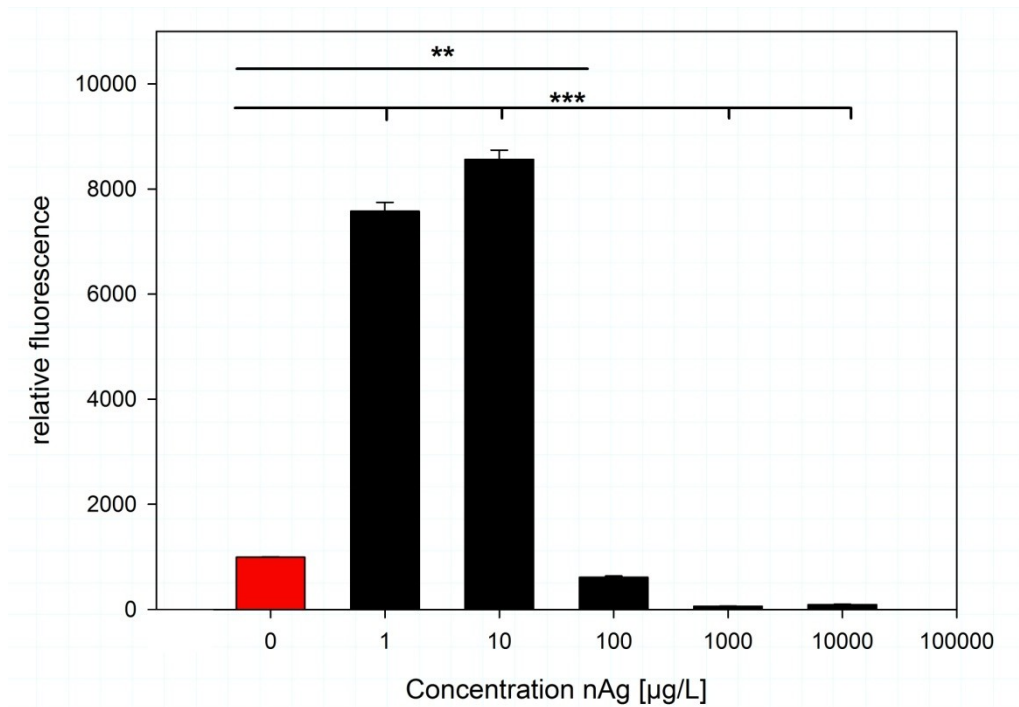


Figure 47: Results of range finder toxicity test with *Nitrobacter vulgaris* and nAg. Note logarithmic scaling of x-axis. Asterisks indicate significant differences according to One-way ANOVA with Holm-Sidak posthoc test. Error bars indicate standard error of means.

Interestingly, at the lowest concentrations tested, relative fluorescence was much higher than in controls, indicating higher viability of these treatments, which could be induced by hormesis effects. At 100 µg nAg/L inhibitory effects were first visible with statistical significance according to One-way ANOVA ($P < 0.008$) and a strong inhibition was observed at the two highest concentrations. Exposure concentrations for subsequent assays were chosen to cover the range of concentrations where inhibitory effects were visible within range finder assay, in order to obtain a concentration response curve. A factor of 2 was applied for concentrations 50 to 200 µg/L, and the highest (1000 µg/L) and lowest (1 µg/L) tested concentrations of the range finder assay were included to test for reproducibility of results.

Results of this assay showed no comparability of viability inhibition between nAg and AgNO_3 (Ag^+) exposure. Relative fluorescence in total was low (figure 48), which might be a result of the slow growth of *Nitrobacter* and consequently comparatively low metabolic activity.

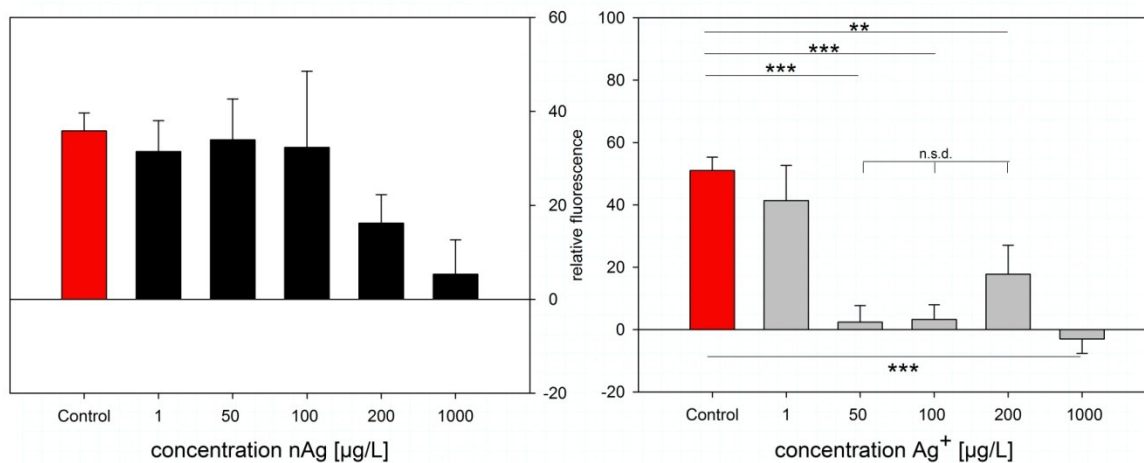


Figure 48: Results of toxicity test with *N. vulgaris* at lower concentrations compared to range finder test. Left side (black bars): nAg exposure, right side (grey bars): AgNO₃ (Ag⁺) exposure. Error bars indicate standard error of means. Asterisks indicate statistical significant difference according to one-way ANOVA (with Holm-Sidak multiple comparison versus control) between bars connected by respective lines (***) P≤0.001), n.s.d. = not significantly different according to One-way ANOVA with pairwise multiple comparison (Holm-Sidak).

No statistically significant effects were observed up to the highest concentration tested in the nAg assay, unlike results obtained from the range finder test and also no hormesis effect was observed at the lowest concentration. Although inhibition was not statistically significant at 200 and 1000 µg/L nAg exposure, a general trend of the mean relative fluorescence values towards lower viability was recognizable. This fact suggests steep concentration response behavior in this range, so that minute deviations in dosage of nAg cause large differences in effects.

In Ag⁺ treatment, statistically significant inhibition effects (P<0.01 and P<0.001, see figure 48) were observed for all exposure concentrations except for the lowest concentration (1 µg/L), but these effects did not clearly mirror concentration-response behavior. Strongest mean inhibitions were observed at 50 and 100 µg/L Ag⁺, although it must be regarded that differences between means of 50 to 200 µg/L exposure were not statistically significant amongst each other. Complete inhibition was observed only at the highest exposure concentration. An EC₅₀ value was not determinable.

It is assumed that exposure with nAg was stable throughout the test period even at the highest concentration according to UV-vis characterization results. Regarding Ag⁺ released from nAg and Ag⁺ in the AgNO₃ treatment, this fact might not hold true, as Ag⁺ is able to build insoluble complexes with different ions, amongst which Cl⁻ and SO₄²⁻ were present in the test media applied here. Nominal concentrations in the

media were 300 mg/L of chloride and 20.08 mg/L SO_4^{2-} , equaling 7.03 mg/L S^{2-} . These concentrations could theoretically (supposed sufficient amounts of Ag^+ provided in the media) yield an amount of 1.21 g/L AgCl complexes under incorporation of 0.9 g/L Ag^+ , 65.2 mg/L of AgSO_4 (consuming 45.1 mg/L Ag^+) or 54.33 mg/L Ag_2S (consuming 47.3 mg/L Ag^+). Precipitation of Ag- complexes formed from released (nAg) or added (AgNO_3) Ag^+ with medium ingredients would result in lower bioavailability of toxic Ag^+ , which might explain a part of the response pattern observed for both exposure scenarios. Generally, the tested *Nitrobacter vulgaris* strain seemed to be less sensitive towards nAg exposure than Ag^+ exposure.

For Ag^+ treatment it is concluded, that either (hypothetical) concentration response curves were very steep in the range between nominal concentrations of 200 to 1000 $\mu\text{g/L}$, so that minute deviations in dosage caused a bias of results regarding inhibition, or that silver resistance mechanisms like efflux pump systems were active up to a certain threshold concentration. This would also be in agreement with results from the range finder test with nAg, where inhibition was observed at concentrations of 1000 and 10000 $\mu\text{g/L}$, however without reaching total inhibition. These assumptions could be evaluated by applying molecular techniques for determination of genes encoding efflux pump systems, as applied in the work of Yang et al. (2014), or by determination of gene copy numbers of 16SrRNA specifically for *Nitrobacter*. With the latter method, as shown before by Zhang et al. (2014) and Liang et al. (2010), better resolution of the response of the culture to exposure with nAg and Ag^+ would be achievable than with cell culture growth quantification and viability measurement methods as applied in this work. In other studies focusing on performance of nitrifying bacteria, substrate consumption rates have been used regarding transformation of $\text{NO}_2\text{-N}$ to $\text{NO}_3\text{-N}$ (Grunditz and Dalhammar, 2001), or oxygen uptake rates (Kim, 2004). The first method however was not feasible to handle in replicated multiple concentration assays and the second method was not available at the laboratory where this study was conducted. It should thus be considered to use molecular methods for effect determination of nAg in nitrifying bacteria in future investigations.

Compared to the other tested bacteria species in this work, *N. vulgaris* was the least sensitive species, supporting the first hypothesis of this thesis, regarding differential sensitivity of test organisms towards nAg exposure.

5 Accumulation tests with nAg in a simple food chain

5.1 Introduction - accumulation of nanoparticles

In previous sections the role of silver ions (Ag^+) released from silver nanoparticles (nAg) concerning toxicity towards bacteria and ciliates has been discussed. It was assumed, that the Ag^+ concentration which was present in exposure medium provoked toxicity in the assay with *P. tetraurelia*. It must be considered however, that uptake of Ag into the cell and thus the internal fraction of Ag might differ substantially from the fraction which was available in the media. Also, uptake of nAg by the cell via ingestion together with food might affect the cells to different extent compared to exposure via surrounding medium, especially in the case of the bacterivorous ciliate *P. tetraurelia*. Within bioaccumulation (i.e. uptake of compounds into the cell), biomagnification and bioconcentration are distinguished. Biomagnification is the uptake via contaminated food and bioconcentration is the uptake from the surrounding environment, especially via cell surface. Accumulation processes play a major role in toxicity of some compounds, such as (heavy) metals or persistent low-level toxins: although their environmental concentration is too low to bear an acute risk for a specific species, they are accumulated in primary consumers and subsequently transferred and accumulated within the trophic cascade, thereby reaching critical concentrations in top predators (MacCormack and Goss, 2008).

As Wang (2011) stated, information on biokinetics and bioaccumulation of NPs in aquatic organisms are lacking. Although some studies exist, which describe the magnification of NPs, little is known about trophic transfer, elimination, chronic toxicity, or partitioning of the material under experimental and environmental conditions (Wang, 2011).

Hou et al. (2013) reviewed available data from literature concerning the bioaccumulation of nanomaterials (NMs). According to the information collected, accumulation of NMs depended on the type and size of NM and the organism under investigation, for different routes of exposure, i.e. via bioconcentration or via biomagnification. Comparatively few studies were available, which focus on trophic transfer of nanoparticles in aquatic food chains. Exposure of ciliates via NP-contaminated bacteria was studied by Werlin et al. (2011) using cadmium selenide quantum dots in experiments with *Tetrahymena thermophila* and by Mielke et al. (2013), who exposed *T. thermophila* to nTiO₂.

In this section of the present study, potential acute and chronic effects of nAg exposure via medium and via food were determined for the ciliate *P. tetraurelia*. The aim of this work was to elucidate whether different uptake pathways of nAg lead to different effects (hypothesis 4) and to bridge the gap in experimental complexity between single species toxicity tests (see previous sections) and whole community tests (see following section).

5.2 Materials and Methods for accumulation experiments

Each accumulation assay contained two types of cell cultures: one with *Paramecium tetraurelia* only, for nAg uptake via medium (bioconcentration) and one with *P. tetraurelia* and addition of exposed *Raoultella planticola*, for uptake via food (biomagnification). These two potential uptake pathways are depicted in figure 49.

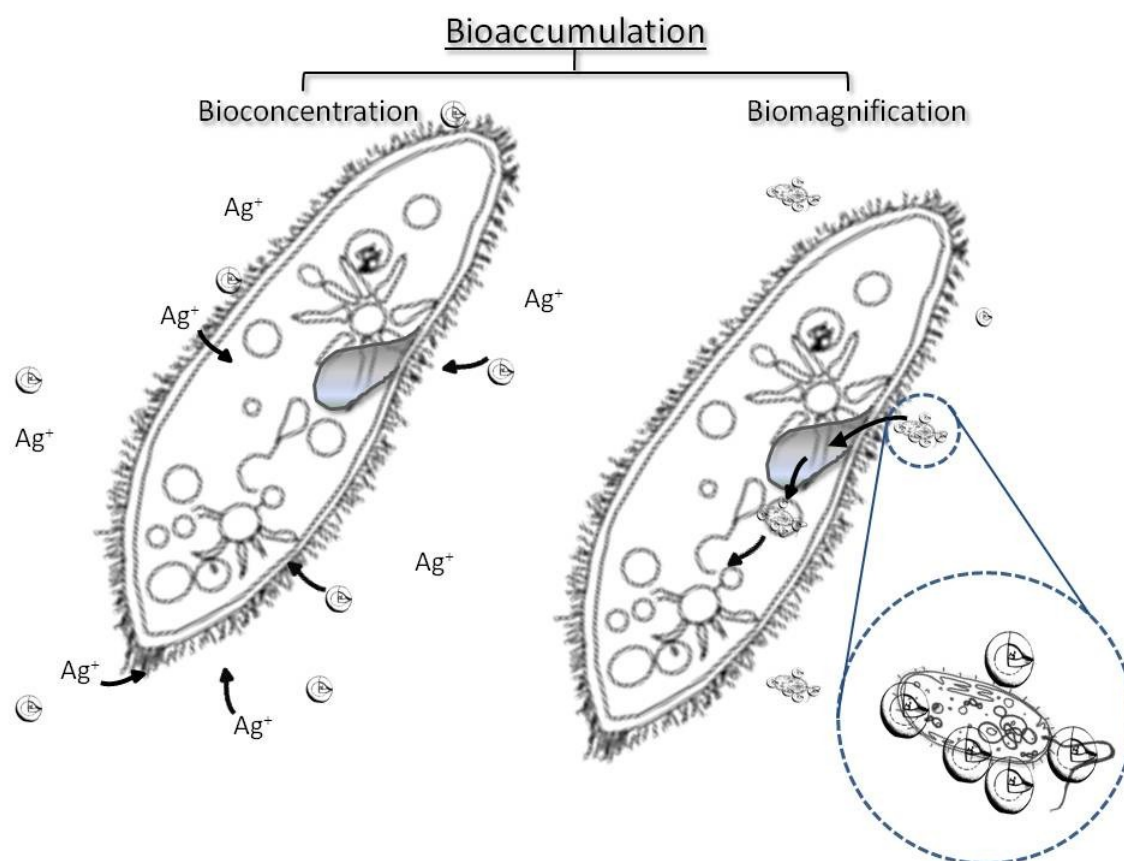


Figure 49: The two modes of bioaccumulation- bioconcentration (uptake from surrounding medium) and biomagnification (uptake via food).

For comparability of these two modes of exposure, the same media needed to be applied in both assays. Cerophyll medium (CM) was used for this purpose, because axenic broth for ciliates (ABC) favors extreme bacterial growth and thus was not suitable for this approach. In order to define exposure concentrations for accumulation experiments and to compare effects of nAg on paramecia in CM to effects on paramecia in ABC (see section 3.3), a preliminary experiment was conducted with *P. tetraurelia* exposed in filtrated ABC and *P. tetraurelia* exposed in conditioned CM. Here 'conditioned' refers to a media, in which bacteria have grown, but which does not contain living bacteria anymore. It was used because fresh CM is toxic to *P. tetraurelia* for unknown reasons (Krenek pers. comm.)⁸. For preparation of conditioned CM, a flask with 500 mL of sterile 0.25% CM (for preparation protocol see ANNEX II) was inoculated under sterile conditions (Hera Safe HS12, Heraeus Instruments, Hanau, Germany) with *R. planticola* cells, which were previously stored in glycerol at -80°C , as follows: one 1.5 mL reaction cup (Eppendorf, Hamburg, Germany) of frozen (-80°C) *R. planticola* stock was thawed at room temperature. An aliquot of 20 mL fresh CM was transferred to a 50 mL reaction tube (TPP, Switzerland). For washing the cells, the reaction cup containing thawed *R. planticola* stock was centrifuged at 8000 rpm (5403 Eppendorf, Hamburg, Germany) for 5 minutes. The supernatant was removed and discarded and the pellet was resuspended by adding 900 μL of CM from the reaction tube and careful mixing by moving the piston of the pipette. Centrifugation and washing was repeated twice, however with 3 minutes centrifugation time. The content of the cup was then transferred to the 500 mL flask and left for growth of the bacteria culture at room temperature for 3 days.

After this incubation, the flask was autoclave sterilized for 20 min at 121°C in order to kill the *R. planticola* bacteria. After settling of dead bacteria by gravitation, the cell free supernatant ('conditioned CM') was subsequently used for assay preparation instead of filtrated ABC for CM exposure. Conditioned CM had a pH of 6.3 after autoclaving, ABC had a pH of 6.9. Both types of exposure were set up as previously described (section 3.3.1) with regard to fluorescent cell viability kit assays (FCVK, Promo Cell GmbH, Heidelberg, Germany) in 96-well plates (pure grade S, transparent F-bottom, Brand GmbH & CO KG, Wertheim, Germany). The toxicity test was carried out with five nAg concentrations between 0.5 and 40.5 mg/L and a spacing factor of 3. Concentration response curves were derived using ToxRat[®] Standard Version 2.10 software and results plotted with Sigma Plot 11.0 software. The experiment was conducted with two exposure durations: 20 h for comparability to previous results,

⁸ Dr. Sascha Krenek, Institute of Hydrobiology, TU Dresden

and 3 h (1h of exposure, addition of FCVK and 2 h of incubation) for evaluation of practicability of the method in short term experiments such as the accumulation experiment.

5.2.1 Characterization of nAg in conditioned CM at exposure concentrations

UV-vis characterization of nAg in conditioned CM was carried out in duplicate at exposure concentrations of the final accumulation assay, i.e. 1.5, 3 and 6 mg/L, as described in section 2.1.2.

5.2.2 Acute biomagnification experiments with *R. planticola* and *P. tetraurelia*

Accumulation of nAg was tested at a concentration range of 0.1 to 10 mg/L in three different assays. These were conducted in order to optimize the strategy for determination of effects and the concentration range for the final assay. Due to the number of different treatments which were necessary for these experiments, only three concentrations per assay were tested.

The experimental setup is sketched in figure 50 and described below.

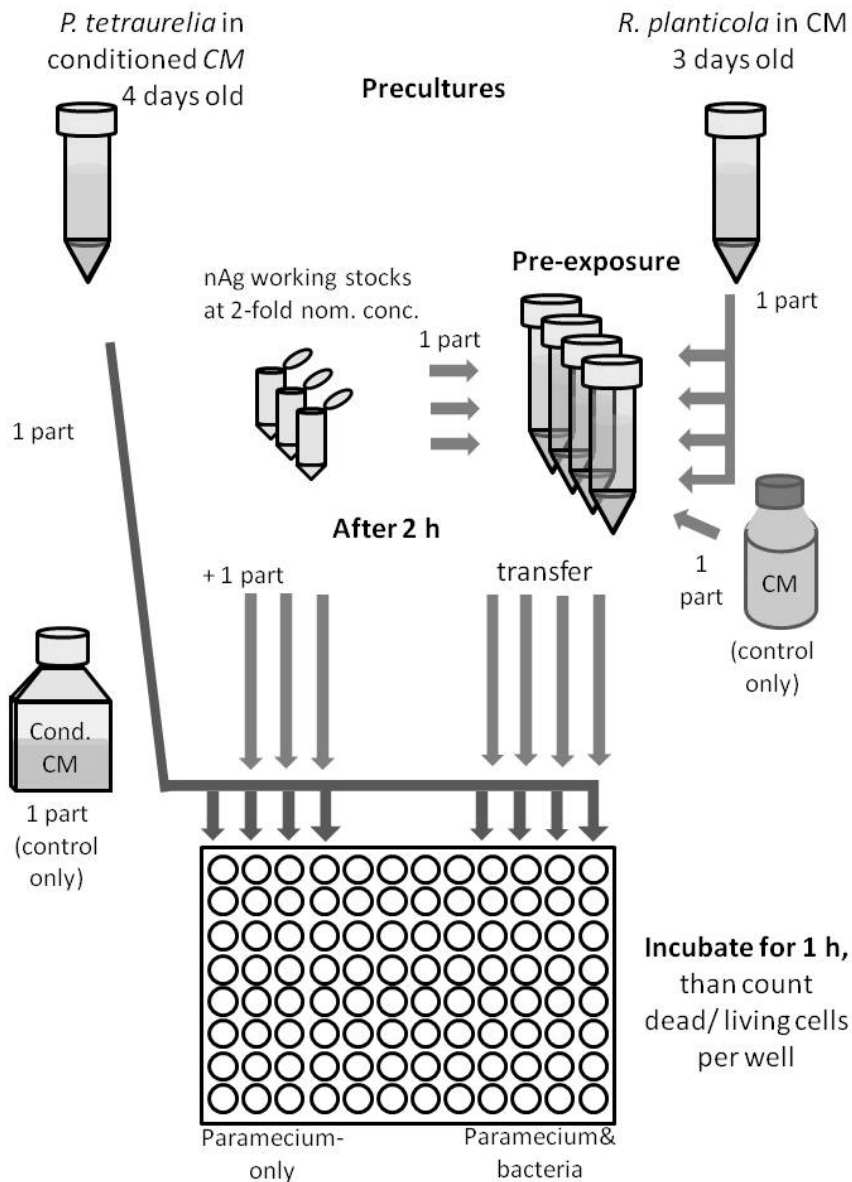


Figure 50: Flowchart of the experimental setup in the biomagnification assay with *P. tetraurelia* and *R. planticola*.

Precultures of *P. tetraurelia* (4 days before test) and *R. planticola* (3 days before test) were prepared in order to provide cell cultures at exponential growth phase for accumulation experiments. Axenic *P. tetraurelia* cells were transferred to filtrated conditioned CM for this purpose.

For preparation of the assay, a 1 g/L nAg stock was prepared as described above (section 3.3.1). Working stocks at twofold exposure concentration were prepared from this stock and conditioned CM in 0.5 mL reaction cups (Eppendorf, Hamburg,

Germany) for exposure-via-medium assays. The tubes were wrapped in aluminum foil for protection from light.

Aliquots of *R. planticola* were taken for each of the three exposure concentrations and supplied with an appropriate volume of nAg stock to reach 2-fold the final nominal exposure concentration. *R. planticola* exposed to nAg and an aliquot of pure culture for control were incubated for 2 h at room temperature in the dark for pre-exposure. In the mean time, *P. tetraurelia* preculture was analyzed regarding cell number as described in section 3.2.1. Subsequently, the test assay was prepared by filling 5 replicate wells per treatment and concentration of a 96-well plate (pure grade S, transparent F-bottom, Brand GmbH & CO KG, Wertheim, Germany) with 50 μ L of *Paramecium* preculture.

For exposure via medium, the same volume of the respective working stock or conditioned CM (as controls) was added to the cells. For exposure via food, the respective pre-exposed *R. planticola* cultures were added at the same volume, using pure bacteria culture as controls.

The assay was incubated for 1 h. This was the estimated duration for complete filtration of the content of a well by a *Paramecium* culture at a certain cell density. The calculation of this duration was based on minimal and maximal filtration rates for *P. caudatum*, taken from Fenchel (1980a). Aliquots from controls (*P. tetraurelia* supplied with conditioned CM and *R. planticola*, respectively) were used for determination of initial pH (WTW Sentix MicB electrode with WTW pH 3110).

At the end of the test in the final assay, an optical evaluation of the 96-well plate was undertaken by means of a stereomicroscope (Leica Wild M10, Wetzlar, Germany) and wells were categorized to contain (a) many living and few or no dead paramecia, (b) living and dead paramecia at almost the same proportion or (c) few or no living and many dead paramecia. In the final assay the definite cell numbers were determined according to optimized strategy as follows: In wells categorized as 'a', dead cells were counted and in wells categorized 'c' living (moving) cells were counted by eye directly in the well without any other treatment. Category 'b' turned out not to be represented in practice and thus needed no special analysis procedure. Aliquots of the respective controls were pooled to determine final pH value (WTW Sentix MicB electrode with WTW pH 3110).

Colony forming units of *R. planticola* were determined to reveal effects of nAg exposure on bacteria and their potential availability as food for *P. tetraurelia*. For this purpose 100 μ L aliquots were taken from each type of exposure and concentration

for plating on Mueller-Hinton-Agar and incubated at 28°C for 24 h. CFU of *R. planticola* were subsequently counted.

In previous assays it was tested, whether living cells in the supernatant could be removed and fixated similar to procedures applied in single species tests with *P. tetraurelia*. This method, however turned out to yield deviating results of accumulation experiments compared to the situation as evaluated optically in the wells (for details see discussion below). Other methods, such as application of live-dead staining or viability assays failed to reflect the effects of nAg in accumulation experiments as well. The preliminary assays were carried out with the following final nAg concentrations: 0.1, 0.5 and 2.5 mg/L in the first assay and 2.5, 5 and 10 mg/L in the second assay. The final assay was undertaken with nAg concentrations of 1.5, 3 and 6 mg/L.

For evaluation of test validity, the total cell number was determined in some of the control wells by fixation of the whole well content through addition of Bouin solution (Sigma-Aldrich, Steinheim, Germany). Aliquots of 15 µL for counting in the counting chamber were drawn and analyzed as described before (section 3.2.1). The number of dead cells was subtracted from total cell number for calculation of surviving cells. This number was compared to the initial cell number at the beginning of the test. Tests were considered valid, if control mortality was below 10 %.

5.2.3 Chronic biomagnification experiments with *R. planticola* and *P. tetraurelia*

For evaluation of effects of nAg on the overall fitness of *P. tetraurelia* populations by biomagnification, growth curves were determined for cultures exposed via medium and via food at nominal nAg concentrations of 0.01, 0.03 and 0.1 mg/L. The setup was similar to the acute test assay, however with 3 replicates for each control and concentration and at a higher initial volume (3 mL culture with nAg working stock or medium in 15 mL-PE tubes). A culture of *R. planticola* was grown for 3 days in CM prior to the experiment and an axenic culture of *P. tetraurelia* (see section 3.2.1) was transferred to filtrated conditioned CM (see section 5.2.2). 1 g/L nAg stocks prepared from NM-300K and HPLC-grade water (Sigma-Aldrich, Steinheim, Germany) were used for preparation of *R. planticola* pre-exposure and working stocks (in filtrated conditioned CM) at 2-fold final nominal nAg concentrations.

Pre-exposure of *R. planticola* cultures was carried out for 1 h. After this period, the same volume of *Paramecium* culture and *R. planticola* (exposed or unexposed) for

exposure via food and the same volumes of *Paramecium* culture and medium or working stocks for exposure via medium were mixed.

Total cell number per mL of paramecia was determined in each replicate after preparation of the whole assay and subsequently every 24 h until stationary phase of the cell cultures was reached. For cell counting, 65 μL were withdrawn from each replicate after gentle mixing and fixed with 1.5 μL Bouin solution (Sigma-Aldrich, Steinheim, Germany) in 0.5 mL reaction cups (Eppendorf, Hamburg, Germany). Cells were counted as previously described (section 3.2.1). In order to control for abundance of living bacteria in the samples from exposure via food at the end of the experiment (day 5), 10 μL aliquots were taken from all replicates previously supplied with *R. planticola* and streaked on LB-agar plates. The plates were incubated for 2 days at 22 °C and checked for growth of bacteria colonies.

5.3 Results and discussion for acute accumulation experiments

5.3.1 Comparison of single species tests with nAg in conditioned CM and ABC

A parallel exposure assay with nAg was conducted with *P. tetraurelia* in conditioned CM and ABC for comparison of cell sensitivity in different media. The results were used for determination of concentration ranges for subsequent accumulation experiments. Results of the 20h exposure assay with FCVK are shown in figure 51 as concentration response curves according to probit analysis.

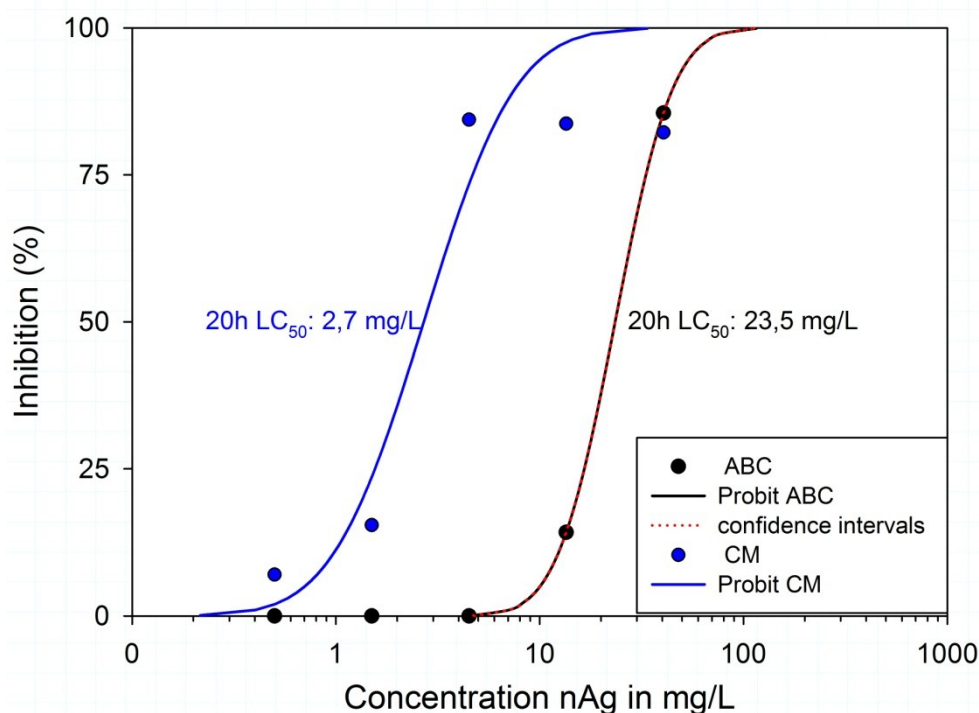


Figure 51: Results of parallel nAg exposure assay with *P. tetraurelia* in conditioned CM and ABC. Red dotted lines indicate 95% confidence intervals for ABC exposure. For CM exposure, confidence intervals could not be determined.

According to these results, 100% mortality was not achieved for either exposure type. 95% confidence intervals (CI) were determinable for ABC exposure only. These appear identical to the probit curve due to the narrow range of the CI and logarithmic scaling of the x- axis. LC₅₀ values were determined and indicated a higher sensitivity of *P. tetraurelia* exposure to nAg in conditioned CM (2.7 mg/L) compared to ABC exposure (23.5 mg/L). Possible reasons for the higher sensitivity of *P. tetraurelia*

observed for exposure in conditioned CM are the properties of the medium in terms of composition and availability of nutrients, as well as the comparatively low pH value. The composition and pH of conditioned CM might substantially enhance the dissolution of Ag^+ from nAg compared to the conditions in ABC and thus boost toxicity towards *P. tetraurelia*. Lower availability of nutrients due to the use of cell free supernatant and low pH might also affect paramecia independently as suggested by the lower intensity of fluorescence in controls with conditioned CM compared to controls in ABC. Yet this fact cannot be proven finally, as cell numbers tended to be generally lower in the assay with conditioned CM from the beginning of the experiment, but could not be determined due to difficulties concerning the cell counting method (see discussion below, section 5.3.3).

In the short term assay (3h), FCVK did not exhibit distinct fluorescence signals, because incubation was obviously too short for transformation of the dye by the cells. Thus, FCVK was unsuitable for accumulation experiments. Hence, concentration ranges for accumulation experiments were derived from the 20h experiments and alternative strategies for determination of endpoints were developed.

5.3.2 UV-vis characterization of nAg in conditioned CM at exposure concentrations of final accumulation assay

According to characterization results from previous single species tests with *R. planticola*, nAg was shown to be stably dispersed in CM. For comparison of dispersion status in pure and conditioned CM, UV-vis characterization was undertaken at exposure concentrations for the final assay (1.5, 3 and 6 mg/L) as described in section 2.1.2.

Spectrograms from UV-vis measures are shown in figure 52. Relative absorption of nAg was comparably low, as tested concentrations were in the lower range of applicability for UV-vis characterization and due to the relatively high turbidity of the medium. Still, distinct peaks were visible in the range of 400 nm wavelength, allowing for determination of particle size. Particle diameter according to equation 1 and equation 2 (page 10) was 20.2 ± 1.9 nm as mean for all concentrations, which is in good agreement with manufacturer's information (see section 2.1.1).

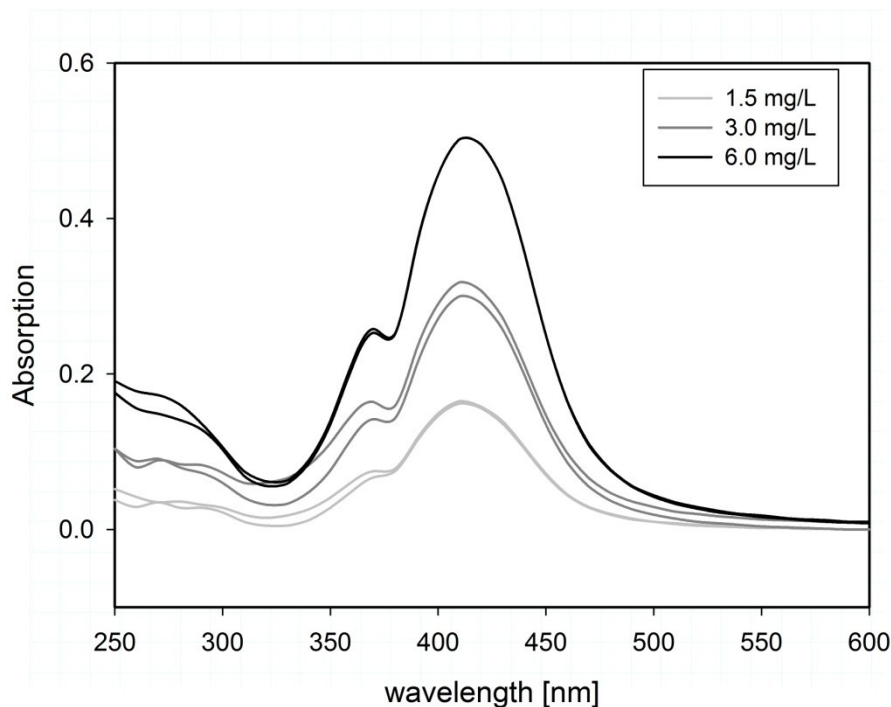


Figure 52: UV-vis spectrograms of nAg in conditioned CM at exposure concentrations.

5.3.3 Results and discussion of acute accumulation experiments with *R. planticola* and *P. tetraurelia*

The evaluation of accumulation test results was carried out ‘by eye’ using a stereomicroscope. As stated before, fixation of living cells in the supernatant led to differing results when compared to the real situation in the wells as determined optically. One reason for this finding was that *Paramecium* cells tended to forage at the bottom of the wells especially in samples with exposure via food, where bacteria flocks had settled probably. Thus, these living cells were not present in the transferred supernatant and led to an underestimation of the number of living cells with this method.

Results according to optical categorization were available for all conducted accumulation assays. In the first assay, all samples were categorized as a) containing few dead cells and a vast majority of living cells. Thus, no effects were observable between nAg treatment at all tested concentrations (0.1, 0.5 and 2.5 mg/L) and respective controls. However, samples with exposure via food seemed to contain slightly lower numbers of *Paramecium* cells than those with exposure via medium.

All tested exposure concentrations (2.5, 5 and 10 mg/L) were lethal in both types of exposure (via food bacteria/via media) in the second test assay. Accordingly, concentrations were chosen for the final assay in the range of the highest concentration where previously no effects were visible and the lowest concentration where 100% effect was visible along with a spacing factor of 2.

Results of the final accumulation test assay with nAg concentrations 1.5, 3 and 6 mg/L, are displayed in figure 53 as number of surviving cells per mL at respective exposure concentrations.

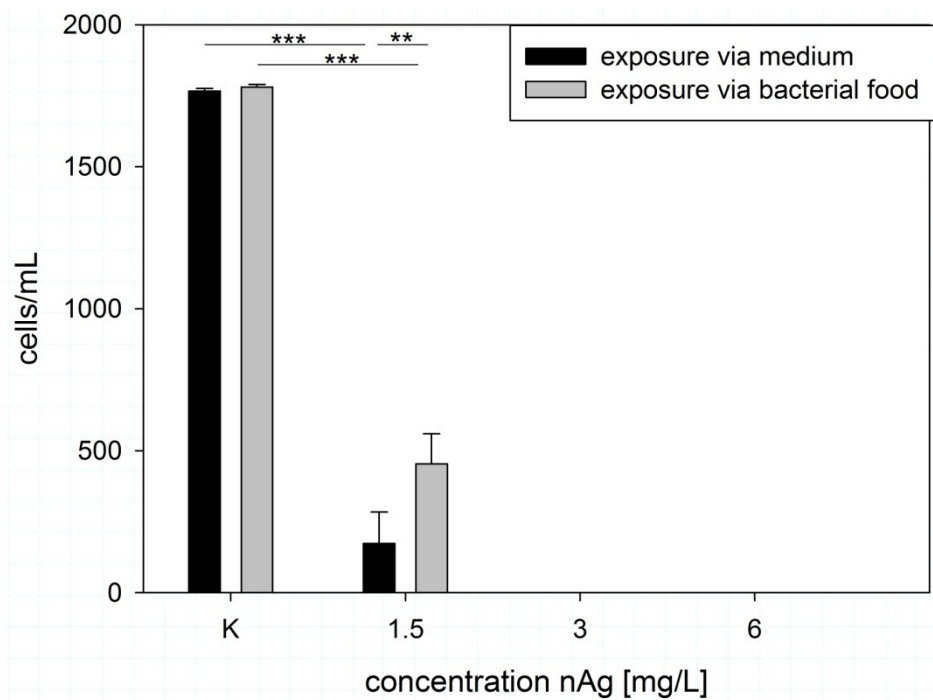


Figure 53: Mean number of surviving cells per mL in the final accumulation test assay at respective nominal nAg concentrations. Black bars indicate *Paramecium*-only samples, gray bars indicate *Paramecium*&bacteria samples. Error bars show standard error of means. Asterisks indicate significance levels as determined by One-way ANOVA with Holm-Sidak post hoc test.

Results cannot be evaluated regarding concentration response behavior, because only three concentrations were tested and effects were observed at 100 % level for the two highest concentrations. Differences between the lowest exposure concentration and controls were highly significant ($P < 0.001$, One-way ANOVA with Holm-Sidak post hoc test) for both exposure types. Hence, the concentration of 1.5 mg/L nAg reflects a lethal effect for both types of exposure. As seen in the first assay, the higher concentration of 2.5 mg/L showed no effect. This discrepancy between the two assays

is in good agreement with the steep concentration response curves obtained from previous *Paramecium* toxicity tests (see section 3.3.2), so that minute deviations in dosage of nAg among the assays led to significantly differing results.

For validation of the effects in the last assay, mortality of controls was calculated as percentage of number of dead cells relating to total cell number. Mortality was determined as 3% of the total cell number in controls from exposure via medium and 2% of total cell number in controls from exposure via food, respectively. With these mortalities being lower than 10%, the test was considered valid. Samples streaked on agar plates from controls with *R. planticola* grew area-wide, indicating availability of bacteria as food source for *Paramecium* in the supernatant. CFU were 0/mL for all samples from exposure via medium, which thus were verified as devoid of contamination.

No statistically significant differences were observed between the two controls according to One-way ANOVA with pair wise comparison of all samples. The differences between the exposure types at the lowest tested concentration were significant ($P < 0.01$) with paramecia exposed to nAg via media being more susceptible than those exposed via food bacteria. Influence of pH value on this difference was excluded, as final pH was 6.6 for both types of exposure, while initial pH was 6.5 ± 0.03 . Another reason could be the toxicity of nAg towards the bacteria. Dead cells would sediment to the bottom of the wells and be less accessible as food source for paramecia. But although exposure concentrations were distinctly higher than those applied in the single species tests with *R. planticola*, colonies on Mueller-Hinton agar plates after exposure to 1.5 mg/L nAg grew area-wide and thus CFU were uncountable in this assay. For that reason, sedimentation of a large fraction of bacteria due to cell death can be excluded as explanation for the observed difference in effects concerning the route of exposure of paramecia.

Generally, effects on *P. tetraurelia* exposed with and without bacteria in CM were more similar to each other, than exposure without bacteria in CM compared to exposure via ABC. Thus, pinocytosis and phagocytosis as potential pathways of nAg uptake do not explain differences in toxic effects for this experiment (hypothesis 4 rejected). This issue is visualized in figure 54.

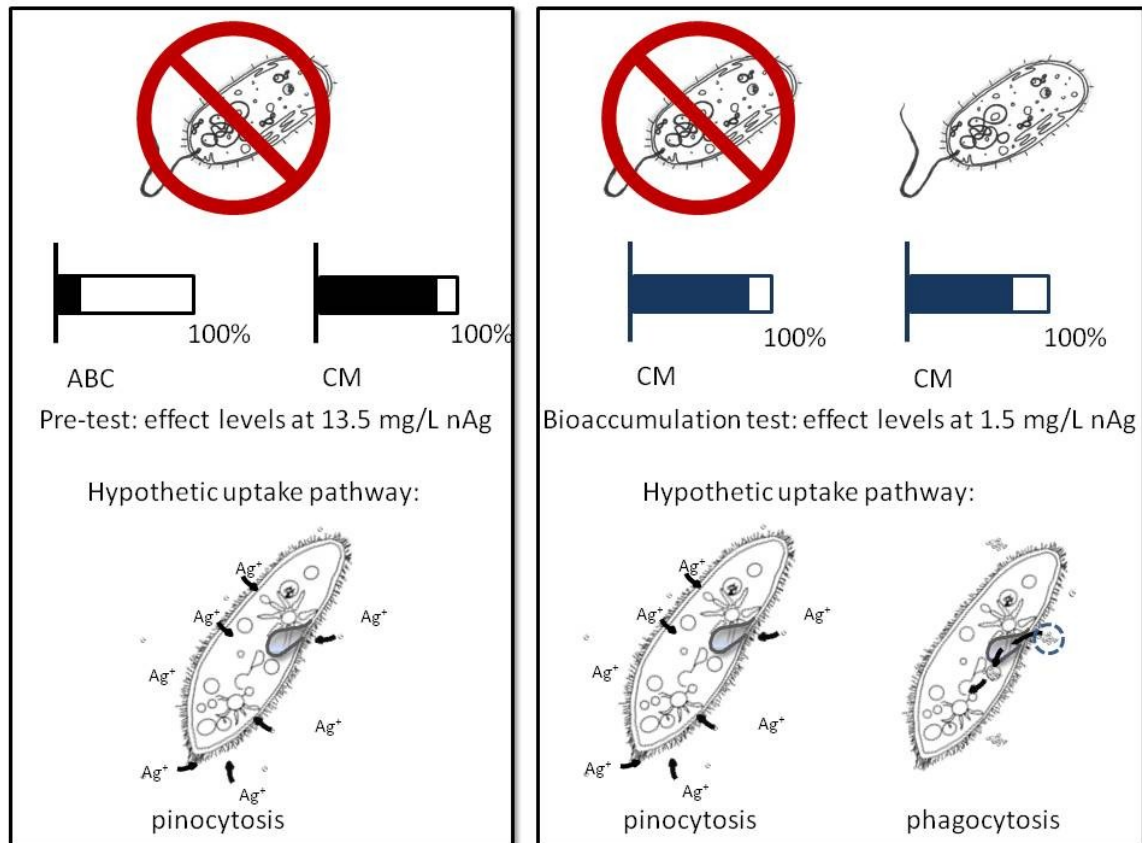


Figure 54: Comparison of effect levels in bioaccumulation experiments depending on the type of exposure (via medium, i.e. without bacteria/ via food, i.e. with bacteria) and the hypothesized uptake pathway. Exposure via different media reveals more different effect levels (left box) than exposure via food compared to exposure via medium (right box).

However, exposure concentration and real dose of Ag (i.e. Ag^+ or nAg actually taken up into the cell) are most probably not the same. Thus, evaluation of the dose should be considered in future research.

Despite the observed similarity of observed effects between the exposure types in CM, statistically significant difference was determined. Potential reasons for this finding are expected to be a consequence of bacterial interaction, or bacterial inactivity, respectively. As shown in several studies in the literature, bacteria can mitigate the toxicity of nAg by excretion of extracellular polymeric substances (EPS), which bind free Ag^+ and nAg and thus diminish contact to the bacterial cell membrane (Joshi et al., 2012; Sheng and Liu, 2011). Henriques et al. (2007) showed that hydrophobic toxins were bound in EPS released from bacteria. By excretion of EPS and concurrent binding of toxins, accumulation in the food chain might be enhanced, as described by Bhaskar and Bhosle (2006) for heavy metals in a marine food chain. The authors reported that the amount of metals (or other toxins) bound by EPS seemed to

be species specific and depended on boundary conditions such as pH and salt concentration. In this work however, exposure via medium (i.e. without EPS excreting bacteria) turned out to show higher toxicity of nAg towards *Paramecium*. This suggests, that EPS did not enhance the availability of nAg or, that paramecia do not feed on EPS or bacteria coated with EPS. Holbrook et al. (2008) studied the uptake of quantum dots (QDs) in simplified aquatic food chains with bacteria and ciliates and found that QDs were associated with aggregated bacteria, which could not be ingested by the ciliate. If EPS excretion led to aggregation of bacteria in this study, uptake by ciliates might have been prevented. Bacteria and/or their EPS might also play a role regarding Ag^+ release from nAg. It cannot be excluded, that the observed toxicity for both types of exposure was triggered by Ag^+ present in the media. In this case, bioconcentration would be the dominant mechanism of Ag uptake in both assays and consequently provoke toxicity. In conclusion, the observed lower toxicity of nAg in exposure via food bacteria could be caused by the inability of *Paramecium* to ingest EPS coated bacteria or by some bacterial influence on the amount of Ag^+ released from nAg into the media.

CFU of *R. planticola* were 60/mL after exposure to 3 mg/L nAg and 0/mL after exposure to 6 mg/L nAg. It is inferred that this result was obtained because bacteria and *Paramecia* were completely inhibited by excessive nAg concentration. *R. planticola* were still present at the end of the toxicity test in samples from exposure at 1.5 mg/L and controls in the liquid according to colonies on agar plates. It is excluded that paramecia cleared the supernatant from bacteria by feeding. This fact supports the above mentioned assumption that *Paramecia* were not able to feed on *R. planticola* probably coated with EPS and nAg. In this context it is very interesting to quantify nAg and Ag^+ uptake into *Paramecium* cells.

5.3.4 Results and discussion of chronic accumulation experiments with *R. planticola* and *P. tetraurelia*

Cell cultures of *P. tetraurelia* were exposed with nAg via food (*R. planticola* bacteria) or medium (conditioned CM) at concentrations 20 to 200 times lower than the determined LOEC from the acute bioaccumulation experiment, in order to determine probable chronic effects on the fitness of the population. The initial cell numbers of all samples were between 850 and 1250 per mL and statistically not significantly different (One-way ANOVA).

In figure 55 the growth curves as mean cell numbers per mL derived from respective replicates are shown. In those replicates which did not contain food bacteria ('exposure via medium'), no growth, but also no decrease of cell numbers was observable throughout the whole experiment.

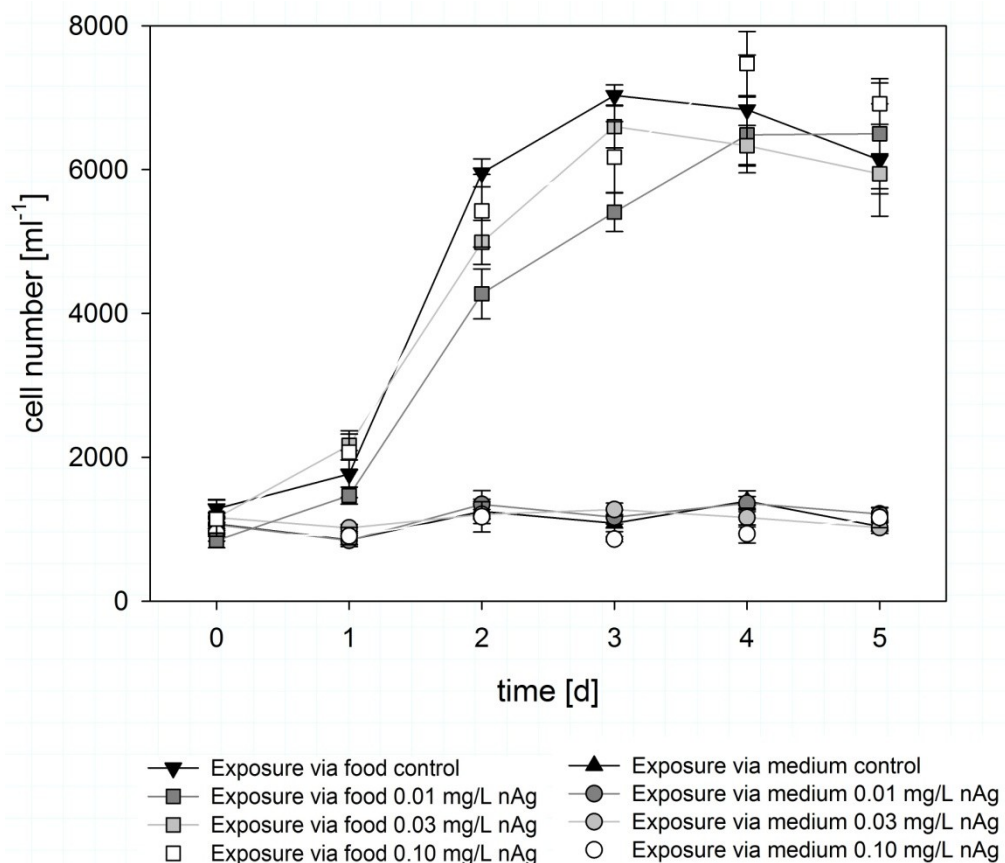


Figure 55: Growth curves of *P. tetraurelia* after exposure with nAg via food or medium and respective controls. Error bars indicate standard error of means.

No differences between controls and treatments in cell number were notable for any sampling date. The constant cell number in all samples without food bacteria indicated that cells were not replicating due to starvation. Regarding the fact that also nAg exposed cell cultures were not inhibited to a greater extent than controls, inhibitory effects through nAg exposure are negated at least for the concentrations applied in this test.

Those samples of *P. tetraurelia* that had been supplied with previously exposed or unexposed *R. planticola* ('exposure via food') started to grow within the first 24 h at a mean increment of $70 \pm 22\%$ relative to initial cell number. Exponential growth endured from day 1 to 3 in all these samples. At the lowest and the highest exposure concentration, exponential growth continued until day 4 with approximately 20% growth from day 3 to 4, while in the other samples cell numbers decreased by 3 to 4% in this period. The maximum cell number was 6834 ± 1320 per mL in controls and ranged from 6334 to 7475 per mL with standard deviations of 489 and 1326 in the nAg exposed samples. Differences in the maximum cell number per mL were statistically not significant (One-way ANOVA) for comparison between control and treatment at varying nAg concentrations, as well as among treatment concentrations. Thus it is inferred, that no inhibitory effects were exerted on *P. tetraurelia* cultures at the nAg concentrations applied in this experiment.

These results contradict the findings of Mielke et al. (2013) who reported that cultures of the ciliate *Tetrahymena thermophila* exposed with nTiO₂ via food bacteria (*Pseudomonas aeruginosa*) grew slower and to lower maximum cell number than cultures exposed via rich media. The medium (SSP) for which this result was obtained, was similar to the ABC medium used in preliminary experiments of this work (see section 5.2). A minimum medium (Dryl's) yielded no cell culture growth in controls and treatments with nTiO₂ for the same study, just as reported for *P. tetraurelia* in conditioned CM with and without nAg in this work. As shown in section 5.3.1, sensitivity of *P. tetraurelia* towards exposure with nAg was much lower in the filtrated ABC than in conditioned CM (without bacteria).

In the study of Mielke et al. (2013), growth rates of *T. thermophila* differed by 0.12/h between SSP medium (0.26/h) and bacteria containing medium (0.14/h). In the work presented here, growth rates derived for *P. tetraurelia* in filtrated ABC according to equation 6 and equation 7 (see page 20) between day 1 and 3 (shown in figure 8, page 22, section 3.2.2), and growth rates of *P. tetraurelia* between day 1 and 3 in the bioaccumulation experiment with *R. planticola* as shown in this section, were very similar with 0.275 and 0.233, respectively. It is thus expected that results from an

experiment with axenic medium and bacteria containing medium with *P. tetraurelia* and nAg as presented by Mielke et al. (2013) for *T. thermophila* with nTiO₂ could be comparable in the case presented here. However, no inhibitory effects were observed for exposure via food at the tested concentrations. According to preliminary experiments, a nominal concentration of 0.5 mg/L nAg, which is 5-fold of the highest concentration tested in this experiment, and 3 times lower than the LOEC from the acute bioaccumulation experiment in the previous section, had caused 100% mortality both in exposure via food and via medium already after one day.

In order to elucidate, why no inhibitory effects were visible in our experiment after chronic exposure at 0.1, 0.03 and 0.01 mg/L nAg for both exposure types, it is necessary to clarify whether nAg was accumulated by *Paramecium* cells at all. For this task it is crucial to study the physiological status of the *Paramecium* cells which were exposed via medium, i.e. if they carry out pinocytosis in a medium which does not serve nutrients. This could be undertaken by adding ink to conditioned CM and ABC medium before filtration. After inoculation of the filtrated media with *Paramecium* cells, the formation of ink-colored vesicles within the cells should be observable by microscopy and hence show whether pinocytosis is a potential uptake pathway for nAg in the experiments. For exposure via food it is indispensable to know whether bacteria were coated by nAg as hypothesized. SEM pictures of bacteria exposed to nAg as shown in section 4.2.3.2 do not doubtlessly prove this assumption, as the allocation of nAg on bacterial cell surfaces could be artifacts from filtration for sample preparation. With more diluted bacterial cultures it could be possible to obtain images of single cells on filter membranes and allow locating of nanoparticles close to, or far from cell surfaces.

Interestingly, in this experiment all replicates from exposure via food contained living bacteria up to the end of the experiment, as shown by the samples which were streaked on agar plates at day 5. On all plates, i.e. in all control and treatment replicates, colonies grew at similar size and density. This is not surprising in terms of the exposure concentrations, which are (except for the highest concentration applied here) below the EC₅₀ concentration of 60 to 80 µg/L for *R. planticola* as obtained from acute toxicity tests as described before (section 4.2.3.2). However, it is surprising that bacteria were still left in the medium at the beginning of the stationary phase of the predators, when assuming that food is the limiting factor at this phase of growth. Whether these bacteria were edible for *P. tetraurelia*, remains unclear at this stage of work and needs further investigation. Release of EPS by bacteria can have a strong influence on binding of nAg and uptake of bacteria into ciliate cells (see discussion in the previous section 5.3.3). Thus it would be necessary to quantify the production of

EPS by *R. planticola* as reaction on exposure with nAg and to study the ability of *P. tetraurelia* to feed on potentially EPS-covered bacteria.

Not at least, the evaluation of the real exposure situation in the experiment as presented here, would require analytical methods which are capable of detection of Ag^+ at very low concentrations in the media and fractions derived from the samples after centrifugation or other particle and cell separation techniques. These time- and cost-intensive experiments should be considered for future work in the field of nAg accumulation studies.

6 Activated Sludge Community Tests

6.1 Introduction – Activated sludge

The most common wastewater treatment strategy throughout Europe is a stepwise approach comprising primary, secondary and tertiary treatment. The primary treatment represents a mechanical purification of the inflow water from coarse material and the tertiary treatment is a gravitational settling of suspended matter downstream from secondary treatment. The major purification of wastewater from organic substances takes place during secondary treatment, which is practiced by biological purification, i.e. degradation of organic matter by a diverse microbial community, referred to as activated sludge. Due to the different skills of the microbial species in activated sludge to degrade certain substances or compounds, their specific demands concerning composition of the wastewater (source of specific compounds versus inhibiting compounds) and the required oxygen supply need to be considered in the technical organization of the wastewater treatment facility. Aerated and unaerated conditions⁹ in activated sludge are generated through spatial separation in conventional WWTPs, where the wastewater passes through the different kinds of tanks which possess specific functions. These functions are explained later within this section.

An alternative approach of biological wastewater treatment is realized by a chronological separation of treatment steps as occurring in sequencing batch reactor (SBR) technique: all treatment steps, except for primary treatment, take place in one single tank but at different times (Al-rekabi et al., 2007; Irvine et al., 1989; Singh and Srivastava, 2011). The two biological treatment options are opposed and illustrated in figure 56 (page 122). SBR setup shall be explained in more detail here, because it was used for the activated sludge community tests in this work.

Usually, SBRs are conducted as discontinuous system, also referred to as unsteady-state activated sludge system (Irvine et al., 1989). That means that wastewater enters the treatment tank periodically and is treated in so called cycles, which consist of at least four time periods: FILL, REACT, SETTLE and DRAW (Al-rekabi et al., 2007; Singh and Srivastava, 2011). During FILL, new wastewater is introduced to the tank, which contains variable amounts of remaining water and sludge from the previous cycle. During REACT, substrates are removed from wastewater. During SETTLE aeration and

⁹ These conditions are often referred to as aerobic, anaerobic and anoxic conditions in wastewater technology. For avoiding confusion with the biological definition of these terms, the words 'aerated' and 'unaerated' will be applied in this work instead.

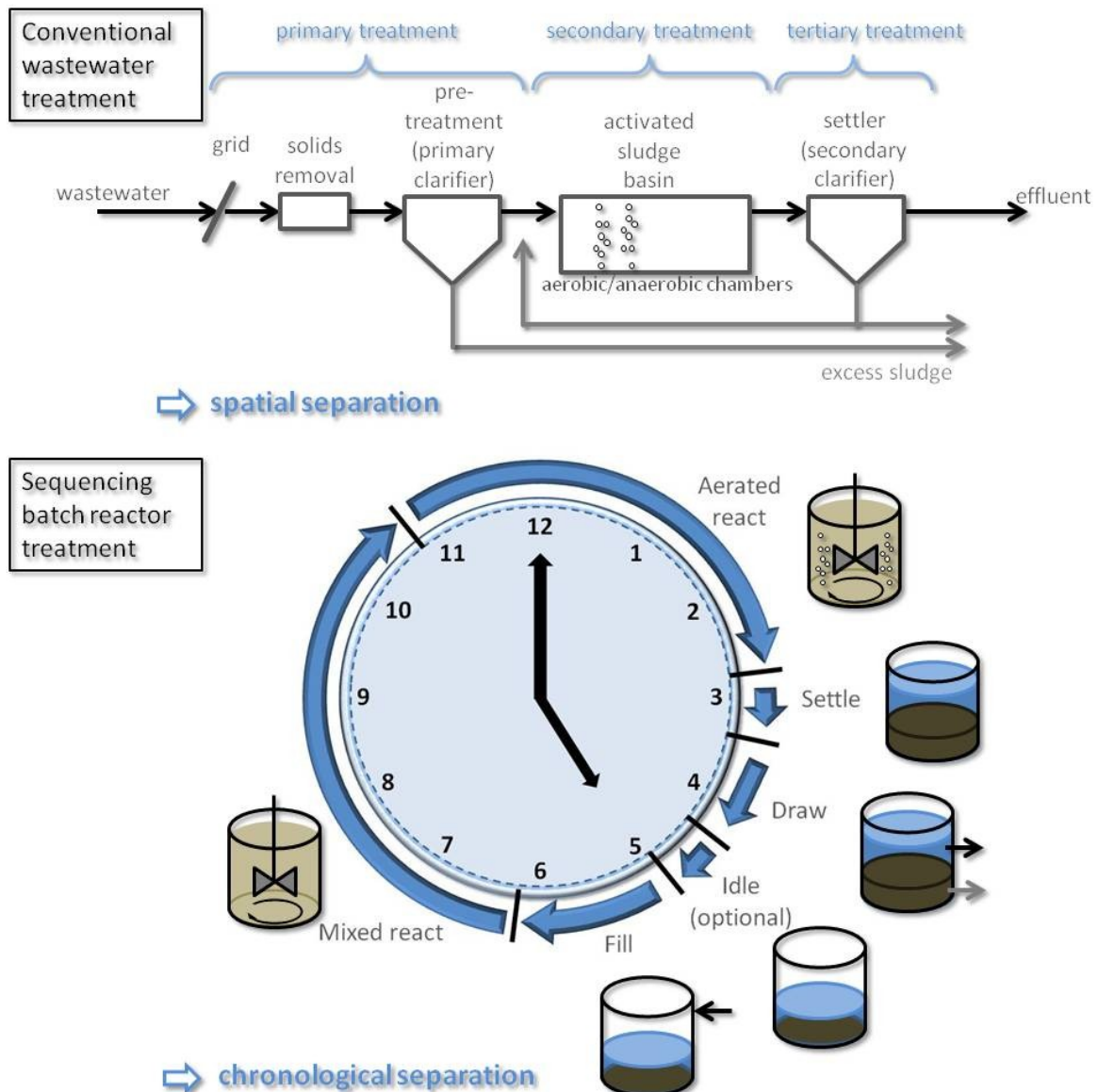


Figure 56: Comparison between spatial separation of treatment steps in conventional wastewater treatment technique (upper section) and chronological separation of treatment steps in sequencing batch reactor technique (lower section). Different aeration and mixing regimes are applied in SBRs to achieve removal of specific compounds.

mixing are turned off to allow the treated wastewater to separate into sludge and effluent, whereas the sludge settles at the bottom of the SBR. Effluent water is removed from the SBR during DRAW (also referred to as 'Decant'). Depending on the operation strategy, these phases can be conducted with varying aeration or mixing conditions, e.g. for removal of carbon, nitrogen compounds and phosphate during REACT phase (aerated and mixed REACT) or static, mixed or aerated FILL (Al-rekabi et al., 2007; Irvine et al., 1989; Singh and Srivastava, 2011). More emphasis on the processes occurring under differing aeration regimes will be given below.

Partially, the aforementioned cycle phases can overlap with each other to a certain extent, depending on the technological setup of the reactor and the operating strategy. This approach enables treatment of wastewater according to its specific composition and demands for effluent water. A so called IDLE phase can optionally be conducted between DRAW and FILL phase (Irvine et al., 1989; Singh and Srivastava, 2011). This is especially feasible for phase shifting of multiple SBR tanks in one treatment plant to allow for continuous wastewater treatment. Most of the cycle phases are also variable concerning their duration relative to the full cycle time. Only SETTLE is relatively time limited, as floating of the settled sludge caused by gas production needs to be avoided (Irvine et al., 1989; Singh and Srivastava, 2011).

The major advantages of SBR application are exhibited through the high degree of flexibility in operation (Irvine et al., 1989). The usage of SBR for wastewater treatment is feasible especially in areas with limited space (only one tank is required in the minimum scenario) and in areas with varying or low wastewater flow (Al-rekabi et al., 2007), as relative tank volumes can be easily shared or redistributed (Irvine et al., 1989). Also, SBRs are very cost effective while reaching excellent wastewater treatment performance (Al-rekabi et al., 2007) although aeration time can be significantly reduced compared to conventional WWTPs (Singh and Srivastava, 2011).

The degradation of substrates present in the wastewater is carried out by the activated sludge microorganisms, namely bacteria. Under aerobic conditions a diverse set of these microbes removes carbon containing compounds by respiration under use of oxygen. On the basis of the biological oxygen demand (BOD) of the organisms, the load of easily degradable organic compounds can be estimated. Usually, this parameter is determined as BOD₅, i.e. the BOD over a period of 5 days without additional aeration (Henze et al., 2008). Organic compounds which are not easily degradable are quantified by the chemical oxygen demand (COD). BOD₅ and COD, besides other parameters, are determined during the wastewater treatment process in influent, activated sludge and effluent for evaluation of treatment efficiency. Further processes occurring under aerobic conditions are nitrification, i.e. the transformation of ammonium to nitrate (NO₃⁻) (for details see section 4.4.1) and polyphosphate formation during the processes of enhanced biological phosphate elimination.

The dissolved oxygen concentration in the activated sludge decreases due to ongoing respiration processes also during unaerated phases, leading to anaerobic or anoxic conditions. Under these conditions, denitrification (transformation of NO₃⁻ to N₂, for details see section 4.3.1) and phosphate resolution occur. The concentration of

nutrients such as nitrogen and phosphorous are usually monitored throughout wastewater treatment processes for evaluation of performance and especially in the effluent for validation of the compliance of legitimate limits.

Apart from bacteria, activated sludge communities are composed of eukaryotic microorganisms, amongst which protozoan predators have a significant impact on the bacterial load of effluent water. Especially ciliates are part of this predator community and are responsible for purification of the water from freely dispersed bacteria, including potentially pathogenic microbes (Curds, 1982).

In activated sludge, the typical protozoan community is dominated by crawling and sessile ciliates (Madoni et al., 1993) and also testate amoeba (Zhou et al., 2008). Among the sessile ciliates, peritrichs are very abundant, especially the genera *Epistylis* and *Opercularia* (Fried and Lemmer, 2003), which are regarded as indicators of high sludge quality (Foissner and Berger, 1996). The community structure is influenced by boundary conditions, for example oxygen supply (Németh-Katona, 2010; Tocchi et al., 2012). Apart from parameters influenced by treatment plant operation strategy, such as the aeration regime, sludge age and loading; toxic substances - introduced into the facility via wastewater - have a major impact on the whole activated sludge community. Protozoan species differ in their sensitivity towards specific compounds and may act as indicator organisms, e.g. flagellates or carnivorous ciliates (Cybis and Horan, 1997; Madoni et al., 1996; Papadimitriou et al., 2013). The differential sensitivity of organisms may lead to shifts in the composition of the community after exposure to toxic compounds, not only in terms of species diversity, but also functional diversity. For example, it has previously been shown, that some ciliates are more efficient in clarifying effluent water from bacteria, due to their high filtration rates (Esteban et al., 1991). The genus paramecium is related to very clear effluents (Curds, 1982). Population shifts thus may impact the performance of biological treatment. For exposure to nAg, Chen et al. (2014) detected a shift in the population composition of functional bacteria groups.

The aim of this chapter is to detect probable changes in the community composition of protozoa and metazoa after exposure to nAg NM-300K with regard to wastewater treatment performance, to test for the fifth hypothesis.

6.2 Acute toxicity test with activated sludge community

6.2.1 Materials and Methods for acute toxicity test with activated sludge

Preparation of nAg stock dispersions

For preparation of 1 g nAg/L HPLC-grade water stock, 0.046 g NM-300K were weighed into a 15 mL PE-tube (Corning Inc., Mexico). HPLC-grade water was added until reaching a weight of 5 g. Two working stocks were prepared from 3 μ L of the 1 g/L stock were dispersed in 299.997 mL of tap water (dispersion 1) and 30 μ L of the 1 g/L stock and 299.97 mL of tap water (dispersion 2), respectively.

General setup

For acute toxicity testing of nAg on activated sludge community, a batch reactor setup was utilized. Exposure was undertaken at two concentrations: one realistic concentration taken from literature (10 μ g/L activated sludge) and a high concentration, which was 10 fold the realistic concentration (i.e. 100 μ g/L activated sludge). Per control and treatment, five replicates were run, accounting for fifteen batch reactors, each with a volume of 1 L. Figure 57 displays a schematic setup of the experiment as top (A) and lateral view (B).

2 L Erlenmeyer flasks (glass; Labsolute, TH. Geyer GmbH & Co. KG, Renningen, Germany; a - figure 57) were used as reactor vessels. For appropriate and constant temperature during the 24 h experiment, flasks were placed into two connected cooling ponds (custom made from hard plastics; b - figure 57). The water filled ponds were traversed by a flexible hose (c - figure 57) which was connected to a cooling aggregate (Lauda UKT 350), set to a temperature of 8.3°C and temperature of the water in the ponds was thus adjusted to $18 \pm 1.1^\circ\text{C}$.

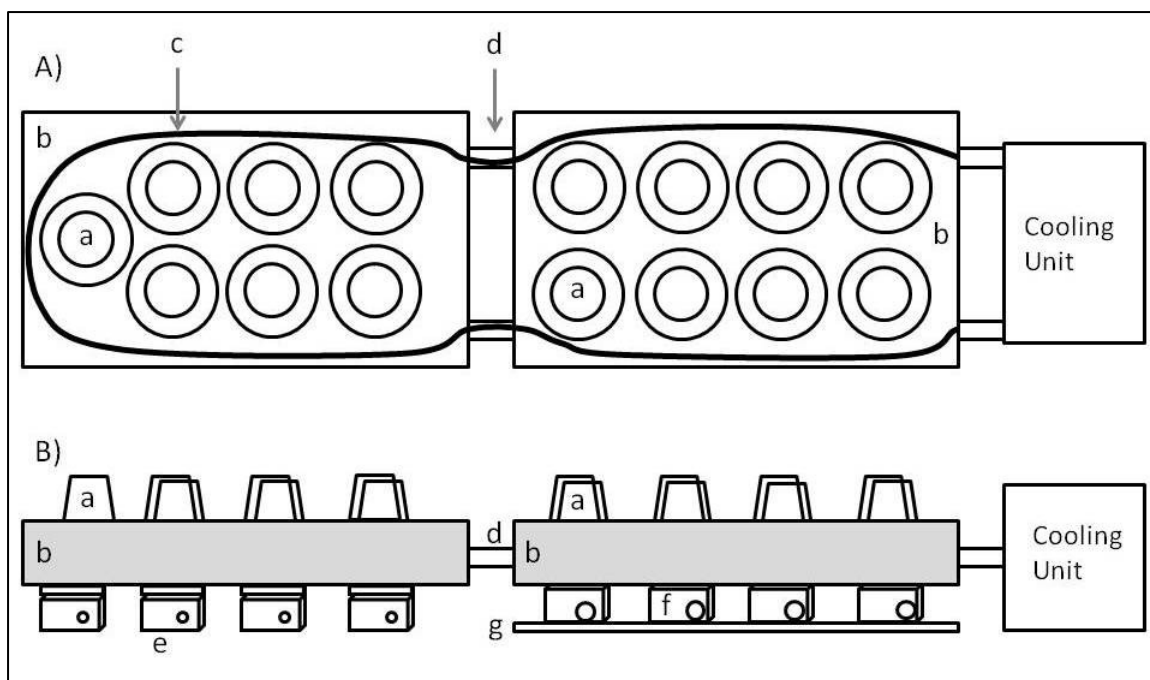


Figure 57: Scheme of the experimental setup: A) in top view, B) in lateral view; a: Erlenmeyer flask; b: cooling pond; c: cooling hose; d: connection of cooling ponds; e: magnetic stirrer type 1; f: magnetic stirrer type 2; g: support for compensation of magnetic stirrer height differences.

For mixing of activated sludge, magnetic stirrers (Heidolph MR3100, e - figure 57; Phoenix Instrument RSM-10B, f - figure 57) were placed under the cooling ponds at the position of the batch reactors and cylindrical magnetic stirring bars were placed into each flask. For aeration (not shown in figure 57; for reference see figure 59, page 128), aquarium air pumps (E2 M1, ASF Thomas Industries, Wuppertal, Germany) were connected with flexible tubing to airflow meters (1.0 L Key instruments, Trevoze, PA, USA) adjusting airflow to 0.5 L per minute. Flexible tubing was connected to the outflow of the airflow meters and on the other end aquarium diffuser stones were used for generation of fine bubbles. Oxygen supply was verified by measuring dissolved oxygen (DO) saturation with an Oxygenmeter, WTW Oxi340I equipped with oxygen probe WTW CelloX325. The experimental setup was tested with three replicates filled with tap water for functionality for a few days.

Experimental setup of acute toxicity test

For filling the Erlenmeyer flasks with activated sludge, a 20 L sample was drawn from wastewater treatment plant Dresden-Kaditz and immediately transported to the laboratory. The sample was transferred to a 20 L PE canister with drainage cock and

stirred with an agitator (IKA RW 20) equipped with custom made propeller and aerated by means of an aquarium air pump (E2 M1, ASF Thomas Industries, Wuppertal, Germany) with two flexible tubes supplied with aquarium diffuser stones. In the activated sludge sample pH was measured with a WTW pH3110. 500 mL aliquots of mixed liquor were drawn from the canister and transferred to the Erlenmeyer flasks working from left side to right side of the setup. In a second round, 450 mL aliquots were transferred to the flasks from right to left side of the setup. It was intended to achieve a homogenous distribution of the activated sludge in shortest time possible, to avoid differences in acclimatization to exposure vessels. The flasks were filled to 1 L by adding 50 mL of tap water to each control replicate, 50 mL of dispersion 1 to each realistic concentration replicate, and 50 mL of dispersion 2 to each high concentration replicate. Flasks were randomly distributed to the cooling ponds and numerated from left to right with abbreviation of treatment and replicate number. In figure 58 the arrangement of treatments and replicates in the cooling ponds is shown schematically.

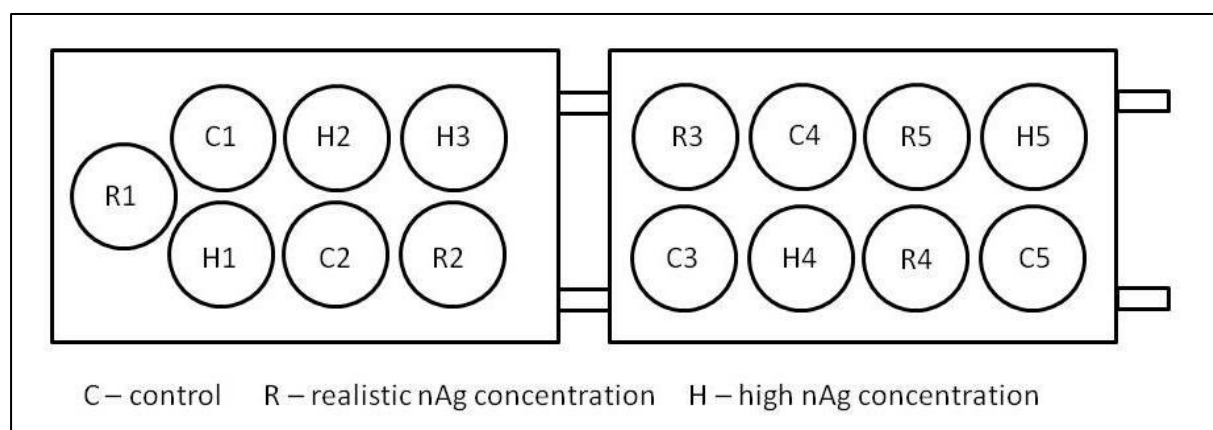


Figure 58: Arrangement of control and treatment replicates in cooling ponds.

Aeration (as described above) was installed and DO was measured after 3 hours of aeration for control of oxygen supply. Full setup is shown in figure 59.

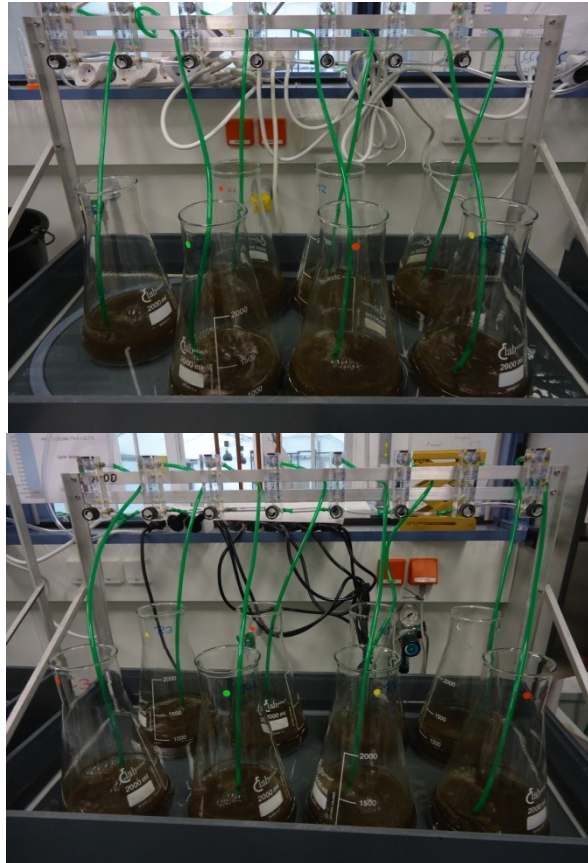


Figure 59: Full setup of acute toxicity test with activated sludge.

Batch reactors were kept for 24 h at these conditions before endpoints were examined. Remaining activated sludge in the PE-canister was used for determination of mixed liquor suspended solids (MLSS), mixed liquor volatile suspended solids (MLVSS), chemical oxygen demand (COD), biochemical oxygen demand (BOD) and protozoan community at beginning of the experiment. Also samples were fixated with different methods as backups.

Vacuum filtration of samples

For determination of MLSS, TSS and backup samples for eventual ion chromatography analytics (see below), sample preparations required vacuum filtration. Filtration equipment was installed as follows.

Each filtration unit consisted of a cylinder funnel with scale (250 mL), respective filter membrane, sand core filter, sand core filter head and a collecting liquid bottle, arranged in this order from top to bottom. Funnel, sand core filter and sand core filter

head were fixed with a metal clamp. Filtration units were linked in series using rubber tubing with hose fittings and connected to a Woulff bottle, and subsequently to a vacuum pump (Type SK 145I). For opportunity of interrupting the vacuum at single filtration units, hose clamps were mounted on the rubber tubing directly connected with filtration units.

Analysis of MLSS and MLVSS

Whatman glass micro fiber filters (ready to use, 934-AHTM RTU, GE Healthcare, USA) were used for MLSS determination. These filters are pre-washed, dried and weighed by the manufacturer. Indicated weight of 30 randomly selected filters was compared to weight determined by the laboratory balance used for MLSS determination. Mean deviation of the results from indicated values was calculated and used as correction factor for dry weight of the filters.

For MLSS analysis the filters were mounted on the sand core filters of vacuum filtration devices and wetted with a few mL of deionized water. After setup of the filtration units, a mixed liquor sample volume of 10 mL per replicate was filled in the cylinder funnel with a serological pipette after mixing the sample by quick shaking. Vacuum was applied and time until completed suction of liquid was measured. If suction was completed within 10 minutes, the procedure was valid. Filters were washed by soaking 10 mL of deionized water through the filter under vacuum. This procedure was repeated twice. After complete suction, filtration was continued for three more minutes. Filters were removed and transferred to their aluminium weighing dishes and dried at 105 °C in a sterilizing oven (Heraeus Instruments GmbH, Hanau, Germany) for at least 1 h. Filters were left to cool down in a desiccator, which kept the samples dry, and subsequently weighed. Drying was repeated until constant weight of filters was determined (less than 4 % change or less than 0.5 mg deviation).

MLSS was calculated from determined weights according to equation 11.

$$MLSS \left[\frac{mg}{L} \right] = \frac{A - B \times 1000}{sample\ volume\ [mL]}$$

equation 11

where A is the weight of dried sample with filter in mg and B is the dry filter weight in mg.

For determination of MLVSS filters from MLSS analysis were ignited in a muffle furnace at 500 °C for 30 minutes. Filters were left in a desiccator for cooling and

weighed subsequently. Igniting and weighing was repeated until constant weights were obtained.

MLVSS was calculated from equation 12:

$$MLVSS = \frac{(C - D) \times 1000}{\text{sample volume [mL]}}$$

equation 12

where C is the weight of sample and filter before ignition and D is the weight of sample and filter after ignition (i.e. Ash and filter weight).

Determination of COD

LCI 400 cuvettes (Hach Lange GmbH, Germany) for a range of 0 to 4000 mg/L were used for COD measures. Cuvettes were inverted prior to sample preparation for dissolving sedimented chemicals. 2 mL of samples were filled into respective cuvettes and mixed thoroughly by inverting the closed cuvettes. 2 mL of deionized water were used as parallel blank in a separate cuvette. Samples were incubated at 148°C for 2 h in a HT2S incubator (Hach Lange GmbH, Germany) and subsequently left to cool to 60°C. At this temperature, cuvettes were removed from incubator and carefully swiveled. After being cooled down to room temperature, cuvettes were read in a DR2800 photometer (Hach Lange GmbH, Germany) using the barcode programmes implemented in the software of the device.

Determination of BOD₅

LCK555 BOD₅ cuvettes (Hach Lange GmbH, Germany) for a range of 4 to 1650 mg/L along with LZC555 Bio-Kit as inoculation material for dilution water were used for BOD₅ determination. Dilution water was prepared at least 3 h before sample preparation. A batch spoon full of inoculation material from BioKit was dispersed in 10 mL of buffer solution (LCK555 B) in the provided reaction vial. After vigorous shaking of the vial for 1 minute, the dispersion was incubated at room temperature for 1 h.

In a Schott laboratory bottle, 500 mL of tap water were supplied with 0.3 mL of trace element solution as provided, and 0.5 mL from the supernatant of inoculated buffer solution were added particle free. The bottle was aerated for 1 h at room temperature. To prevent over saturation of the dilution water with oxygen, the bottle was left unaerated for 1 h prior to cuvette preparation.

For sample preparation, degree of dilution was chosen according to categorization of samples in the LCK555 manual. For mixed liquor samples, range B3 was applied by mixing 1 mL of sample with 5 mL of dilution water in a 15 mL PE tube. From this dilution, 0.5 mL were transferred into LCK555 cuvettes, which were filled with dilution water to the brim, resulting in a dilution factor of 75. Parallel to samples, a blank cuvette was prepared from dilution water exclusively. Cuvettes were closed and controlled for air bubbles, labeled and kept incubated for 5 days in the dark at 20 °C. After incubation, chemicals enclosed in the lid of cuvettes were added to the samples, cuvettes were closed and for 3 minutes repeatedly shaken in order to dissolve the chemicals. After 3 minutes settling time cuvettes were analyzed on DR2800 photometer (Hach Lange GmbH, Germany) in barcode reading mode.

Examination of protozoan community

According to Madoni (1994)¹⁰ two aliquots of 20 µL activated sludge per sample (i.e. all control and treatment replicates) were analyzed. Aliquots were mounted on microscope slides. The edges of cover slips were sealed with petrolatum using a syringe with needle, and carefully mounted on the droplet of activated sludge. Protozoa were identified with a stereomicroscope at 100 x magnification by screening the full area of the cover slip. Testate and naked amoeba, rotifers and nematodes were determined to genus level. Ciliates were categorized into sessile, crawling, free swimming and suctorian and also determined to genus level. Flagellates were categorized into small or large. On the basis of total numbers of respective cells counted in the two aliquots (40 µL volume in total), individuals per L were calculated for the functional groups of testate amoeba, naked amoeba, metazoa (nematodes and rotifers), flagellates and carnivorous ciliates in addition to the three categories of ciliates. Total microfauna number was calculated as sum of individuals per L from these groups. Further, the numbers of taxonomic units per functional group were listed and the sum of taxonomic units was calculated. Dominant key groups were determined, based on the functional groups mentioned before and some intersection groups or species groups, which were: sum of crawling and sessile ciliates and testate amoeba, sessile ciliate genus *Opercularia*, sessile ciliate species *Vorticella microstoma* and the group of small flagellates. These dominant key groups were converted to percentages of respective individuals per L respective to total microfauna

¹⁰ Madoni suggests one or two aliquots of 25 µL, which volume was found to leak from the cover slips in practice and was thus reduced to 20 µL

(individuals/L). It was further registered, whether the density (individuals/L) of each dominant key group exceeded 10^6 .

From these data, according to table 15, sludge biotic index was determined for each control and treatment replicate. SBI values were converted into quality evaluation classes according to table 14.

Table 14: Conversion of SBI values into four quality classes (I – IV) and respective evaluation. Modified after Madoni (1994).

SBI value	Class	Evaluation
8 -10	I	Very well colonized and stable sludge, excellent biological activity, very good performance
6 - 7	II	Well colonized and stable sludge, biological activity in decrease; good performance
4 - 5	III	Insufficient biological depuration in the aeration tank; mediocre performance
0 - 3	IV	Poor biological depuration in the aeration tank; low performance

Backups for ciliate community and for bacteria community in eventual posterior analysis, samples were fixated with differing agents. Ciliate community samples were prepared at in 15 mL PE tubes at two replicates each with 50% Glycerol, with 80% ethanol, with 37% para- formaldehyde (PFA) and with Bouin solution. For Glycerol preservation, 2 mL sample were mixed with equal volume of 50% glycerol and immediately stored in a freezer at -18°C . For ethanol preservation 2 mL of sample were added to 3 mL 80% EtOH. For PFA fixation, 2 mL samples were spiked with $114\ \mu\text{L}$ of 37% PFA, resulting in 2% PFA concentration. Fixation with Bouin solution was carried out mixing 2 mL sample with $3\ \mu\text{L}$ Bouin solution. Except for glycerol samples, all tubes were stored in a fridge at 4°C .

Bacteria community samples were prepared by freezing 10 mL aliquots in PE tubes and by fixation of 10 mL sample with $570\ \mu\text{L}$ of 37% PFA at two replicates, which were incubated over night at 4°C in a fridge. Subsequently, samples were fixed on special fluorescence microscopy filters (IsoporeTM membrane filters, $0.2\ \mu\text{m}$ GTBP, Merck Chemicals GmbH) by vacuum filtration as described previously. Paper filters (MN85/70, Macherey-Nagel GmbH &Co. KG, Düren, Germany) were used as support filters. Filters were left to dry in open petridishes at room temperature in a laboratory hood and subsequently stored in a freezer at -18°C .

Table 15: Two-way table for determination of SBI on basis of dominant keygroups, density and number of taxonomic units in microfauna of activated sludge, modified after Madoni (1994).

Total number of taxonomic units		>10		8 - 10		5 - 7		< 5	
		Number of small flagellates							
Dominant keygroup	Density (ind./L)	F<10	10< F <100	F<10	10< F <100	F<10	10< F <100	F<10	10< F <100
Crawling + sessile* Ciliates and testate amobae	$\geq 10^6$	10	8	9	7	8	6	7	5
	$< 10^6$	9	7	8	6	7	5	6	4
Sessile ciliates* >80 %	$\geq 10^6$	9	7	8	6	7	5	6	4
	$< 10^6$	8	6	7	5	6	4	5	3
<i>Opercularia spp.</i>	$\geq 10^6$	7	5	6	4	5	3	4	2
	$< 10^6$	6	4	5	3	4	2	3	1
<i>Vorticella microstoma</i>	$\geq 10^6$	6	4	5	3	4	2	3	1
	$< 10^6$	5	3	4	2	3	1	23	0
Swimming bacterivorous ciliates	$\geq 10^6$	5	3	4	2	3	1	2	0
	$< 10^6$	4	2	3	1	2	0	1	0
Small swimming flagellates (>100)	$\geq 10^6$	4		3		2		1	
	$< 10^6$	3		2		1		0	

**Opercularia spp.* and *Vorticella microstoma* not abundant

Samples for Ag analytics

After setting up the acute toxicity experiment, two aliquots of 10 mL were transferred from each of the dispersions 1 and 2 to 15 mL PE-tubes (Corning Inc., Mexico) and supplied with 3 to 4 drops of 69% HNO₃ for digestion. From the 1 g/L stock two replicates at 100-fold dilution were prepared. For this purpose, 9.9 mL deionized water were mixed with 100 µL stock dispersion in a 15 mL PE-tube for each replicate and acidified with 69% HNO₃ as described before. Samples were stored in a fridge until being sent to Helmholtz centre for environmental research Magdeburg for chemical analysis via ICP-MS. Results of these analytics were not available at the time of thesis submission.

Sampling at the end of acute toxicity test

After 24 h of exposure under aeration, mixing and cooling of the batch reactors, DO, temperature and pH were measured and mixed liquor samples were taken for analyses of MLSS, MLVSS, COD, BOD₅ and protozoan community, as well as storage samples (backups and bacteria community), as described for the beginning of the experiment (see above).

Aeration and magnetic stirrers were switched off to enable settling of activated sludge. From effluent water, samples were drawn for determination of total suspended solids (TSS), volatile suspended solids (VSS), COD, BOD₅, and ammonium, nitrate, nitrite, ortho-phosphate and Ag analyses.

TSS and VSS determinations correspond to the procedures of MLSS and MLVSS analysis, except that sample volume per filter was 100 mL. Cuvette tests (Hach Lange GmbH, Germany) were used to determine COD (LCI 400), BOD₅ (LCK 555) and the compounds NH₄-N (LCK 305), NO₂-N (LCK 341), NO₃-N (LCK 340), total and ortho-phosphate (LCK 348). Additionally, for chemical compound backups and potential IC- chromatography analyses, 5 mL sample were vacuum filtrated using cellulose acetate filters (Sartorius RC210S) with 0.45 µm pore diameter and samples were stored in 15 mL PE tubes at -18°C. BOD cuvettes were prepared at dilution range B1, mixing 1 mL sample and 1 mL dilution water of which 0.5 mL were filled into cuvette and procedure was continued as described above.

For ammonium and ortho-phosphate analyses, dilutions were prepared with deionized water if needed. Cuvettes were prepared as indicated by the manufacturer. For Ag analyses in effluent water, samples were prepared as previously described for analyses of stock dispersions.

A backup sample of effluent water was prepared for each batch reactor by transferring 34 mL of liquid into a 50 mL PE tube, which was stored at -18°C. Finally, effluent was removed from batch reactors as far as possible using serological pipettes.

15 Erlenmeyer flasks were supplied with glass funnels (Duran) carrying pleated paper filters. The settled sludge from batch reactors was poured into the filters and left until remaining liquid had run off completely. Sludge was scratched off the filter papers using a spatula and transferred to previously weighed and labeled 50 mL PE tubes. Samples were frozen at -18°C and subsequently freeze dried for 48 h (Alpha 1-2, Christ). Samples were weighed and sent to Helmholtz centre for environmental research, Magdeburg, for chemical analysis via ICP-MS. Results of these analytics were not available at the time of thesis submission.

Data analyses

Basic statistical analyses (t-tests, ANOVAs and regressions) on results from the acute activated sludge experiment with nAg were calculated and plotted with Sigma Plot 11.0 software.

Principal component analysis (PCA) was conducted in order to reduce dimensions due to collinear parameters in the dataset, excluding abundance of protozoa and metazoa. PCA was performed in R system (R core team, 2014) with add-on packages 'vegan' and 'MASS'. Canonical correspondence analysis (CCA) was conducted in order to identify those parameters which explain the abundance of protozoa and metazoa, applying R system with add-on packages 'vegan' and 'MASS'. A scree plot was drawn in order to determine which principal components should be retained.

In order to address random effects, which might explain variance in the dataset, linear mixed effect (LME) model approaches were used by applying R system with the add-on package lme4 (Bates et al., 2015). Measured parameters which showed collinearity according to previously conducted PCA were omitted and those parameters in principal components explaining most of the variance were determined as random or fixed effects for LMEs and tested in varying combinations. The model with the lowest Aikaike information criterion (AIC) was identified by applying an ANOVA according to maximum likelihood fits. Results were plotted as estimated realistic averages derived as intercepts from the identified best LME.

6.3 Results and Discussion of acute toxicity test with activated sludge community

Analyses of mixed liquor from inoculation material

Inoculation material obtained from WWTP Dresden - Kaditz was characterized regarding MLSS, MLVSS, $\text{NH}_4^+\text{-N}$, $\text{NO}_2^-\text{-N}$, $\text{NO}_3^-\text{-N}$, pH, BOD_5 and protozoan community at the beginning of the experiment.

BOD_5 was 194 mg/L which is lower than BOD_5 values expected for influent water, with 300 to 500 mg/L (Fuchs, 2014). MLSS and MLVSS were determined with 2010.5 and 1151.5 mg/L. These results are in good agreement with typical values of activated sludge ranging from 1 to less than 4 g MLSS/L and a F/M (food to microorganism) ratio of 0.17, calculated from the quotient of BOD_5 and MLVSS. This value meets the acceptable range of F/M between 0.05 and 0.5 (Glymph, 2005). $\text{NH}_4^+\text{-N}$, $\text{NO}_2^-\text{-N}$ and $\text{NO}_3^-\text{-N}$ in the mixed liquor (ML) were 22.3 mg/L, 0.811 mg/L and 4.98 mg/L, respectively. The pH was 6.7 and thus providing good physiological conditions for microorganisms.

The protozoan community was diverse with 12 taxonomic units, which is in the highest range for SBI determination (>10 taxonomic units). The sum of taxonomic units would eventually even be higher, if protozoa were determined unto species level. However this was not possible in the study presented here, as species determination is time consuming and would have lead to a large time shift in evaluation of the community throughout all batch reactor replicates at the end of experiment. The initial community was dominated by sessile and crawling ciliates as well as testate amoeba genera, indicating a very high sludge quality (Lee et al., 2004; Madoni, 1994; Salvado et al., 1995). The number of small flagellates was determined throughout the whole cover slip areas, deviating from the suggestion by Madoni et al. (1994) to enumerate them using a Fuchs-Rosenthal chamber diagonal. As no small flagellates were observed in the samples, this procedure was omitted. SBI for the inoculation material was determined with 10, indicating the highest quality class I.

In figure 60 the composition of taxa in inoculation material is displayed. The most abundant genera were the (sessile) peritrich ciliate *Epistylis* and the testate amoeba *Arcella*, though for the latter it is precarious whether the observed individuals were alive, as vitality is difficult to verify due to the theca. This result should thus be regarded with care. For *Epistylis*, which is a colony forming ciliate, every cell body is counted. Thus, a single large colony can account for a massive number of individuals. Growth of colonies originates from a single cell body, which divides in longitudinal plane if environmental conditions are sufficient.

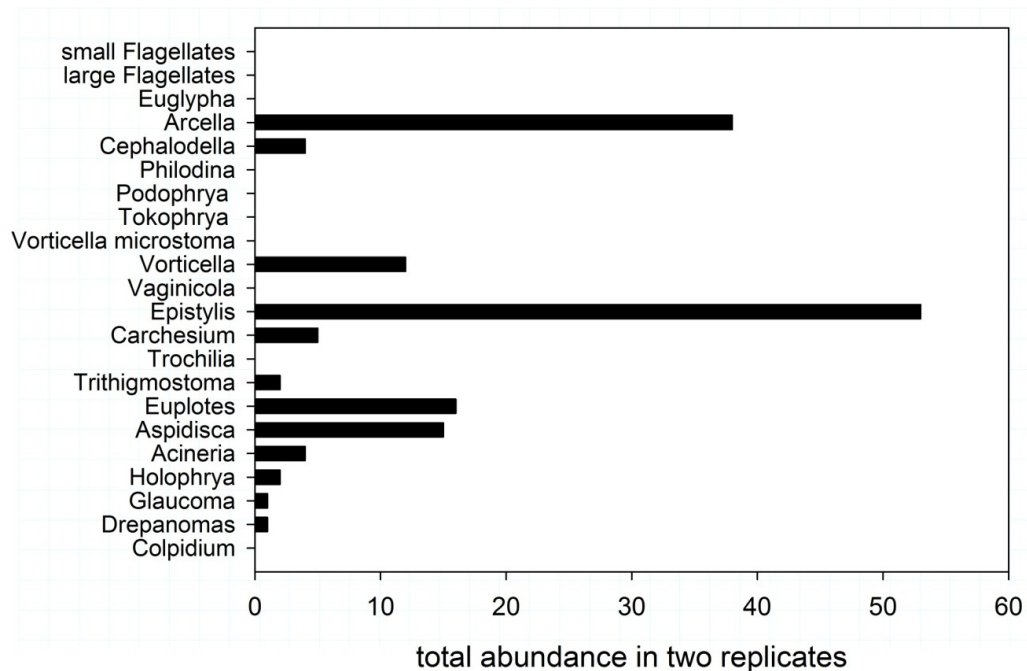


Figure 60: Total abundance of genera in the two analyzed replicates (20 μ L each) of inoculum material. Note that *Vorticella microstoma* is listed separately from genus *Vorticella* as species complex.

For this reason, cell body numbers of colonies are still valid enumerators for abundance and sludge quality. The intermediate abundant genera *Vorticella*, *Euplotes* and *Aspidisca* belong to the functional groups of sessile and crawling ciliates, respectively. All these are indicators of very high sludge quality.

The 15 batch reactors were analyzed regarding DO content after 3 hours of mixed aeration, as equilibration of conditions after physical impact through batch reactor setup were assumed to be completed after this time. DO was determined at an average of 7.0 ± 0.2 mg/L throughout all batch reactors. Regarding the required DO for activated sludge with > 1 to 2 mg/L (Environmental Protection Agency, 1997), oxygen supply was optimal in this experiment.

As stated in the methods section before, aeration was set on for the whole duration of the experiment and only switched off at the end of the sampling after 24 h in order to separate sludge from effluent water. Usually, an intermittent aeration and mixing regime would be conducted in wastewater treatment via SBI, in order to initiate nitrification, denitrification and - where applicable - biological phosphorous removal. In this experiment aeration was kept constant, because many protozoa and metazoa are very sensitive to oxygen depletion. Thus, if aeration would have been switched off, effects due

to oxygen deficit would be more probable than effects due to the treatment with nAg. In a real WWTP this would not be as problematic as in this experiment, because loss of organisms is compensated by organisms introduced into the treatment facility via the periodical inflow of wastewater which is entering the system.

Analyses of mixed liquor in batch reactors after exposure

After 24 h, at the end of the experiment, temperature, pH, DO, MLSS, MLVSS, COD and BOD₅ were determined in the 15 batch reactors. Temperature was $17 \pm 0.1^\circ\text{C}$ in all replicates and pH was 7.8 ± 0.1 , DO was 6.9 ± 0.36 mg/L. Thus, temperature was slightly lower than intended and pH had increased in all samples compared to the inoculum. The reason for the latter could have been the addition of stock dispersions or tap water, respectively, or metabolic activity of the microfauna. As pH was not measured after addition of stock dispersions in the batch reactors, this cannot be elucidated. Still, pH values were in physiological range so that negative effects on the organisms were excluded. DO at test end proved optimal conditions for activated sludge.

MLSS values were in a range of 1052 to 2398 mg/L with a mean of 1693.5 and a standard deviation of 450.8 mg/L throughout all reactors and thus were within optimum range. MLVSS values ranged between 686 and 1440 mg/L with an average of 1043.7 and a standard deviation of 258 mg/L. BOD₅ values were between 48 and 195 mg/L throughout the reactors. No treatment effect was observed in terms of solids concentration. Instead, a position effect was ascertainable. For statistical analysis positions of batch reactors in cooling ponds were assigned as follows (figure 61):

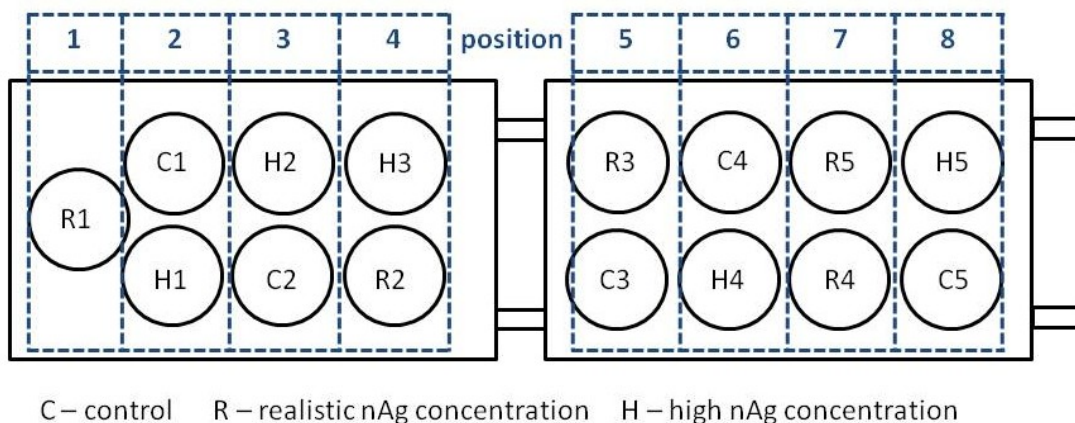


Figure 61: Assignment of batch reactor positions in cooling ponds.

Filling of batch reactors with inoculums at the beginning of the experiment was conducted in two steps, with aliquots of 500 and 450 mL activated sludge. The first filling step was planned to be undertaken proceeding from batch reactors at position 1 to 8 and the second filling step vice versa. In practice, filling was executed from position 1 to 7 and the second step was begun at position 7. The omitted batch reactors at position 8 were subsequently filled in one step and filling procedure was continued from positions 6 to 1. The order of filling was designed to achieve a homogenous distribution of inoculum material. From MLSS analysis results it can be inferred that homogenous mixture was achieved only at the beginning of filling step one. As the volume of inoculum material in the PE canister decreased, we assume stirring was not efficient anymore resulting in progressive settlement of sludge at the bottom, where material was taken for filling reactors at positions 5 to 8 from the drain cock. Through removal of larger proportions of sludge during the first filling step, solids density decreased during progress of the second filling step, resulting in overall lower solids concentrations in batch reactors at positions 1 to 3. This effect was visible by eye from turbidity of liquids in the batch reactors and in the MLSS and MLVSS concentrations at test end (figure 62). MLSS concentration was only approximately half of the MLSS of inoculum material in these reactors.

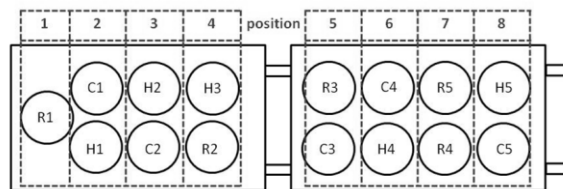
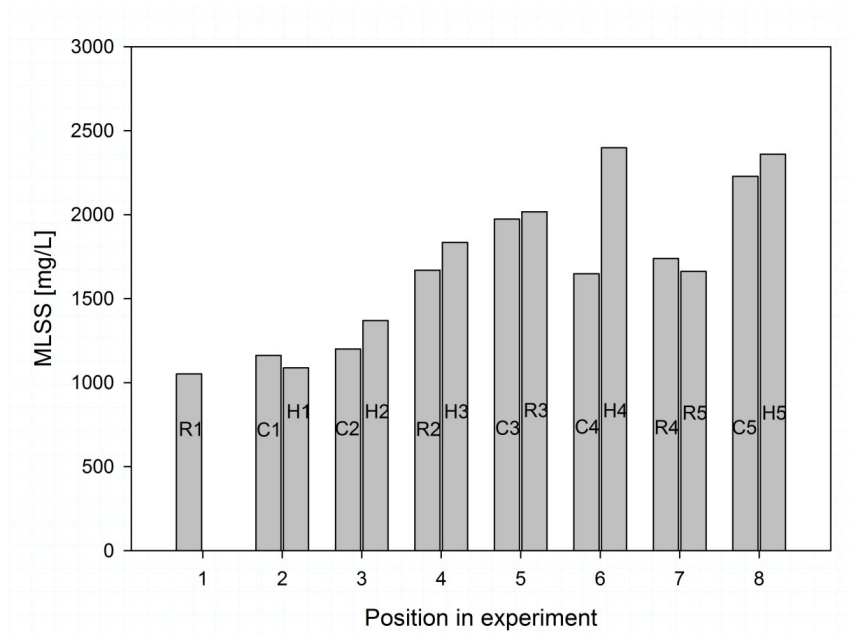


Figure 62: MLSS assigned to positions of batch reactors in cooling ponds (for reference see small insertion of figure 61 below the graph). Abbreviations at bars indicate sample type (C - control; R – realistic nAg concentration, H – high nAg concentration) and replicate number.

The role of the position (i.e. filling order) of batch reactors on interpretation of results will be further analyzed and discussed below.

The abundance of protozoa and metazoa genera was determined microscopically in duplicate samples from all batch reactors. Only living organisms were recorded by this method, except for tecamoeba, where dead and living individuals cannot be distinguished at 100 x magnification without any further treatment. For the group of flagellates, taxonomic units were distinguished as small and large flagellates. *Vorticella microstoma* was recorded separately as the only species, because it has a strong indicator value for activated sludge quality. All other *Vorticella* species were included in the counts of the genus *Vorticella*. For avoidance of confusion, the genera, species and taxonomic groups will be summed up and hereafter referred to as ‘taxonomic units’.

The sludge quality derived from SBI determined according to table 14 and 15 was categorized in class I for all batch reactors and SBI value was 10 in all reactors, except for

control replicate 1, where the SBI value was 8. Hence, sludge quality was very good in all replicates and all treatments and it was not possible to distinguish any inhibitory effects regarding SBI. However, in terms of numbers of individuals and diversity of samples, differences within and between treatments were observable. In total, 22 taxonomic units were found in the various samples. The number of taxonomic units per batch reactor ranged between 11 and 15. The cumulative abundance of the genera, according to those determined for SBI classification from duplicate samples of each batch reactor, is illustrated in figure 63.

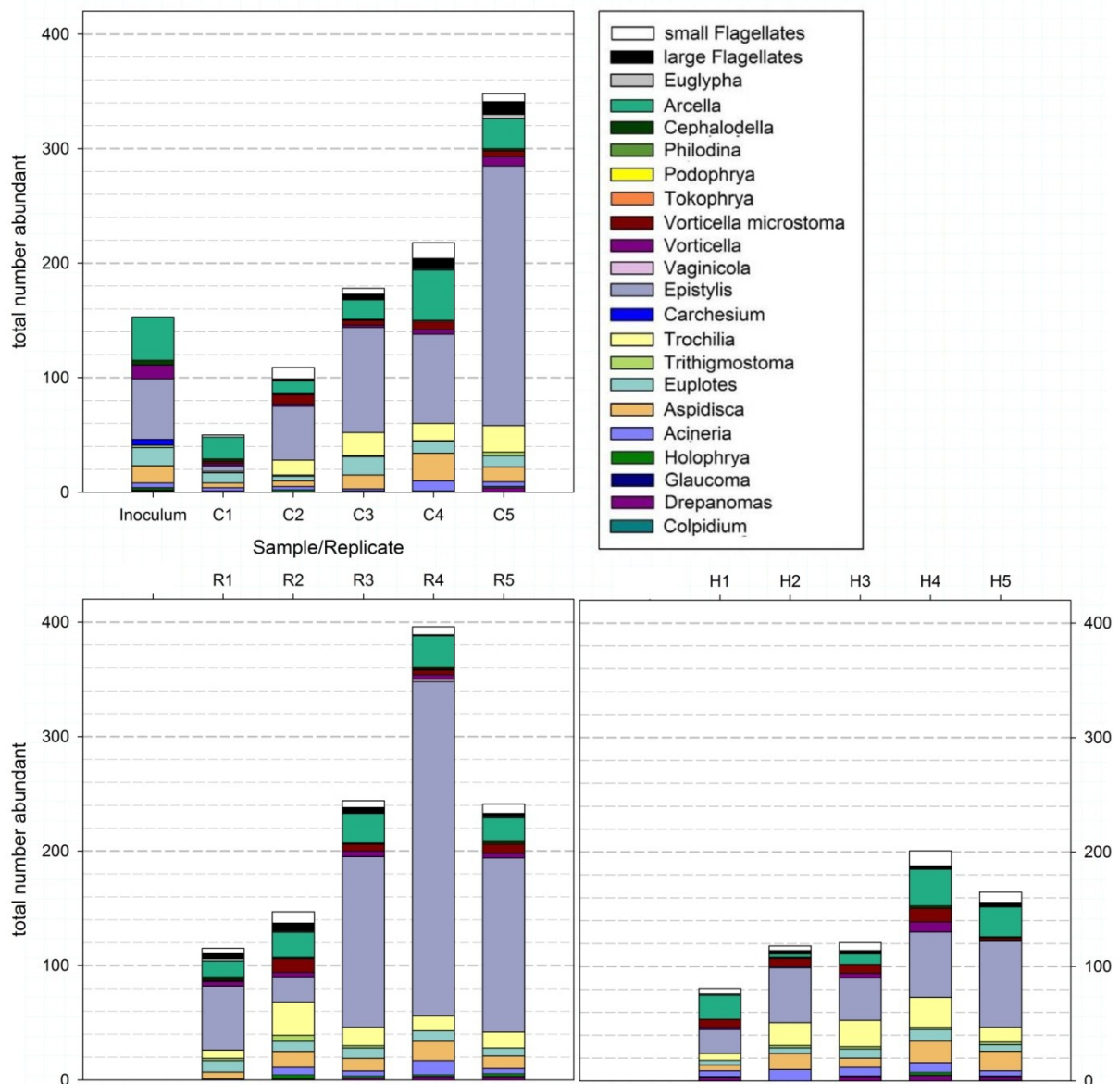


Figure 63: Cumulative abundance of the protozoa and metazoa genera in two microscopy replicates per treatment replicate. Upper row: Control replicates including inoculum samples. Lower row left: replicates with nAg exposure at realistic concentration. Lower row right: replicates with nAg exposure at high concentration. Abbreviations at x - achsis indicate sample type (C - control; R – realistic nAg concentration, H – high nAg concentration) and replicate number.

A high abundance of *Epistylis* cells was noticeable in all samples, relative to the total number of individuals per sample. *Epistylis* is a peritrich ciliate which forms colonies with many cell bodies on a single stalk. Peritricha are generally regarded as indicators of good sludge quality (Foissner and Berger, 1996). Also, a relatively constant abundance of *Arcella* individuals was observed. As the latter is a genus of tecamoeba, it cannot be ascertained that the counted individuals in the samples were alive or whether empty shells were included in the quantification. The sum of individuals per duplicate sample from the batch reactors is opposed to the number of taxa in the respective samples in table 16. Figure 64 depicts the regression of these two parameters with each other.

Table 16: Results of microscopical enumeration of taxonomic units in batch reactors. Abbreviations indicate sample type (C - control; R – realistic nAg concentration, H – high nAg concentration) and replicate number. t_{0h} : beginning of experiment.

Batch reactor	Sum of individuals	Number of taxa
C t_{0h}	153	12
C1	50	11
C2	109	13
C3	178	13
C4	218	14
C5	348	15
R1	115	14
R2	147	15
R3	244	14
R4	396	15
R5	241	15
H1	81	12
H2	118	12
H3	121	13
H4	201	14
H5	165	15

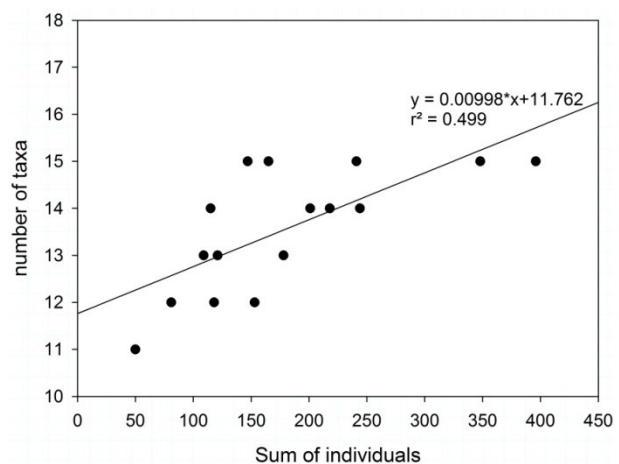


Figure 64: Linear regression of number of taxa against sum of individuals in the batch reactors.

Although a relation between the two parameters seems to exist to a certain extent, the coefficient of determination ($r^2=0.499$) was low. Especially in the range of 100 to 250 individuals, the number of taxa among these animals was varying. This means diversity generally trended to increase with higher density of individuals, but other factors must

exist, which contributed to the observed variance. Probable candidates for these factors will be traced and discussed below.

Effluent analyses showed very good removal of suspended solids in all batch reactors as TSS were between 0 and 7.2 mg/L. The only exception was control replicate 4, in which accidentally a small amount of settled sludge was withdrawn together with the effluent. This sample contained 17.3 mg/L TSS. In table 17 the requirements for effluent water, which are released from WWTPs into the environment, according to EU guideline (EU, 1991) are opposed to the measured values in batch reactor effluent and the respective reduction compared to initial mixed liquor values is depicted.

Table 17: Requirements for effluent waters released to the environment according to EU guideline (EU, 1991) and measured values in batch reactor samples for parameters TSS, CSB and BSB₅.

Parameter	EU requirement	Range of measured values [mg/L]	Reduction respective to ML
TSS	< 35 mg/L or - 90 %	0 to 17.3	99 to 100 %
COD	< 125 mg/L or - 75 %	23.7 to 32.9	98 to 99 %
BOD ₅	< 25 mg/L or - 90 %	0 to 16	92 to 100 %

All three parameters were within the required ranges for effluent water as claimed by EU guideline, as indicated in table 17. Further requirements do exist for total phosphorous and total nitrogen concentrations, which were not separately analyzed in this work except for NH₄-N, NO₃-N, NO₂-N and ortho-phosphate. Measured concentrations of nitrogen compounds, ortho-phosphate and COD in the effluent of inoculation material at the beginning of the experiment are opposed to the mean concentrations in all batch reactors at the end of the experiment in table 18.

Table 18: Measured concentrations of nitrogen compounds, ortho-phosphate and COD in effluent samples of inoculation material (t_{0h}) and batch reactors (t_{24h}).

Parameter [mg/L]	Inoculation material effluent	Mean ± standard deviation from all batch reactor samples after 24 h
NH ₄ -N	0.16	0.12 ± 0.110
NO ₂ -N	0.024	0.01 ± 0.006
NO ₃ -N	1.99*	6.07 ± 0.960
Ortho-PO ₄	0.608	0.61 ± 0.050**
COD	104	23.73 ± 3.990

*: measure was below detection range of applied cuvette test. **: sample from control replicate 4 was excluded, because it contained settled sludge.

In all samples, $\text{NH}_4\text{-N}$ and $\text{NO}_2\text{-N}$ concentrations were below 0.2 mg/L and 0.04 mg/L, respectively. Throughout the experiment period, $\text{NH}_4\text{-N}$ concentration did not change significantly (t-test, $P = 0.170$), while $\text{NO}_2\text{-N}$ concentration was significantly lower at the end of the experiment (t-test, $P < 0.001$). $\text{NO}_3\text{-N}$ concentration increased significantly from 1.99 mg/L in the inoculation material effluent to 6.07 ± 0.96 mg/L in the batch reactor effluent samples at test end. The increase of $\text{NO}_3\text{-N}$ concentration and the decrease of $\text{NO}_2\text{-N}$ concentration over time confirm nitrification activity and denitrification inactivity in the batch reactors, just as expected according to the aeration regime in the experiment. Ortho- PO_4 concentration was below 0.7 mg/L in all samples, except for control replicate 4, which contained some sludge accidentally removed with the effluent water. The ortho- PO_4 concentration in inoculation material effluent was constant over time in all batch reactors (t-test, $P = 0.878$), indicating that also biological phosphorous removal was inhibited due to continuous aeration during the experiment. A One-way ANOVA was carried out for the mean concentrations of the quantified compounds in effluent for the different treatment types and the inoculation material. No adverse effects of nAg were observed regarding N- and P- concentration, as no difference in reduction of matter concentrations among treatments were detected. Conversely, matter concentrations differed among replicates of the different treatments. This fact once more stresses the significance of the initial composition of the content in the batch reactors, because strong deviations between the replicates due to filling order might obscure treatment effects. For this reason, all data were analyzed with multivariate statistical methods. First, the influence of the position of the batch reactors in the experiment, which is synonymous for the filling order, was investigated using principal component analysis (PCA). The resulting plot is shown in figure 65. The two axes PC1 and PC2 explained 66 % of the variance in the data. The contribution of further components (axes) to explain variance in the data was negligible.

Two obvious clusters of replicates were identified in the PCA plot, marked with blue ellipses in figure 65: one cluster was aligned with pH and temperature and included replicates 1 and 2 of controls and high nAg exposure and replicate 1 of realistic concentration exposure.

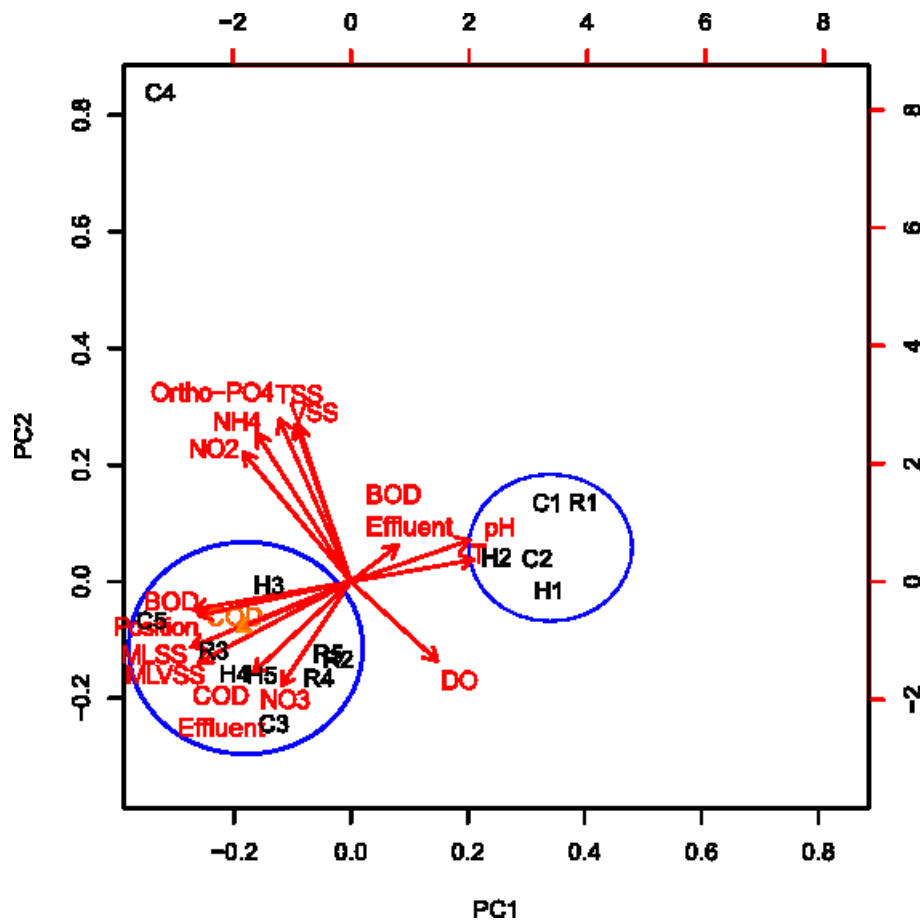


Figure 65: PCA of treatment replicates and abiotic parameters in the acute batch reactor experiment. Abbreviations: PC1: principal component 1, PC2 – principal component 2, T – temperature. For the other abbreviations see previous text.

In the second cluster, which is aligned with position of batch reactors, solids concentrations in ML, as well as COD and BOD₅ concentrations in ML and effluent, all other samples except for control replicate 4 were included. This outlier is explained by the deviating nutrient concentrations in effluent, derived from sludge accidentally withdrawn with the sample. As expected, indicators for high sludge content in the ML strongly grouped with position, i.e. filling order of reactors. The two clusters of samples were opposed on this axis. Effluent parameters grouped strongly in direction of PC2 axis, except for COD and BOD₅. The latter explained only few of the variance in data, as indicated by the short arrow in the plot.

With canonic correspondence analysis (CCA), the impact of measured parameters on taxonomic units composition in the samples was examined, as shown in figure 66 (page 146).

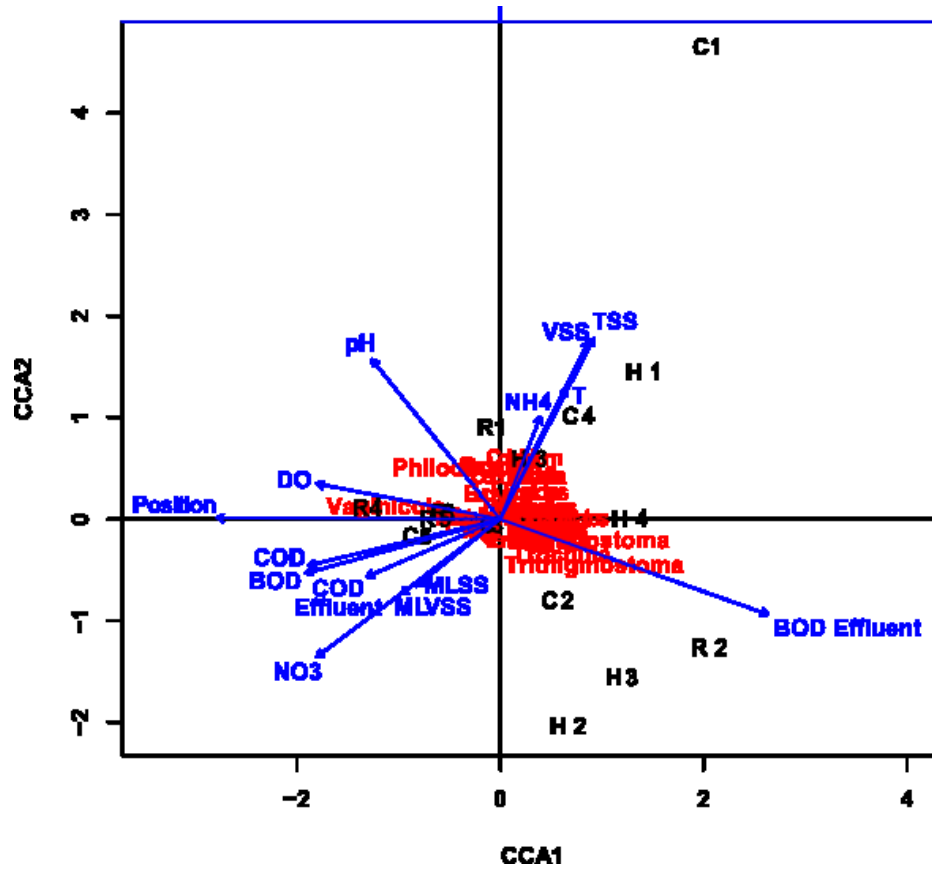


Figure 66: CCA plot with all measured parameters (blue) and taxonomic units (red) in the batch reactors (black). CCA1 – Canonical correspondence analysis achsis 1, CCA2 - Canonical correspondence analysis achsis 2.

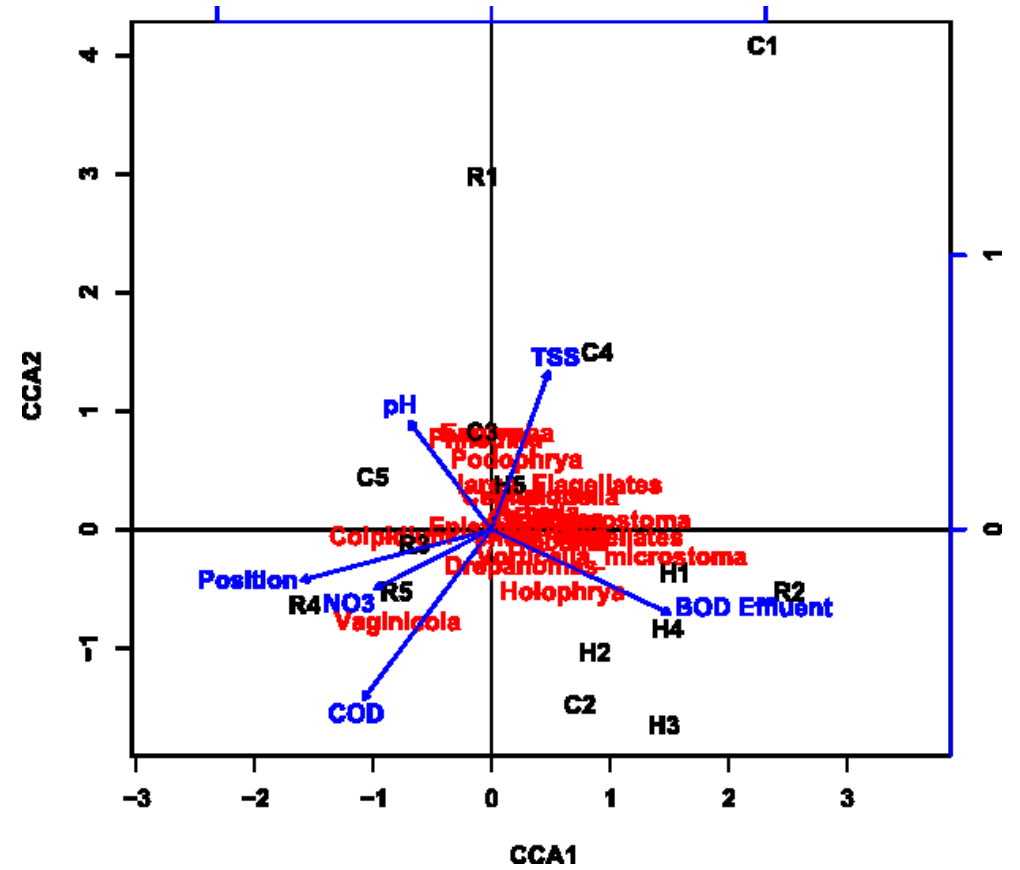


Figure 67: CCA plot with selected parameters (blue) for analysis of taxonomic units (red) variance in batch reactors (black). CCA1 – Canonical correspondence analysis achsis 1, CCA2 - Canonical correspondence analysis achsis 2.

The variance in data which was explained by constrained axes was 26%. The clustering of the taxonomic units in the center of the plot indicated that only few of the variance is explained by the measured parameters included in the plot. The only exceptions were *Vaginicola*, which was aligned with position and DO, and *Trithigmostoma*, which was aligned with BOD₅ in the effluent. Interestingly, the grouping of batch reactors according to position was much lesser pronounced in the CCA plot compared to PCA. All parameters which were displayed with short arrows in this CCA plot were excluded for subsequent analyses. Consequently, a CCA analysis with TSS, pH Position, NO₃ and BOD₅ in effluent was conducted. The results are plotted in figure 67 (page 146). In this plot, the variance within data explained by constrained axes was 14%. The clusters of taxonomic units were less condensed compared to the CCA with all parameters. *Vaginicola* was still aligned with position, but also with NO₃ and COD. The extent of scattering of batch reactors was similar in both plots. The alignment of *Trithigmostoma* with BOD₅ in the effluent was not displayed in the CCA plot with selected parameters. Instead, *Holophrya* was more strongly aligned with the latter parameter.

Generally, taxonomic unit abundance was neither well explained by the measured parameters (potentially leading to rejection of hypothesis 5 concerning community composition), nor by the filling order of batch reactors. A reason for this observation could be that the parameters assessed in this experiment did not include those parameters which explain a greater part of the variance in abundance data. Another reason could be that the previous assumption, which was filling order of batch reactors explains all variance in the data, was partly falsified. Analysis of the data regarding a potential treatment effect, which might have been obscured by the differences in batch reactor contents, was carried out.

When analyzing the sum of individuals of protozoa and metazoa as depicted in figure 63 (page 141), the abundance of individuals at all high nAg exposure replicates seemed to be lower than the abundance in control and realistic nAg exposure replicates. However, it was assumed that a higher number of individuals correlated with higher mass of activated sludge in a batch reactor. Hence MLSS was used as a measure for sludge content of the batch reactors. Surprisingly, a regression of the sum of individuals (abundance) with MLSS had a coefficient of determination of 0.29 only. This means that sludge concentration (i.e. differences due to filling) influences the abundance of individuals by about 30% and the other 70% of variance need to be explained by other factors, such as treatment effects.

To test for this assumption, the relative abundance of protozoa and metazoa was calculated as sum of individuals divided by MLSS (in g/L) of the respective batch reactor sample. Subsequently, the sum of individuals in the dataset was substituted with relative

abundance of individuals and the dataset was analyzed as linear mixed-effect model (LME), in R software (Bates et al., 2015; R core team, 2014). With this model, the true averages of the replicates were estimated. In a null-model, parameter position was included as separate random effect, because it was shown previously that this parameter explained a comparably large fraction of variation. The model resulted in an Akaike information criterion (AIC) of 161.34. When including treatment as fixed parameter, i.e. exposure situation of the respective replicates in the model, the AIC improved to 160.1, while additional parameters such as pH, temperature and nitrite concentration led to an impairment of the model quality. Hence it is concluded, that treatment had a significant influence on the abundance of protozoa and metazoa.

The influence of treatment becomes even more prominently visible, when plotting the estimated real mean values of relative abundance as derived from the LME model against BOD₅ in ML for the different treatments (figure 68). The AIC was significantly reduced to 158.31 (P=0.05) for this model.

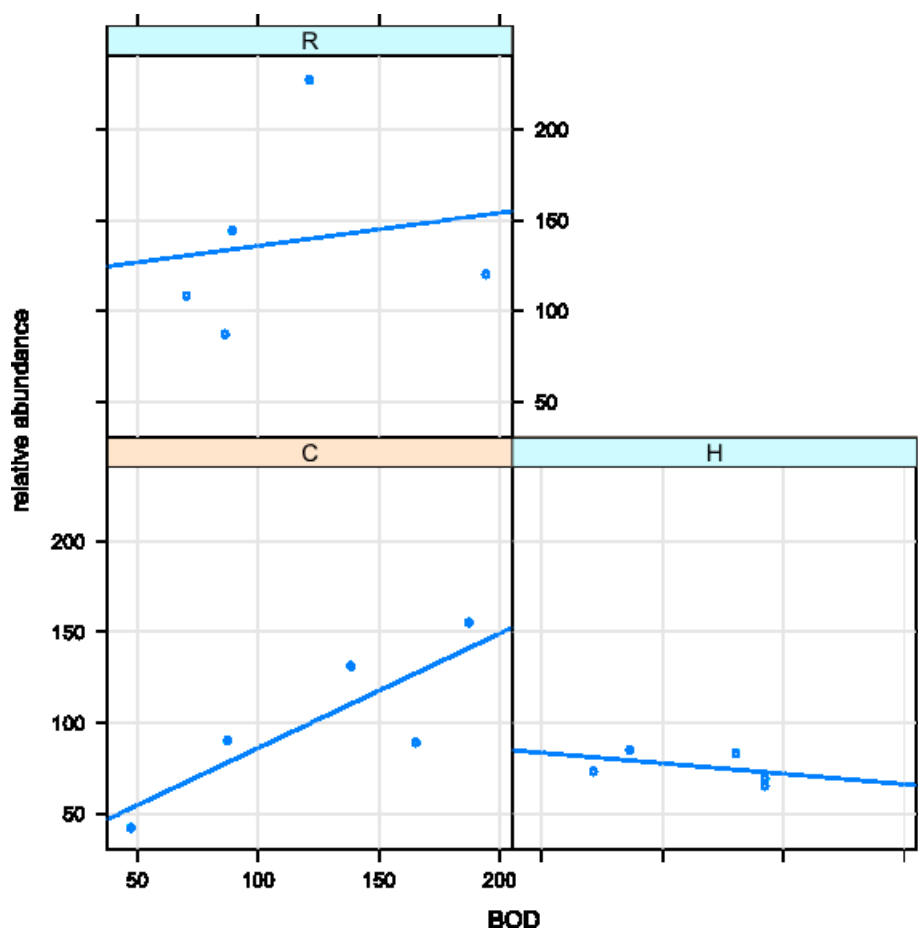


Figure 68: Estimated real averages of relative abundance (y-axis) and BOD₅ in ML (x-axis) with regard to the treatments (C - control; R - realistic nAg exposure; H - high nAg exposure) as derived from LME model.

In controls and realistic exposure samples, relative abundance of protozoa and metazoa increased with BOD₅ in ML. As explained in section 6.1, BOD₅ represents the amount of easily degradable biomass, i.e. organic matter which is consumed by bacteria. An increase of this biomass consequently yields good growth conditions for these bacteria, which in turn are the food source of protozoa. Consequently, populations of protozoa and their predators (metazoa) increase along with food supply. In the high nAg exposure however, the relative abundance of protozoa and metazoa decreased slightly, with increasing BOD₅ in ML. This fact suggests, that survival of these organisms was inhibited either directly through exposure with nAg or, indirectly via inhibition of their food source (bacteria). The exposure concentration in these treatment samples (100 µg/L nominal concentration) was comparably high regarding determined EC₅₀ values for bacteria in this work (e.g. *R. planticola* nominal EC₅₀~82 µg/L) and in the literature (e.g. growth inhibition of nitrifying bacteria with EC₅₀ = 140 µg/L, reported by Choi and Hu (2008)). Thus it is plausible, that a part of the bacterial community in the batch reactors was inhibited or even killed through nAg exposure at the high exposure concentration. Consequently, less bacteria were available as food source for protozoa, for which reason their abundance decreased as well. To test this hypothesis, the bacterial community should be analyzed in future studies regarding relative abundance and community composition. For this purpose, molecular methods such as sequencing techniques and real-time quantitative PCR targeting on 16SrRNA gene copies would be applicable for determination of the bacteria and their abundance in the samples.

Summing up, effects occur at the highest exposure concentration which is therefore construed as the nominal effect concentration, although random effects like filling order (position) of the batch reactors had a considerable influence on the overall result of the experiment. This supports hypothesis 5 partially, concerning the influence on the abundance of activated sludge organisms.

Regarding risk assessment, characterization of NPs in the wastewater is recommended in order to transform mass concentrations into surface area concentration, as proposed in section 3.3.2 (page 28 ff.). However, currently adequate methods for NP characterization in particle rich environmental samples such as activated sludge, are lacking. To date, techniques focusing on this issue are very time-consuming and laborious, or not affordable in terms of costs. As characterization of nAg in the sludge was not feasible in this experiment, evaluation of effect data for risk assessment was performed on nominal mass concentrations, with the assumption of correct dosage, as well as stable and constant dispersion in this experiment. Effects occurring due to high nAg exposure on the

protozoan and metazoan community of activated sludge were observed here, although determination of EC_{10} as equivalent of a LOEC value was not applicable according to the experimental design and the resulting dataset. However, it is assumed that the real nominal LOEC would be equal or lesser than the high exposure concentration. For this reason, it is included as such in the general environmental risk assessment in section 7, (page 155 ff.).

6.4 Chronic toxicity test with activated sludge community

6.4.1 Materials and Methods for chronic toxicity test

For the two weeks exposure experiment, feeding of the batch reactors was required to maintain nutrient supply and constant exposure to nAg in the assay. In order to avoid effects of additionally introduced organisms from wastewater, artificial wastewater (AWW) was used as medium. A 100-fold concentrated stock of AWW was prepared as follows. 325 g EDTA (Sigma-Aldrich, Steinheim, Germany, purity >99%) were dissolved in deionized water. The pH was measured and adjusted to 7.3 with 10 M NaOH.

Ingredients were weighed as specified in table 19 and dissolved in 1 L of deionized water:

Table 19: Ingredients for 100 fold concentrated stock of AWW.

Compound	mass	CAS
Peptone from gelatin ⁵	208 g	91079-38-8
Meat extract ⁵	143 g	91079-40-2
Urea ⁵	39 g	10034-99-8
K ₂ HPO ₄ ⁶	29.25 g	63231-63-0
KH ₂ PO ₄ ⁵	22.75 g	
NaCl ⁵	9.1 g	57-10-3
CaCl ₂ ⁵	5.2 g	57-11-4
MgSO ₄ x 7 H ₂ O ⁵	2.6 g	112-80-1

⁵ Carl Roth GmbH + Co. KG, Karlsruhe, Germany

⁶ Merck, Darmstadt, Germany

A trace element solution was prepared from 10 g ZnSO₄ x 7 H₂O, 0.03 g MnCl₂ x 4 H₂O, 0.3 g H₃BO₃, 0.2 g CoCl₂ x 6 H₂O, 0.01 g CuCl₂ x 2 H₂O, 0.02 g NiCl₂ x 6 H₂O, 0.03 g Na₂MoO₄ x 2 H₂O dissolved in 1 L deionized water (MiliQ) and autoclaved at 121°C for 20 min. From this stock, 65 mL were added to the medium, which was filled up to 6.5 L with deionized water (ASTM standard 1), mixed and aliquoted to 1 and 0.5 L Schott bottles (DURAN glass, Duran Group, Wertheim/Main, Germany) for autoclavation at 121 °C for 20 min.

The respective amount of 100x AWW stock was diluted with deionized water to 1x AWW and pH was adjusted to 6.8 to 6.9 with 10 N NaOH prior to use of medium. Conductivity was determined for medium characterization by using a WTW Conductometer LF 340 A equipped with a TetraCon 325 conductivity probe (WTW, Weilheim, Germany). Cuvette tests (Hach-Lange, Germany) were used for the determination of BOD₅ values (LCK555

with LZC555) and content of $\text{NH}_4\text{-N}$ (LCK 305), $\text{NO}_2\text{-N}$ (LCK 341), $\text{NO}_3\text{-N}$ (LCK 340), total and ortho-phosphate (LCK 348).

For acclimatization to operation conditions, activated sludge was kept in a mixed and aerated 20 L PE canister with drainage cock for a 4 weeks period prior to the test in order to establish a stable protozoan community, adapted to the AWW medium and boundary conditions. After inoculating the PE canister with 20 L fresh activated sludge from the wastewater treatment plant Dresden-Kaditz, two operation cycles were run per day, each consisting of 30 minutes decantation and feeding, 10 hours of mixed aeration and 1.5 h settling. Starting after 6 hours of mixed aeration (agitator IKA RW 20 equipped with custom made propeller; aquarium air pump (E2 M1, ASF Thomas Industries, Wuppertal, Germany) with two flexible tubes supplied with aquarium diffuser stones), a first settling phase (no aeration, no mixing) started to separate sludge from effluent water. After 1.5 h, a volume of 9.5 L effluent water was withdrawn from the canister (decantation) and replaced with AWW (feeding). The reactor was mixed and aerated for 10 h subsequently, before a new settling phase began.

It was planned to spread the inoculation material after 4 weeks acclimatization period to batch reactors as previously described (section 6.2.1) and continue the cycle operation at a smaller scale with continuous spiking of treatment reactors with nAg through addition of medium supplied with nAg at the respective concentrations. However, as difficulties arose to keep the protozoan community alive throughout acclimatization period, the experiment was aborted (see results and discussion).

6.4.2 Results and Discussion of chronic toxicity test

The artificial wastewater, which was used for feeding of the batch reactor, was characterized as follows: pH was 6.96, DO was 73% and conductivity was 614 $\mu\text{S}/\text{cm}$. The $\text{NH}_4\text{-N}$ content was 12.4 mg/L, orthophosphate was 18 mg/L, $\text{NO}_3\text{-N}$ and $\text{NO}_2\text{-N}$ were below the measuring range of the cuvette tests.

Chronic toxicity tests with a whole activated sludge community were not finalized, because protozoa and metazoa were not able to survive at experimental conditions during the 4 weeks adaptation period prior to the experiment. Microscopic examination of samples revealed high abundance of unspecified bacteria before and after the disappearance of protozoa and metazoa. Most probably, the artificial wastewater was selective for those bacteria, which were not edible for protozoa by means of their properties (e.g. size, or toxicity). A probable scenario for the development of the activated sludge community during acclimatization period, resulting in a breakdown of the protozoan fraction of the community, is illustrated in figure 69. Note that data in the graph are fictitious. On the left axis, numbers of bacteria are scaled, while the number of protozoa is scaled on the right axis. At the beginning of the acclimatization period, the majority of bacteria were assumed to be edible for the protozoa.

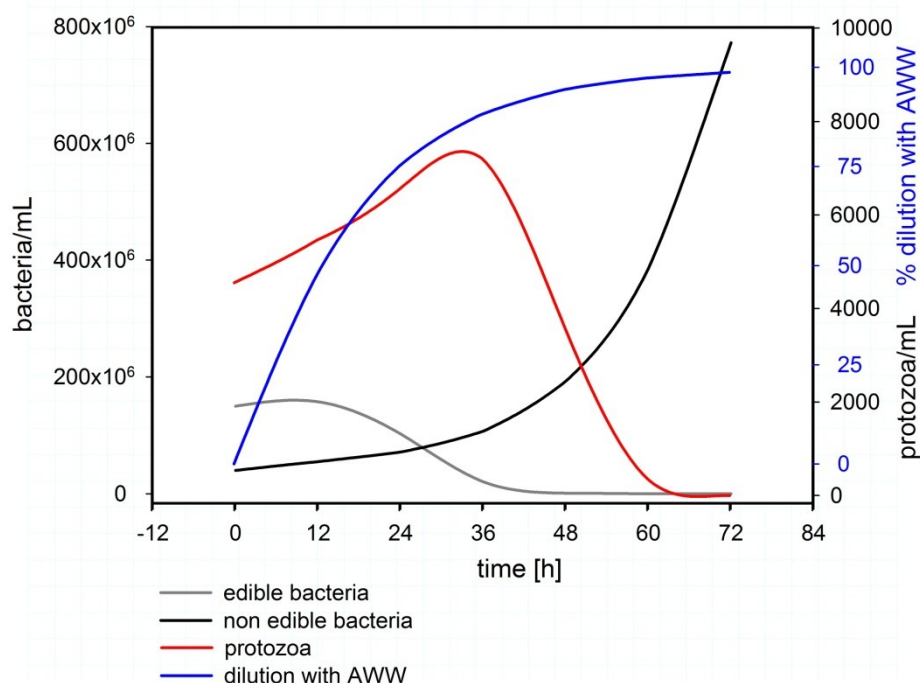


Figure 69: Development of the microbial community over acclimatization period with exchange of liquid with AWW. Note that data are fictitious.

The fraction of non edible bacteria is assumed to be lower than that of edible bacteria at the beginning. The population of protozoa increases in the first 36 h of acclimatization as they feed on the edible bacteria, which decrease in number through predation and probable unfavorable conditions due to the addition of artificial wastewater every 12 h (indicated by axis on the right in blue). After complete removal of edible bacteria through predation, protozoa become extinct and non edible bacteria overgrow the system.

Whether this fictitious scenario applies in reality, could be elucidated by screening of the samples regarding the bacteria species and cross testing of protozoa with the different bacteria strains regarding edibility and different combinations of bacteria and protozoa regarding population development, as reported by Lawler (1993). However, essentially for chronic toxicity testing, an AWW needs to be identified which is non-selective for specific bacteria. The protocol for preparation of AWW as applied in this study was derived from protocols for AWW in acute toxicity testing, which lack potentially essential compounds for long term survival. For this reason, trace element stocks as applied in cell culturing, were added to the AWW protocols. Other researchers have successfully applied similar media in chronic batch reactor experiments (Zhang et al., 2014). It should thus be considered, to test different AWW media in preliminary experiments for future long term experiments with activated sludge communities. Regarding the results from acute toxicity tests with nAg in batch reactors, it is hypothesized that treatment effects will be more clearly pronounced in chronic toxicity tests which should be undertaken in future research.

7 Conclusions & Prospects

Nanomaterials possess innovative properties and are increasingly manufactured for various applications. Especially nanosilver (nAg) is appreciated for its antibacterial effects and belongs to the most intensively deployed nanomaterial in housekeeping articles. An introduction of nAg released from such consumer products into sewer facilities and finally the occurrence in waste water treatment plants (WWTPs) is very likely. The potentially adverse effects on activated sludge when exposed to these NMs are still poorly understood. In this thesis work, the effects of nAg (NM-300K) on organisms related to activated sludge were explored in a stepwise approach: based on single species acute toxicity tests carried out on several bacteria and one ciliate species, complexity of toxicity tests was increased by conducting a basal artificial food chain experiment and finally a whole community experiment with real activated sludge. The purpose of this experimental setup was to test the following hypotheses:

1. The sensitivity towards nAg exposure differs between the separately tested species and organism groups (chapter 3 and 4).

When comparing effects of NM-300K nAg based on nominal concentrations, as chemical analytics of silver content were not conducted for all test assays, the bacterium *R. planticola* was clearly more sensitive (average 5h EC₅₀ = 0.14 mg/L) than the other tested bacteria (24h EC₅₀ = 4.99 mg/L for *Hyphomicrobium sp.*, no EC determinable for *Nitrobacter vulgaris*) and the ciliate *Paramecium tetraurelia* (20h EC₅₀ = 11.3 mg/L). These results confirm the findings of other scientists. The first hypothesis is thus regarded as not rejected.

Differential sensitivity of bacteria towards NPs is sometimes explained as a result of gram staining characteristics in the literature (Shrivastava et al., 2007; Liu et al., 2010b; Marambio-Jones and Hoek, 2010). In this work, gram-negative bacteria were investigated exclusively. The differential sensitivity among these gram-negative bacteria contradicts the aforementioned explanation, at least for the work presented here. However, the two alphaproteobacteria were less sensitive to nAg than the gammaproteobacterium. Although the phylogenetic groups within the proteobacteria are based on RNA sequence similarities and not on physiological or morphological characteristics, they might play a role in the toxicological response of microorganisms. Whether this hypothesis is plausible, should be regarded in future work.

2. The determined toxic effects of nAg are triggered by ions released from particles (chapter 3 and 4).

Regarding the results of this thesis, the plausibility of the second hypothesis is not easy to be answered. EC_{50} values of Ag^+ from nAg and $AgNO_3$ were the same in single species tests with *P. tetraurelia*, leading to the conclusion, that toxic effects of nAg are indeed triggered by silver ion release. For *R. planticola* however, results led to doubt concerning this implication, although difficulties with the chemical analytics and the resulting uncertainty influenced the interpretation of results. Lacking chemical analytics in *Hyphomicrobium* and *Nitrobacter* experiments made it even more complicated to answer this question clearly. It is further hypothesized that resistance mechanisms might trouble the deduction of triggers which are responsible for nAg toxicity. Apart from this fact and the required improvement of Ag chemical analytics, it is advisable to change the experimental design in order to fully elucidate the mechanisms that drive nAg toxicity based on the experiences from this work. First of all, dissolution behavior of nAg under investigation (and $AgNO_3$) should be addressed, requiring dialysis of nAg and $AgNO_3$ in the respective medium, as well as extensive chemical analysis. Ag^+ obtained from nAg and $AgNO_3$ after dialysis could then be transferred into the toxicity test assays. For the latter, those organisms and assays should be applied, which yielded interpretable results and did not suggest resistance to Ag. At this stage of work, the question whether nAg toxicity is triggered by released Ag^+ , remains open. Also, it cannot be excluded that the toxicity mechanisms differ from case to case in dependence of the boundary conditions and NP under investigation. This idea also reflects the previously mentioned discussion in the literature with contradictory results between and within studies. Generally, the hypothesis can neither be clearly supported nor clearly rejected.

3. nTiO₂ exhibits toxic effects on *P. tetraurelia*, which are enhanced by photocatalysis through UV radiation (chapter 3).

In acute and chronic toxicity tests, no adverse effects of nTiO₂ were found for *P. tetraurelia*. Results of toxicity tests with UV radiation showed that photocatalysis, if it occurred in the samples at all, did not affect the triggering of effects. Thus, the third hypothesis was falsified for the specific material which was applied in this work.

4. Different uptake pathways in *P. tetraurelia* lead to different effect concentrations of nAg in toxicity tests (chapter 3 and 5).

According to results from exposure via food and via medium experiments the hypothesis is neither clearly falsified, nor clearly supported regarding results from acute biomagnification assays. Here, effects from exposure in CM with and without food bacteria were more similar to each other, than those obtained from exposure in ABC. However, it must be noted that conclusions were drawn from the nominal exposure situation in the experiment and eventual uptake of nAg into the cells was not validated, for instance by means of electron microscopy. Availability and edibility of potentially nAg covered bacteria could not be verified within this work, but should be considered for future research. When considering the chronic experiment, interpretation of results was even more difficult, due to differences in growth of the cells between the two exposure modes. Despite the detailed discussed limitations of the experiments, comparison of the exposure samples with their respective controls revealed no adverse effects on population fitness at the tested concentrations (up to 0.1 mg/L). Further chronic tests with higher concentrations (up to EC_{50} from acute tests) led to full population mortality after 24 h in both assays and thus did not reveal information about differential sensitivity of populations. Additional tests with intermediate concentrations, supplementing chronic exposure in ABC would help to draw more meaningful conclusions. Further, methods need to be developed which enable quantification of nAg uptake into the cells.

5. nAg affect the community composition and abundance of organisms from activated sludge, probably leading to deterioration of wastewater purification processes (chapter 6).

Although the outcome of the acute activated sludge community experiment was influenced by the filling order of batch reactors, a treatment effect was observed for high nAg exposure (100 $\mu\text{g/L}$), suggesting plausibility of the hypothesis for the tested material NM-300K. In order to fully elucidate this issue, it is advisable to supplement the experimental data with results for the bacterial part of the community. With these results, probable deterioration of wastewater purification through nAg would be identifiable. Regarding long term effects on microbial WWTP communities, the experimental setup for

chronic nAg exposure requires further improvement in order to clarify the impact of recurring nAg input into WWTPs and its fate in the purification processes.

All in all, these hypotheses contributed to the main aim of this work: to identify possible risks of nAg NM-300K for activated sludge organisms which are crucial for wastewater treatment plant processes.

For this purpose, all available effect values from toxicity tests on the specific material are obliged to be gathered and compared. All existing data for NM-300K nAg from this work and the literature is displayed in table 20. According to European commission technical guidance document (Technical-Guidance-Document, 2003), the most sensitive organism is selected from the list of tested species for determination of hazard.

Table 20: Overview on available effect values from toxicity tests with NM-300K nAg on different organisms.

test organism (group)	type of test*, duration (h)	endpoint	Type of tox. Value	Nominal EC _x (mg/L)	source
<i>P. tetraurelia</i> (ciliate)	A, 20	mortality and viability	∅ EC ₅₀	11.3	1)
WWTP community (protozoa & metazoa)	A, 24	abundance	indirect effect	0.1	1)
<i>Raphidocephalus subcapitata</i> (algae)	A, 4.5	Inhibition of photosynthesis	EC ₅₀	0.9	2)
<i>Chydorus sphaericus</i> (cladocera)	A, 48	immobility	EC ₅₀	0.009	2)
<i>Danio rerio</i> embryo (fish)	A, 96	mortality/ inhibition of development	EC ₅₀	0.08	2)
<i>R. planticola</i> (bacterium)**	C, 5	viability and cell density	∅ EC ₅₀ ∅ EC ₁₀ NOEC	0.14 0.068 0.063	1)
<i>Hyphomicrobium sp.</i> (bacterium)	C, 24	cell density	EC ₅₀	4.99***	1)

* Usually, chronic toxicity tests require determination of NOEC values or EC₁₀ as substitute for NOEC. ** Determination of NOEC was possible and is given here for comparison to EC₁₀ values. ***EC₁₀ was not determinable for *Hyphomicrobium*, for which reason EC₅₀ values were included in this table for both chronic assays to enhance comparability of toxicity levels. A – acute, C – chronic, ∅ – average, tox. – toxicity, conc. - concentration. 1) this work 2) Wang et al. 2012

In this case, the cladocera *C. sphaericus* would be identified as most sensitive species. However, this organism, as well as fish and algae (gray shaded in table 20), are not

relevant for risk assessment in WWTPs as they are not part of the community of activated sludge. When excluding these organisms from the evaluation, *R. planticola* is the most sensitive species tested. Also, a NOEC was determinable for *R. planticola*, which is applied in risk assessment. For calculation of the predicted no effect concentration (PNEC), a safety factor is applied on the effect level determined in the toxicity test. The safety factor is defined based on the number and kind of toxicity tests conducted, as depicted in table 21.

Table 21: Determination of safety factors for PNEC calculation according to OECD and EU guidelines.

Available toxicity test data	Safety factor according to OECD & EU
LC/EC ₅₀ values from acute tests of 1 or 2 aquatic organisms	1000
LC ₅₀ values for fish, crustacean and algae from acute tests	100
NOEC/LOEC values for 2 aquatic organisms (chronic)	50 (EU)
NOEC/LOEC values for fish, crustacean, algae (chronic)	10

The principle behind this categorization is that with each further toxicity test conducted regarding a specific material, the uncertainty for interpretation of the hazard level decreases. Chronic tests are of special importance, because they help to estimate long term impacts of the tested material on populations. Regarding the data available for NM-300K toxicity testing as presented in table 20, a safety factor of 100 would be applicable, if strictly addressing the suggestions of the European regulatory agencies. However, the tests with *R. planticola* and *Hyphomicrobium sp.* are regarded as chronic experiments and thus contribute to a reduction of uncertainty concerning environmental risk. For *R. planticola*, a NOEC was determinable at a nominal concentration of 63 µg/L, but not for *Hyphomicrobium sp.* Uncertainty in hazard identification is further reduced through the availability of results from the whole community assay, which justifies the application of a safety factor of 10 for the calculation of the PNEC with the NOEC of *R. planticola*. The resulting PNEC is 6.3 µg/L.

As discussed before (see section 3.3.2, p.28 ff), the predicted environmental concentrations (PEC) for a realistic and a worst case scenario were deduced from Hendren et al. (2013), with 1.6 and 4.5 µg NM-300K per L activated sludge. Consequently, the risk quotients (PEC/PNEC) are 0.25 for the realistic scenario and 0.7 for the worst case scenario and would not result in a risk, posed by NM-300K to activated sludge organisms. It should be noted, that the risk quotient would increase slightly, when taking into account the effective concentrations as determined by ICP-OES and that many assumptions were made concerning the PEC. Further, the safety factor was chosen very strictly.

Thus, the risk for an unobstructed purification of wastewater in the treatment processes as functional endpoint must be assessed in future experiments. In order to elucidate this issue, chronic whole community experiments should be undertaken under laboratory and realistic conditions and special focus should be laid on functional diversity. For the bacterial part of the activated sludge community, shifts in functional groups have already been observed after exposure to nanomaterials. For protozoa and metazoa these data are still lacking for nAg in general. Because the specific properties of NPs depending on size, coating and boundary conditions require particle specific risk assessment, as also demanded by the European commission (2012), the impact of NM-300K on functional diversity of the whole activated sludge community needs to be investigated along with the performance (i.e. effluent quality) in chronic experiments.

Summarizing, a general conclusion on the impact of NM-300K on wastewater purification is not possible at this stage of nano-ecotoxicological work. However, through the experiences gained from experiments of this thesis, new insights were gathered concerning essential features to complement the understanding of nanosilver toxicity on the different levels of complexity. Further, data on effects for some of the tested organisms were accomplished, which are now available for the scientific community and will help to fill the lack of knowledge especially regarding material specific toxicity.

8 Summary

Among all nanomaterials, which are intentionally manufactured and applied, nanosilver (nAg) and nano titanium dioxide (nTiO₂) are two of the most frequently applied nanomaterials. Especially nAg is introduced into wastewater treatment plants (WWTPs) due to its use as antimicrobial resource in household and medical care products and hence concern raised regarding its impact on activated sludge organisms and their purification efficiency. In contrast, nTiO₂ plays an economical role in paints and sunscreens and less frequently in food as white pigment. Within this thesis, the effects of nAg on single species, simple food chains and communities related to activated sludge were investigated. Potential effects of nTiO₂ were tested in single species tests with the ciliate *P. tetraurelia*. Results were implemented into environmental risk assessment.

When regarding effects in nanotoxicology, characterization of the respective particles in the matrix (i.e. medium) as applied in the test system is crucial. On one hand, information is required concerning the agglomeration behavior and particle size under experimental conditions to evaluate the availability of NPs in the experiment. On the other hand, particle number concentrations are more meaningful for interpreting the test results, than mass concentrations. For their determination, particle size and exposure concentrations need to be determined as exactly as possible. For this reason, chemical analytics should accompany the experiments as far as possible. In this thesis, different spectroscopy techniques (ICP-OES and ICP-MS) were applied in combination with centrifugation, to determine nanoparticle and ion concentrations in the experiments with *P. tetraurelia* and the bacterium *R. planticola*. It was shown that dosage of nAg was difficult and nearly not replicable between independent tests. Further refinement of the analytical technique for these experiments is required. Concerning particle size and agglomeration behavior of NPs in heterogenous aqueous matrices, UV-vis spectroscopy appeared to represent the most plausible particle sizes, also confirmed by scanning electron microscopy, while dynamic light scattering (DLS) contradicted the DLVO theory and was thus disregarded in subsequent experiments.

Among all tested species in this thesis, the gammaproteobacteria *R. planticola* was the most sensitive organism regarding the tested nAg material, NM-300K. Based on data from the literature, only the cladocera *Chydorus sp.* was more sensitive. For environmental risk assessment (ERA) in WWTPs it was disregarded, as it is not abundant in activated sludge. The ERA, based on an assumed predicted environmental concentration derived from modeled concentrations of other types of nAg, revealed no risk for the activated sludge. This result should be interpreted with care, considering the tolerantly chosen safety factor

for calculation of the predicted no effect concentration and the assumptions which were made concerning environmental concentrations.

Differences in acute toxic effects of nAg on *P. tetraurelia* were observed depending on the type of medium and the exposure pathway (via medium or via bacterial food). More detailed investigations are required to analyze the distribution, availability and uptake of nAg into ciliates in the respective tests (i.e. whether nAg is dispersed or attached to bacteria, whether bacteria are distributed in the liquid column or settled and whether coated bacteria are edible for the ciliates). In chronic experiments concentration response was very steep in the range between the effect concentration determined in acute toxicity testing (resulting in 100% mortality) and a tenfold lower concentration (no effect observed) for both exposure pathways.

Community experiments with activated sludge exposed to realistic and high concentrations of nAg revealed acute effects on the protozoan community at high nAg concentration using multivariate statistics for data analysis. In contrast, the sludge biotic index was not meaningful for data interpretation, as no differences were observed between the samples of different treatments. The evaluation of acute toxicity should be extended to the bacterial part of the activated sludge community for completion of the environmental risk assessment. For chronic testing, more preliminary work is required to develop a protocol for artificial wastewater which serves the needs of activated sludge organisms over longer time periods and which retains a typical composition of the activated sludge community.

9 References

- Abbott, L. C. and Maynard, A. D., 2010: Exposure Assessment Approaches for Engineered Nanomaterials. *Risk Analysis*. 30, 11, 1634-1644.
- Abhilash and Pandey, B. D., 2012: Synthesis of zinc-based nanomaterials: a biological perspective. *IET Nanobiotechnology*, Institution of Engineering and Technology.
- Aitken, R. J., Chaudhry, M. Q., Boxall, A. B. A. and Hull, M., 2006: Manufacture and use of nanomaterials: current status in the UK and global trends. *Occupational Medicine*. 56, 5, 300-306.
- Al-rekabi, W. S., Qiang, H. and Qiang, W. W., 2007: Review on Sequencing Batch Reactors. *Pakistan Journal of Nutrition, Asian Network for Scientific Information* 6, 1, 11-19.
- AWWA, 2002: Nitrification. p. Agency, U. S. E. P.
- Badawy, A. M. E., Luxton, T. P., Silva, R. G., Scheckel, K. G., Suidan, M. T. and Tolaymat, T. M., 2010: Impact of Environmental Conditions (pH, Ionic Strength, and Electrolyte Type) on the Surface Charge and Aggregation of Silver Nanoparticles Suspensions. *Environ Sci Technol*. 44, 4, 1260-6.
- Bates, D., Maechler, M., Bolker, B. and Walker, S., 2015: Fitting Linear Mixed-Effects Models Using lme4. *Journal of Statistical Software*, 67, 1, 1-48.
- Battin, T. J., Kammer, F. V. D., Weilhartner, A., Ottofuelling, S. and Hofmann, T., 2009: Nanostructured TiO₂: Transport Behavior and Effects on Aquatic Microbial Communities under Environmental Conditions. *Environmental Science & Technology*. 43, 21, 8098-8104.
- Beer, C., Foldbjerg, R., Hayashi, Y., Sutherland, D. S. and Autrup, H., 2012: Toxicity of silver nanoparticles—Nanoparticle or silver ion? *Toxicology Letters*. 208, 3, 286-292.
- Berger, H., Foissner, W. and Kohmann, F., 1997: Bestimmung und Ökologie der Mikrosaprobien nach DIN 38410 : 26 Bildbestimmungsschlüssel, 10 Tabellen. Gustav Fischer Verlag, Stuttgart, Germany,
- Bhaskar, P. V. and Bhosle, N. B., 2006: Bacterial extracellular polymeric substance (EPS): A carrier of heavy metals in the marine food-chain. *Environment international*. 32, 2, 191-198.
- Bilberg, K., Hovgaard, M. B., Besenbacher, F. and Baatrup, E., 2012: In Vivo Toxicity of Silver Nanoparticles and Silver Ions in Zebrafish (*Danio rerio*). *Journal of Toxicology*. 2012,
- Blaser, S. A., Scheringer, M., MacLeod, M. and Hungerbühler, K., 2008: Estimation of cumulative aquatic exposure and risk due to silver: Contribution of nano-functionalized plastics and textiles. *Science of the Total Environment*. 390, 2-3, 396-409.
- Bondarenko, O., Ivask, A., Käkinen, A., Kurvet, I. and Kahru, A., 2013: Particle-Cell Contact Enhances Antibacterial Activity of Silver Nanoparticles. *PLoS ONE*. 8, 5, e64060.
- Boon, B. and Laudelout, H., 1962: Kinetics of nitrite oxidation by *Nitrobacter winogradskyi*. *Biochemical Journal*. 85, 3, 440-447.
- Bouin, P., 1897: *Phenomenes Cytologique anoramoux dans. 1 Histogenes*, Nancy.
- Boverhof, D. R. and David, R. M., 2010: Nanomaterial characterization: considerations and needs for hazard assessment and safety evaluation. *Analytical and Bioanalytical Chemistry*. 396, 3, 953-961.

- Brar, S. K., Verma, M., Tyagi, R. D. and Surampalli, R. Y., 2010: Engineered nanoparticles in wastewater and wastewater sludge - Evidence and impacts. *Waste Management*. 30, 3, 504-520.
- Chen, J., Tang, Y.-Q., Li, Y., Nie, Y., Hou, L., Li, X.-Q. and Wu, X.-L., 2014: Impacts of different nanoparticles on functional bacterial community in activated sludge. *Chemosphere*. 104, 141-148.
- Choi, O., Deng, K. K., Kim, N. J., Ross, L., Surampalli, R. Y. and Hu, Z. Q., 2008: The inhibitory effects of silver nanoparticles, silver ions, and silver chloride colloids on microbial growth. *Water Research*. 42, 12, 3066-3074.
- Choi, O. and Hu, Z. Q., 2008: Size dependent and reactive oxygen species related nanosilver toxicity to nitrifying bacteria. *Environmental Science & Technology*. 42, 12, 4583-4588.
- Choi, O. K. and Hu, Z. Q., 2009: Nitrification inhibition by silver nanoparticles. *Water Science and Technology*. 59, 9, 1699-1702.
- Clemente, Z., Castro, V. L., Jonsson, C. M. and Fraceto, L. F., 2012: Ecotoxicology of Nano-TiO₂ An Evaluation of its Toxicity to Organisms of Aquatic Ecosystems. *International Journal of Environmental Research*. 6, 1, 33-50.
- Coleman, V. A., Jämting, Å. K., Catchpoole, H. J., Roy, M. and Herrmann, J., 2011: Nanoparticles and metrology: a comparison of methods for the determination of particle size distributions. 810504-810504.
- Consumer-Products-Inventory, 2009: The Project on Emerging Nanotechnologies. Woodrow Wilson International Center for Scholars, 12/2009.
- Curds, C. R., 1982: The Ecology and Role of Protozoa in Aerobic Sewage Treatment Processes. *Annual Review of Microbiology*. 36, 1, 27-28.
- Cybis, L. F. D. A. and Horan, N. J., 1997: Protozoan and metazoan populations in sequencing batch reactors operated for nitrification and/or denitrification. *Water Science and Technology*. 35, 1, 81-86.
- Dhandapani, P., Maruthamuthu, S. and Rajagopal, G., 2012: Bio-mediated synthesis of TiO₂ nanoparticles and its photocatalytic effect on aquatic biofilm. *Journal of Photochemistry and Photobiology B: Biology*. 110, 0, 43-49.
- Drancourt, M., Bollet, C., Carta, A. and Rousselier, P., 2001: Phylogenetic analyses of *Klebsiella* species delineate *Klebsiella* and *Raoultella* gen. nov., with description of *Raoultella ornithinolytica* comb. nov., *Raoultella terrigena* comb. nov. and *Raoultella planticola* comb. nov. *International Journal of Systematic and Evolutionary Microbiology*. 51, 3, 925-32.
- Dror-Ehre, A., Mamane, H., Belenkova, T., Markovich, G. and Adin, A., 2009: Silver nanoparticle-E. coli colloidal interaction in water and effect on E-coli survival. *Journal of Colloid and Interface Science*. 339, 2, 521-526.
- Environment Canada, 2005: Guidance Document on Statistical Methods for Environmental Toxicity Tests. Report EPS 1/RM/46. p. Environmental Technology Center.
- Environmental Protection Agency, 1997: Wastewater treatment manuals - Primary, secondary and tertiary treatment. EPA Ardavan, Wexford, Ireland.
- Esteban, G., Tellez, C. and Bautista, L. M., 1991: DYNAMICS OF CILIATED PROTOZOA COMMUNITIES IN ACTIVATED-SLUDGE PROCESS. *Water Research*. 25, 8, 967-972.
- EU, 1991: RICHTLINIE DES RATES über die Behandlung von kommunalem Abwasser. Gemeinschaften, A. d. E., Nr. L 135/40.

- European-comission, 2012: Communication from the comission to the European Parliament, the council and the European economic and social committee - Second Regulatory Review on Nanomaterials.
- Fenchel, T., 1980a: Suspension feeding in ciliated protozoa: Feeding rates and their ecological significance. *Microbial Ecology*. 6, 1, 13-25.
- Fenchel, T., 1980b: Suspension feeding in ciliated protozoa: Functional response and particle size selection. *Microbial Ecology*. 6, 1, 1-11.
- Feng, Q. L., Wu, J., Chen, G. Q., Cui, F. Z., Kim, T. N. and Kim, J. O., 2000: A mechanistic study of the antibacterial effect of silver ions on *Escherichia coli* and *Staphylococcus aureus*. *Journal of Biomedical Materials Research*. 52, 4, 662-668.
- Fent, K. 2013: *Ökotoxikologie. Umweltchemie - Toxikologie – Ökologie*, 4. Auflage, Georg Thieme Verlag.
- Filipkowska, Z., Janczukowicz, W., Krzemieniewski, m. and Pesta, J., 2000: Microbiological Air Pollution in the Surroundings of the Wastewater Treatment Plant with Activated-Sludge Tanks Aerated by Horizontal Rotors. *Polish Journal of Environmental Studies* Vol. 9, 4, 273-280.
- Finlay, B., 1977: The dependence of reproductive rate on cell size and temperature in freshwater ciliated protozoa. *Oecologia*. 30, 1, 75-81.
- Finlay, B. J. and Fenchel, T., 1996: *Ciliates: Cells as Organisms*. Gustav Fischer Verlag, Stuttgart, Germany, Ecology: role of ciliates in the natural environment).
- Foissner, W. and Berger, H., 1996: A user-friendly guide to the ciliates (Protozoa, Ciliophora) commonly used by hydrobiologists as bioindicators in rivers, lakes, and waste waters, with notes on their ecology. *Freshwater Biology*. 35, 2, 375-482.
- Fried, J. and Lemmer, H., 2003: On the dynamics and function of ciliates in sequencing batch biofilm reactors. *Water Science and Technology*. 47, 5, 189 - 196.
- Fuchs, G., 2007: *Allgemeine Mikrobiologie*. Georg Thieme Verlag,
- Gao, J., Youn, S., Hovsepian, A., Llanaez, V. L., Wang, Y., Bitton, G. and Bonzongo, J. C. J., 2009: Dispersion and Toxicity of Selected Manufactured Nanomaterials in Natural River Water Samples: Effects of Water Chemical Composition. *Environmental Science & Technology*. 43, 9, 3322-3328.
- Garrity, G., Brenner, D., Krieg, N. and Staley, J., 1974: *Bergey's manual of determinative bacteriology*. Springer-Verlag US, (Gliesche, C., Fesefeldt, A. and Hirsch, P., Genus I. *Hyphomicrobium*).
- Görtz, H.-D., 1988: *Paramecium*. Springer Verlag, Berlin, Germany, (Takagi, Y., Aging).
- Gottschalk, F., Sonderer, T., Scholz, R. W. and Nowack, B., 2009: Modeled Environmental Concentrations of Engineered Nanomaterials (TiO₂, ZnO, Ag, CNT, Fullerenes) for Different Regions. *Environmental Science & Technology*. 43, 24, 9216-9222.
- Grunditz, C. and Dalhammar, G., 2001: Development of nitrification inhibition assays using pure cultures of *Nitrosomonas* and *Nitrobacter*. *Water Research*. 35, 2, 433-440.
- Gunawan, C., Teoh, W. Y., Marquis, C. P. and Amal, R., 2013: Induced Adaptation of *Bacillus* sp. to Antimicrobial Nanosilver. *Small*. 9, 21, 3554-3560.
- Gupta, A., Matsui, K., Lo, J.-F. and Silver, S., 1999: Molecular basis for resistance to silver cations in *Salmonella*. *Nat Med*. 5, 2, 183-188.
- Handy, R. D., von der Kammer, F., Lead, J. R., Hassellöv, M., Owen, R. and Crane, M., 2008: The ecotoxicology and chemistry of manufactured nanoparticles. *Ecotoxicology*. 17, 287-314.

- Handy, R. D., Al-Bairuty, G., Al-Jubory, A., Ramsden, C. S., Boyle, D., Shaw, B. J. and Henry, T. B., 2011: Effects of manufactured nanomaterials on fishes: a target organ and body systems physiology approach. *Journal of Fish Biology*. 79, 4, 821-853.
- Hassellöv, M., Readman, J., Ranville, J. and Tiede, K., 2008: Nanoparticle analysis and characterization methodologies in environmental risk assessment of engineered nanoparticles. *Ecotoxicology*. 17, 5, 344-361.
- Hayes, A. C., Liss, S. N. and Allen, D. G., 2010: Growth Kinetics of *Hyphomicrobium* and *Thiobacillus* spp. in Mixed Cultures Degrading Dimethyl Sulfide and Methanol. *Applied and Environmental Microbiology*. 76, 16, 5423-5431.
- Hendren, C. O., Badireddy, A. R., Casman, E. and Wiesner, M. R., 2013: Modeling nanomaterial fate in wastewater treatment: Monte Carlo simulation of silver nanoparticles (nano-Ag). *Science of the Total Environment*. 449, 0, 418-425.
- Henriques, I. D. S. and Love, N. G., 2007: The role of extracellular polymeric substances in the toxicity response of activated sludge bacteria to chemical toxins. *Water Research*. 41, 18, 4177-4185.
- Henze, M., van Loosdrecht, M. C. M., Ekama, G. A. and Brdjanovic, D., 2008: *Biological Wastewater Treatment: Principles, Modelling and Design*. IWA Publishing, London, UK.
- Holbrook, R. D., Murphy, K. E., Morrow, J. B. and Cole, K. D., 2008: Trophic transfer of nanoparticles in a simplified invertebrate food web. *Nat Nano*. 3, 6, 352-355.
- Hou, W.-C., Westerhoff, P. and Posner, J. D., 2013: Biological accumulation of engineered nanomaterials: a review of current knowledge. *Environmental Science: Processes & Impacts*. 15, 1, 103-122.
- Hu, Z. Q., Chandran, K., Grasso, D. and Smets, B. F., 2002: Effect of nickel and cadmium speciation on nitrification inhibition. *Environmental Science & Technology*. 36, 14, 3074-3078.
- Hu, Z. Q., Chandran, K., Grasso, D. and Smets, B. F., 2004: Comparison of nitrification inhibition by metals in batch and continuous flow reactors. *Water Research*. 38, 18, 3949-3959.
- Hwang, E. T., Lee, J. H., Chae, Y. J., Kim, Y. S., Kim, B. C., Sang, B.-I. and Gu, M. B., 2008: Analysis of the Toxic Mode of Action of Silver Nanoparticles Using Stress-Specific Bioluminescent Bacteria. *Small*. 4, 6, 746-750.
- Irvine, R. L., Ketchum, L. H. and Asano, T., 1989: Sequencing batch reactors for biological wastewater treatment. *Critical Reviews in Environmental Control*. 18, 4, 255-294.
- Jeong, E., Chae, S. R., Kang, S. T. and Shin, H. S., 2012: Effects of silver nanoparticles on biological nitrogen removal processes. *Water Science and Technology*. 65, 7, 1298 - 1303.
- Jiang, J., Oberdoerster, G. and Biswas, P., 2009: Characterization of size, surface charge, and agglomeration state of nanoparticle dispersions for toxicological studies. *J Nanopart Res*. 11, 77 - 89.
- Jin, X., Li, M. H., Wang, J. W., Marambio-Jones, C., Peng, F. B., Huang, X. F., Damoiseaux, R. and Hoek, E. M. V., 2010: High-Throughput Screening of Silver Nanoparticle Stability and Bacterial Inactivation in Aquatic Media: Influence of Specific Ions. *Environmental Science & Technology*. 44, 19, 7321-7328.
- Joshi, N., Ngwenya, B. T. and French, C. E., 2012: Enhanced resistance to nanoparticle toxicity is conferred by overproduction of extracellular polymeric substances. *Journal of Hazardous Materials*. 241-242, 0, 363-370.

- Kaegi, R., Sinnet, B., Zuleeg, S., Hagendorfer, H., Mueller, E., Vonbank, R., Boller, M. and Burkhardt, M., 2010: Release of silver nanoparticles from outdoor facades. *Environmental Pollution*. 158, 9, 2900-2905.
- Kaempfer, P., 1989: Numerische Identifizierung aquatischer Mikroorganismen mittels automatisierter Methoden am Beispiel von Bakterien aus dem belebten Schlamm. *Zentralblatt für bakteriologie Mikrobiologie und Hygiene Serie B*. 187,
- Kaempfer, P., Eisentraeger, A., Hergt, V. and Dott, W., 1990: Untersuchungen zur bakteriellen Phosphateliminierung. I. Mitteilung: Bakterienflora und bakterielle Phosphatspeicherung in Abwasserreinigungsanlagen. *gwf Wasser Abwasser*. 131,
- Kahru, A. and Dubourguier, H.-C., 2010: From ecotoxicology to nanoecotoxicology. *Toxicology*. 269, 2-3, 105-119.
- Kaneshiro, E. S., Beischel, L. S., Merkel, S. J. and Rhoads, D. E., 1979: The Fatty Acid Composition of *Paramecium aurelia* Cells and Cilia: Changes with Culture Age. *The Journal of Protozoology*. 26, 1, 147-158.
- Khan, S., Mukherjee, A. and Chandrasekaran, N., 2011: Silver nanoparticles tolerant bacteria from sewage environment. *Journal of Environmental Sciences-China*. 23, 2, 346-352.
- Kim, B. H. and Gadd, G. M., 2008: *Bacterial physiology and metabolism*. Cambridge University Press, UK,
- Kim, J. S., Kuk, E., Yu, K. N., Kim, J.-H., Park, S. J., Lee, H. J., Hyun, K. S., Park, Y. K., Park, Y. H., Hwang, C.-Y., Kim, Y.-K., Lee, Y.-S., Jeong, D. H. and Cho, M.-H., 2007: Antimicrobial effects of silver nanoparticles. *Nanomedicine: Nanotechnology, Biology and Medicine*. 3, 95 - 101.
- Kim, S.-J., 2004: ESTIMATION OF ACTIVE NITROSOMONAS AND NITROBACTER CONCENTRATIONS IN ACTIVATED SLUDGE USING NITROGENOUS OXYGEN UPTAKE RATE. *Environmental Engineering Research*. 9, 3, 130-142.
- Kim, S., Baek, Y.-W. and An, Y.-J., 2011: Assay-dependent effect of silver nanoparticles to *Escherichia coli* and *Bacillus subtilis*. *Applied Microbiology and Biotechnology*. 92, 5, 1045-1052.
- Kiser, M. A., Westerhoff, P., Benn, T., Wang, Y., Perez-Rivera, J. and Hristovski, K., 2009: Titanium Nanomaterial Removal and Release from Wastewater Treatment Plants. *Environmental Science & Technology*. 43, 17, 6757-6763.
- Kittler, S., Greulich, C., Diendorf, J., Köller, M. and Epple, M., 2010a: Toxicity of Silver Nanoparticles Increases during Storage Because of Slow Dissolution under Release of Silver Ions. *Chemistry of Materials*. 22, 16, 4548-4554.
- Kittler, S., Greulich, C., Gebauer, J. S., Diendorf, J., Treuel, L., Ruiz, L., Gonzalez-Calbet, J. M., Vallet-Regi, M., Zellner, R., Koller, M. and Epple, M., 2010b: The influence of proteins on the dispersability and cell-biological activity of silver nanoparticles. *Journal of Materials Chemistry*. 20, 3, 512-518.
- Koops, H.-P. and Pommerening-Röser, A., 2001: Distribution and ecophysiology of the nitrifying bacteria emphasizing cultured species. *FEMS Microbiology Ecology*. 37, 1, 1-9.
- Kovárová, K., Zehnder, A. J. and Egli, T., 1996: Temperature-dependent growth kinetics of *Escherichia coli* ML 30 in glucose-limited continuous culture. *Journal of Bacteriology*. 178, 15, 4530-4539.
- Krenek, S., Berendonk, T. U. and Petzoldt, T., 2011: Thermal performance curves of *Paramecium caudatum*: A model selection approach. *European Journal of Protistology*. 47, 124-137.

- Lawler, S. P., 1993: Direct and indirect effects in microcosm communities of protists. *Oecologia*. 93, 184 - 190.
- Lee, S., Basu, S., Tyler, C. W. and Wei, I. W., 2004: Ciliate populations as bio-indicators at Deer Island Treatment Plant. *Advances in Environmental Research*. 8, 3–4, 371-378.
- Lee, Y.-J., Kim, J., Oh, J., Bae, S., Lee, S., Hong, I. S. and Kim, S.-H., 2012: Ion-release kinetics and ecotoxicity effects of silver nanoparticles. *Environmental Toxicology and Chemistry*. 31, 1, 155-159.
- Lees, H. and Simpson, J. R., 1957: The biochemistry of the nitrifying organisms. 5. Nitrite oxidation by *Nitrobacter*. *Biochemical Journal*. 65, 2, 297-305.
- Lemmer, H., Griebe and Flemming, 1995: *Ökologie der Abwasserorganismen*. Springer (Gliesche, H., Holm, *Hyphomicrobium* spp; im Klärwerk und im Abwasserbelasteten Gewässer).
- Leps, H., 2011: Effekte von Silbernanopartikeln auf den Ciliaten *Paramecium tetraurelia* in einem akuten Toxizitätstest in axenischem Medium. Diplomarbeit im Fachbereich Biowissenschaften der Goethe-Universität Frankfurt am Main, durchgeführt am Institut für Hydrobiologie der TU Dresden.
- Li, Q. L., Mahendra, S., Lyon, D. Y., Brunet, L., Liga, M. V., Li, D. and Alvarez, P. J. J., 2008: Antimicrobial nanomaterials for water disinfection and microbial control: Potential applications and implications. *Water Research*. 42, 18, 4591-4602.
- Li, X. and Lenhart, J. J., 2012: Aggregation and Dissolution of Silver Nanoparticles in Natural Surface Water. *Environmental Science & Technology*. 46, 10, 5378-5386.
- Liang, Z., Das, A. and Hu, Z., 2010: Bacterial response to a shock load of nanosilver in an activated sludge treatment system. *Water Res.* 44, 18, 5432-8.
- Liau, S. Y., Read, D. C., Pugh, W. J., Furr, J. R. and Russell, A. D., 1997: Interaction of silver nitrate with readily identifiable groups: relationship to the antibacterial action of silver ions. *Letters in Applied Microbiology*. 25, 4, 279-283.
- Lin, Q. and Sun, Z., 2010: Optical Extinction Properties of Aggregated Ultrafine Silver Nanoparticles on Silica Nanospheres. *The Journal of Physical Chemistry C*. 115, 5, 1474-1479.
- Lin, Q. and Sun, Z., 2011: Study on optical properties of aggregated ultra-small metal nanoparticles. *Optik - International Journal for Light and Electron Optics*. 122, 12, 1031-1036.
- Lindqvist, R., 2006: Estimation of *Staphylococcus aureus* Growth Parameters from Turbidity Data: Characterization of Strain Variation and Comparison of Methods. *Applied and Environmental Microbiology*. 72, 7, 4862-4870.
- Liu, J. and Hurt, R. H., 2010: *Environ. Sci. Technol.* 44, 2169.
- Liu, J., Sonshine, D. A., Shervani, S. and Hurt, R. H., 2010a: Controlled Release of Biologically Active Silver from Nanosilver Surfaces. *ACS Nano*. 4, 11, 6903-6913.
- Liu, H.-L., Dai, S. A., Fu, K.-Y. and Hsu, S.-h., 2010b: Antibacterial properties of silver nanoparticles in three different sizes and their nanocomposites with a new waterborne polyurethane. *International Journal of Nanomedicine*. 5, 1017-1028.
- Lok, C. N., Ho, C. M., Chen, R., He, Q. Y., Yu, W. Y., Sun, H. Z., Tam, P. K. H., Chiu, J. F. and Che, C. M., 2006: Proteomic analysis of the mode of antibacterial action of silver nanoparticles. *Journal of Proteome Research*. 5, 4, 916-924.
- Lu, H., Chandran, K. and Stensel, D., 2014: Microbial ecology of denitrification in biological wastewater treatment. *Water Research*. 64, 0, 237-254.

- MacCormack, T. J. and Goss, G. G., 2008: Identifying and Predicting Biological Risks Associated With Manufactured Nanoparticles in Aquatic Ecosystems. *Journal of Industrial Ecology*. 12, 3, 286-296.
- Madoni, P., 1994: A sludge biotic index (SBI) for the evaluation of the biological performance of activated sludge plants based on the microfauna analysis. *Water Research*. 28, 1, 67-75.
- Madoni, P., Davoli, D. and Chierici, E., 1993: COMPARATIVE-ANALYSIS OF THE ACTIVATED-SLUDGE MICROFAUNA IN SEVERAL SEWAGE-TREATMENT WORKS. *Water Research*. 27, 9, 1485-1491.
- Madoni, P., Davoli, D., Gorbi, G. and Vescovi, L., 1996: Toxic effect of heavy metals on the activated sludge protozoan community. *Water Research*. 30, 1, 135-141.
- Marambio-Jones, C. and Hoek, E., 2010: A review of the antibacterial effects of silver nanomaterials and potential implications for human health and the environment. *Journal of Nanoparticle Research*. 12, 5, 1531-1551.
- Maurer-Jones, M. A., Mousavi, M. P. S., Chen, L. D., Buhlmann, P. and Haynes, C. L., 2013: Characterization of silver ion dissolution from silver nanoparticles using fluoros-phase ion-selective electrodes and assessment of resultant toxicity to *Shewanella oneidensis*. *Chemical Science*. 4, 6, 2564-2572.
- Mielke, R. E., Priester, J. H., Werlin, R. A., Gelb, J., Horst, A. M., Orias, E. and Holden, P. A., 2013: Differential Growth of and Nanoscale TiO₂ Accumulation in *Tetrahymena thermophila* by Direct Feeding versus Trophic Transfer from *Pseudomonas aeruginosa*. *Applied and Environmental Microbiology*. 79, 18, 5616-5624.
- Morones, J. R., Elechiguerra, J. L., Camacho, A., Holt, K., Kouri, J. B., Ramirez, J. T. and Yacaman, M. J., 2005: The bactericidal effect of silver nanoparticles. *Nanotechnology*. 16, 10, 2346-2353.
- Müller, N. C. and Nowack, B., 2008: Exposure modeling of engineered nanoparticles in the environment. *Environmental Science & Technology*. 42, 12, 4447-4453.
- Musee, N., Thwala, M. and Nota, N., 2011: The antibacterial effects of engineered nanomaterials: implications for wastewater treatment plants. *Journal of Environmental Monitoring*. 13, 5, 1164-1183.
- Obert- Rauser, P., 2012: Etablierung eines Toxizitätstest zur Quantifizierung der Effekte von Silbernanopartikeln auf das Wachstum des Bakteriums *Raoultella planticola*. Diplomarbeit im Fachbereich Biowissenschaften der Goethe-Universität Frankfurt am Main, durchgeführt am Institut für Hydrobiologie der TU Dresden.
- Navarro, E., Baun, A., Behra, R., Hartmann, N. B., Filser, J., Miao, A. J., Quigg, A., Santschi, P. H. and Sigg, L., 2008: Environmental behavior and ecotoxicity of engineered nanoparticles to algae, plants, and fungi. *Ecotoxicology*. 17, 5, 372-386.
- Németh-Katona, J., 2010: The Environmental Significance of Bioindicators in Sewage Treatment. *Acta Mechanica Slovaca*. 14, 2, 92.
- Nickel, C., Angelstorf, J., Bienert, R., Burkart, C., Gabsch, S., Giebner, S., Haase, A., Hellack, B., Hollert, H., Hund-Rinke, K., Jungmann, D., Kaminski, H., Luch, A., Maes, H., Nogowski, A., Oetken, M., Schaeffer, A., Schiwy, A., Schlich, K., Stintz, M., von der Kammer, F. and Kuhlbusch, T. J., 2014: Dynamic light-scattering measurement comparability of nanomaterial suspensions. *Journal of Nanoparticle Research*. 16, 2, 1-12.
- Nyberg, D. and Bishop, P., 1983: High Levels of Phenotypic Variability of Metal and Temperature Tolerance in *Paramecium*. *Evolution*. 37, 2, 341-357.

- Pal, S., Tak, Y. K. and Song, J. M., 2007: Does the antibacterial activity of silver nanoparticles depend on the shape of the nanoparticle? A study of the gram-negative bacterium *Escherichia coli*. *Applied and Environmental Microbiology*. 73, 6, 1712-1720.
- Papadimitriou, C. A., Petridis, D., Zouboulis, A. I., Samaras, P., Yiangou, M. and Sakellaropoulos, G. P., 2013: Protozoans as indicators of sequential batch processes for phenol treatment; an autoecological approach. *Ecotoxicology and Environmental Safety*. 98, 210-218.
- Petit, C., Lixon, P. and Pileni, M. P., 1993: In situ synthesis of silver nanocluster in AOT reverse micelles. *The Journal of Physical Chemistry*. 97, 49, 12974-12983.
- Poda, A. R., Bednar, A. J., Kennedy, A. J., Harmon, A., Hull, M., Mitrano, D. M., Ranville, J. F. and Steevens, J., 2011: Characterization of silver nanoparticles using flow-field flow fractionation interfaced to inductively coupled plasma mass spectrometry. *Journal of Chromatography A*. 1218, 27, 4219-4225.
- Porkodi, K. and Arokiamary, S. D., 2007: Synthesis and spectroscopic characterization of nanostructured anatase titania: A photocatalyst. *Materials Characterization*. 58, 6, 495-503.
- R core team, 2014: R: A language and environment for statistical computing. R Foundation for Statistical Computing, Vienna, Austria.
- Radniecki, T. S., Stankus, D. P., Neigh, A., Nason, J. A. and Semprini, L., 2011: Influence of liberated silver from silver nanoparticles on nitrification inhibition of *Nitrosomonas europaea*. *Chemosphere*. 85, 1, 43-49.
- Reidy, B., Haase, A., Luch, A., Dawson, K. and Lynch, I., 2013: Mechanisms of Silver Nanoparticle Release, Transformation and Toxicity: A Critical Review of Current Knowledge and Recommendations for Future Studies and Applications. *Materials*. 6, 6, 2295-2350.
- Robinson, T. P., Aboaba, O. O., Kaloti, A., Ocio, M. J., Baranyi, J. and Mackey, B. M., 2001: The effect of inoculum size on the lag phase of *Listeria monocytogenes*. *International Journal of Food Microbiology*. 70, 1-2, 163-173.
- Salvado, H., Gracia, M. P. and Amigo, J. M., 1995: CAPABILITY OF CILIATED PROTOZOA AS INDICATORS OF EFFLUENT QUALITY IN ACTIVATED-SLUDGE PLANTS. *Water Research*. 29, 4, 1041-1050.
- Schluesener, J. and Schluesener, H., 2013: Nanosilver: application and novel aspects of toxicology. *Archives of Toxicology*. 87, 4, 569-576.
- Schulze, K., 2013: Effekte von Nano-Titandioxid auf den Ciliaten *Paramecium tetraurelia* im akuten Toxizitätstest. Bachelorarbeit am Institut für Mikrobiologie der TU Bergakademie Freiberg, durchgeführt am Institut für Hydrobiologie der TU Dresden.
- Shehata, T. E. and Marr, A. G., 1975: Effect of temperature on the size of *Escherichia coli* cells. *Journal of Bacteriology*. 124, 2, 857-862.
- Sheng, Z. and Liu, Y., 2011: Effects of silver nanoparticles on wastewater biofilms. *Water Research*. 45, 18, 6039-6050.
- Shrivastava, S., Bera, T., Roy, A., Singh, G., Ramachandrarao, P. and Dash, D., 2007: Characterization of enhanced antibacterial effects of novel silver nanoparticles. *Nanotechnology*. 18, 22.
- Singh, M. and Srivastava, R. K., 2011: Sequencing batch reactor technology for biological wastewater treatment: a review. *Asia-Pacific Journal of Chemical Engineering*. 6, 1, 3-13.

- Soldo, A. T. and Van Wagendonk, W. J., 1969: The Nutrition of *Paramecium aurelia*, Stock 299. *The Journal of Protozoology*. 16, 3, 500-506.
- Solomon, S. D., Bahadory, M., Jeyarajasingam, A. V., Rutkowsky, S. A., Boritz, C. and Mulfinger, L., 2007: Synthesis and study of silver nanoparticles. *Journal of Chemical Education*. 84, 2, 322-325.
- Sondi, I. and Salopek-Sondi, B., 2004: Silver nanoparticles as antimicrobial agent: a case study on E-coli as a model for Gram-negative bacteria. *Journal of Colloid and Interface Science*. 275, 1, 177-182.
- Sonneborn, T. M., 1970: *Methods in Paramecium Research*. Academic Press, New York, (Prescott, D. M., *Methods in Cell Physiology*).
- Sonneborn, T. M., 1975: The *Paramecium aurelia* Complex of Fourteen Sibling Species. *Transactions of the American Microscopical Society*. 94, 2, 155-178.
- Sotiriou, G. A. and Pratsinis, S. E., 2010: Antibacterial Activity of Nanosilver Ions and Particles. *Environmental Science & Technology*. 44, 14, 5649-5654.
- Spieck, E. and Bock, E., 2005: 19, *The Lithoautotrophic Nitrite-Oxidizing Bacteria*. p. 149-153; Brenner, D., Krieg, N., Staley, J. and Garrity, G.; *Bergey's Manual® of Systematic Bacteriology*; Springer US.
- Technical-Guidance-Document, 2003: Technical Guidance Document on Risk Assessment in support of Commission Directive 93/67/EEC on Risk Assessment for new notified substances. (ECB), E. C. J. R. C. I. f. H. a. C. P. E. C. B.,
- Teeguarden, J. G., Hinderliter, P. M., Orr, G., Thrall, B. D. and Pounds, J. G., 2007: Particokinetics In Vitro: Dosimetry Considerations for In Vitro Nanoparticle Toxicity Assessments. *Toxicological Sciences*. 95, 2, 300-312.
- Tejamaya, M., Römer, I., Merrifield, R. C. and Lead, J. R., 2012: Stability of Citrate, PVP, and PEG Coated Silver Nanoparticles in Ecotoxicology Media. *Environmental Science & Technology*. 46, 13, 7011-7017.
- Tocchi, C., Federici, E., Fidati, L., Manzi, R., Vincigurerra, V. and Petruccioli, M., 2012: Aerobic treatment of dairy wastewater in an industrial three-reactor plant: Effect of aeration regime on performances and on protozoan and bacterial communities. *Water Research*. 46, 10, 3334-3344.
- Van Dong, P., Ha, C., Binh, L. and Kasbohm, J., 2012: Chemical synthesis and antibacterial activity of novel-shaped silver nanoparticles. *International Nano Letters*. 2, 1, 9.
- Vertelov, G. K., Yu, A. K., Efremenkova, O. V., Olenin, A. Y. and Lisichkin, G. V., 2008: A versatile synthesis of highly bactericidal Myramistin® stabilized silver nanoparticles. *Nanotechnology*. 19, 35, 355707.
- Viessmann, W. and Hammer, M. J., 2005: *Water supply and pollution control*. Upper Saddle River, NJ : Pearson Education,
- Wang, W.-X., 2011: Incorporating exposure into aquatic toxicological studies: An imperative. *Aquatic Toxicology*. 105, 3-4, Supplement, 9-15.
- Wang, Z., Chen, J., Li, X., Shao, J. and Peijnenburg, W. J. G. M., 2012: Aquatic toxicity of nanosilver colloids to different trophic organisms: Contributions of particles and free silver ion. *Environmental Toxicology and Chemistry*. 31, 10, 2408-2413.
- Werlin, R., Priester, J. H., Mielke, R. E., Kramer, S., Jackson, S., Stoimenov, P. K., Stucky, G. D., Cherr, G. N., Orias, E. and Holden, P. A., 2011: Biomagnification of cadmium selenide quantum dots in a simple experimental microbial food chain. *Nature Nanotechnology*. 6, 1, 65-71.
- Wichtermann, R., 1986: *The biology of Paramecium*. Plenum Press, New York,

- Wiesner, M. R., Lowry, G. V., Jones, K. L., Hochella, J. M. F., Di Giulio, R. T., Casman, E. and Bernhardt, E. S., 2009: Decreasing Uncertainties in Assessing Environmental Exposure, Risk, and Ecological Implications of Nanomaterials†‡. *Environmental Science & Technology*. 43, 17, 6458-6462.
- Wyrwoll, A. J., Maes, H. M., Hollert, H., Schaeffer, A., Meister-Werner, A. and Ralf, P., 2014: Environmental hazard of selected TiO₂ nanomaterials under consideration of relevant exposure scenarios. *Texte*. 72/2014, p. 137,
- Xia, S., Duan, L., Song, Y., Li, J., Piceno, Y. M., Andersen, G. L., Alvarez-Cohen, L., Moreno-Andrade, I., Huang, C.-L. and Hermanowicz, S. W., 2010: Bacterial Community Structure in Geographically Distributed Biological Wastewater Treatment Reactors. *Environmental Science & Technology*. 44, 19, 7391-7396.
- Xiu, Z.-M., Ma, J. and Alvarez, P. J. J., 2011: Differential Effect of Common Ligands and Molecular Oxygen on Antimicrobial Activity of Silver Nanoparticles versus Silver Ions. *Environmental Science & Technology*. 45, 20, 9003-9008.
- Xiu, Z.-m., Zhang, Q.-b., Puppala, H. L., Colvin, V. L. and Alvarez, P. J. J., 2012: Negligible Particle-Specific Antibacterial Activity of Silver Nanoparticles. *Nano Letters*. 12, 8, 4271-4275.
- Yang, Y., Li, M., Michels, C., Moreira-Soares, H. and Alvarez, P. J. J., 2014: Differential sensitivity of nitrifying bacteria to silver nanoparticles in activated sludge. *Environmental Toxicology and Chemistry*. 33, 10, 2234-2239.
- Zhang, C., Liang, Z. and Hu, Z., 2014: Bacterial response to a continuous long-term exposure of silver nanoparticles at sub-ppm silver concentrations in a membrane bioreactor activated sludge system. *Water Research*. 50, 0, 350-358.
- Zheng, X., Chen, Y. and Wu, R., 2011: Long-Term Effects of Titanium Dioxide Nanoparticles on Nitrogen and Phosphorus Removal from Wastewater and Bacterial Community Shift in Activated Sludge. *Environmental Science & Technology*. 45, 17, 7284-7290.
- Zhou, K. X., Xu, M. Q., Liu, B. A. and Cao, H., 2008: Characteristics of microfauna and their relationships with the performance of an activated sludge plant in China. *Journal of Environmental Sciences-China*. 20, 4, 482-486.

10 Danksagung

„Nach unserer Überzeugung gibt es kein größeres und wirksameres Mittel zu wechselseitiger Bildung als das Zusammenarbeiten.“

- Johann Wolfgang von Goethe -

Diesem Ausspruch wird Jeder ohne Zögern zustimmen. Für mich ist es aber nicht nur die gegenseitige Bildung, die aus der Zusammenarbeit mit Anderen resultierte. Ohne Zusammenarbeit wäre mein wissenschaftlicher Werdegang sehr kurz geworden und diese Dissertationsschrift nie entstanden. Neben der finanziellen Förderung durch die Klaus Tschira Stiftung gemeinnützige GmbH (ein ganz besonderer Dank!), waren viele Menschen direkt oder indirekt daran beteiligt, „mein“ Projekt zu realisieren. Zunächst war das ganz klar Professor Thomas Berendonk, der mich bereits während meiner Diplomarbeit in Leipzig betreute, und mir die Gelegenheit gab, am Institut für Hydrobiologie der TU Dresden Fuß zu fassen. Der Sprung (oder Schubser?) ins kalte Wasser mit dem ersten Projektantrag hat sicherlich zum späteren Erfolg mit dem Antrag für dieses Projekt beigetragen und die Überbrückung der vertragslosen Zeit mit den Forschungsaufenthalten in Brasilien hat mich nicht nur fachlich, sondern am allermeisten persönlich voran gebracht. Hierfür und für die spätere Unterstützung während der Projektdurchführung und darüber hinaus ein großer Dank!

Außergewöhnlich großes Überzeugungsvermögen und positive Bestärkung habe ich von Dr. Dirk Jungmann erfahren. Dazu kam eine riesig große Portion Unermüdlichkeit und Optimismus beim Schreiben der unzähligen Anträge im Bereich Nano-Ökotoxikologie, nachdem ich die ersten vorbereitenden Arbeiten unter seiner Betreuung durchgeführt hatte. Besonders bedanken möchte ich mich auch für die Geduld wenn wir nicht einer Meinung waren oder ich kurz davor war, alles hinzuwerfen. Auch nach Ende der Projektlaufzeit habe ich uneingeschränkte Unterstützung erhalten. Ich wurde von ihm ermutigt, meine Ideen, bei denen ich Angst vor der eigenen Courage hatte, in die Tat umzusetzen, was ich meistens nachträglich nicht bereuen musste. Neben der Unterstützung bei der Einwerbung des Projekts bin ich sehr dankbar für Alles, was ich lernen durfte.

Weitere Personen, die zum Gelingen der Antragstellung beigetragen haben, sind Dr. Astrid Weigert und Klaus Dorschner. Für ihr Know-how, Hilfsangebote, sowie Bildmaterial sei hiermit herzlich gedankt.

Bei den laborpraktischen Arbeiten wurde ich vielfältig unterstützt, zum Einen von Studenten, die ich während Abschlussarbeiten und Praktika betreuen durfte und die mir im Gegenzug die erhobenen Daten zur Verfügung stellten: Dipl.-Biol. Henriette Leps, Dipl.-Biol. Patrick Obert-Rausser, M.Sc. Simbisai Mashiri, M. Sc. Elisa Brode, B. Sc. Katharina Schulze, B. Sc. Katrin Burkhardt und B. Sc. Daniel Pfitzner. Ganz besonders großer Danke gilt der Studentin Annika Stoll, die mir und Patrick Obert-Rausser mit außerordentlichem persönlichen Einsatz bei der Durchführung der Batchreaktor-Experimente, sowie bei den Magnifikations- Experimenten und den unzähligen Wachtsumskurven-Versuchen mit den Nitrobactern geholfen hat.

Generelle praktische Unterstützung bekam ich während der Laborarbeiten von meinen Kollegen, besonders den Technischen Assistenten, die durch ihr tägliches Werk die Laboratorien am Laufen hielten, aber auch Ansprechpartner für jegliche Probleme, technische Fragen, Bestellungen und/oder Bereitstellung von Material, Medien und Arbeitskraft waren. Vielen Dank an Christiane Zschornack, Steffen Kunze, Ulrike Mogck, Frau Benndorf und Frau Egerer.

Neben den Arbeiten, die hier im Labor gemeistert werden konnten, gab es viele technische Herausforderungen, für die wir hier nicht ausgerüstet waren und die deshalb an anderen Instituten und Einrichtungen durchgeführt wurden. In diesem Zusammenhang möchte ich mich bei Professor Michael Stinz, Dipl.-Ing. Petra Fiala, Professor Wolf von Tümping, Dr. Norbert Scheibe, Dr. Thomas Klinger, Dr. Alexandra Kroll, Dr. Klaus Ripl, Jana Brückner und den Technikern der Kläranlage Dresden-Kaditz für alle Hilfe bedanken.

Nach Verlassen des Labors blieb noch immer die Datenanalyse und Auswertung der Ergebnisse, wobei ich Unterstützung von vielen Kollegen bekam. Neben meinem Betreuer Dr. Dirk Jungmann möchte ich namentlich für offene Ohren, konstruktive Beiträge und zum Teil praktische Hilfe Dr. Sascha Krenek, Dr. Marcus Rybicki und Dr. Eike Dusi danken. Allen anderen Kollegen sei generell für ihr Interesse und den ein oder anderen hilfreichen Hinweis gedankt, besonders den Mit-Doktoranden in der vorübergehend etablierten Zielvereinbarungsgruppe.

In der Hoffnung, dass ich Niemanden vergessen habe, der an meiner wissenschaftlichen Arbeit Anteil hatte, möchte ich mich an dieser Stelle bei den Menschen bedanken, die mich persönlich, beziehungsweise mental unterstützt haben. Dabei kommt meine Familie an erster Stelle, die Interesse an meiner Arbeit zeigte, obwohl es sicher manchmal schwer war, das Fachchinesisch zu begreifen. Aber auch die Nachfragen nach dem Stand der Dinge, der Verträge und Anträge, das Mitfiebern und Daumendrücken und sämtliche Hilfe haben mir den nötigen Rückhalt gegeben um „Das hier“ durchzuziehen. Besonders dankbar bin ich auch, dass ihr nie Zweifel an meiner beruflichen Entscheidung gehegt

habt, denn die hatte ich selbst oft zur Genüge. Die Zuversicht, dass ich das alles schaffe und die Freiheit meinen Weg gehen zu dürfen, war eine große Stütze, besonders wenn nicht alles optimal lief. Danke, dass ich von euch nie Sätze gehört habe, die mit „Hättest du nicht besser...?“ anfangen. Das Allerbeste ist aber, dass ich mit euch immer sehr viel Lachen konnte, egal, in welcher Situation ihr und ich uns gerade befanden. Denn wie sagte Charles Dickens: *„Ein schöner, gerechter und vornehmer Ausgleich der Dinge besteht darin, dass, wie Krankheit und Kummer übertragbar sind, Nichts in der Welt so sehr ansteckend wirkt, wie Gelächter und gute Laune.“*

List of figures

Figure 1: Estimated product numbers containing nanoparticles	1
Figure 2: Dispersion, agglomeration and aggregation of particles.....	3
Figure 3: Flowchart of stepwise approach for studying effects of silver nanoparticles	7
Figure 4: Principle of DLS. Modified, from R. Nitzsche.....	10
Figure 5: Illustration of zeta potential and electrophoretic mobility.	11
Figure 6: Modified 24-well plate as counting chamber.....	19
Figure 7: Ten days growth curves of <i>P. tetraurelia</i> batch culture in unfiltered ABC.	21
Figure 8: Growth of <i>P. tetraurelia</i>	22
Figure 9: Experimental setup, preparation of assays and analyses.....	26
Figure 10: Intensity weighted size distribution of nAg.....	29
Figure 11: Concentration dependent particle diameters.....	30
Figure 12: SEM pictures of a 60 mg/L nAg dispersion.....	32
Figure 13: Analyzed values of total Ag (a) and Ag ⁺ (b) in recovery experiment.	34
Figure 14: Concentration response curves based on effective concentrations	37
Figure 15: Regression functions of Ag ⁺ release quotient	39
Figure 16: Intensity weighted size distribution of nTiO ₂ in filtrated ABC,	45
Figure 17: Bar charts for acute toxicity test results regarding cell counts and FCVK,	46
Figure 18: Bar charts of results from acute toxicity test with UV irradiation	48
Figure 19: Chronic exposure with nTiO ₂	49
Figure 20: Growth rates as cells/h in different treatments.....	50
Figure 21: Flowchart of experimental setup for growth kinetic of <i>R. planticola</i>	54
Figure 22: Correlation of CFU/mL with OD ₆₀₀ values	56
Figure 23: Growth curves obtained from a) OD ₆₀₀ , b) CFU/mL, and c) relative fluorescence	58
Figure 24: Correlations of all determined endpoints against each other,.....	59
Figure 25: SEM photograph of CM with 270 µg/L Ag.....	64
Figure 26: SEM photograph of 270 µg/L nominal total Ag and <i>R. planticola</i>	65
Figure 27: Measured concentrations of total Ag plotted against nominal concentrations of total Ag. .	66
Figure 28: Relative inhibition of <i>R. planticola</i> exposed to nAg.....	67
Figure 29: Derived inhibition of <i>R. planticola</i> exposed to nAg	68
Figure 30: Relative inhibition of <i>R. planticola</i> exposed to AgNO ₃	70
Figure 31: Growth kinetics of a freshly inoculated <i>Hyphomicrobium</i> culture over 28 h	76
Figure 32: Growth kinetics of <i>Hyphomicrobium</i> sp. over 9 days determined as OD ₆₀₀ in cuvettes.	77
Figure 33: Scheme of toxicity test preparation with <i>Hyphomicrobium</i> sp. and nAg or AgNO ₃ , respectively.....	78
Figure 34: UV-vis spectrograms of nAg dispersions in R2A medium.....	80
Figure 35: UV-vis spectrograms of nAg working stock dispersions in R2A medium.....	81
Figure 36: Viability of <i>Hyphomicrobium</i> cells exposed to nAg,.....	82
Figure 37: Toxicity test results for <i>Hyphomicrobium</i>	83
Figure 38: Viability of <i>Hyphomicrobium</i> cells after 24 h exposure to nAg and AgNO ₃	84
Figure 39: a) Viability of <i>Hyphomicrobium</i> after exposure to nAg	85

Figure 40: Concentration response curve of <i>Hyphomicrobium</i> exposed to nAg according to OD ₆₀₀	85
Figure 41: Results of the preliminary FCVK assays with differently diluted <i>N. vulgaris</i> culture.	91
Figure 42: Nitrite consumption and nitrate release during growth of <i>Nitrobacter</i>	92
Figure 43: Growth kinetic experiments with <i>N. vulgaris</i>	94
Figure 44: Scheme of toxicity test preparation with <i>Nitrobacter vulgaris</i>	96
Figure 45: UV-vis spectrogram of nAg in <i>Nitrobacter</i> medium.....	97
Figure 46: UV-vis spectrograms of nAg in <i>Nitrobacter</i> medium over 72 h	98
Figure 47: Results of range finder toxicity test with <i>Nitrobacter vulgaris</i> and nAg.....	99
Figure 48: Results of toxicity test with <i>N. vulgaris</i> at lower concentrations	100
Figure 49: The two modes of bioaccumulation	103
Figure 50: Flowchart of the experimental setup in the biomagnification assay	106
Figure 51: Results of parallel nAg exposure assay with <i>P. tetraurelia</i> in conditioned CM and ABC.	110
Figure 52: UV-vis spectrograms of nAg in conditioned CM at exposure concentrations	112
Figure 53: Mean number of surviving cells per mL in the final accumulation test assay.....	113
Figure 54: Growth curves of <i>P. tetraurelia</i> after exposure with nAg via food or medium	117
Figure 55: Comparison between spatial separation of treatment steps in conventional wastewater treatment technique (upper section) and chronological separation of treatment steps in sequencing batch reactor technique (lower section).	122
Figure 56: Scheme of the experimental setup.....	126
Figure 57: Arrangement of control and treatment replicates in cooling ponds	127
Figure 58: Full setup of acute toxicity test with activated sludge.	128
Figure 59: Total abundance of genera in the two analyzed replicates	137
Figure 60: Assignment of batch reactor positions in cooling ponds	138
Figure 61: MLSS assigned to positions of batch reactors in cooling ponds.....	140
Figure 62: Cumulative abundance of the protozoa and metazoa genera.....	141
Figure 63: Regression of number of taxa against sum of individuals in the batch reactors.....	142
Figure 64: PCA of treatment replicates and abiotic parameters.....	145
Figure 65: CCA plot with all measured parameters	146
Figure 66: CCA plot with selected parameters	146
Figure 67: Estimated real averages of relative abundance (y-axis) and BOD ₅ in ML (x-axis).....	148
Figure 68: Development of the microbial community over acclimatization period.....	153

List of tables

Table 1: Overview on characterization methods applied for identification of nAg.....	13
Table 2: nAg Particle sizes as mean diameters.....	30
Table 3: Results of zeta potential (ζ in mV) analyses of nAg test concentrations in filtrated ABC.	33
Table 4: Nominal and determined concentrations of Ag and Ag ⁺	35
Table 5: Toxicity values of NM-300K.....	40
Table 6: OD ₆₀₀ values with assigned dilution levels for agar plating.....	57
Table 7: Generation time <i>gt</i> of <i>R. planticola</i> at 22 °C.....	60
Table 8: Hydrodynamic diameters of nAg in CM.....	63
Table 9: Ag-concentrations according to ICP-OES analysis in CM	66
Table 10: Nominal and inferred concentrations derived from regression function.....	67
Table 11: Median effective concentrations derived from the toxicity tests	69
Table 12: EC ₅₀ values with CI for <i>R. planticola</i> toxicity tests with AgNO ₃	70
Table 13: Median effective concentration according to OD ₆₀₀ and fluorescence	71
Table 14: Conversion of SBI values into four quality classes (I – IV) and respective evaluation.....	132
Table 15: Two-way table for determination of SBI.....	133
Table 16: Results of microscopical enumeration of taxonomic units in batch reactors.....	142
Table 17: Requirements for effluent waters released to the environment	143
Table 18: Measured concentrations of nitrogen compounds, ortho-phosphate and COD.....	143
Table 19: Ingredients for 100 fold concentrated stock of AWW.....	151
Table 20: Overview on available effect values from toxicity tests with NM-300K	158
Table 21: Determination of safety factors for PNEC calculation	159

Erklärung zur Eröffnung des Promotionsverfahrens

1. Hiermit versichere ich, dass ich die vorliegende Arbeit ohne unzulässige Hilfe Dritter und ohne Benutzung anderer als der angegebenen Hilfsmittel angefertigt habe; die aus fremden Quellen direkt oder indirekt übernommenen Gedanken sind als solche kenntlich gemacht.

2. Bei der Auswahl und Auswertung des Materials sowie bei der Herstellung des Manuskripts habe ich Unterstützungsleistungen von folgenden Personen erhalten:
Prof. Dr. rer. nat. habil. Thomas Berendonk
Dr. Dirk Jungmann
Dr. Marcus Rybicki
Dipl.-Biol. Patrick Obert- Rauser
Dipl.-Biol. Henriette Leps
B. Sc. Katharina Schulze
Dr. Ana Tshvediani
Annika Stoll

3. Weitere Personen waren an der geistigen Herstellung der vorliegenden Arbeit nicht beteiligt. Insbesondere habe ich nicht die Hilfe eines kommerziellen Promotionsberaters in Anspruch genommen. Dritte haben von mir weder unmittelbar noch mittelbar geldwerte Leistungen für Arbeiten erhalten, die im Zusammenhang mit dem Inhalt der vorgelegten Dissertation stehen.

4. Die Arbeit wurde bisher weder im Inland noch im Ausland in gleicher oder ähnlicher Form einer anderen Prüfungsbehörde vorgelegt und ist – sofern es sich nicht um eine kumulative Dissertation handelt – auch noch nicht veröffentlicht worden.

5. Sofern es sich um eine kumulative Dissertation gemäß § 10 Abs. 2 handelt, versichere ich die Einhaltung der dort genannten Bedingungen.

6. Ich bestätige, dass ich die Promotionsordnung der Fakultät Umweltwissenschaften der Technischen Universität Dresden anerkenne.

Dresden,

Unterschrift des Doktoranden

Übereinstimmungserklärung

Die Übereinstimmung dieses Exemplars mit dem Original der Dissertation zum Thema:

“Ecotoxicology of nanoparticles – effects on organisms from activated sludge in wastewater treatment plants”

wird hiermit bestätigt.

Dresden,

References to own original publications used in this thesis

Section 3.3 'Toxicity tests with *P. tetraurelia* and nAg' has been published with major alterations under the title:

Burkart, C., von Tümpling, W., Berendonk, T. und Jungmann, D., 2015: Nanoparticles in wastewater treatment plants: a novel acute toxicity test for ciliates and its implementation in risk assessment. *Environmental Science and Pollution Research*. 22, 10, 7485-7494.

The section differs from the original publication in the following respects:

The introduction of the section was completely rewritten for the thesis, as the contents of the publication introduction were mentioned in the general introduction of the thesis. **Materials and methods section:** From the publication, the part 'Cultivation of axenic *P. tetraurelia*' was moved into section 3.2.1 of the thesis. The section 'Chemicals' from the publication was moved into the section 2.1.1 'Properties of silver nanoparticles'. A minor part of the section 'Characterization of silver nanoparticles in exposure media' from the publication was moved into section 2.1.2 'Characterization methods for silver nanoparticles'. In the toxicity test section, figure 9 was inserted into the main text of the thesis, which was originally added to the supplementary material of the publication. Validity criteria were added at the beginning of section 'Data analysis' in the thesis. The equations according to Teeguarden et al. (2007), originally contained in the same section of the publication, were moved to the section 2.1.2 'Characterization methods for silver nanoparticles' of the thesis, along with respective explanations. **Results and discussion section:** in the section 'Characterization of nAg', the figure and tables from supplementary material of the publication was inserted into the main text of the thesis. In the section 'Analytics' the first paragraph of the publication was extended for the supplemental material from the publication. The following paragraph was changed to minor extent. In the third paragraph of the section 'Toxicity tests' of the thesis an additional equation was introduced for comparison of EC_x values. The paragraph about environmental risk assessment according to REACH legislation in the publication was moved to 2.1.2 'Characterization methods for silver nanoparticles' in the thesis. The supplemental material figure was inserted into the main thesis text as figure 15. Supporting information table S4 was also included into the thesis text. The last paragraph of the publication was rewritten for the thesis.

Dresden,

Curriculum Vitae

Corinna Burkart

Education

Contents removed for reason of privacy protection

Employment

Contents removed for reason of privacy protection

Extracurricular activities

Research internships

Publications

2015: **Burkart, C.**, von Tuempling, W., Berendonk, Th. and Jungmann, D. 2015: Nanoparticles in wastewater treatment plants: a novel acute toxicity test for ciliates and its implementation in risk assessment. *Environmental Science and Pollution Research*

Alexandra Kroll , [...], **Corinna Burkart**, [...], Dirk Jungmann [...] and Claus Svendsen 2015: Mixed messages from benthic microbial communities exposed to nanoparticulate and ionic silver. *Environmental Science and Pollution Research*

2014:

Carmen Nickel, [...], **Corinna Burkart**, Stephan Gabsch, [...], and Thomas A.J. Kuhlbusch 2014: Dynamic light-scattering measurement comparability of nanomaterial suspensions. *Journal of Nanoparticle Research*

Dresden,

Corinna Burkart

Annex I: Protocol for Axenic Broth for Ciliates (ABC)

modified after Soldo, Godoy, van Wagtenonk: 1966 J. Protozool., 13, 492 and Kaneshiro et al.: 1979 J. Protozool., 26, 147, supplied by Dr. Eva-Maria Ladenburger (University of Konstanz)

Solution A:

- Dissolve 1g of ribonucleic acid in 20 ml 0.5 M NaOH (RNA-Solution)
- Weigh
 - 10 g Proteose Peptone
 - 5 g Trypticase
 - 0.5 g Mg SO₄ x 7 H₂Oin a beaker and dissolve with ddH₂O
- Add RNA- Solution

Solution B: Fatty acids

Dissolve: (*under a chemical hood!*)

- 0,06 g Palmitinsäure in 18 ml ddH₂O in a beaker, carefully add some drops (c. 0,2 ml) of Triethylamine
- Add 0.04 g Stearic acid, let stirr for a while
- Add 100 µl olic acid &
 - 5 µl Linoleic acid, stirr
- add 1 mg Linolenic acid (solution crystallizes)
- adjust pH with Triethylamine to 10,5 - 11 if necessary (Linolenic acid should dissolve)

Solution B can be stored in the freezer for several months.

Solution C: Vitaminsolution

Weigh:

- 0.005 g Calcium – D – Pantothenat
- 0.005 g Nikotinsäureamid
- 0.005 g Pyridoxal – HCl
- 0.0025 g Pyridoxamin – HCl
- 0.015 g Thiamin – HCl
- 0.005 g Riboflavin

Dissolve in 8.8 ml ddH₂O

This solution can be prepared in bigger volumes and stored frozen in aliquots for several months.

When preparing fresh medium:

Dissolve also:

- 0.025 g Folic acid in 1 ml 0,1 N NaOH (Folic acid solution)
- 0.00125 g Biotin in 50 ml ddH₂O (Biotin solution)
- 0.005 g Lipoic acid in 10 ml 70% Ethanol (Lipoic acid solution)
- add 1 ml Folic acid solution
 0.05 ml Biotin solution
 0,1 ml Lipoic acid solution to solution C

Completion:

- prepare 50 mg/ml Stigmasterole solution
- prepare Phosphatidyl-ethanol-cholin (Cephalin) solution: weigh 250 mg and dissolve in 10 ml ddH₂O while slightly heating (ca 40 °C) and stirring for 20 min

Add:

10 ml Solution C
1 ml Stigmasterol solution
10 ml Cephalin solution
5 ml solution B (under hood)
to solution A , fill up to 1 Liter with ddH₂O and let stir

Adjust pH to 6.8 – 7 if necessary

Autoclave for 20 min at 120°C at the same day. (*Do not leave unautoclaved overnight.*)

ANNEX II: Protocol for 0.25% Cerophyl-Medium (CM)

- 2.5g Cerophyl
- 990 ml deionized H₂O
- 5ml Cerophyl buffer pH 7.0 (see below), final concentration:
 - Na₂HPO₄ 500mg/l
 - NaH₂PO₄ 120mg/l
- 5ml Balanced Salt Solution (BSS) pH 6.95
 - NaCl 1040mg/l
 - MgSO₄ 40mg/l
 - MgCl₂ 85mg/l
 - CaCl₂ 10mg/l
 - KCl 230mg/l
- 100 µl Stigmasterol solution* 0,5mg/l

Boil Cerophyl for 5min in 500ml dH₂O and pass through two paper filters. Let cool down, add Cerophyl buffer, BSS and Stigmasterol solution, fill to 1000ml with deionized H₂O and mix. Autoclave for 20 min at 120°C.

Cerophyl buffer pH 7.0:

- 100ml ddH₂O
- 10g Na₂HPO₄ · 2H₂O
- 2.4g NaH₂PO₄ · H₂O

Balanced Salt Solution (BSS):

- 100ml ddH₂O
- 20.8g NaCl
- 0.8g MgSO₄
- 1.7g MgCl₂
- 0.2g CaCl₂
- 4.6g KCl

Stigmasterol-Lösung:

- 100ml 96%iger Ethanol (undenatured)
- 500mg Stigmasterol

* not mandatory

ANNEX III: Protocol for R2A Medium

According to variation of DSMZ protocol 830. R2A MEDIUM, without addition of agar:

Yeast extract	0.50 g
Proteose Peptone	0.50 g
Casamino acids	0.50 g
Glucose	0.50 g
Soluble starch	0.50 g
Na-pyruvate	0.30 g
K ₂ HPO ₄	0.30 g
MgSO ₄ x 7 H ₂ O	0.05 g
Distilled water	1000.00 ml

adjust with crystalline K₂HPO₄ or KH₂PO₄ to final pH 7.2, autoclave for 20 min at 121 °C.

ANNEX IV: Protocol for Nitrobacter medium 756.c

According to DSMZ medium 756 and 756.c

Stock solution:

CaCO ₃	0.07 g
NaCl	5.00 g
MgSO ₄ x 7 H ₂ O	0.50 g
KH ₂ PO ₄	1.50 g
Distilled water	1000.00 ml

Trace element solution:

MnSO ₄ x H ₂ O	33.80 mg
H ₃ BO ₃	49.40 mg
ZnSO ₄ x 7 H ₂ O	43.10 mg
(NH ₄) ₆ Mo ₇ O ₂₄	37.10 mg
FeSO ₄ x 7 H ₂ O	97.30 mg
CuSO ₄ x 5 H ₂ O	25.00 mg
Distilled water	1000.00 ml

Autoclave stock solution and trace element solution for 20 min at 121 °C and store in a fridge at 4 °C.

For completion:

NaNO ₂	2 g
Trace element solution	1.00 ml
Stock solution	100.00 ml
Distilled water	899.00 ml

Adjust pH to 8.6 with NaOH or KOH. Autoclave and leave the medium to stand for 2 - 3 days so that pH can adjust itself to pH 7.4 - 7.6.

ANNEX V: Protocol for aniline violet staining

According to personal communication with Dipl.-Biol. Claudia Seiler, Institute of Hydrobiology, TU Dresden/Helmholtz center for environmental research Magdeburg

- Prepare a 0.1 % aniline violet solution, by dissolving aniline violet with 96% ethanol (here Sigma-Aldrich, Steinheim, Deutschland) and diluting to respective concentration with sterile filtrated¹¹ deionized water (Milli-Q Direct8, Millipore, Merck KGaA, Darmstadt, Germany)
- Fill a 96-well plate (here pure grade S, transparent F-bottom, Brand GmbH & CO KG, Wertheim, Germany) with 200 μ L of the *Nitrobacter vulgaris* culture per well and incubate at the respective temperature (here 28 °C)
- At each sampling date, discard the supernatant of the respective replicate wells (8 wells per sampling in this work) and wash the biofilm in the wells five times using 100 μ L of sterile filtrated Milli-Q deionized water
- Let dry for 45 minutes
- Stain the biofilm with the 0.1 % aniline violet solution (150 μ L) and incubate for 45 minutes
- Wash with 200 μ L Milli-Q deionized water (sterile filtrated) five times per well
- Dissolve the aniline violet from the biofilm by adding 200 μ L 96% ethanol
- Transfer 100 μ L of the alcohol with the aniline violet into a fresh 96-well plate
- Measure the absorption of the samples in a plate reader at 595 nm (Synergy H1 plate reader (BioTek Instruments, Inc., Winooski, VT, USA) used in this thesis work)

¹¹ carried out with syringes equipped with 0.45 μ m and 0.2 μ m syringe connected cellulose acetate PES filters (TPP, Switzerland)